Neural Bases of Breathing in the Mouse : Monosynaptic Tracing and Genetic Dissection of Phrenic Premotor Neurons

Jinjin Wu

NNT : 2016SACLS151

THESE DE DOCTORAT

DE
L'UNIVERSITE PARIS-SACLAY
PREPAREE A
L'UNIVERSITE PARIS SUD-XI

ECOLE DOCTORALE N° 568 : BIOSIGNE

Signalisations et réseaux intégratifs en biologie

SPECIALITE DE DOCTORAT: Aspects moléculaires et cellulaires de la biologie
NEUROSCIENCES

Par

JINJIN WU

Neural bases of breathing in the mouse: monosynaptic tracing and genetic dissection of phrenic premotor neurons

Thèse présentée et soutenue à Gif-sur-Yvette, le 28 Juin 2016

Composition du Jury :

Gilles Fortin	DR2	Directeur de thèse
Muriel Thoby-brisson	CR1	Rapporteurs
Thomas Similowski	PUPH	Rapporteurs
Alessandra Pierani	DR2	Examinateurs
Hervé Daniel	PU2	Président du jury

université PARIS-SACLAY
ÉCOLE DOCTORALE
Signalisation et réseaux intégratifs en biologie (BIOSIGNE)

Titre : Bases neurales de la respiration : traçage monosynaptique et dissection génétique des neurones pré-moteurs phréniques

Mots clés : pré-moteurs, respiratoire, tronc cérébral

Résumé : Le comportement respiratoire est unique en ce qu'il requiert l'activation permanente de muscles squelettiques. Le contrôle exécutif de la respiration repose sur des groupes d'interneurones connectés par des synapses et formant un réseau ordonné : le générateur central respiratoire (CPG). Nous cherchons à comprendre l'implication de types neuronaux définis dans la logique de l'organisation du CPG respiratoire. Nous avons précédemment démontré que les neurones constitutifs du – complexe preBötzinger (preBötC) – le générateur du rythme inspiratoire, dérivaient de progéniteurs neuraux exprimant le gène à homéoboite *Dbx1*. J'étudie ici, par traçage viral monosynaptique chez des souriceaux, les neurones prémoteurs à l'interface entre le générateur de rythme et les motoneurones phréniques innervant le diaphragme. Je montre que les principaux neurones prémoteurs formant – le groupe respiratoire ventral rostral (rVRG) – sont aussi des neurones de type V0. Ce travail révèle une organisation des circuits inspiratoires dans laquelle les lignages cellulaires de types V0 sont cruciaux pour établir (i) le preBötC (générateur du rythme) et le rVRG (suiveur du rythme) et (ii) un dessin de connectivité assurant bilatéralement l'amplitude équilibrée et la synchronisation de la commande motrice des nerfs phréniques requise pour respirer efficacement.

Title: Neural bases of breathing in the mouse: monosynaptic tracing and genetic dissection of phrenic premotor neurons

Keywords: premotor, respiration, brainstem

Abstract: Breathing uniquely engages permanent rhythmic contractions of skeletal muscles in a bilaterally synchronized manner. The executive control of respiration imparts on sets of brainstem interneurons synaptically assembled into an ordered network: the respiratory central pattern generator (CPG). We investigate the relationship of defined neuronal subtypes to the organizational logic of the respiratory CPG. We have previously demonstrated that neural progenitors expressing the homeobox gene *Dbx1* give rise to V0 neurons that go on forming the – preBötzinger complex (preBötC) – the inspiratory rhythm generator. I now study, via monosynaptic viral tracing in early postnatal mice, the premotor neurons that interface the rhythm generator to output phrenic motor neurons innervating the main inspiratory pump muscle, the diaphragm. I show that the principal premotor neurons in the – rostral ventral respiratory group (rVRG) – are also V0 interneurons. This work reveals an organization of inspiratory circuits in which V0 cell lineages are crucial for establishing (i) the preBötC (rhythm generator) and the rVRG (rhythm follower) and (ii) a connectivity design that secures the bilaterally balanced amplitude and temporal synchronicity of rhythmic phrenic motor drives necessary for efficient breathing.

ACKNOWLEDGEMENTS

Time flies so fast, after five years of PhD study in France, finally, I am able to defense and tell the story of my project. The scientific training and life experience I've gotten in France and in the lab during the past few years is my invaluable treasure, which will have big impact on my future scientific career and personal life.

Above all, I would like to express my special thanks to my supervisor, Gilles Fortin, who has given me great support and excellent guidance during this critical period of my career. I deeply appreciate your patient and motivating discussion of scientific issues with me, and the great opportunities you've provided for international scientific communication. The rigorous training you've provided during my PhD period gave me a solid foundation and good start to continue my scientific career.

I would like to thank all the members of the jury. It is a great honor to have Hervé Daniel as president of jury, Alessandra Pierani as examiner, and Muriel Thoby-brisson and Thomas Similowski as reviewers. Thank you all for accepting to evaluate my thesis. Especially, I would like to thank the reviewers, Muriel Thoby-brisson and Thomas Similowski, for their time and efforts to evaluate my manuscript.

My thanks also go to all our collaborators. To Martyn Goulding (Salk Institute, US), who offered the first opportunity to apply the cutting edge viral tracing to my project, and to all his lab members for their kind help during my stay. To Silvia Arber (FMI, Switzerland), who accepted me to continue this part of work in her lab, and especially the kind help from her lab member Paolo Capelli, thank you for your great help with my daily work and life during my stay in Switzerland, I really appreciated all the efforts you've invested in this thesis work.

I would like to also thank all the past and present members of our lab for creating the pleasant and motivating atmosphere. Julien, thank you for your very nice discussion of my project and the patient explanation and generous sharing of new technologies and ideas. Thank you Pierre-Louis and John, the ancient members of our team, for teaching me the basic techniques used in our lab and the kind help from you whenever I had a problem. And the thanks also go to our great technician team, Sandra and Séverine, thanks for your efficient and brilliant work, without you some experiments were not possible to finish on time, and I really appreciate your special care of me both inside and outside of the lab. Laure, really thank you for your assistance in the in situ hybridization, and your personal support gave me

great courage during the hardest time of my study. I also would like to thank Jean for the nice scientific discussions, and Marie-Pierre for the communication of some techniques. In addition, I would like to thank the new comers: to our beautiful blond master student Coralie, I really enjoy the time we've spent together, you have great talent in science, I am sure you will be great in the scientific field; to the Brazilian team, Luciane, Marcelo and Luis Gustavo, thanks for friendly sharing your technique with me. And I would like to thank Gustavo for his good advices to deal with my documental work to stay in France. To all our lab members, thank you all for your special care of me, many thanks to your friendship and kindly help.

In addition, I would like to thank the Animal facility in our institute, especially Valérie Lavallée, Aurélien Drouard and Krystel Saroul for the maintenance of the mice colonies. I am really grateful for the daily effort of Valérie to take care of hundreds of cages of our mice and her great work to set up the mice used for experiments. And I would like to thank the Imagif platform in our institute for their proper training for using the confocal and imaging analysis.

My thanks must be given to all the members in building 32 for their help whenever I needed. My special thanks go to Philippe Vernier, Odile Lecquyer and Nadia Iafrate for taking care and handling all my administrative procedures.

I would like to thank ENP (École des Neurosciences Paris Île de France) for offering me this great PhD program to study in Paris. And all the faculty and staff in the ENP are extremely nice and helpful, who helped me a lot both for the scientific and personal lives.

Also to my friends both in and out of France: Jiajia Pan, Tiantian He, Xia Sun, Sumen, Xinhe Liu, Yihui Cui, Chenju Yi, Jiewen Hua, Maria Teleńczuk, Xiangyi Dong, Wendi Sun, and many others… Thanks for all the good moments you've shared with me, and your support and help when I encountered difficulties.

Last but not least, I would like to deeply thank all my family members. To my parents for their strongest support and respect of my own choice. They always stand by my side and believe in me, and their encouragements have inspired me to overcome a lot of difficulties during my stay in France. I would like to thank specially my fiancé, Guangxin Ren, for supporting my decision of PhD study in France, being far way from China, thank you for always being there, and for your constant care, trust and encouragement no matter when I needed.

CONTENTS

FOREWORDS

Breathing controls gas exchange in the lungs to support metabolism by regulating blood (and brain) O_2, CO_2, and pH. The neural command controlling respiratory movements is characterized by permanent rhythmicity, bilateral synchronicity and obligation to operate at birth. Over the past decades, progress in clarifying principles of respiratory motor control has benefitted from a wide range of ideas and approaches in cellular neurophysiology in vivo (**Bianchi, 1971**; **Cohen, 1979**; **Richter and Spyer, 2001**; **Richter et al., 2000**) and in vitro (**Del Negro et al., 2005**; **Onimaru and Homma, 2003**; **Paton, 1996**; **Rekling and Feldman, 1997**; **Rivera et al., 1999**; **Smith et al., 1991**), anatomy (**Bertrand et al., 1973**; **Dobbins and Feldman, 1994**; **Kalia, 1981**; **McCrimmon et al., 2004**), comparative physiology (**Milsom, 2008**; **Vasilakos et al., 2005**), as well as computational descriptions of simulated central networks (**Guerrier et al., 2015**; **Rubin et al., 2009**; **Rybak et al., 1997**). This has revealed, the locations and the functional diversity of interneurons involved in regulating the respiratory motor output and some operating principles of rhythm generation.

This corpus was recently augmented by seminal molecular studies that have unraveled cell specification schemes, conserved across vertebrate species, giving rise to neuronal type diversity, revealed most clearly by profiles of transcription factor expression (**Goulding, 2009**; **Jessell, 2000**; **Lupo et al., 2006**). Interneurons that settle in the developing neural tube with presumed functional roles, let it be respiratory, derive from cardinal progenitor populations, which give rise at cell cycle exit to cardinal classes of dorsal and ventral interneuron and motor neuron types. Each progenitor and post-mitotic set is marked by its own distinctive set of progenitor and postmitotic transcription factors (**Jessell, 2000**). It is hoped that established molecular signatures will help the investigation of cellular functional fates. Major progress has been made in the elucidation of the transcriptional codes that define the assembly of components of inspiratory command circuits, starting with the rhythm generator in the preBötC (**Bouvier et al., 2010**; **Gray et al., 2010**), some of its attendant modulatory control (**Li et al., 2016**; **Rose et al., 2009**; **Ruffault et al., 2015**; **Thoby-brisson et al., 2009**) and its output motoneurons that innervate the diaphragm (**Philippidou et al., 2012**).

The goal remains to determine the relationship of defined neuronal subtypes to the organizational logic of interneuron circuitry, and to ask whether molecular interventions that

target individual neuronal subsets can reveal new aspects of the logic of interneuron networks in respiratory control. We pursue here this goal, leaving aside rhythmogenic aspects and focusing on inspiratory premotor neurons, a yet missing component of the genetic dissection of respiratory circuit described above, that bridge the inspiratory rhythm generator and the inspiratory motor neurons controlling contractions of the diaphragm. Because interneurons are by definition precisely inserted in neural circuits, their molecular identities need to be addressed jointly with the generally missing dimension of neural networks, connectivity. In this Ph.D. work I have combined molecular genetics tools with transsynaptic tracing methods to reveal the identity, impair the commissural navigation of axon and photostimulate phrenic premotor neurons to establish the neural bases whereby respiratory movements (by necessity) are bilaterally synchronized.

The results obtained demonstrate that a single type of interneurons known as V0s in the brainstem contribute both the inspiratory rhythm generator and the prominent premotor module conveying the motor command to phrenic motor neurons, the two neuronal groups are redundantly commissural and secure bilateral synchronicity of the command. These data also point to the importance of P0 progenitors for the advent of aspiration breathing in tetrapods.

INTRODUCTION

I. General view of respiration

Breathing, like locomotion, is a behavior used by integrative neurobiologist as a model system to study how the nervous system functions normally, how it balances inherent robustness with highly regulated lability and how it adapts to changing conditions of the environment. Breathing is a "simple" yet vital behavior regulating the gas exchange in the lung to support energetic homeostasis throughout life. Simplicity of the system comes from stereotypic respiratory movements associated to stereotypic neuronal discharges of neurons sufficient to define them as respiratory neurons, this is not the case in most brain circuits where the sole activity pattern of a neuron is a poor predictor of its functional involvement. In early tetrapods, air is driven into the lungs by positive pressure generated in the buccopharyngeal cavity via buccal pumping of the pharyngeal muscles. Unlike amphibians, amniotes are aspiration breathers, they draw air in by expanding the thorax via body wall muscles, which releases the skull from the vital air acquisition to other behaviors such as vigilance and defense. In mammals, a unique inspiratory muscular septum named diaphragm has developed. This muscle acts like a pump moving up and down to change the volume of thoracic cavity, which is directly responsible for the lung inflation (inspiration) while in basal condition deflation of the lung (expiration) is due to passive recoiling of the rib cage. The body wall muscles such as intercostal and abdominal muscles become accessory pump muscles, which help to stiffen the rib cage and thus increase the efficiency of diaphragm contraction. The upper airway muscles such as striated muscles of the nose, tongue, and throat, which open and close the upper airways, become valve muscles that regulate the rate at which the air flows in and out of the lungs (**Figure 1**). During exercise, expiration becomes active (active expiration) and requires the contraction of expiratory abdominal and internal intercostal muscles. From an evolutionary point of view, this breathing strategy helps mammals to reduce the conflicts between breathing and other behaviors such as locomotion, thus the mammals are able to breathe with high efficiency to meet high metabolic demands.

We breathe continuously in an effortless and often unconscious manner, whatever the arousal state, owing to the existence of a dedicated neuronal circuit that can generate a rhythmic activity, integrate sensory informations and pattern the coordinate contractions of multiple respiratory muscles to produce a reliable and adapted motor behavior. The central respiratory control network is comprised of three main levels. First, a central pattern generator

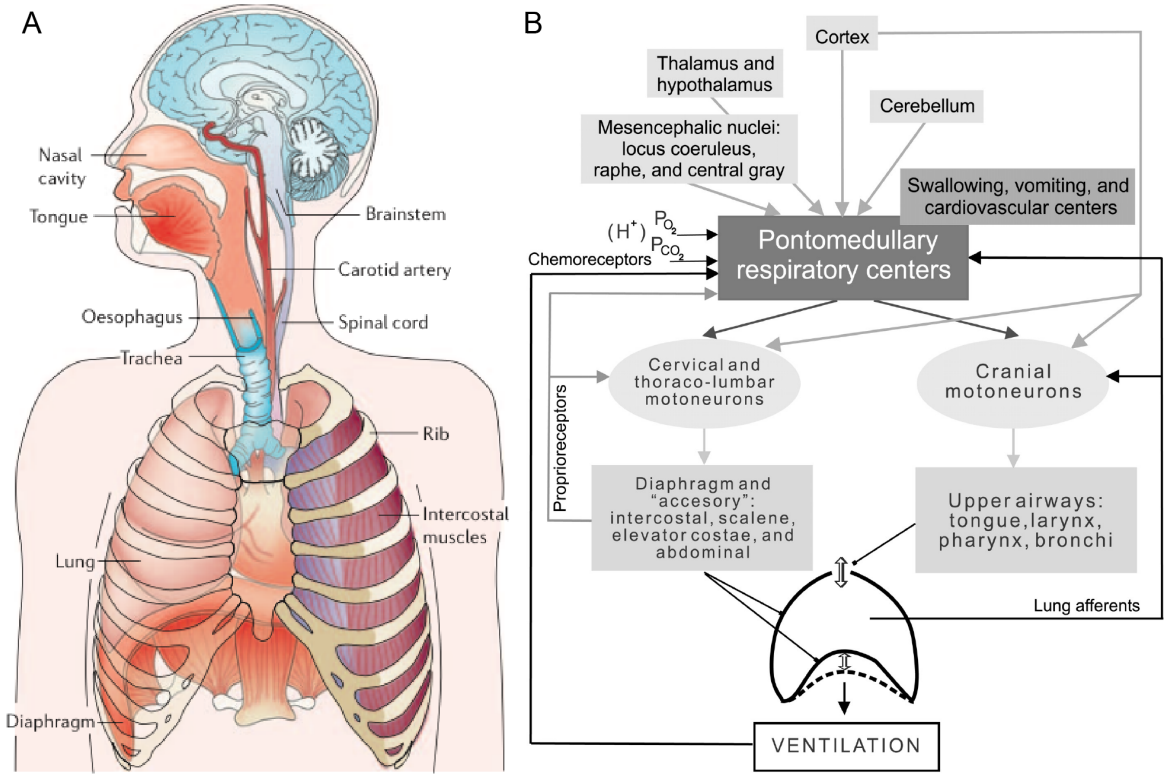

Figure 1. Respiratory system in human. (A) Anatomy of respiratory system. (B) Neuronal control of respiration. During inspiration, gas exchange in the lungs results from contraction of the pump muscles-diaphragm and external intercostal muscles, and the valve muscles, such as the striated muscles of tongue and nose, help to change the airflow rate. Expiration is often passive, especially at rest, as the inspiratory muscles relax. The respiratory neurons that control and regulate the respiratory rhythm are located in the brainstem and spinal cord. The pontomedullary respiratory network produces the central respiratory command for breathing that controls cranial, cervical, and thoracolumbar respiratory motoneurons commanding the upper airways, the diaphragm, and the "accessory" rib cage respiratory muscles, respectively. During breathing, respiratory centers receive sensory information from the chemosensors in the carotid bodies and brainstem that monitor the blood O_2, CO_2 and pH levels to adapt the respiration to the metabolic states. In addition, under physiological condition, the activity of respiratory centers is also modulated from nonrespiratory centers (e.g. swallowing, vomiting centers) and upper structures such as cortical structures to coordinate with other behaviors such as walking, vocalizing and swallowing under different emotional and arousal states. Adapted from Feldman and Del Negro, 2006 and Hilaire and Pasaro, 2003.

(CPG) in the brainstem is the core rhythmogenic system. Second, premotor neurons (pMNs) relaying the CPG command to motoneurons. Third, respiratory motoneurons (MNs) that innervate and directly control the contraction of respiratory muscles. The latter include the pump motoneurons innervating effector muscles through spinal nerves and the upper airway patency controlling motoneurons projecting through cranial nerves. Breathing centers receive sensory information reporting O_2, CO_2 and pH levels from chemosensors in the carotid bodies and brainstem to adapt the respiration to the metabolic states (**Figure 1**A). Under physiological condition, breathing must be combined to multiple non-respiratory activities some of which may involve common muscular effectors such as walking/postural control, vocalizing and swallowing under different emotional and arousal states (**Figure 1**B). Finally, breathing needs to operate at birth and thus is a model system to link neural tube development with neural network assembly and function.

The current knowledge about the circuits underlying respiratory control of their anatomy and physiology is still rudimentary, significantly lagging behind that of the spinal cord, cerebellum or cortex. The reason for this is twofold. First, the hindbrain, due to its size and position, is not easily amenable to functional exploration. Second, most of the literature deals with ill-defined “regions”, “centers” and “complexes” in the apparently amorphous anatomy of the hindbrain, subsumed under the vague term “reticular formation”. Even extensively studied respiratory neuronal groups in the pons and medulla still await a cell-level definition. This situation is poised to change thanks to the advent of new genetic technologies in mice that allow the visualization, the activity recording, the killing, the silencing or activation of specific respiratory neuronal groups, identified by their molecular make-up or developmental origin. *Furthermore, as this PhD will illustrate, the generally missing dimension in the description of neural networks--the connectivity of neural elements-- can now be considered with novel tracing tools that should rapidly and firmly establish the links between the nodes in respiratory neural circuits.*

In the past decades, with the development of electrophysiology, neuronal tracers and genetic tools, the connectivity of the respiratory neurons and their genetic recruitment have been extensively studied, especially the respiratory motoneurons and the CPG, but little is known about the premotor neurons that convey the rhythm to motoneurons. The premotor neurons, which are the interneurons that directly project to the motoneurons, are the last station receiving a variety of inputs from the brain and sensory afferents to process and shape

the activity of motoneurons. In this thesis, I study the premotor neurons projecting onto phrenic motor neurons controlling the diaphragm. Their genetic identity from development and their role in the maintenance of bilateral synchronized inspiration are carefully investigated.

In the following sections, backgrounds elements are provided on the central control of breathing, with emphasis on the respiratory CPG and its motor output, the upstream and downstream partners of premotor neurons. I also describe fetal breathing to insist on the developmental regulatory mechanisms that enable robust breathing at birth and that incidentally, provide molecular correlates that can be used to gain genetic access to specific neuronal populations.

II. Neuronal control of breathing

II.1. The respiratory central pattern generator

Breathing in mammals relies on a neuronal network located in the brainstem (**Von Euler, 1983**; **Feldman and Del Negro, 2006**). Central control implies that the central nervous system is intrinsically capable of providing the proper timing of muscle activation, although sensory inputs can modulate respiratory rhythm and pattern and adapt breathing to changes in state. If the basic elements making up this network are located in the brainstem, structures outside the brainstem can and do affect respiration. However, these distant components are not essential to the network because their elimination does not impair rhythmogenesis. Therefore the neurons with obligatory role for respiratory rhythm generation form the central pattern generators (CPGs)(**Delcomyn, 1980**). This respiratory CPG develops a rhythm essentially based on three phases: 1) inspiration (I) in which inspiratory muscles contract; 2) post-inspiration (post-I) or passive expiration (stage 1 expiration, E1) in which inspiratory muscles cease progressively to contract while activity of the adductor muscles of the upper airway reduces exhalation; and 3) active expiration (stage 2 expiration, E2) in which internal intercostal and abdominal muscles contract (**Figure 2**)(**Richter, 1982**; **Richter et al., 1986**).

These distinct phases clearly indicate that the rhythmic respiratory motor command is not a simple oscillation but rather a neuronal sequence organizing temporally the coordination of activities destined to the maintenance in distinct activation states of multiple neuronal populations to (i) condition maintenance of the rhythm and (ii) dispatch harmoniously activities to diverse synergistic and antagonistic motor neuronal pools controlling respiratory effector muscles. Even the phrenic nerve that controls contraction of the diaphragm does not present with an inspiratory activity that can be considered plain. It starts with a synchronized onset burst of activity preceding a steadily increasing activity (inspiratory ramp) reaching a maximum when it abruptly ends with a complete breakdown of activity. This is followed by a post-inspiratory phase (Post-I) where the phrenic nerve activity that has partially recovered with a much weaker amplitude progressively declines. The post-I phase represents the part of "passive" (not engaging expiratory muscles, stage 1 expiration) exhalation during which upper airway adductor muscles act to narrow the airway to provide a mechanical brake of expiratory airflow to allow continued gas exchange in the lung. Then comes the phase of

active expiration (stage 2 expiration) during which expiratory muscles contract to cause lung deflation (**Figure 2**).

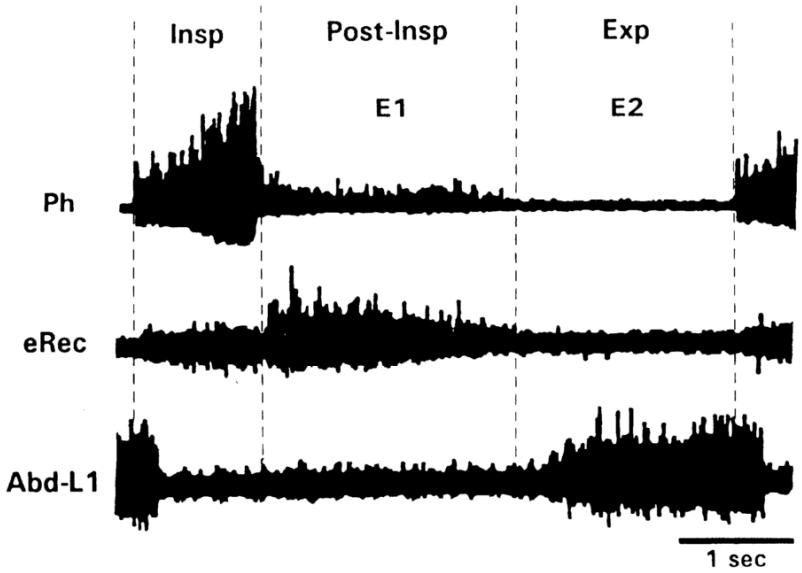

Figure 2. Three phases of a typical respiratory cycle and corresponding efferent discharge activities recorded in phrenic nerve (Ph) innervating diaphragm, expiratory branch of recurrent laryngeal nerve (eRec) innervating laryngeal adductor muscles, and lumbar nerve (Abd-L1) innervating abdominal muscles in anesthetized cat and rat. Inspiratory phase (Insp) is characterized by linear augmenting activity in inspiratory nerves and muscles, which ends with a sudden complete breakdown of activity. This is followed by declining bursting activity during post-inspiration (Post-Insp) or passive expiration (El), controlled by the activation of adductor muscles of larynx (thyroarythenoid), which narrow the airway to reduce the expiratory airflow allowing continued gas exchange in the lungs. These two phases are usually supplemented by a third activity during active expiration, named stage 2 expiration (E2), in which expiratory nerves and muscles exhibit ramp discharge patterns which end abruptly at inspiratory onset, but this phase is either weak or absent during quiet breathing. Reproduced from Bianchi et al., 1995.

The respiratory neurons are classified based on their preferential firing during these phases and according to their firing patterns (e.g. decrementing and augmenting) (**Bianchi et al., 1995**; **Richter, 1996**). Recording of the membrane potential trajectories of respiratory neurons in vivo gave access to some robust interaction in between functional types of respiratory neurons mostly based on reciprocal inhibitions e.g. I-augmenting neurons probably inhibit I-decrementing neurons and vice versa. A synthetic summary of the ideas about respiratory rhythm generation inferred from in vivo electrophysiological investigations

performed up to 1990's was that the rhythm resulted from the sequential activation of at least six neuronal population (pre-I > early-I <> I-Aug > late-I > post-I > E-Aug > pre-I….) leading to two fast phase-switching transitions (inspiratory-offswitch and expiratory-offswitch) and three relatively long respiratory phases (inspiration, post-inspiration and expiration). Each process is conditioned by the previous one and initiates the next (**Bianchi et al., 1995**). I will skip here detailed description of the attempts made to correlate this functional description to the anatomical location of principal respiratory areas because the literature is difficult to synthetize as it is replete with interspecific differences and a diversity of defining criteria for activities. A succinct anatomical description of respiratory compartments with a consensual assignment of the included respiratory types is proposed on **Figure 3**. In any case, the sole knowledge of the type of discharge of a neuron if enabling to rule its inspiratory or expiratory nature is far from being predictive of its role in the network that will depend on its excitatory or inhibitory nature and knowledge about its synaptic targets. *Absent knowledge about connectivity still constitutes the main limitation to the understanding of the neuronal bases supporting neuronal sequences of activity in the CNS. This of course applies to the respiratory network and my PhD work modestly begins to fill up this gap.*

A major breakthrough regarding respiratory rhythm generation probably inspired from studies of invertebrate system was the introduction in the debate of putative "pacemaker neurons" (**Del Negro et al., 2005**; **Pena et al., 2004**). Before this, as described above, the rhythm was not envisioned to rely on a single class of neurons but rather emerged from the synaptic interaction among many types of neurons possibly in distant structures acting mostly through reciprocal inhibitory influences (admitted assumption of a tonic excitatory drive without which inhibitions would lack effect). The respiratory CPG then began to evolve into a respiratory rhythm generator (RRG) following spectacular results obtained on reduced in vitro slice preparations that retained a respiratory-like rhythm (**Smith et al., 1991**). Therefore, the respiratory CPG can be defined as including a rhythmogenic module the RRG (see detailed presentation below) and all the neurons that contribute to the patterning of the primary clock activity, those that convey the patterned command to motor neurons that translate it into contraction of respiratory muscles.

The respiratory neurons are concentrated in three main areas in the brainstem: the pontine respiratory group (PRG) within the dorsolateral pons, the dorsal respiratory group (DRG)

within the nucleus of the solitary tract (NTS), and the ventral respiratory column (VRC) that occupies the ventrolateral medulla (**Figure 3**). The VRC hosts crucial respiratory areas including the RRG itself and as we will see in the present work a main inspiratory premotor areas.

In the following section, the function and connectivity of these spatially arranged respiratory compartments are introduced.

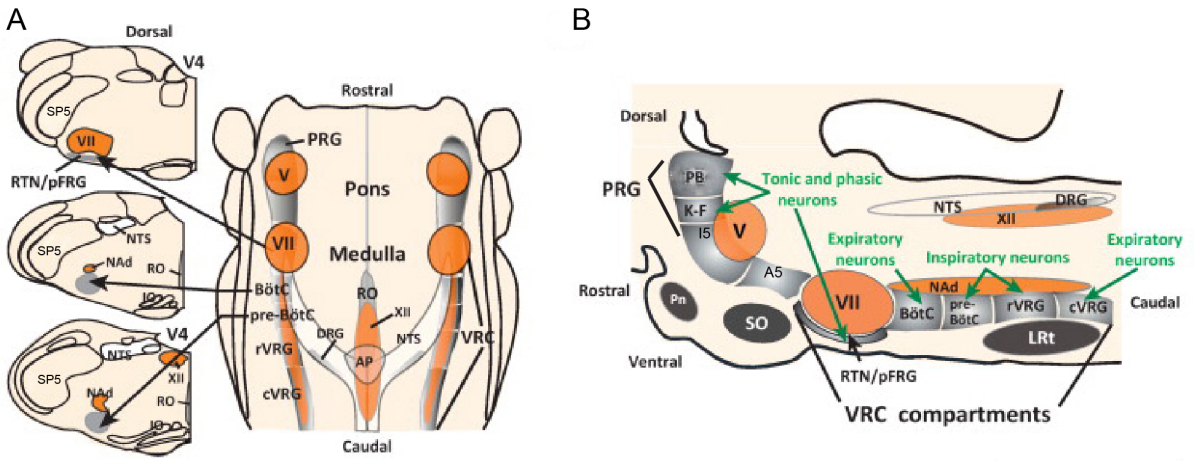

Figure 3. Brainstem respiratory compartments bilaterally arranged from the rostral pons to caudal medulla shown in (A) horizontal (right) and transverse (left) and (B) parasagittal view. Respiratory compartments are indicated in grey and their main functions are written in green. Different motor nucleus is shown in orange. Abbreviations: A5, A5 noradrenergic neuronal group; AP, area postrema; BötC, Bötzinger complex; cVRG, caudal division of ventral respiratory group; DRG, dorsal respiratory group; I5, intertrigeminal area; IO, inferior olive; KF, Kölliker-Fuse nucleus; PB, parabrachial complex; LRt, lateral reticular nucleus; NAd, nucleus ambiguus, dorsal division; NTS, nucleus of the solitary tract; pFRG, parafacial respiratory group; Pn, ventral pontine nucleus; preBötC, preBötzinger complex; PRG, pontine respiratory group; RO, raphe obscurus; RTN, retrotrapezoid nucleus; rVRG, rostral division of ventral respiratory group; SO, superior olive; SP5, spinal trigeminal nucleus; V, trigeminal motor nucleus; V4, fourth ventricle; VII, facial nucleus; VRC, ventral respiratory column; XII, hypoglossal motor nucleus. Adapted from Smith et al., 2013.

II.2. Brainstem respiratory centers

II.2.1 The ventral respiratory column

The core respiratory circuits that generate respiratory rhythm and shape the inspiratory and expiratory activity are located in the ventrolateral medulla along its entire length, which form the ventral respiratory column (VRC). The respiratory rhythm emerges mainly in the rostral half of the VRC including the retrotrapezoid nucleus (RTN), the Bötzinger complex (BötC)

and the preBötzinger complex (preBötC), while the caudal half of the VRC, named the ventral respiratory group (VRG) includes rostral (rVRG) and caudal (cVRG) subdivisions, that contains premotor neurons that convey the rhythmic command to the spinal respiratory motoneurons (**Figure 3**).

The **RTN**, which was first identified in the adult cats (**Smith et al., 1989**), is located below and extend through the rostrocaudal levels of the facial nucleus (VII). The RTN, in adult rodents, contains tonically discharging neurons whose activity is regulated by the blood and tissue CO_2 level or pH and the inputs from peripheral chemoreceptors, therefore RTN is a central chemosensory region (**Guyenet et al., 2005**; **Mulkey et al., 2004**). It has been shown that RTN neurons provide extensive excitatory (glutamatergic) drives to the neurons in VRC (**Mulkey et al., 2004**; **Rosin et al., 2006**), which modulates the respiratory activity to meet the homeostatic needs. In the study of the in vitro brainstem preparation from neonatal rats, Onimaru and Homma (**Onimaru and Homma, 2003**; **Onimaru et al., 2006**) identified a group of pre-inspiratory (pre-I) discharging neurons which is spatially overlapping with the RTN, named **pFRG**, and they have proposed that the pFRG interact with the preBötC neurons as a coupled oscillator for respiratory generation (see Introduction II.3). During active expiration, the RTN/pFRG acts as an expiratory oscillator to coordinate the inspiratory and expiratory activity (**Feldman and Del Negro, 2006**; **Janczewski and Feldman, 2006**).

The **BötC,** which is located immediately caudal to the VII, contains predominately expiratory (post-I, E-Aug, E-Dec) neurons. This region is thought to be a major source of expiratory activity during normal breathing. The BötC neurons make widely interaction with other VRC compartments as well as the phrenic motoneurons (**Jiang and Lipski, 1990**; **Tian et al., 1998**, **1999**), and the BötC contains mainly inhibitory glycinergic neurons (**Ezure et al., 2003a**; **Schreihofer et al., 1999**) that project on inspiratory neurons and contributes to their inhibition during expiration.

The **preBötC**, just caudal to the BötC, is the core rhythmogenic neuronal module. Because of its essential role for inspiratory rhythm generation, this structure will be detailed in a separate section (see Introduction II.3.1).

The **rVRG**, directly adjacent and caudal to the preBötC, contains mainly excitatory (glutamatergic) bulbospinal inspiratory neurons that project to phrenic and inspiratory external intercostal motoneurons (**Dobbins and Feldman, 1994**; **Stornetta et al., 2003a**).

The rVRG receive excitatory inputs from the preBötC and inhibitory inputs (during expiration) from BötC as well as other modulatory drives such as that from the Kölliker-Fuse (**Ezure et al., 2003b**; **Tan et al., 2010**; **Yokota et al., 2007**), therefore the rVRG is a convergent site of multiple inputs to transmit the inspiratory rhythm to the inspiratory motoneurons and shape their output pattern. It should be noted that there is no clear boundary between the end of preBötC and the beginning of rVRG, but the rVRG neurons can be discriminated functionally from the preBötC, they do not have intrinsic rhythmogenic capability and have in vivo an I-augmenting discharge pattern (**Smith et al., 2007**).

The caudal part of the VRG **(cVRG)**, mainly contains excitatory bulbospinal expiratory neurons (E-Aug) that innervate the abdominal and internal intercostal motoneurons controlling the expiratory muscles. The cVRG is thought to be a convergent site that receive multiple inputs such as the ones from the RTN, BötC and NTS, and thus shape the activity of expiratory motoneurons (**Ezure et al., 2003b**; **Iscoe, 1998**).

II.2.2 The dorsal respiratory group

The dorsal respiratory group (DRG) in the dorsomedial medulla contains mainly inspiratory neurons of the nucleus of the solitary tract (NTS) (**Castro et al., 1994**; **Ezure et al., 1988**). The NTS is the entry point of sensory afferent inputs conveying respiratory-related information from the lungs and airways (**Kalia et al., 1980**; **Kubin et al., 2006**), in which lung inflation terminates an ongoing inspiration or prolongs an ongoing expiration. Also, the NTS is the principal target of afferents from peripheral chemoreceptors in the carotid body detecting arterial pO2 and in a much more limited manner pCO2 (regarding breathing, CO_2 chemosensitivity relies only for about 25% on peripheral sensors, most of this sensory modality falls on central chemosensors among which those in the RTN) to maintain homeostasis (**Vardhan et al., 1993**). It has been shown that the caudal third of NTS regions (cNTS) mediate the afferent control of respiration via inhibitory projections to pontine and VRC compartments including the RTN (**Alheid et al., 2011**) as well as a small fraction of excitatory neurons projecting to the phrenic nucleus in adult rats (**Castro et al., 1994**; **Dobbins and Feldman, 1994**).

II.2.3 Pontine respiratory group

Electrical and chemical stimulations or inhibitions have revealed that the pontine respiratory

group (PRG), is composed of four or more distinct but contiguous pontine regions have been identified with different respiratory facilitation or inhibition abilities (**Figure 3**). The **parabrachial complex (PB)** and **Kölliker-Fuse nucleus (KF)** in the dorsolateral pons, as well as **intertrigeminal area (I5)** that is sandwiched between the motor and the sensory trigeminal nucleus and dorsally merges with the KF and PB, are the main components of the PRG. This region includes, in adult rats, various respiratory-related neurons, phasic inspiratory (I, EI, IE) and expiratory (E-Dec, E-Aug, E-whole) neurons (**Ezure and Tanaka, 2006**). Although in this region, heterogeneous groups of neurons are found both physiologically and neurochemically, it has been shown to interact with multiple medullary regions to regulate respiratory activity and the inspiratory-expiratory phase transition (**Alheid et al., 2004**; **Ezure and Tanaka, 2006**; **Mörschel and Dutschmann, 2009**). The KF provides the densest projections to the VRC, and additional projections to ventrolateral NTS, as well as to the phrenic motoneurons (**Ezure and Tanaka, 2006**; **Yokota et al., 2007**). With the retrograde tracing and in situ hybridization study, most of the bulbospinal and phrenic projecting neurons in the KF are glutamatergic (**Yokota et al., 2004**, **2007**). It also appears that individual KF neurons innervate both the rVRG region and phrenic motoneurons by axon collaterals (**Yokota et al., 2004**). The KF also contains laryngeal and hypoglossal premotor neurons controlling upper airway resistance, and thus it is thought to be critical for the coordination of the activity of expiratory and upper airway muscles during expiration and post-I activity (**Dobbins and Feldman, 1995**; **Dutschmann and Herbert, 2006**; **Kuna and Remmers, 1999**).

A5 group is a small group of noradrenergic neurons located ventral to the KF and I5 in the ventrolateral pons. Electrolytic lesion and local application of noradrenergic agonists in the A5 area, which destruct or inhibit the A5 neurons, increase the phrenic burst frequency, revealing that the A5 neurons are responsible for the inhibition of respiratory CPG both in neonatal rats and mice (**Hilaire et al., 1989**, **2004**; **Viemari et al., 2004**), and this inhibition persists in adult (**Dawid-Milner et al., 2001**; **Jodkowski et al., 1997**). In vitro the stimulation of nasal trigeminal inputs is able to relieve the A5 inhibition of respiratory-like activities (**Viemari et al., 2004**).

II.3. Respiratory rhythm generator

II.3.1 The preBötC: the core circuit for inspiratory rhythm generation

As early as the 19th century, the physiologists have localized the respiratory centers within the medulla, and a long lasting debate about the existence of a "*vital node"* (**Flourens, 1851**) i.e. a most spatially restricted area of the brainstem that would suffice to ensure breathing, seems to have found incarnation with the discovery of the preBötzinger complex. This owes to the establishment of in vitro brainstem-spinal cord preparation that were shown to maintain a respiratory-like rhythm (**Suzue, 1984**). In 1991, Jeffrey Smith along with German colleagues (**Smith et al., 1991**) found that after serial transverse sections of in vitro isolated brainstem preparation the respiratory rhythm recorded from the XII nerve persisted in a 450 micrometer thick transverse medulla slice retained a small ventrolateral region just caudal to the BötC (**Figure 4**). Injection of CNQX, an AMPA/kainate glutamate receptor antagonist, into this region of the slice completely abolished the rhythm. This region was named the preBötzinger complex (preBötC) and suggested to be the kernel of respiratory rhythm generation. Because this rhythm could be recorded from hypoglossal and phrenic cervical motor roots the paced rhythm is an inspiratory rhythm. This is in keeping with basal breathing that includes only one active rhythmic phase, inspiration while expiration results from the passive recoiling of the lung. Many confirmatory experiments have been produced. For example, in situ working heart-brainstem preparations with brainstem transection at the rostral border of the preBötC are still able to generate the respiratory rhythm spontaneously (**Smith et al., 2007**). Neurotoxic lesion or transient suppression of defined subsets of preBötC in adult rats in vivo induce ataxic breathing during wakefulness and apneas during sleep (**Gray and Janczewski, 2001**; **Tan et al., 2008**). Optogenetic excitation of the preBötC can effectively drive the inspiratory activity in vivo (**Alsahafi et al., 2015**). Also, the neuroanatomical location of the human preBötC has been studied and described (**Schwarzacher et al., 2011**). Nowadays there is a broad consensus that the preBötC is the core site for inspiratory rhythm generation.

The preBötC, as described above, is located caudal to the BötC and ventral to the semi-compact region of nucleus ambiguus (**Figure 3**). The preBötC mainly contains excitatory neurons that express the neurokinin-1 receptor (NK1R) that can be used as a marker to distinguish preBötC from adjacent VRC regions such as BötC and rVRG (**Figure 5**) (**Gray and Janczewski, 2001**; **Gray et al., 1999**; **Wang et al., 2001**). The application of substance P (SubP), the endogenous agonist for NK1R, into the preBötC in vitro increases the

frequency of endogenous respiratory rhythm (**Gray et al., 1999**), and selective destruction of the NK1R neurons in the preBötC in vivo induces ataxic breathing (**Gray and Janczewski, 2001**). Many of the NK1R preBötC neurons are characterized as pre-inspiratory/inspiratory (pre-I/I) and early-inspiratory (early-I) neurons that are thought to be critical for initiation of inspiration and rhythm generation (**Guyenet and Wang, 2001**; **Sun et al., 1998**). It has been shown that glutamatergic phenotype such as expression of the vesicular glutamate transporter 2 (vGlut2) of the NK1R preBötC neurons is the essential excitatory component for the preBötC rhythmogenesis (**Guyenet et al., 2002**). Genetic deletion of the vGlut2 completely eliminates respiratory motor activity and the mouse mutants die immediately after birth (**Wallén-Mackenzie et al., 2006**). And the injection of a non-NMDA receptor antagonist, CNQX, into the preBötC region completely abolished the respiratory rhythm in the slice, indicating that respiratory rhythmogenesis depends on the activation of non-NMDA glutamatergic receptors (**Smith et al., 1991**). A subpopulation of glutamatergic NK1R neurons in preBötC has been found to co-express somatostatin (Sst) and these neurons perform propriobulbar projections (**Stornetta et al., 2003b**) , and thus Sst is another marker for the preBötC neurons. Some NK1R neurons in the preBötC also express μ-opiate and $GABA_B$ receptors, whose agonists decrease respiratory frequency (**Gray et al., 1999**). Besides the majority of glutamatergic populations, small subpopulations of inspiratory glycinergic (**Morgado-Valle et al., 2010**) and GABAnergic (**Kuwana et al., 2006**) neurons are also found in the preBötC and they are thought to inhibit expiratory neurons during inspiration.

There is now little doubt that the preBötC is the prime site pacing the inspiratory rhythm and debates are open as to the rhythmogenic mechanisms. The rhythm is now perceived to not be caused by true pacemaker neurons whose activities would rely purely on intrinsic membrane properties. Rather, the current hypothesis, the "group pacemaker" rhythm generation is one where redundant synaptic connectivity among glutamatergic neurons through activating intrinsic sodium and calcium ionic conductances lead to cellular recruitment and ultimately to collective firing of preBötC neurons thus generating a burst of inspiratory activity. This burst is terminated by powerful potassium conductances that lead to depressed excitability of preBötC neurons. As preBötC neurons regain progressively excitability, the synaptic dialogue with other preBötC neurons is re-initiated and the process repeats itself so that permanent generation of rhythmic burst of activity is maintained to pace the inspiratory rhythm (**Feldman and Del Negro, 2006**; **Del Negro and Hayes, 2008**; **Del**

Negro et al., 2010).

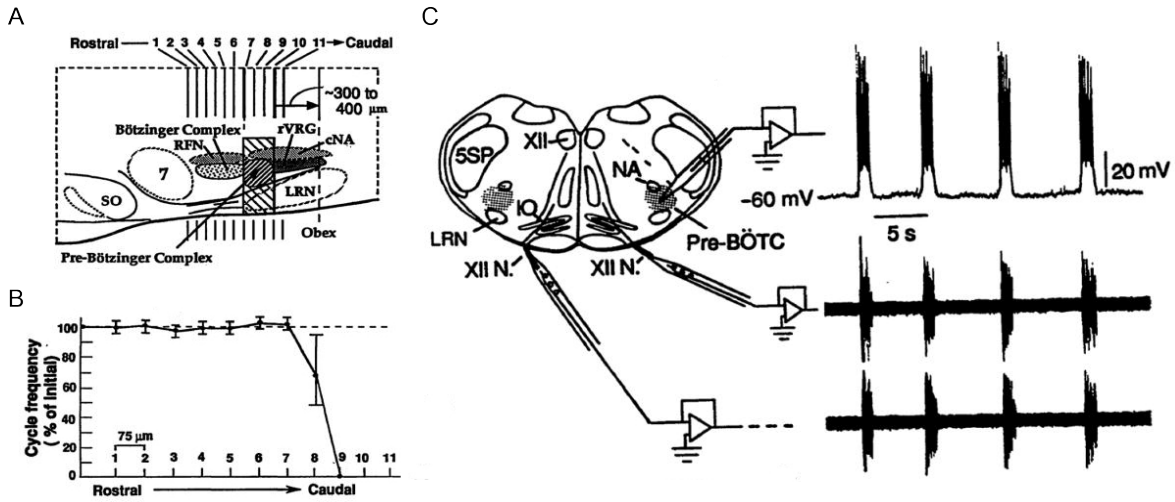

Figure 4. In vitro preparations from neonatal rats illustrate that the preBötC is the kernel for respiratory rhythm generation. (A) Sagittal view of medulla illustrates the position of preBötC and neighboring regions. The numbers 1-11 indicate the axial level where sections were made. (B) Serial transverse microsections were made from rostral to caudal medulla and a single 75µm section through the boundary of preBötC resulted in a decrease of cycle frequency of the phrenic motor outputs and instable respiratory rhythm. The numbers 1-11 correspond to the ones in A. (C) The medullary slice enclosing the preBötC is able to generate the respiratory motor output. Traces at right show whole cell recording from a rhythmically active neuron in the preBötC (upper trace) and the bilateral respiratory motor discharge of XII nerve roots (middle and lower traces). Abbreviations: SO, superior olive; 7, facial nucleus; LRN, lateral reticular nucleus; RFN, retrofacial nucleus; rVRG, rostral ventral respiratory group; NA, nucleus ambiguous; 5SP, spinal trigeminal nucleus; XII N, hypoglossal nerve; IO, inferior olive. Adapted from Smith et al, 1991.

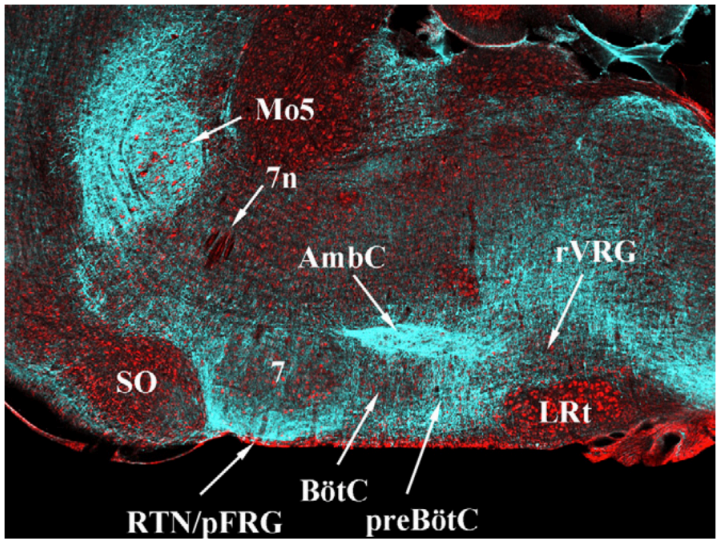

Figure 5. NK1R in the VRC. Pseudocolored sagittal view of the brainstem of the mouse with immunolabeled NK1R (Cyan) and Nissl (red). The preBötC and RTN/pFRG are densely labeled by the NK1R, whereas the adjacent BötC and rVRG region are devoid of the NK1R. Note that the trigeminal motor nucleus (Mo5) and nucleus ambiguus (AmbC) are also densely labeled. SO, superior olive; LRt, lateral reticular nucleus; 7, facial nucleus; 7n, facial nerve. Reproduced from Alheid et McCrimmon, 2008.

II.3.2 A second oscillator: the parafacial respiratory group

If the preBötC can explain generation of the inspiratory rhythm, a later finding in 2003 questioned its prominent role. A Japanese group then reported the existence of a second oscillator (**Onimaru and Homma, 2003**) found in en bloc preparations from neonatal rats to contain pre-inspiratory (pre-I) neurons. If a rhythmic group of neuron exist with pre-I activity they should be prime candidates for the generation of the inspiratory rhythm. These neurons were located in the so called parafacial respiratory group (pFRG), in perfect anatomical overlap with the retrotrapezoid nucleus (RTN) in adult cats and rats. These pre-I neurons have intrinsic burst generating properties and they fire before and after but are inhibited during inspiratory activity. This was taken to indicate that these neurons instead of being considered pre-I neurons should better be considered expiratory like neurons (inhibited during inspiration) and that the most should be made to the contrary of their post-I activity. Indeed, separate manipulation of preBötC and RTN/pFRG by pharmacological methods provides evidences that there is an independent oscillator located in the RTN/pFRG responsible for the generation of active expiration. For example, in anaesthetized and vagotomized juvenile rats in vivo, brainstem transections that remove the RTN/pFRG from the medulla but leave the preBötC intact abolish active expiratory bursts without affecting inspiratory rhythm (**Janczewski and Feldman, 2006**). The μ-opiate agonist such as DAMGO and fentanyl induces quantal slowing (skipped inspiratory bursts) due to the hyperpolarization of a subset of preBötC inspiratory neurons, but the firing ability of pre-I neurons are not affected because of their opiate non-sensitive nature, and expiratory outputs persist both in vivo and in vitro preparations (**Janczewski and Feldman, 2006**; **Mellen et al., 2003**; **Onimaru et al., 2006**). Moreover, in adult anesthetized rats, activation of RTN/pFRG neurons by photostimulation or by suppression of synaptic inhibition can induce active expiration (**Pagliardini et al., 2011**). Collectively, there is increasing consensus that, in addition to its major role in central chemoception, the RTN/pFRG contributes as a second oscillator for the generation of active expiration, which coupled with preBötC so that respiratory rhythm generation may have a dual organization.

It has been proposed that, in quiet breathing when mammals breathe with active inspiration and passive expiration, the preBötC is dominant for respiratory generation, whereas the RTN/pFRG mainly acts as a central chemosensory region. Under special conditions such as hypercapnia, hypoxia and exercise, the RTN/pFRG can generate active

expiration to promote ventilation (**Feldman and Del Negro, 2006**; **Janczewski and Feldman, 2006**). In perinatal stage, the existence of two oscillators may play a special role. It has been proposed that at this stage, RTN/pFRG provides excitatory drive to entrain preBötC in order to prevent the depression of the preBötC in response to an existing opiate surge accompanying birth (**Feldman and Del Negro, 2006**).

II.4. Inspiratory motoneurons

Motoneurons (MNs) are the only source of neurons that directly innervate and control the contraction of muscles. As early as the 2nd century A.D., Galen observed the close relation between spinal cord and the contraction of respiratory muscles by a series of spinal cord sections and muscle denervations and thus described *"the nerves that transmit the power of the mind from the brain to muscles"* (**Derenne et al., 1995**; **Furley and Wilkie, 1984**). With the development of electrophysiological and anatomical investigations using various neuronal tracer molecules (see Introduction V.1 for tracing principles), a comprehensive knowledge about the innervation of respiratory muscles including the location of motoneuronal pools has been obtained. In this section, the anatomy and function of the MNs primarily controlling inspiration and upper airway patency are introduced. The muscles powering inspiratory efforts are skeletal muscles and include the diaphragm, external intercostals, parasternal, sternomastoid and scalene muscles.

II.4.1 Phrenic motoneurons (Phr-MNs)

The diaphragm, the principal inspiratory muscle, is a dome-shaped structure that separates the thoracic and abdominal cavities, consisting of a central tendon surrounded by a ring of predominantly radially oriented striated muscle divided into crural and costal parts (**Figure 6**). The left and right phrenic nerves comprise the axons of phrenic motoneurons (Phr-MNs) and exit from the spinal cord at cervical (C) C3-C6 segments on the left and the right side and then project ipsilaterally and caudally through the thoracic cavity to each innervate a hemi-diaphragm. Three main branches are formed after making contact with the diaphragm, one branch projects ventrally and one dorsally to innervate the costal diaphragm, and another branch projects dorsomedially to innervate the crural diaphragm (**Figure 6**).

The anatomical location of Phr-MNs is conserved across mammalian species (**Goshgarian and Rafols, 1981**; **Hollinshead and Keswani, 1956**; **Mantilla et al., 2009**; **Qiu**

et al., 2010; **Takahashi et al., 1980**). Phr-MNs occupy the ventral horn of the spinal cord from the third to the sixth cervical (C) segments (C3-C6, **Figure 7**B) (**review in Lane, 2011)**. Phr-MNs somata are pyramidal or fusiform in shape with large diameter and they are tightly packed at the lamina IX of spinal cord to form the phrenic motor column (PMC) (**Figure 7**C,D). In the horizontal plane, the motoneurons in the column are seen in discrete clusters with their dendrites organized with a major rostrocaudal orientation (**Figure 7**A). Although in neonatal rats some dendrites occasionally cross the midline, none of these dendrites extend to the somata of the contralateral Phr-MNs (**Lindsay et al., 1991**; **Prakash et al., 2000**), and in adult animals crossed Phr-MN dendrites are extremely rare (**Prakash et al., 2000**; **Qiu et al., 2010**). It has been suggested that the dendro-dendritic interactions may exist and contribute to synchrony of Phr-MNs because of the proximities of Phr-MN dendrites. However, the electronic coupling between neonatal Phr-MNs seems to be low (26%) in comparison with that of lumbar MNs (77%) (**Martin-Caraballo and Greer, 1999**; **Walton and Navarrete, 1991**), and no gap junctions and electrical interaction are detected between apposing adult Phr-MNs (**Lipski, 1984**) and their primary dendrites appear to be separated by astrocytes (**Goshgarian and Rafols, 1984**).

II.4.2 Upper airway motoneurons

The nose, the pharynx, the larynx, and the extra-thoracic portions of the trachea constitute the upper airway, a vital part of the respiratory tract. Dynamic changes in the upper airway size and resistance occur throughout the respiratory cycle. Over twenty pairs of muscles located around the upper airway can potentially influence its size, shape and function. Some are active during eupnea; others are recruited when respiratory drive increases. In addition to their respiratory role, most upper airway muscles participate in non-respiratory tasks such as mastication, deglutition, vocalization, olfaction, and upper airway protection. Based on their location, upper airway muscles can be divided into nasal, palatal, pharyngeal, laryngeal, and cervical. Most of these muscle groups can modify air flow resistance through valve-like mechanisms. The pharyngeal dilators are located on the lateral and ventral aspects of the pharynx. The genioglossus, an extrinsic muscle of the tongue, is the most extensively studied pharyngeal dilator and is innervated by the hypoglossal nerve.

During inspiration, the genioglossus muscle is activated just prior to the diaphragm to maintain open the upper airway for effective breathing. Reduction of the genioglossus tone

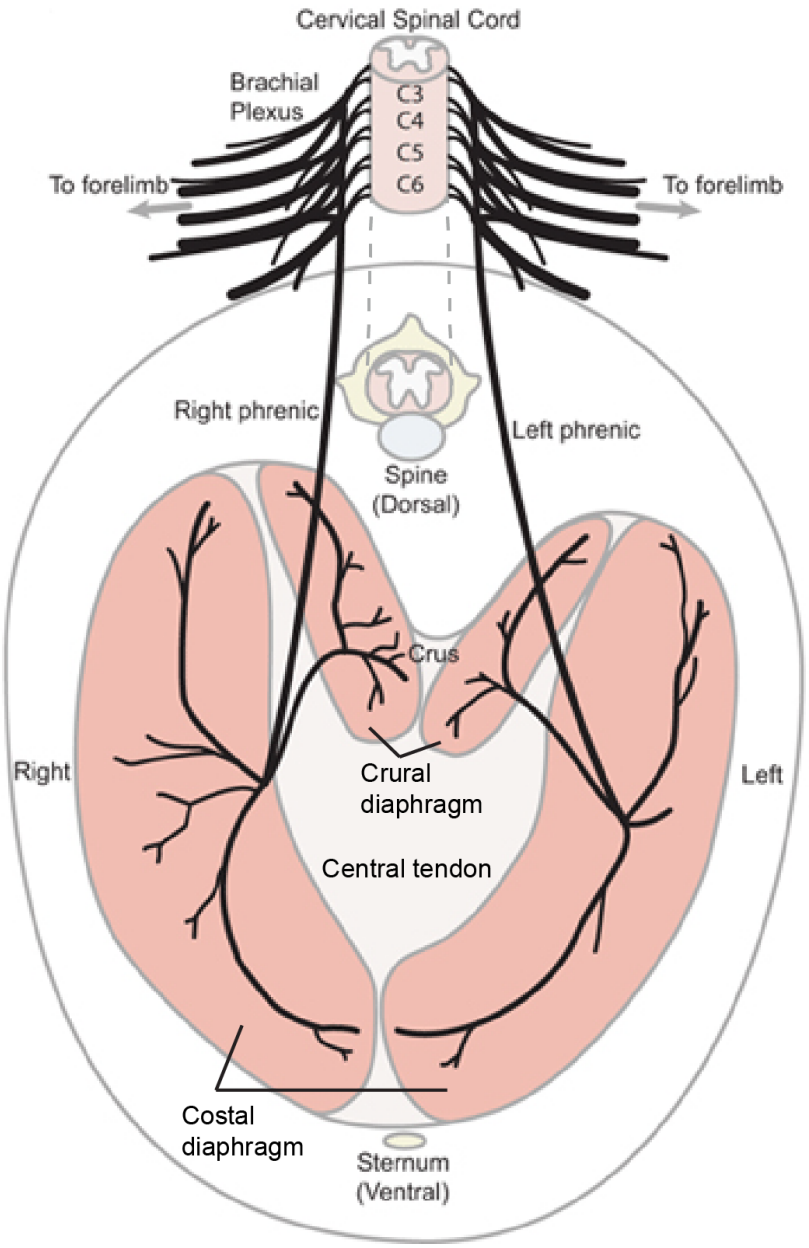

Figure 6. Diaphragm innervation (thoracic surface view). Phrenic nerves arise bilaterally from the ventral horn of the cervical spinal cord (C3 through C6), and then courses caudally through the thoracic cavity to contact the diaphragm. They form three main branches, a ventral and a dorsal branch that innervate the costal diaphragm, and a dorsomedial branch that innervates the crural diaphragm. Adapted from Burgess et al. 2006.

during sleep can result in airway obstruction and apnea suggesting an important role in sleep-disordered breathing (**Brouillette and Thach, 1980**; **Chan et al., 2006**; **Deegan and McNicholas, 1995**).

Although the tongue is involved in multiple motor behaviors such as swallowing, chewing, vocalizing and breathing, the hypoglossal nerve (XII) provides the only motor innervation to the tongue. The intrinsic muscles constitute the body of the tongue, and the extrinsic muscles serve as either tongue protruders (genioglossus) or retractors (hyoglossus and styloglossus), and the medial and lateral branch of XII nerve innervate the protruders and retractors respectively. The XII MNs are located in the dorsal part of the brainstem and consist of the genioglossal MNs in the ventral subnucleus of XII MNs and the hyoglossal and styloglossal MNs in the dorsal subnucleus (**Dobbins and Feldman, 1995**; **Sawczuk and Mosier, 2001**).

The axons of XII MNs course ventrally in a radial manner from the XII nucleus to the ventral surface of medulla and their dendrites are found extensively intermingled at all rostrocaudal levels. Contrary to the Phr-MNs, a portion of the dendrites of genioglossal MNs extend to the contralateral XII nucleus (**Altschuler et al., 1994**). In neonatal rats ≤ P8, electronic coupling is present in 42.5% of genioglosssal MNs, but disappear in the rats older than P10 (**Mazza et al., 1992**). The inspiratory-related XII activity are more often observed in anaesthetized or decerebrated animals than awake ones, and in isolated brainstem-spinal cord preparations and brainstem slices, XII MNs are rhythmically depolarized and discharge during the inspiratory phase (**Figure 8**) (**Funk et al., 1994**; **Morin et al., 1992**; **Smith et al., 1991**). Aside from XII MNs, other cranial MNs innervating the oro-pharyngeal muscles such as MNs in nucleus ambiguus (nA) and facial nucleus (VII) are also active during respiration to facilitate the upper airway dilation.

II.5. Bilateral connectivity

Mechanical considerations about ventilation indicate that alternating inspiratory/expiratory phases together with left/right balanced motor drives to respiratory muscles is adapted to the design of the upper airways that end in a unique tract imposing unidirectional air flows, in or

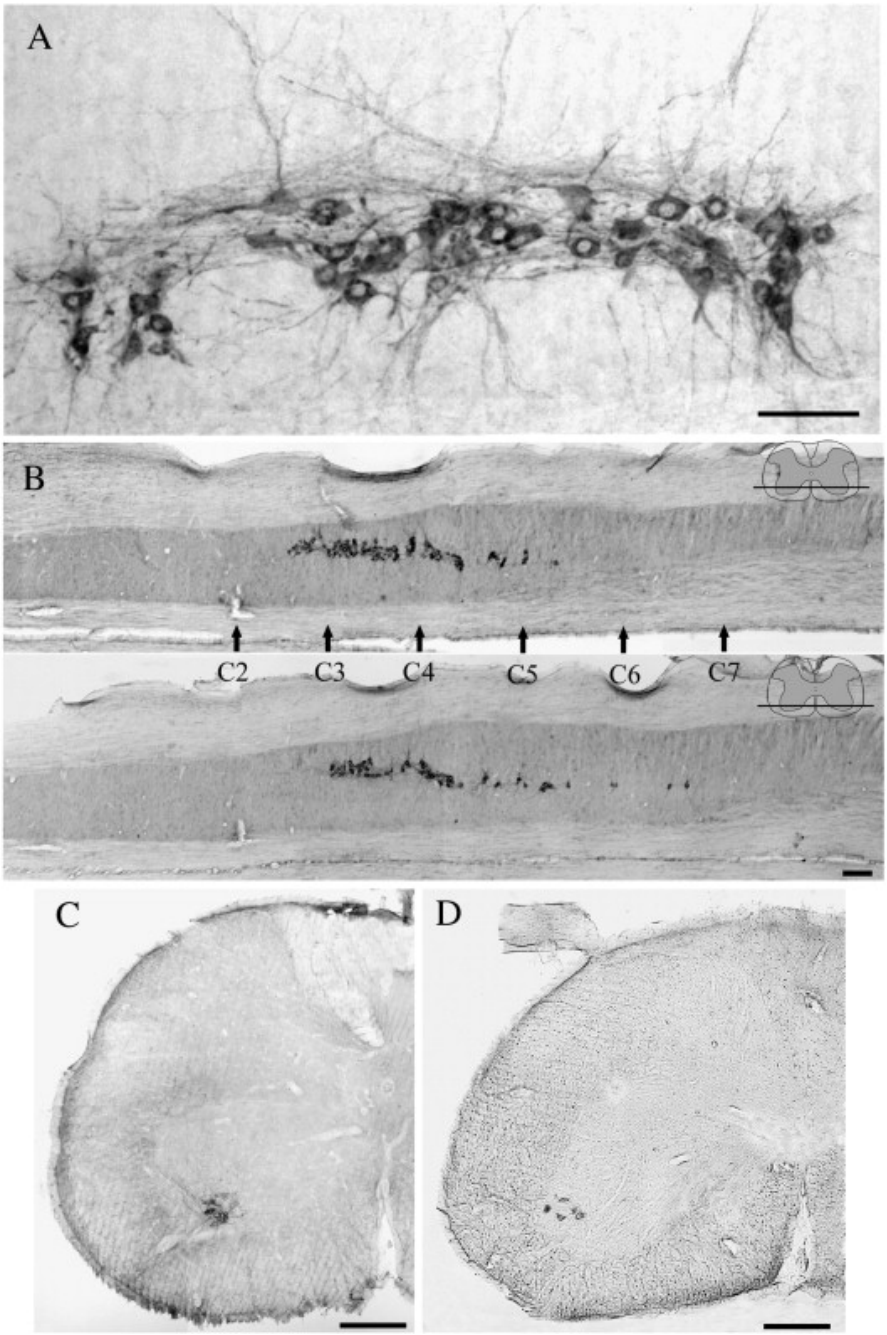

Figure 7. The Phr-MNs in the adult mouse labeled by Cholera Toxin B subunit (CTB). (A) A horizontal section from the C3 spinal cord shows the primarily rostrocaudal orientation of Phr-MN dendrites. (B) Horizontal sections at lower magnifications and at two different depths along the dorsoventral axis (inset at top right). The arrows indicate the approximate locations of the cervical dorsal roots. (C) Transverse spinal cord hemi-sections at C3 (C) and C5 (D) levels. Scale bars: 50μm in A; 100μm in B; 200μm in C-D. Reproduced from Qiu et al., 2010.

out. As seen above the innervation of the diaphragm arise from distinct left and right phrenic motoneuronal pools giving rise to a left and a right phrenic nerve each innervating a hemi-diaphragm. This sets a constraint on the design of the respiratory control circuit in that it must ensure that the left and right motor drives be necessarily balanced in amplitude and temporally synchronized for efficient inflation of the lung. How is the circuit managing bilateral control? In the brain bilateral control imparts on commissural interneurons, i.e. neurons bearing axons that can navigate across the midline and transmit activity from one side of the brain to the other.

The respiratory rhythm is produced and controlled by respiratory groups with symmetric locations in each half of the brainstem. A midline section in the medulla of de-cerebrated adult rat reveals that each half of the brainstem is able to produce a respiratory rhythm independently (**Peever et al., 1998**). In transverse slice preparations, the activities of the preBötC on both sides of the medulla are synchronized, and it has been shown by many reports that the preBötC neurons project to the contralateral preBötC both anatomically and functionally (**Bouvier et al., 2010**; **Koizumi et al., 2013**; **Koshiya et al., 2014**; **Stornetta et al., 2003b**; **Tan et al., 2010**; **Thoby-brisson et al., 2005**; **Wang et al., 2001**). A section along the midline results in independent rhythms of the left and right preBötC (**Thoby-brisson et al., 2005**). Thus commissural connections ensure preBötC bilateral synchrony but are dispensable for rhythm generation per se. Later experiments have demonstrated that these commissural interneurons were preBötC proper neurons that required a roundabout receptor 3 mediated signaling for axonal midline crossing (**Bouvier et al., 2010**). These data indicated that bilateral synchronicity of the motor command was established at the level of the rhythm generator. In fact, the projections of somatostatinergic (Sst+) preBötC neurons, outside the preBötC itself, to the VRG, RTN/pFRG, BötC, NTS and PB/KF were all found to be bilateral (**Figure 9**) (**Tan et al., 2010**), indicating that the preBötC bilaterally broadcasts its left-right synchronous activity. In principle, the dispatching of activity achieved by the preBötC is sufficient to ensure bilateral coordination of respiratory motor activity even if downstream neuronal relay neurons were to all be ipsilaterally projecting. *My work will directly inspect this possibility.*

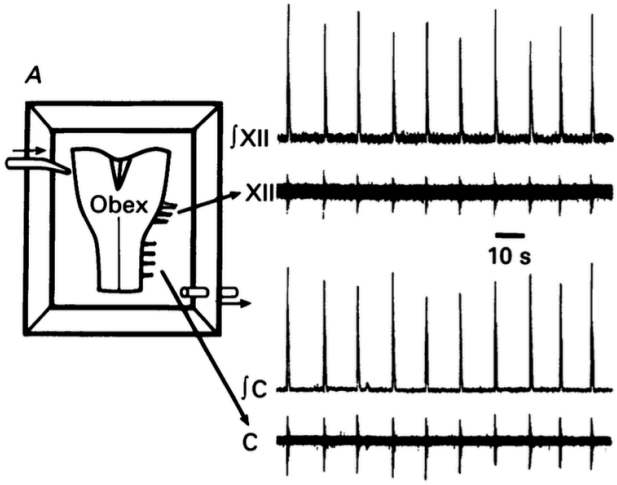

Figure 8. Spontaneous inspiratory discharges of XII and cervical (C) ventral roots in brainstem-spinal cord en bloc preparations in neonatal rats. Integrated (∫) and raw discharges of XII and cervical ventral roots are illustrated. Reproduced from Morin et al., 1992.

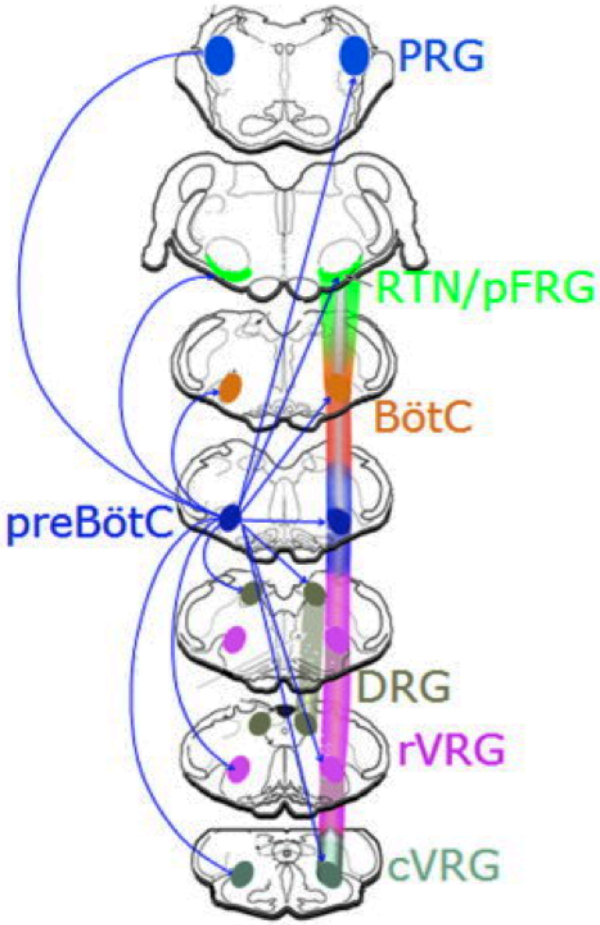

Figure 9. Schematic presentation of the projections of preBötC in the brainstem. The preBötC send projections to contralateral preBötC, ipsi- and contralateral RTN/pFRG, BötC, rVRG, cVRG, dorsal respiratory group (DRG) and pontine respiratory group (PRG). Adapted from Tan et al., 2010.

III. Fetal breathing

In mammals, most of the brain structures are not fully functional until they undergo several important developmental steps after birth. This is also true for breathing, yet neonates must breathe efficiently at birth to survive, therefore the respiratory system must be prepared and functional before birth. In human embryos, fetal breathing-like movement (FBM) can be detected at approximately 10 to 12 weeks gestation and become more strong and regular at 36 weeks, which is prepared to generate adequate ventilation after birth. Pathologies of newborns often result from the failure or inadequate prenatal development of the respiratory apparatus such as the respiratory CPGs, MNs and muscles. Therefore, understanding of the embryology, the plasticity, and the genetic and pharmacologic control of the respiratory system, can provide basic understanding of the infant respiratory disorders.

In this section, the development of FBM is introduced with emphasis on respiratory CPGs and phrenic MNs in mice. Their functional onsets, connectivity and pharmacology are introduced. Their genetic control will be introduced in the next section.

III.1. Fetal respiration in the rodents - practice makes perfect

The fetal breathing-like movement (FBM) has been observed in many different species such as sheep (**Dawes et al., 1972**), human (**De Vries et al., 1986**) and rat (**Kobayashi et al., 2001**). In the mice, the typical respiratory-like movement, in which the fetus open its mouth, bend the neck dorsally and flex the body ventrally, is observed as early as embryonic day (E) 15.5 by using a transplacental perfusion method, which can keep the fetuses alive and maintain their physiological activities for 24h ex utero (**Suzue, 1994**). This observation has been confirmed in the calcium imaging and electrophysiological recordings of the preBötC in the fetal medullary slices (**Thoby-brisson et al., 2005**) and phrenic nerve (C4) recording in the isolated brainstem-spinal cord preparations from the mice embryo (**Bouvier et al., 2010**; **Viemari et al., 2003**). In rat, the FBM first emerges at E17 in the fetal rats (**Greer et al., 1992**; **Kobayashi et al., 2001**), fitting with the longer gestational period of rats compared with mice,

Although the respiratory network has already established and starts drive fetal respiratory-like activities and movements at E15.5 in mice, plethysmographic recordings of

caesarean delivered mice fetuses, in which the ventilations in vivo are measured, have shown that the fetuses younger than E18 are not able to ventilate and survive whereas at E18 they can breathe at a frequency (110 cycles/min) similar to newborns (P0-P2) (**Viemari et al., 2003**), indicating that the respiratory networks and the respiratory effectors such as the diaphragm and lungs rapidly undergo important developmental steps from the onset of the respiratory rhythm, and the respiratory system are fully prepared one day before the natural birth. It has been observed that the amplitude and duration of the respiratory bursts increase with the gestational age with decreasing variability (**Greer et al., 2006**; **Viemari et al., 2003**). Also, it has been suggested that fetal inspiratory activity play an important role in the maturation of the respiratory motor system to prepare for the generation of the robust respiratory activity at birth (**Greer, 2012**). In addition, it has been shown that the FBMs are required for the proliferation and differentiation of the lung, lack of which in fetus results in lung hypoplasia and pulmonary hypertension at birth (**Inanlou et al., 2005**). Therefore, the fetal respiratory-like activity is not only essential for the postnatal survival but also required for the proper development of the respiratory system.

III.2. Ontogeny of phrenic motoneurons

To perform respiratory behavior, the phrenic motoneurons (Phr-MNs) must be properly developed and innervate the diaphragm. In mice, the observation of the FBM and C4 outputs at E15,5 suggests that the Phr-MNs at this stage although still developing are already functional. In mice, the Phr-MNs with other motoneurons differentiate and proliferate in the neural tube at E10. Phr-MNs then migrate in packed clusters to their final position to form the phrenic motor column (PMC) around E11. Then the axons of Phr-MNs exit from the ventral spinal cord (E12) and extend to the diaphragm. As development proceeded, the axons of Phr-MNs fasciculate and branch on the diaphragm during E14-E17, and at E18 the intramuscular branches are completely formed (**Figure 10**) (**Castellani and Kania, 2012**; **Greer, 2012**; **Philippidou et al., 2012**).

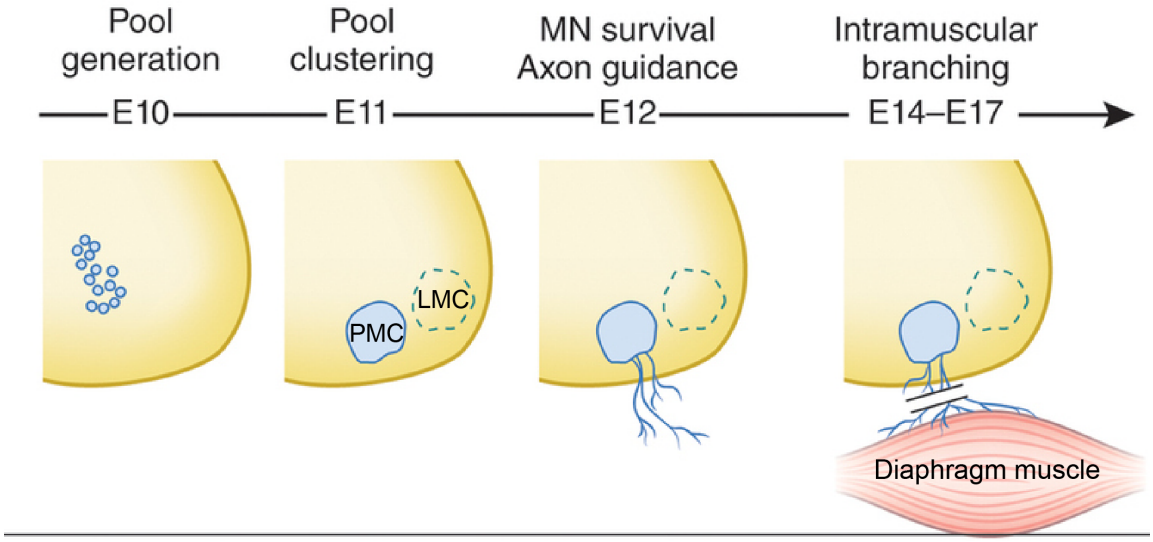

Figure 10. Development of phrenic motor column (PMC). After their generation together with other motoneurons, phrenic motoneurons migrate to their own position, which is distinct from other motor pools such as lateral motor column (LMC). Then the axons of phrenic motoneurons exit from the ventral horn of the spinal cord, and then extend towards and innervate the diaphragm. Adapted from Castellani and Kania, 2012.

III.3. Ontogeny of respiratory rhythm generator

III.3.1 Ontogeny of preBötC

Anatomical emergence

In neonates and adult, the preBötC mainly contains glutamatergic neurons expressing NK1R, which provides the basis to examine ontogeny of preBötC in prenatal development. After the injection in the pregnant females at precise gestational stages of the 5-bromo-2'-deoxyuridine (BrdU), a thymidine analog that incorporates within the DNA of actively dividing cells, the massive co-labeling (71%) of BrdU and NK1R in the preBötC is found in the BrdU injection at E12-E13 in the rat, indicating that the preBötC neurons were born at E12-E13 in the rat, 2 days later than the adjacent NK1R positive neurons in the nucleus ambiguus (**Pagliardini et al., 2003**). The same birth dating has been confirmed in the mice at E10-E11 (comparable to E12-E13 in the rat) (Bouvier et al., 2010). Analysis of the spatiotemporal distribution of the NK1R positive neurons by NK1R immunostaining have shown that the NK1R neurons reach the preBötC region at E15 (mice)/ E17 (rat). Although at E14 in mice and E16 in rat, weak NK1R labeling is detected in the preBötC, the NK1R expression is much stronger with

increasing spatial extension from E15 (mice)/ E17 (rat) (**Figure 11**). In addition, the Sst expression pattern in the region has been shown to follow the same time and spatial course (**Pagliardini et al., 2003**; **Thoby-brisson et al., 2005**).

Functional emergence

Anatomical ontogeny of the preBötC coincides with the first emergence of the fetal respiratory-like activity, strongly suggesting that the preBötC is functional at this stage (E15 in mice, E17 in rat). The following observations have confirmed this hypothesis. First, at E15, calcium imaging and electrophysiological recording of the transverse slices from mouse embryo has shown a bilateral rhythm generator located in a spatially restricted site ventral to the nucleus ambiguous, which corresponds to the location of the NK1R immunoreactivity in the preBötC (**Figure 12**). When bath application of the NK1R agonists SubP in fetal slice, the frequency of the rhythmic respiratory activity produced by this ventral generator increases whereas strongly decreases with the application of μ-opiate agonists DAMGO. And the synchrony of the generator neurons is intensively disrupted when applying the non-NMDA receptor antagonist CNQX, indicating that the synchrony of these ventral generator populations depends on the AMPA/kainite receptors in glutamatergic synapse (**Pagliardini et al., 2003**; **Thoby-brisson et al., 2005**). All these properties found in this fetal rhythm generator at E15 in mice and E17 in rat demonstrate a similar profile of preBötC in postnatal rodents. Therefore, the preBötC emerges anatomically and functionally at E15 in mice and E17 in rat.

Emergence of bilateral connectivity

Commissural connectivity of the preBötC on each side of medulla is important for the bilateral synchronization of the respiratory rhythm. In mice transverse slice, pharmacological stimulation of the preBötC on one side of the medulla fail to trigger the activation the preBötC on the other side at E14, whereas at E15 the stimulation of preBötC on one side results in the preBötC bursts on both sides, and the spontaneous activity of the preBötC on each side of the medulla are well synchronized (**Figure 12**A), indicating that the bilateral connectivity of the preBötC has settled at E15 in mice (**Thoby-brisson et al., 2005**).

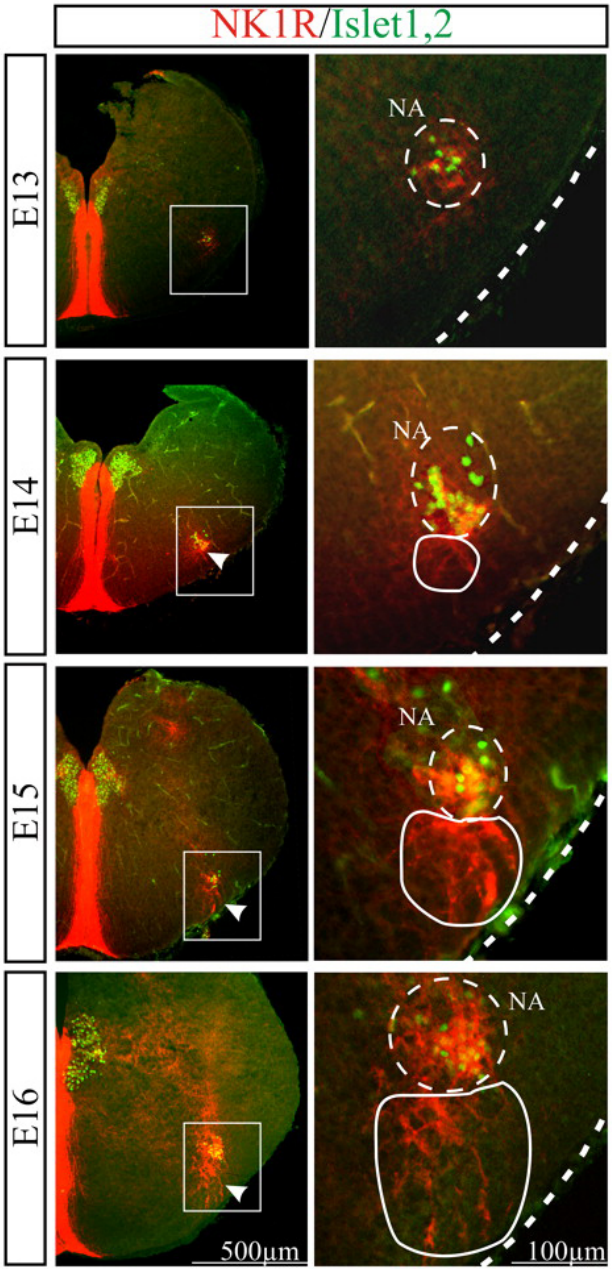

Figure 11. Anatomical ontogeny of preBötC examined by spatio-temporal distribution of NK1R neurons in transverse brainstem slices from mouse embryos. Immunostaining of NK1R positive neurons (red) and Islet positive motoneurons (green) is shown in transverse brainstem slices at different developmental stages (E13-E16). The images in the left column represent half of the transverse slices, and the regions highlighted by white rectangle are shown at high magnification in the right column. Note that the midline is intensively labeled by NK1R immunostaining at all the ages. Weak NK1R immunoreactivity is detected at E14 in the area ventral to the nucleus ambiguus (NA) (recognized by Islet1,2 labeling, dashed outline in the right column) corresponding to the preBötC (arrowhead in the left column, continuous white outline on the right). From E15 the NK1R is more strongly expressed with increasing spatial extension in the same region. Adapted from Thoby-brisson et al., 2005.

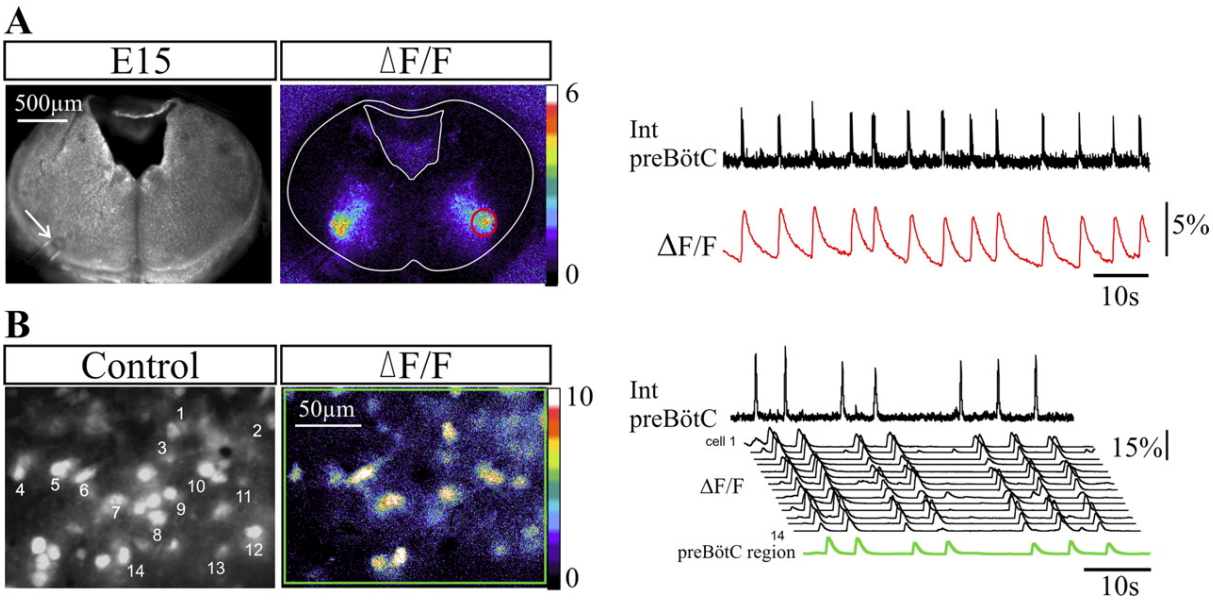

Figure 12. Spontaneous respiratory activity of the preBötC detected by calcium imaging and electrophysiological recording in E15 mouse medullary slice. (A) Left, fluorescent image of an E15 transverse medullary slice loaded with the calcium indicator. Middle, spontaneous calcium transients illustrated as relative changes in fluorescence (ΔF/F) is detected on this medullary slice. Right, black trace illustrates the spontaneous burst of electrical activity recorded from the ventrolateral area corresponding to the preBötC region (arrow in the left panel), and the red trace indicates the calcium transients of the contralateral preBötC region (red circle in the middle panel). (B) Calcium imaging also allows examination at the cellular level at higher magnification in the preBötC region. Traces in the right panel represent calcium changes in individual cells (1–14 corresponding to cells numbered in the left panel) and for the entire preBötC region (green trace and green rectangle) recorded simultaneously with the population activity (Int preBötC). Reproduced from Thoby-brisson and J.Greer, 2009.

III.3.2 Ontogeny of parafacial respiratory group

As described previously, there is a second respiratory CPG located in the parafacial region that is thought to generate the active expiratory activity and to be coupled to the preBötC in postnatal animals. In vitro preparation from the mouse embryos, using calcium imaging and population electrophysiological recording, a group of rhythmic neurons is detected in the parafacial region as early as E14 (**Figure 13**), located in the same region as pFRG/RTN, named fetal parafacial respiratory group (e-pF), and these spontaneous rhythmic activities are preserved in the transverse slices. Similar as pFRG/RTN neurons, e-pF neurons are not sensitive to µ-opioid, since at E14, one day before the onset of spontaneous rhythm generation in the preBötC, the rhythm generation of the e-pF neurons is preserved in the presence of DAMGO. Moreover, the frequency of e-pF is increased by a low pH challenge, indicating their role in chemosensitivity as pFRG/RTN. In addition, pharmacological

applications and genetic manipulation have shown that the synchronization of the e-pF population does not require the glutamatergic transmission but relies on the gap junction communication (**Thoby-brisson et al., 2009**). Therefore, the parafacial respiratory group also exists in the embryo and emerges as early as E14 in the mice.

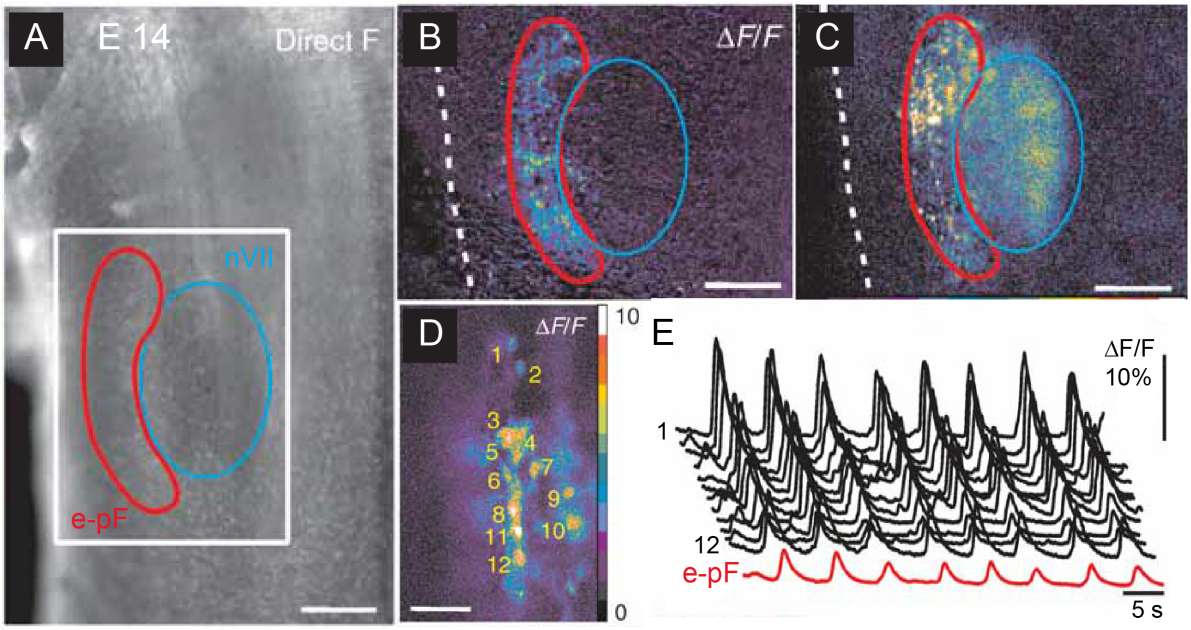

Figure 13. Functional emergence of the e-pF oscillator at E14 in the mice. (A) Fluorescent image of a whole brainstem preparation from E14 mice embryo loaded with the calcium indicator shows the location of the e-pF (red outline) and facial nucleus (nVII, cyan). Fluorescence changes (ΔF/F) are detected restricted in the e-pF oscillator (B) and are sometimes concomitant to activity of the nVII (C). Calcium imaging of the parafacial region at the cellular level with higher magnification allows examination of calcium changes in individual cells (black traces in E, 1–12 corresponding to cells numbered in D) and for the entire e-pF region (red trace in E). Adapted from Thoby-brisson et al., 2009.

III.3.3 Functional coupling of the two oscillators

Although e-pF neurons are rhythmic active and bursting continuously at E14, the nVII and XIIn bursts show a discrete failing pattern similar to those observed in the quantal slowing (skipped inspiratory bursts) induced by hyperpolarization of a subset of preBötC inspiratory neurons, and the onset of each individual motor burst has a delay than that of the e-pF. During E14-E15, there is a dynamic developmental transition in which the occurrences of the motor bursts progressively synchronize with e-pF bursts. At E15, when the preBötC neurons are

functional mature, the motor outputs become continuous and totally in phase with the discharges of the two oscillators, and this synchronization maintains in all the preparations at all the developmental stages onwards, indicating that the two oscillators are coupled to produce a single respiratory phase (**Figure 14**). A transverse section made between the e-pF and preBötC to separate these two oscillators at E15 in the whole brainstem preparation has shown that the interaction between e-pF and preBötC is important to maintain the respiratory rhythm at a normal frequency. After the section, the respiratory rhythm generated from the preBötC becomes slower (**Thoby-brisson et al., 2009**). Also, there is evidence that at E15, the e-pF is able to evoke the respiratory motor activity in the C4 only when preBötC and glutamatergic transmission are both present, suggesting that the e-pF provides glutamatergic drive to the preBötC to entrain its activity (**Ruffault et al., 2015**). Collectively, the dual organization of the respiratory rhythm generator, one in the e-pF and the other in the preBötC, is also found in the fetus and is established around E15 in the mice.

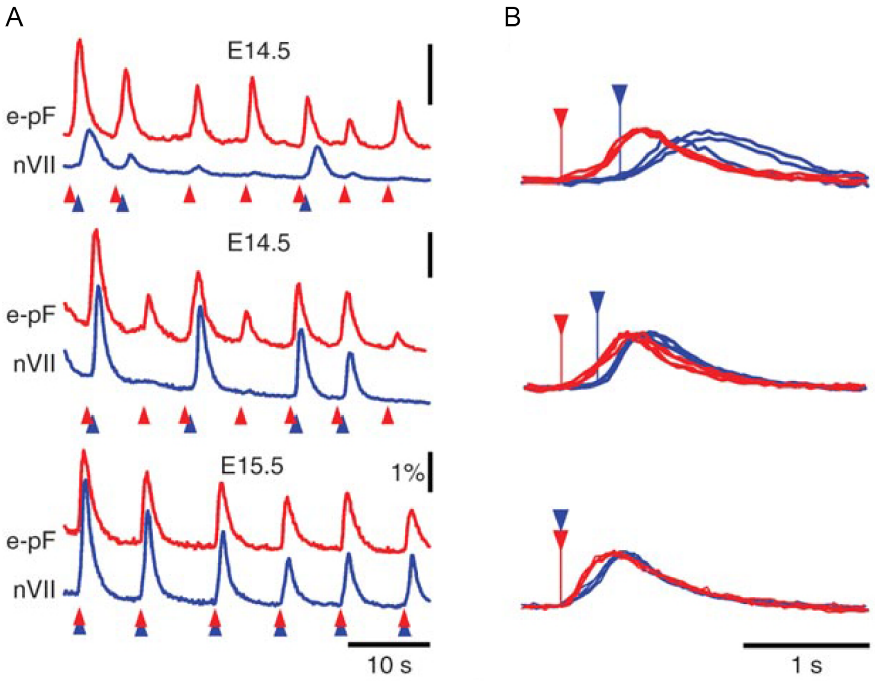

Figure 14. Progressively coupling between the e-pF oscillator and motor activity during development in the mice. The traces represent the spontaneous calcium changes in the e-pF (in red) and nVII (in blue) in E14.5 and E15.5 mouse brainstem preparations (A), and all the individual bursts are overlapped to show the time lag (B). Note the increase of the occurrence of motor bursts coupled to the e-pF with the reduction of the time lag indicated by distance between the red (e-pF) and blue (nVII) arrowheads. Adapted from Thoby-brisson et al., 2009.

IV. Developmental specification of respiratory circuit elements

The mammalian nervous system is made up of a great variety of neural cell types with distinct morphology, anatomical location, projection pattern, neurotransmitter identity, pharmacological sensitivity, firing pattern…properties subsumed individually or collectively under the term phenotype. Over the past decade, studies of regulatory developmental genes have open ways to put in register classical functional findings with defined cellular identities inherited from particular developmental histories. The understanding of cell specification programs is thus important to understand how neural networks assemble and function. Moreover, knowledge about cell specification programs is required to appreciate their putative alterations that may predispose to dysfunction.

In this chapter, first I will consider neuronal type specification applied to respiratory oscillators. I will also introduce an axon guidance scheme critical for establishment of commissural connectivity underlying bilateral coordination of neural activities.

IV.1. Transcription factors and patterning of brainstem

Transcription factors (TFs) are proteins that control the expression of genes. In the development of neural tube to generate different types of neurons, the TFs with a basic-helix-loop-helix (bHLH) domain and a homeodomain (HD) are expressed in a nested manner, in which the progenitor cells in specific location of the neural tube express a defined combination of TFs, forming the so-called "lineage specific" genetic codes and progenitor zones. This developmental genetic program plays an important role in patterning the neuroaxis including the hindbrain and spinal cord along its antero-posterior (A-P) and dorso-ventral (D-V) axis, and provides markers to identify specific subsets of neurons in the neuronal circuits (**Jessell, 2000**).

IV.1.1 Hox genes and A-P patterning of the brainstem

During early embryogenesis, the part of neural tube that will become the hindbrain, the rhombencephalon, is segmented into seven to eight compartments termed rhombomeres (r) along its antero-posterior (A-P) axis, with r1 the most anterior part connected with the mesencephalon (midbrain) and r8 the most posterior part connected with the spinal cord

(**Figure 15**). In the mice, this hindbrain segmentation is achieved at E8.5 and disappears around E11.5. Each rhombomere generates similar sets of neurons such as motoneurons, but with distinct differentiation programs in different rhombomeres. For example, trigeminal (V) motoneurons are derived from r2 and r3, facial (VII) motoneurons originates from r4, whereas vagus nucleus (X) originates from r6 and r7 and the hypoglossal (XII) motoneurons from r8 (**Borday et al., 2004**; **Guthrie, 2007**; **Krumlauf et al., 1993**).

In the vertebrates, the specification of each rhombomere depends on expression of different sets of homeobox (Hox) genes, encoding a family of highly evolutionarily conserved transcription factors, homologs of HOM-C genes that encode parasegmental information in their *Drosophila* counterparts. In all vertebrates, there are four separate clusters of Hox genes (Hox-a, b, c and d), and genes in each of the four Hox clusters are highly related both in structure and organization, forming 13 sets of paralogous groups (1-4 paralogous expressed in the hindbrain and 5-13 in the spinal cord). Their linear order in the chromosome and domain restricted expression pattern are highly correlated with the spatial and segmental order of the rhombomeres. Expression of the 3' ends genes of the Hox clusters in the early structures gives rise to their anterior segment identity whereas the later structures gain their posterior identity by expression of 5' ends genes of the Hox clusters (**Krumlauf et al., 1993**; **Lumsden and Krumlauf, 1996**). This Hox gene based segmentation is important for the development of neurons, especially the cranial nerve innervation (**Figure 15**). For example, inactivation of Hoxa1 results in the deletion of r5 and reduction of r4, and thus defects of facial motoneurons development and malformations of several cranial nerves (**Gavalas et al., 2003**; **Guthrie, 2007**).

The molecular programs controlling the activation of *Hox* genes in appropriate levels of the A-P axis have been suggested such as morphogen signaling. Morphogens are molecules that form a long-range concentration gradient that influence the cell fate according to the position of the cell along the gradient in a dose dependent manner. Retinoic acid (RA) and fibroblast growth factor (FGF), act as morphogens, forming opposing posterior to anterior concentration gradients along the hindbrain and spinal cord, to transiently control the activation of the *Hox* gene in neuroepithelium (**Del Corral and Storey, 2004**; **Glover et al., 2006**). Through auto- and cross- regulations the *Hox* genes plays an important role in maintaining their rhombomere-restricted expression pattern (**review in Krumlauf, 2016; Tümpel et al., 2007)**. In addition, transcription factors that regulate the *Hox* genes expression

also regulate the expression pattern of other genes, especially *Krox-20* (also known as *Egr2*) and *MafB* (**Figure 15**). *Krox-20* encodes a zinc finger transcription factor expressed in r3 and r5, and it is a direct regulator to activate *Hoxa2* and *Hoxb2* expression. MafB is a bZIP transcription factor expressed in r5 and r6, which is required for the activation of Hoxa3 and Hoxb3 gene transcription. Disruption of *Krox-20* results in the elimination of r3 and r5, and thus formation of a partially fused r2/r4/r6 region. Similarly, in *kreisler* mouse embryo, a naturally occurring mutant with *MafB* ectopic expression, loss of neural tube segmentation in r5 and r6 is found (**review in Lumsden and Krumlauf, 1996**). *Krox20* null and *kreisler* mutants present with respiratory deficits (**Chatonnet et al., 2002**; **Jacquin et al., 1996**)

IV.1.1 Cell type specification and D-V patterning

Similar to A-P patterning, along the D-V axis of the rhombomeres and spinal cord, developing neural tube can be subdivided into different progenitor (p) domains defined by the expression pattern of TFs genes in both the progenitor cells as well as their early postmitotic progenies. This spatial expression pattern of TFs is determined by graded morphogen signaling molecules, primarily based on experiments in the spinal cord (**Briscoe and Ericson, 2001**; **Jessell, 2000**), and the hindbrain most likely shares the same mechanism. The ventral neural tube patterning, for example, is induced by Sonic hedgehog (Shh) concentration gradient secreted by the notochord and the floor plate (**Figure 16**A). The TFs expressed by the progenitor cells serve as intermediate factors that interpret this position inductive cue. They can be divided into two classes depending on their repression (class I) or induction (class II) manner by Shh, and the combinational expression of these two classes of TFs, who repress the expression of each other, delineates the boundaries between progenitor domains and finally defines five progenitor (p) domains (p0, p1, p2, pMN, p3) that generate corresponding five neuron cell types (V0, V1, V2, V3 interneurons and motoneurons) (**Figure 16**B). Similarly, the dorsal progenitor domains are mainly induced by TGF-like bone morphogenic proteins (BMPs) from the ectoderm and roof plate (**Lee and Jessell, 1999**), as well as other molecular signal such as Wnts (especially Wnt1 and Wnt3α) (**Muroyama et al., 2002**). With development, the progenitor cells exiting the cell cycle migrate from the original ventricular zone to their adjacent mantle zone, and thus generate their early postmitotic progenies. These postmitotic neurons begin to express new TFs that are required for the cell type specification such as the neurotransmitter phenotype and axonal projection pattern, which diverges the postmitotic neurons into subpopulations of neurons. For example, the

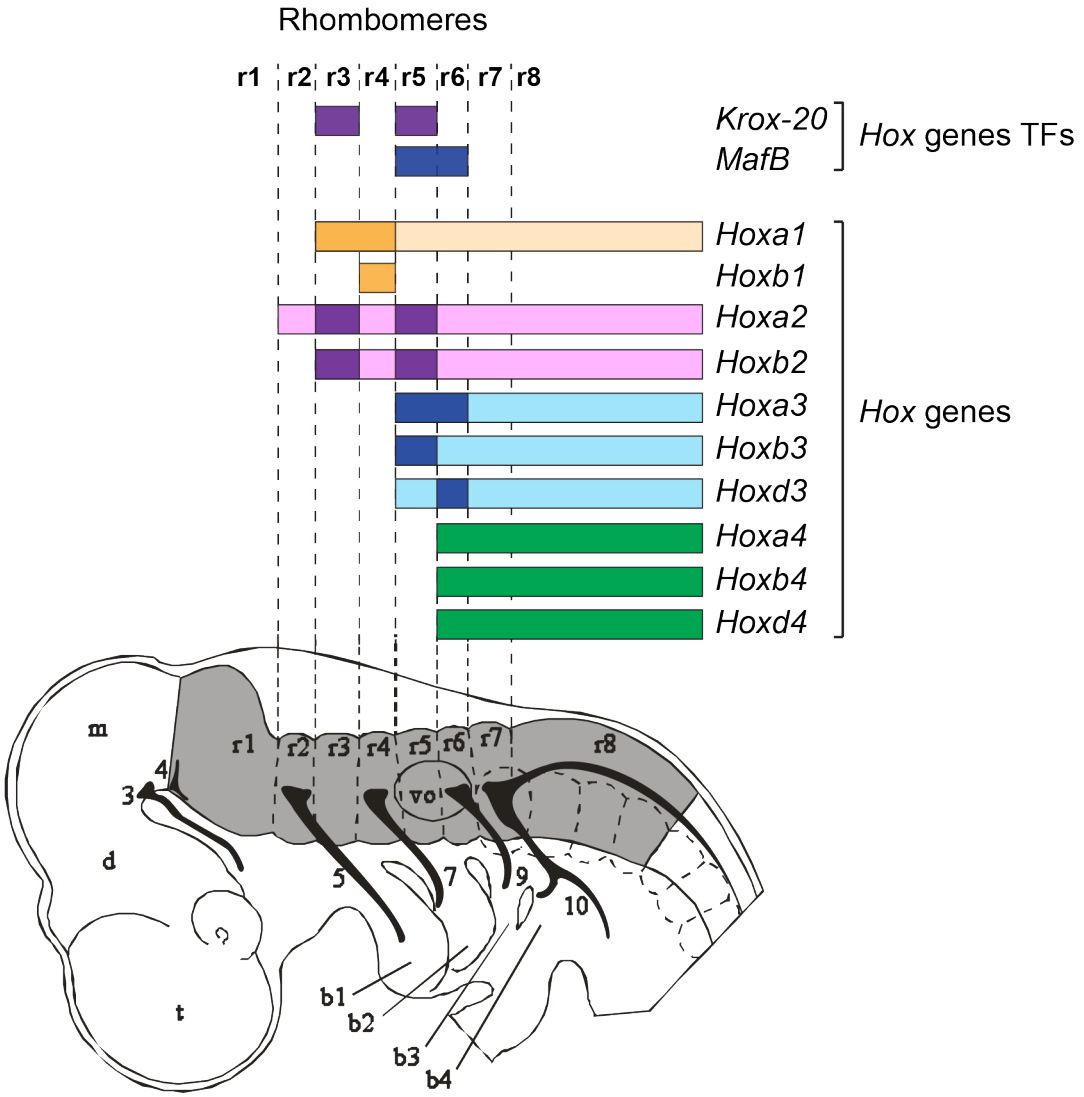

Figure 15. A-P segmentation of vertebrate hindbrain by expression patterns of Hox genes. Lateral view of the mouse embryo at E9 illustrates the segmentation of hindbrain into eight rhombomeres (r1-r8, grey color). Dashed line indicates the boundaries between rhombomeres. The bars labeled the different Hox genes expression as well as the transcription factors (TFs) that regulate Hox gene expression with the darkest color meaning the highest level of expression. Note that the nerves of branchiomotor neurons derived from certain rhombomeres project to specific branchial arch. t, telencephalon; d, diencephalon; m, mesencephalon; vo, otic vesicle; b1-b4, branchial arch 1-4. Digit numbers denote the cranial nerves: 3, oculomotor; 4, trochlear; 5, trigeminal; 7, facial; 9, glossopharyngeal; 10, vagus.

postmitotic transcription factor Evx1 is specific to ventral p0 domain-derived $V0_V$ neurons that are mostly glutamatergic, but is not expressed in the dorsal derived GABA/glycinergic $V0_D$ neurons (**Pierani et al., 2001**). Altogether, in the brainstem, the TFs in the progenitors cells and their early postmitotic neurons define at least 17 distinct neuronal types, at or before E11.5 in mice (**Figure 17**) (**Gray, 2008**, **2013**; **Jacob et al., 2013**; **Pattyn et al., 2003**; **Storm et al., 2009**). The most striking feature of this D-V defines TF coding is that the neurons with same lineage cell type share major neuronal properties such as neurotransmitter phenotype and projection pattern (**Figure 17**) (**Alaynick et al., 2011**; **Gray, 2008**; **Jessell, 2000**). And thus, this "lineage cell type" determines the neuronal cell fate and their ensuing recruitment during behavior.

Note that although the composition of cell populations is remarkably similar between rhombomeres and spinal cord, not every population is present in every rhombomere or segments. For example, dA3 is present in rhombomeres 4-7 but not in more rostral rhombomeres, and dA2 only exists in r7 but not other rhombomeres whereas dB2 is only absent in this rhombomere (**Sieber et al., 2007**; **Storm et al., 2009**). Also, p3 progenitor domain in the ventral spinal cord (**Figure 16**), which produces V3 interneurons expressing transcription factor Sim1, do not exist but replaced by pvMN progenitor domain in the hindbrain, which produces visceral motoneurons expressing Phox2b and 5HT interneurons expressing Pet1 (**Figure 17**). All these suggest that A-P and D-V signaling interact with each other and coordinately shape the brain organization. And there are several evidences that reveal this coordination. For example, Hoxb1 which is expressed only in r4, suppresses the production of 5HT neurons and promote vMN in r4, which results in the unique absence of 5HT neuronal production in this rhombomere (**Pattyn et al., 2003**). In addition, it has been shown that Retinoic acid (RA) signaling, whose gradient is important for the A-P segmentation, specifies the production of 5HT neurons in the hindbrain and Sim1-positive V3 interneurons in the spinal cord (**Jacob et al., 2013**).

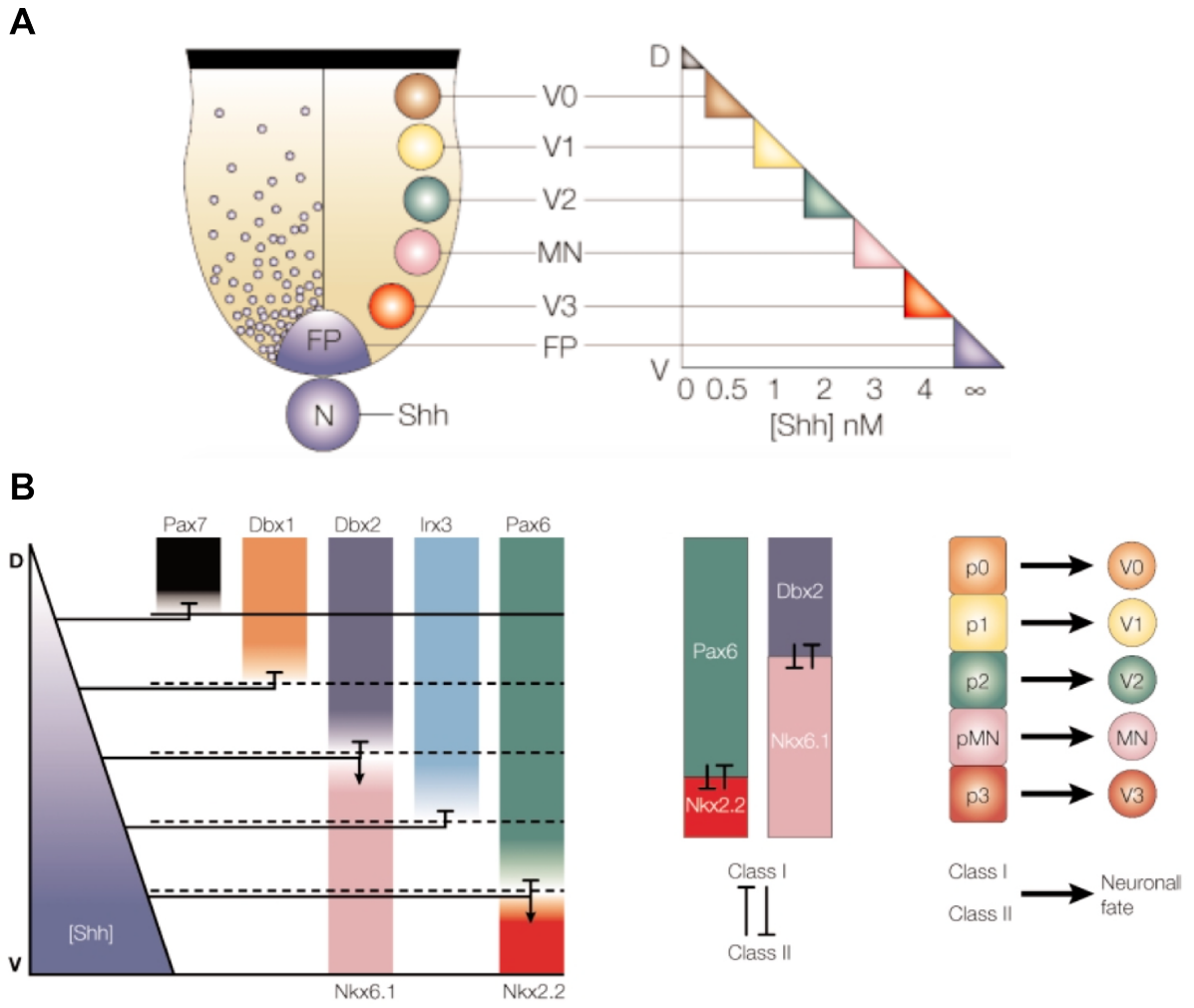

Figure 16. Shh-mediated ventral neural tube patterning. (A) Schematic transverse view of the ventral neural tube. The morphogen Shh is expressed from the notochord (N) and the floor plate (FP) with a ventral-high and dorsal-low gradient (purple dots), which induces four classes of interneurons (V0-V3) and motoneurons (MNs). (B) Three phase interpretation of the Shh signaling to induce different classes of neurons. Left, Shh mediates the repression of class I TFs and induction of class II TFs at different threshold concentrations. Dash line is the boundary between progenitor domains, continuous line is the boundary between dorsal and ventral neural tube. Middle, the paired expression of two classes of TFs, with cross-repression, delineate the boundary between progenitor domains. Right, five neural progenitor (p) domains (p0-p3, pMN) generates their corresponding ventral (V) postmitotic neurons (V0-V3, MN). D, dorsal; V, ventral. Adapted from Jessell, 2000.

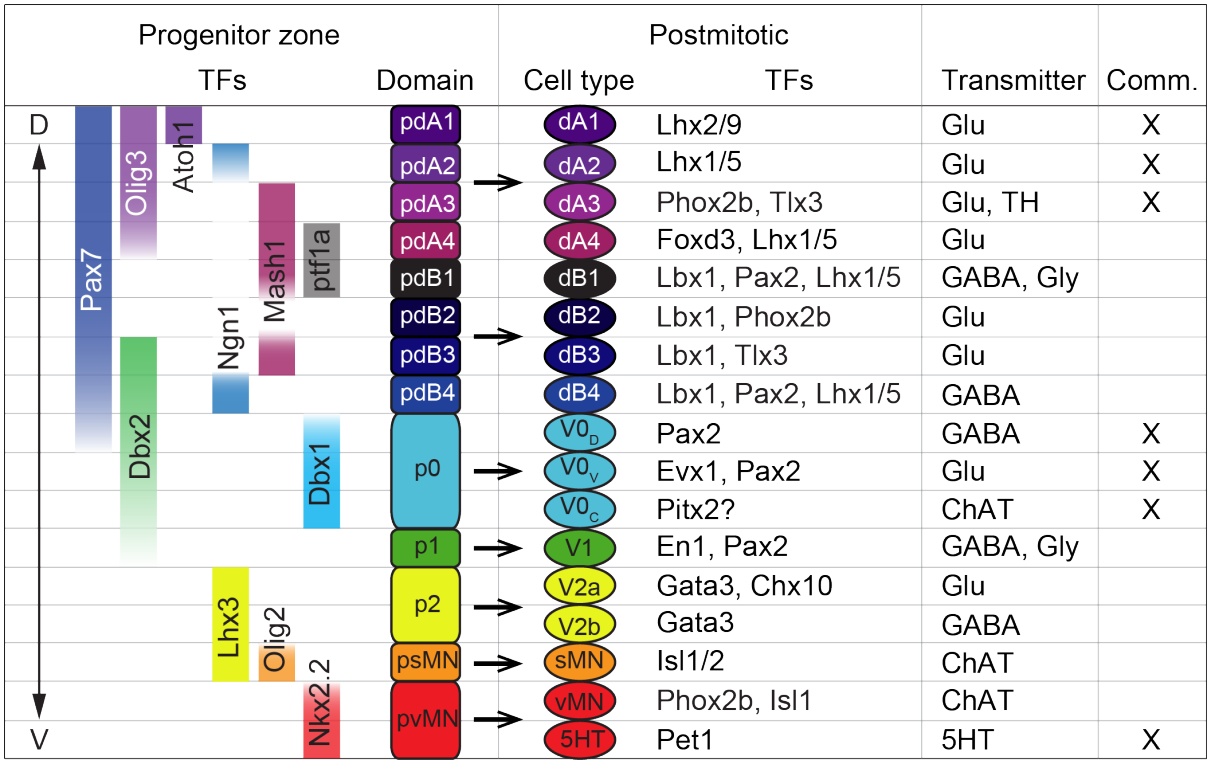

Figure 17. Schematic diagram illustrates transcription factor (TF) coding D-V populations in the brainstem at or before E11.5 in mice. Subsets of TFs that code the progenitor domains and their corresponding early postmitotic neurons are listed, which specify 17 distinct lineage cell types. A given TF can present in different domains with adjacent or not adjacent manner. Note that the neurons with the same lineage cell type share the same neurotransmitter phenotype and projection pattern, which is listed on the two right columns. Comm., commissural. D, dorsal; V, ventral. Glu, glutamate; Gly, glycine; GABA, g-aminobutyric acid; 5HT, 5-hydroxytryptamine (serotonin); TH, tryrosine hydroxylase; ChAT, choline acetyltransferase.

IV.2. A-P and D-V origin of respiratory CPGs

IV.2.1 P0 origin of the preBötC

The transcription factor Dbx1 is essential for the generation of preBötC neurons. Dbx1 is only expressed in p0 progenitor cells and turns off when progenitors exit the cell cycle to give rise to V0 type neurons (**Pierani et al., 2001**). The V0 neurons consist of three subpopulations, $V0_D$, $V0_V$ and $V0_C$ (**Feldman et al., 2012**; **Lanuza et al., 2004**; **Pierani et al., 2001**; **Zagoraiou et al., 2009**). $V0_D$ neurons are mainly GABAergic and arise from dorsal p0 progenitors that also express Pax7. $V0_V$ neurons express Evx1 and are predominantly glutamatergic. $V0_C$ neurons are cholinergic interneurons probably expressing Pitx2. All these three neuronal populations bear commissural axons (**Figure 17**).

The preBötC neurons expressing NK1R and Sst were found to derive from

Dbx1-expressing progenitors. These Dbx1-derived preBötC neurons are glutamatergic neurons expressing the vesicular glutamate transporter 2 (vGlut2), and are spontaneously rhythmic in transverse medullary slices. In Dbx1 null ($Dbx1^{LacZ/LacZ}$) mutants, the rhythm is absent in slices and cannot be recovered by stimulation, and thus no respiratory activity can be detected in vivo (**Figure 18**). Further anatomical analysis has shown that in this mutant Dbx1-derived neurons are able to migrate to the preBötC region but are not able to express NK1R or Sst, and no longer express vGlut2, which indicates that Dbx1 is required for proper specification of preBötC neurons but is not essential for their survival and migration. In addition, in $Pax7^{cre}$; $Dbx1^{DTA}$ mutants, in which the $V0_D$ neurons with both Pax7 and Dbx1 expression history are eliminated, the preBötC is still functional, indicating that preBötC neurons are not $V0_D$ but $V0_v$ Evx1-expressing neurons (**Bouvier et al., 2010**).

Currently, there is no direct knowledge about the A-P origin of the preBötC neurons. In mice, nucleus ambiguous (nA), which is located just dorsal to the preBötC, is derived from r7 and r8, indicating that the preBötC may have the same rhombomeric origin.

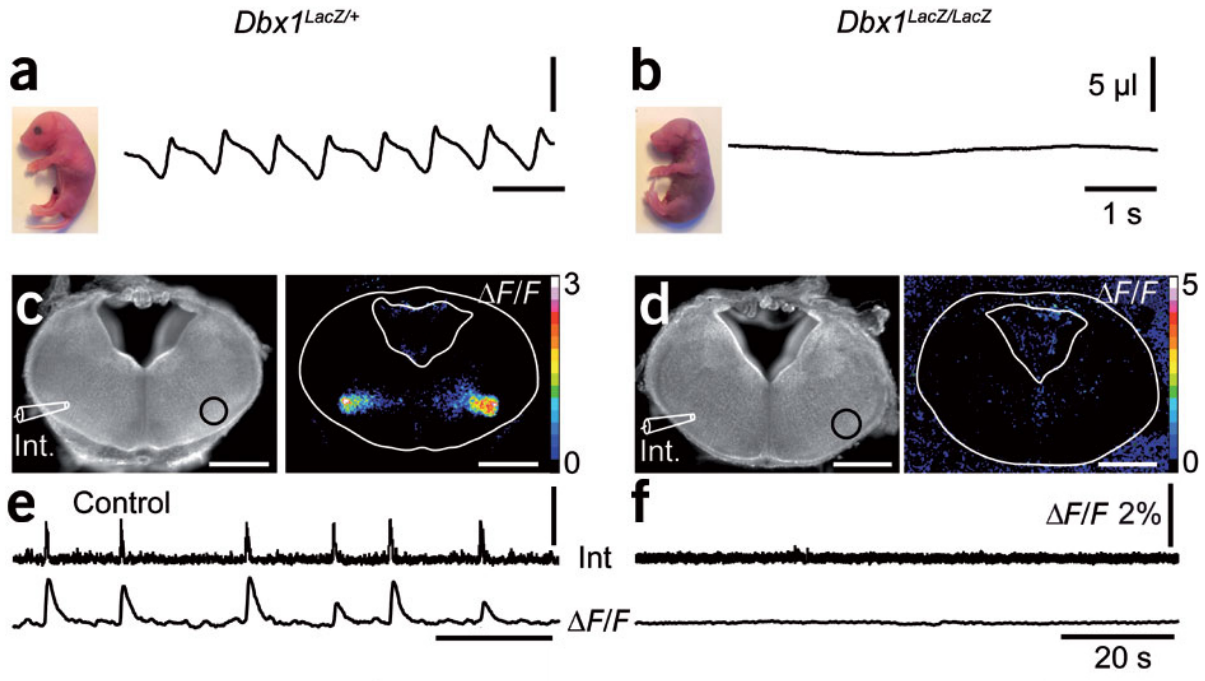

Figure 18. Respiratory activity generation from the preBötC is disrupted in the Dbx1 null mice. (a,b) Plethysmographic recording of the Dbx1LacZ/+ mice (a) E18.5 breathe normally whereas Dbx1LacZ/LacZ mutants (b) at the same age show no ventilation. (c,d) Calcium imaging of E15.5 slice preparations in WT (c) and mutants (d) shows that the bilateral rhythmic activity of the preBötC, indicated by the fluorescent changes (ΔF/F), is absent in mutant. Their corresponding electrophysiological (Int) and optical recordings (ΔF/F) are shown in e and f. Adapted from Bouvier et al., 2010.

IV.2.2 The parafacial respiratory group

The first genetic characterization for the parafacial respiratory group is that its neurons express Phox2b. The paired-like homeobox gene Phox2b is expressed in neurons with only three dorsoventral origins dA3, dB2 and vMN origins (**Figure 17**). Phox2b is expressed in all the neurons that will go on forming the visceral reflex circuits that control the digestive, cardiovascular and respiratory systems. Phox2b expression is required for survival of the cells expressing it so that Phox2b null animals miss all visceral neuronal elements (**Brunet and Goridis, 2008**; **Dubreuil et al., 2009a**; **Pattyn et al., 2000**). In the respiratory system, Phox2b is required for the development of chemoreceptive and chemoafferent visceral neurons such as the ones in carotid bodies and NTS (**Dauger et al., 2003**). It has been identified that Phox2b is expressed by RTN neurons and is required for the chemoreception to hypercapnia in adult rat (**Stornetta et al., 2006**). The Phox2b expressing neurons have also been found in the parafacial region in the neonatal and embryonic preparations, and these neurons are essential to sense the pH and CO_2 (**Dubreuil et al., 2009b**; **Onimaru et al., 2008**; **Thoby-brisson et al., 2009**), so that the e-pF in embryos, the pFRG in neonates and the RTN in adults probably correspond to distinct developmental states of a single entity. In the rest of this document independent of the developmental stage considered this structure will be referred to as the RTN. Dominant mutation of the Phox2b locus have become diagnostic for a rare respiratory syndrome in humans, the Congenital Central Hypoventilation Syndrome (CCHS) (**Amiel et al., 2003**). CCHS patients present with an abnormally high incidence of apneas at birth and severely blunted to absent response to hypercapnia, an elevation of blood P_{CO2} above a tightly regulated set point. A mouse model of CCHS bearing a human (*Phox2b*^{27Ala}) mutation recapitulated the human respiratory deficit and was found associated to a selective hypoplasia of the RTN (**Dubreuil et al., 2009b**).

Another transcription factor expressed by RTN neurons is the ladybird homeobox gene Lbx1, which defines the dB class of neurons (**Figure 17**). It has been shown that the Phox2b expressing RTN neurons have a history of Lbx1 expression, indicating their dB2 origin. In Lbx1 null mutant mice, these Phox2b expressing RTN neurons do not exist because dB2 neurons change their fate to dA3, resulting in a slow respiratory rhythm in vitro and respiratory deficits in vivo (**Pagliardini et al., 2008**). This probably corresponds to a lack of entrainment of the preBötC by the RTN. Such a lack of entrainment had been first noticed in Krox20 null animals and later experiments indeed established that the RTN was derived from

Krox20-expressing rhombomeres (**Thoby-brisson et al., 2009**). RTN neurons also express the transcription factor Atoh1 (also known as Math1) (**Rose et al., 2009**; **Ruffault et al., 2015**). Therefore, the RTN neurons coexpress Lbx1, Phox2b and Atoh1 and thus are derived from dB2 progenitor cells. A recent study has shown that loss of *Atoh1* in Phox2b+ neurons or loss of *Phox2b* in Atoh1+ neurons or loss of *vGlut2* in Atoh1+/Phox2b+ cells similarly result in functional impairment of the RTN and loss of CO_2 chemoreflex (**Ruffault et al., 2015**).

In summary, the parafacial and preBötC oscillator are two independently produced neuronal populations with the former derived from dB2 neurons probably in r5 and the latter from $V0_V$ neurons in r7 and r8. The preBötC is able to emerge and function at birth in the absence of the RTN (**Thoby-brisson et al., 2009**), the reverse is true for the RTN in the absence of the preBötC (**Bouvier et al., 2010**). These independent developmental programs are in line with a possible sequential appearance during evolution of first a visceral Phox2b-derived branchiomotor apparatus for ventilation followed later in mammals by a novel Dbx1-derived rhythmogenic center destined to control the diaphragm.

IV.3. Axon guidance cue and bilateral synchrony of respiratory behavior

IV.3.1 The Robos/Slits signaling and commissural axons

During development, different neuronal populations must be assembled and project to their proper target neurons to form a functional nervous circuit. In the developing neural tube, cells located the midline secrete several axon guidance cues that guide growing axons to their synaptic partner. Some guidance cues attract the axon such as Netrin and Shh, whereas some act as repellents such as BMP and Slit, and they function as addictive parallel signaling or crosstalking pathways (**review in Dudanova and Klein, 2013**). For commissural axons, there are two steps to make them cross the midline, pre-crossing and post-crossing. First, the commissural axons are guided towards the floor plate by dorsal repellents and ventral attractants, at this time the growth cone is not sensitive to the midline repellents. Then at the midline, axon growth cones are exposed to some permissive factors, which allow the growth cone to sense the midline repellents and to be expelled and pushed to the contralateral side,

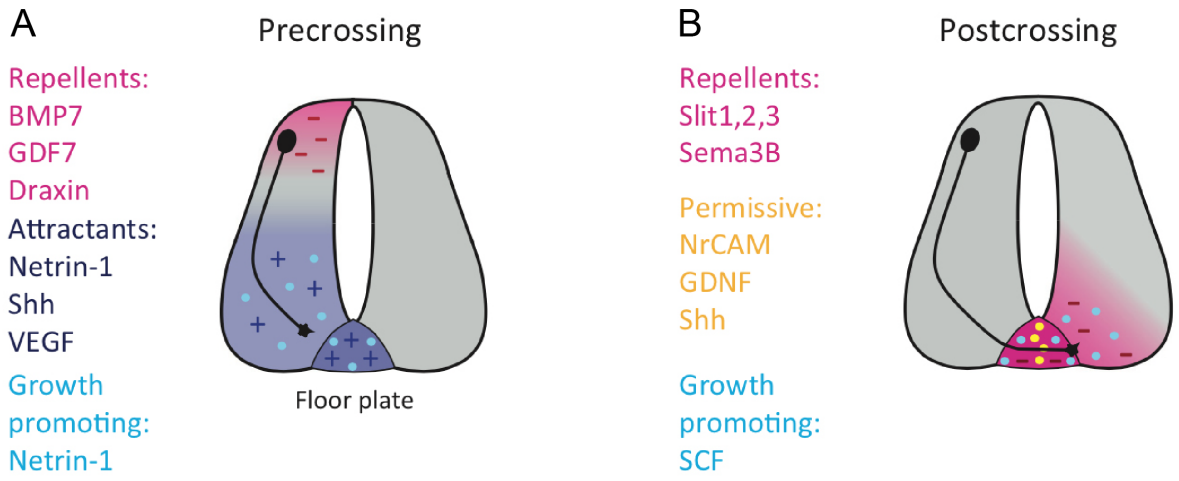

Figure 19. Axon guidance of the commissural axons. The commissural axons cross the midline in two phases, precrossing (A) and postcrossing (B). (A) Commissural axons are first guided to the floor plate by dorsal repellents (pink gradient) and ventral attractants (purple gradient). (B) At the midline, axons are exposed to the permissive molecules (yellow dots) which release them to sense the midline repellents to push the axon across the midline. At the same time, growth factors (cyan dots) promote the axon extension. Adapted from Dudanova and Klein, 2013.

and at the same time the growth factors promote the axon extension (**Figure 19**).

The Robos/Slits signaling is important for the axon pathfinding of the commissural neurons in hindbrain and spinal cord (**Marillat et al., 2004**; **Renier et al., 2010**; **Sabatier et al., 2004**). Slits are large extracellular matrix proteins secreted in the floor plate and they function as repellent guidance cue in the midline through interaction with their Roundabout (Robo) transmembrane receptors expressed in developing axon growth cone, preventing the ipsilateral axon from crossing the midline and the commissural axons from re-crossing it. In mammals, three Slits (Slit1-3) and four Robos (Robo1-4) genes have been identified (**Huminiecki et al., 2002**; **Wong et al., 2002**). Since Robo4 is only expressed in endothelial cells, it is not discussed here. In commissural neurons, expression of Robo1 and Robo2 proteins is low in pre-crossing and high in post-crossing axons, in contrast, Robo3 (also known as Rig1) protein is expressed at high level before crossing the midline and downregulated after crossing (**Long et al., 2004**; **Sabatier et al., 2004**). Robo1 and Robo2 mediate the Slit repulsion of the axon growth cone, and Robo1 has been suggested to silence the Netrin-1 attraction by interaction with Netrin receptor DCC (**Stein and Tessier-Lavigne, 2001**). However, Robo3 plays a contrary role in axon guidance, which is to inhibit the interaction of Slits with Robo1 and thus make the growth cone insensitive to the Slit repulsion

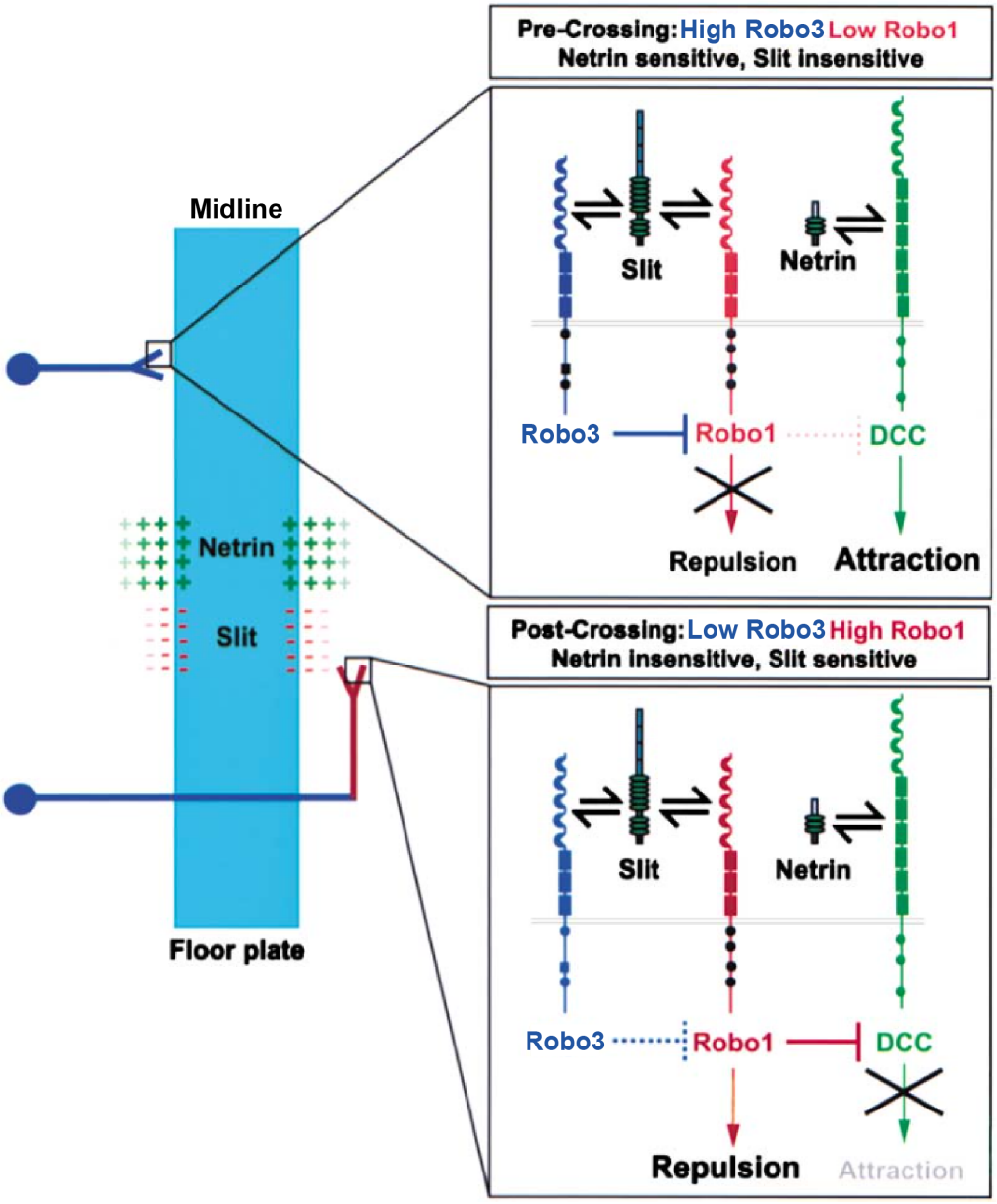

Figure 20. Model for the commissural axons cross the midline mediated by Slits/Robos signaling. Precrossing commissural axon growth cones are initially attracted to the floor plate by Netrin1 and its receptor DCC. At the midline, although the Slits repelling cue are also present, Robo3 on the growth cone membrane inhibits the Slit receptor Robo1 from exhibiting a repulsive response and a Netrin 1 attraction-silencing manner, resulting in Slit insensitive axon growth cones. After crossing the floor plate, the inhibition of Slit sensitivity is relieved due to the downregulation of Robo3 on postcrossing commissural axons and the upregulation of Robo1 expression, resulting in repellents sensitive axons, and thus the repellents expels the axons onto the contralateral side. Adapted from Sabatier et al., 2004.

but sensitive to Netrin attraction. In commissural neurons, the high level of Robo3 and low level of Robo1 expression in pre-crossing growth cones may ensure that the commissural axons sense the attractive guidance to the floor plate. And once they reach the floor plate and enter the contralateral side, the downregulation of Robo3 and upregulation of Robo1 re-instates the sensitivity of axons to Slit repellents to promote growth of the cone towards contralateral targets (**Figure 20**) (**Sabatier et al., 2004**).

IV.3.2 Robo3 and bilateral synchronized respiration

Although there are several modulations in the axon guidance, Robo3 is essential for the midline crossing of the commissural neurons both in brainstem and spinal cord. In Robo3 null mutants, axons are not able to cross midline, remain exclusively ipsilateral and the mutant mice die shortly after birth (**Marillat et al., 2004**). In humans, mutations in the Robo3 gene cause a rare syndrome named horizontal gaze palsy with progressive scoliosis (HGPPS), with which the patient is not able to perform conjugate lateral eye movements (**Jen et al., 2004**). In addition, conditional deletion of the Robo3 in specific type of neurons using cre transgenic lines results in severe functional deficits. For example, in $Krox20^{cre}$;$Robo3^{lox/lox}$ mice, Cre-mediated excision of exons 12-14 of Robo3 gene leaves truncated Robo3 proteins in neurons origin from r3 and r5. These truncated Robo3 proteins have no transmembrane and cytoplasmic domains and thus not functional, therefore commissural neurons derived from r3 and r5 lack of Robo3 signaling in their axons. In this mutant, severe reduction of commissural projections in r3 and r5 has been observed, and the mutants show abnormal eye movements and auditory brainstem responses (**Renier et al., 2010**). Interestingly, although the commissural axons are not able to cross the midline in the absence of Robo3, they still project to their normal postsynaptic partners but on the ipsilateral side (**Renier et al., 2010**). Therefore, this Cre;Robo3 strategy can be applied to dissect the function of different types of commissural neurons in specific circuits.

In the respiratory system, Robo3 is critical for its bilateral synchronized feature. Robo3 null mutants ($Robo3^{GFP/GFP}$), lacking commissural axons in the hindbrain and spinal cord, show left and right independent rhythmic C4 outputs in vitro, and the diaphragm contraction of the mutants in vivo are also left-right de-synchronized and all the Robo3 null mutants die within 8h after birth. In vitro transverse slice preparations from E15.5 Robo3 null or $Dbx1^{cre}$; $Robo3^{lox/lox}$ mutant, the preBötC neurons, which are commissural neurons derived from Dbx1

expressing p0 progenitors, are not able to project their axons to the contralateral preBötC, and left-right independent inspiratory rhythmic preBötC bursts have been observed (**Figure 21**) (**Bouvier et al., 2010**). Therefore, Robo3 is required for bilateral synchronization of respiratory behavior as well as the bilateral rhythm generation of the preBötC oscillator.

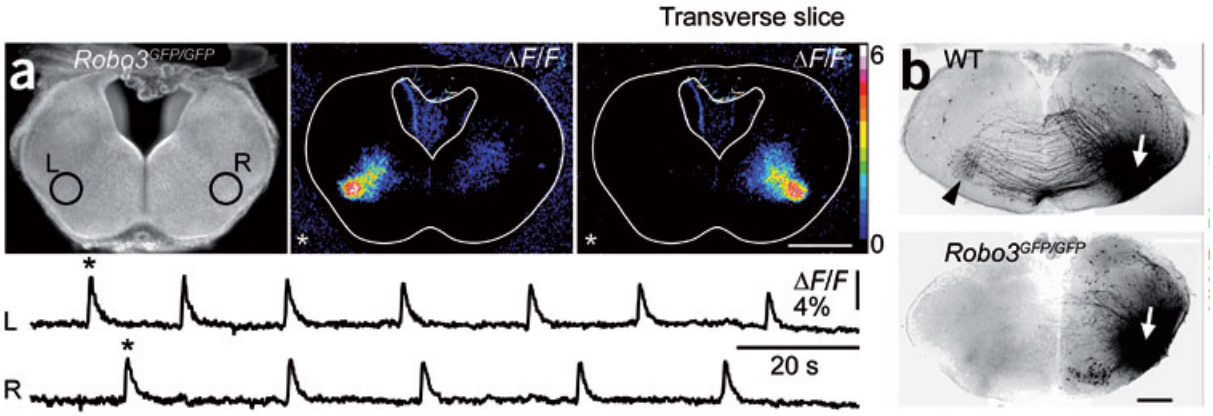

Figure 21. Left-right desynchronization of the preBötC in Robo3GFP/GFP mutants. (a) Calcium imaging of E15.5 slice preparations of Robo3GFP/GFP mice shows left (L, circle outline) and right (R, circle outline) independent burst of preBötC, indicated by the fluorescent changes (ΔF/F). Their corresponding optical recordings (ΔF/F) are shown below. (b) Biocytin injections (white arrow) in WT and Robo3GFP/GFP slices show the absence of contralateral labeled preBötC neurons. Adapted from Bouvier et al., 2010.

V. Tracing premotor neuronal circuits using genetically-modified virus

Premotor neurons (pMNs) are the interneurons that directly innervate the motoneurons and modulate their activity. Mapping the premotor neuronal circuits is important to understand the modulation and coordination of specific behavior. Although previous studies using conventional neuronal tracers and transsynaptic virus provide valuable information about the location of the premotor neurons to the phrenic motoneurons (**Dobbins and Feldman, 1994**; **Ellenberger, 1999**; **Ellenberger and Feldman, 1988**; **Feldman et al., 1985**; **Gaytán et al., 2002**; **Stornetta et al., 2003a**; **Yokota et al., 2001**), they have significant limitations such as non-specific labeling and transportation of the tracers and lacking strong criteria to discriminate mono and multi-synaptic connections. In recent years the development of gene-modified monosynaptic virus, which can be used to trace the pre-synaptic partner of cell population of interest, provides a useful tool to decipher the premotor circuits.

In this chapter, the basic knowledge of neuronal network tracing, the detailed principles of the monosynaptic tracing method to reveal the premotor network connectivity are provided, which is used in this thesis to identify the premotor inputs to inspiratory motoneurons.

V.1. Anterograde, retrograde and conventional tracers

The use of tracers to reveal neuronal network is based on the knowledge of axonal transport, which is important for the growth and survival of neurons, occurring throughout the neuronal life. Microtubules, which are cytoskeletal elements, provide the main track for axonal transport. Axonal transport proceeds in two directions- anterograde (from soma to axon terminals) and retrograde (from axon terminals to soma) depending on different motor proteins. Kinesins, the motor proteins for anterograde transport, move cargos such as neurotransmitter to the axon terminals, whereas dyneins mediate the retrograde transport (**Figure 22**) (**Hirokawa and Takemura, 2005**; **Oztas, 2003**).

Different series of markers have been developed as anterograde or retrograde tracers according to their axonal transport direction, such as the subunit B of cholera toxin (CTB), biocytin and dextran (**review in Vercelli et al., 2000**). These conventional tracers can be

applied into the region of interest to reveal the groups of neurons directly projecting to or from this region. The fluorescent conjugation on these tracers makes it easier to detect and reveal the traced cells. These tracers are still widely used nowadays because of their safe and easy application. The development of new forms of these conventional tracers allow their faster transport and brighter emission such as TMR biocytin (transportation speed of 5.4mm/h), which retrogradely labels the neurons in few hours and can be used in combination with blue-light excited calcium dyes to reveal the activity in live traced neurons (**Harsløf et al., 2015**). However, most common limitations of these conventional tracers are signal dilution and absent specificity of the labeling in relation to synaptic contacts.

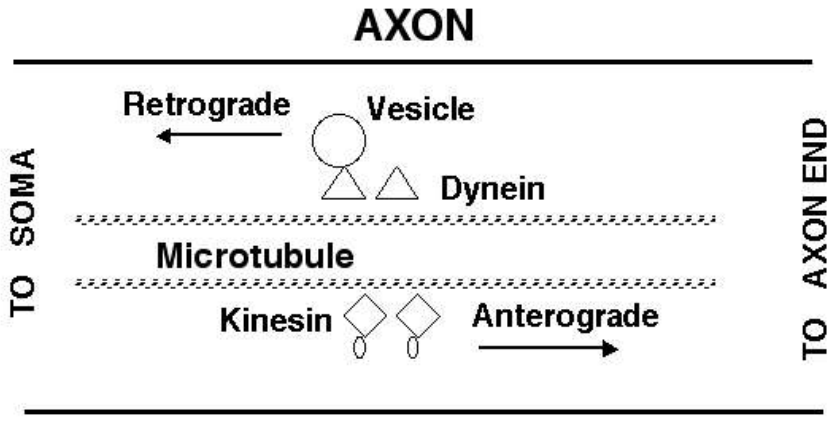

Figure 22. Molecular mechanism of axonal transport. Microtubules provide the main track for axonal transport. The motor proteins, kinesins and dyneins, move the cargos in anterograde (from soma to axon end) and retrograde (from axon end to soma) direction respectively. Reproduced from Oztas, 2003.

V.2. Transsynaptic neuronal circuit tracing with rabies virus

The limitations of conventional tracers can be overcome by the use of viral tracers. These tracers are neurotropic viruses, which have the ability to infect neurons and spread through synapses in the nervous system. Furthermore, the transsynaptic signal is amplified due to self-replication nature of viruses in the infected cells. Rabies virus is one of the most widely used viral tracers because of its synapse-restricted, retrograde directional spread in the CNS (**Callaway, 2008**; **Ugolini, 2010**, **2011**), and its somewhat limited cytotoxicity makes it useful to label the neurons without altering neuronal metabolism (**Ugolini, 2011**).

V.2.1 Rabies virus

The Rabies virus is a neurotropic enveloped virus with a cylindrical morphology, a diameter of 75nm and an average length of 180nm. It has a small negative-sense single-stranded (-ss) RNA genome about 12kb, which encodes the genes of five structural proteins: nucleoprotein (N), phosphoprotein (P), matrix protein (M), glycoprotein (G), and polymerase (L) (**Figure 23**). As an RNA virus, rabies virus completes its life cycle in the cytoplasm of the host cell. First, it binds and enters into the host cell by endocytosis. Second, the virus performs uncoating to release the viral genome by fusion of the viral membrane and endosome membrane. In the cytoplasm, the virus takes advantage of the host cell's machinery (transcription, replication and translation) to produce and amplify virion components (rabies genome, mRNA and proteins). And then, the viral components assemble to form new viral particles, which then bud and are released from the primary infected cells to spread to other neurons (**Figure 24**). (**review in Ghanem and Conzelmann, 2015; Schnell et al., 2009**)

V.2.2 Rabies glycoprotein and retrograde spread

During rabies virus life cycle, rabies glycoproteins (RG) on the surface of viral envelope play a crucial role in virus infection and trans-neuronal spread. As infection is mediated by the binding of glycoproteins with cell surface receptors, rabies can only infect cells that express receptors for RG. And its exclusive retrogradely transsynaptic nature may be explained by the enrichment of RG receptors in the presynaptic nerve terminals (**Lafon, 2005**), but the molecular mechanism of this unidirectional spread remains unclear. After entering the cell, rabies virus need to be transported from the axon to the cell body in order to process protein synthesis. This dynein-dependent axonal transport also relies on the RG, as lentiviral vectors pseudotyped with RG are transported in the same manner as rabies (**Mazarakis et al., 2001**). It is interesting that original G gene of the vesicular stomatitis virus (VSV) vectors substituted by RG gene can cross multiple synapses specifically in a retrograde direction while replaced by glycoproteins gene from lymphocytic choriomeningitis virus (LCMV) spread anterogradely (**Beier et al., 2011**), which provides definitive evidence about the essential role of glycoprotein in defining spread directionality. Also, it has been observed that the G-deficient rabies virus, which has the entire G gene deleted from the genome, is not able to be transferred from the primary infected cells to secondary neurons (**Etessami et al., 2000**). This study demonstrates that the glycoproteins are exclusively required for the transsynaptic

spread. In all, rabies virus is a useful retrograde transsynaptic tracer and G proteins play an essential role in its unidirection and transneuronal spread (**Figure 26**A).

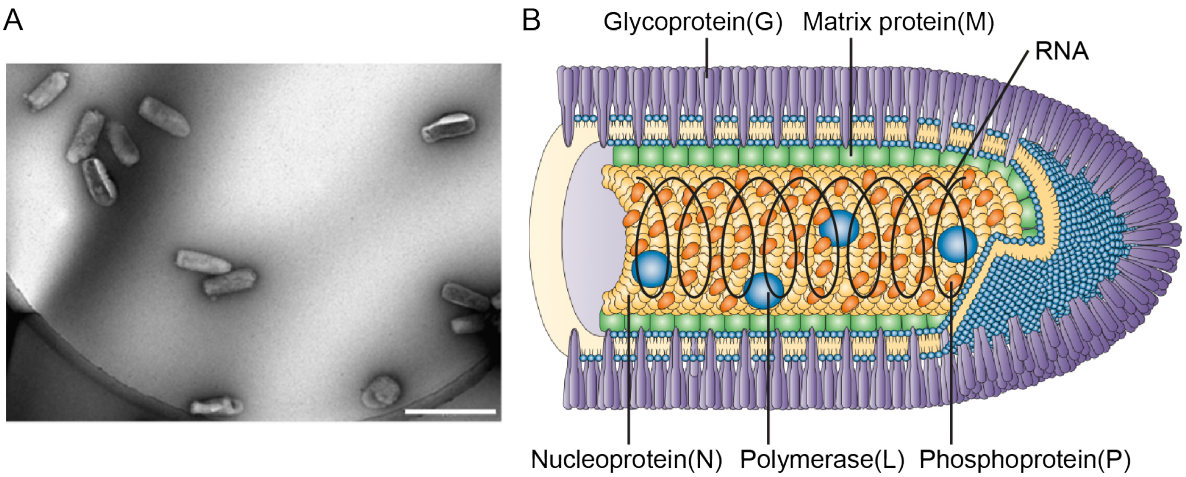

Figure 23. The rabies virus virion. (A) Electron micrographs of rabies virus particles. (B) Schematic structure of a rabies virus particle. Scale bar, 500nm. Adapted from Ghanem and Conzelmann, 2015 and Schnell et al., 2009.

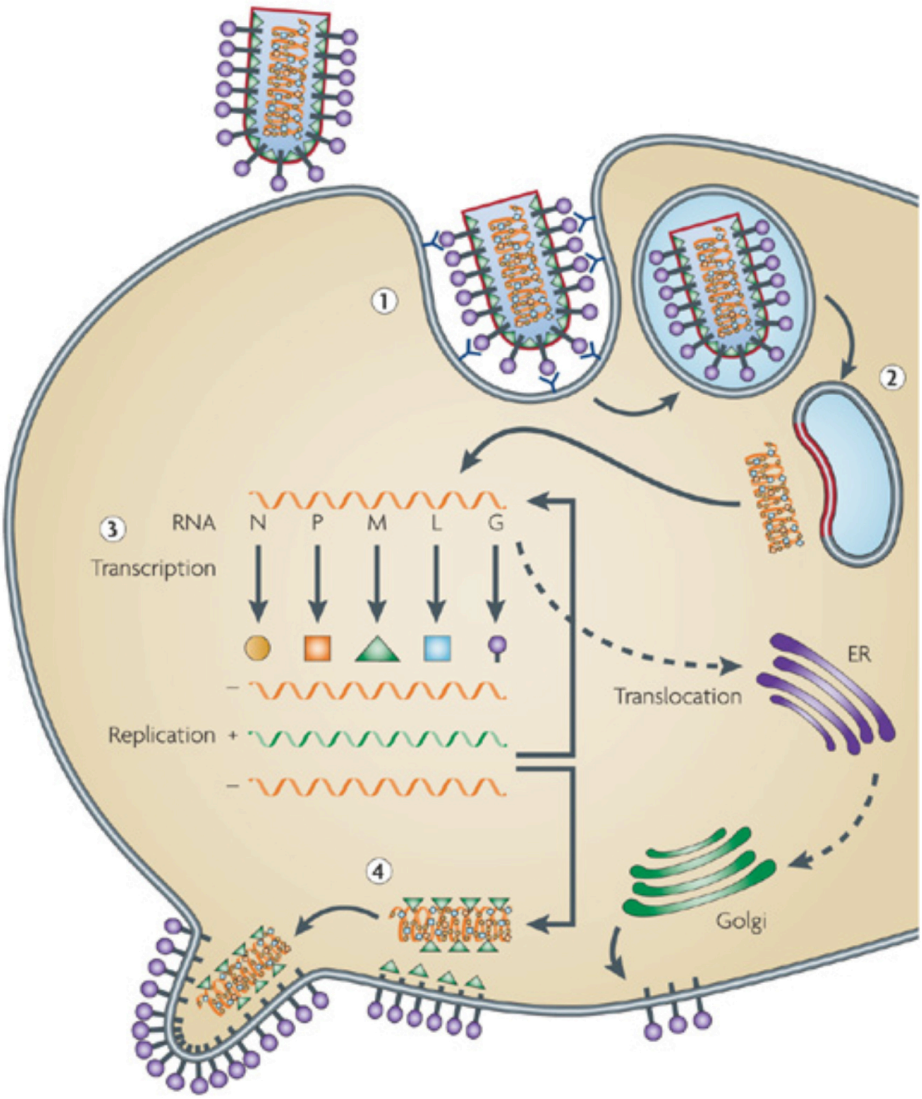

Figure 24. Life cycle of the rabies virus. Step1, binding and entry into the host cell by endocytosis; Step2, fusion of the viral membrane and endosome membrane to release the viral genome (uncoating) and; Step3, production of viral components; Step4, assembly of viral components and budding of the rabies virons to start a new cycle. Rabies glycoprotein (purple) plays essential role for viral entry and transsynaptic spread. Reproduced from Schnell et al., 2009.

V.3. Monosynaptic tracing strategy

Virus tracers are useful tools to reveal the anatomical connectivity within neuronal circuits, but they are not able to distinguish mono or multi synaptic connection due to their transsynaptic nature. To overcome this obstacle, a rabies virus-based monosynaptic tracing system has been developed in recent years **(review in Ghanem and Conzelmann, 2015; Ginger et al., 2013**), allowing the visualization of only the direct connected presynaptic partner of interested neurons. This strategy is discussed below.

V.3.1 ΔG rabies virus

Rabies has only a single gene coding for the glycoprotein (G). G gene-deficient (ΔG) rabies virus, which had the entire G gene deleted from the genome of SAD B19 vaccine strain of rabies virus, was first generated in 1996 to address the essential role of glycoprotein in rabies transsynaptic spread (**Etessami et al., 2000**; **Mebatsion et al., 1996**). In 2007, Wickersham in Callaway's lab further modified this ΔG rabies virus by replacing the full G gene with the gene encoding the enhanced green fluorescent protein (EGFP) (**Figure 25**) (**Wickersham et al., 2007a**). This ΔG rabies can infect axon terminals because the ΔG viral vectors are coated with their natural glycoproteins through prior growth in RG-expressing packaging cell lines. However, as the ΔG virus cannot synthetize the glycoproteins in the primary infected cells, newly formed viral particles are not able to spread beyond the primary infected (1st order) neurons (**Figure 26**B) (**Etessami et al., 2000**; **Mebatsion et al., 1996**; **Wickersham et al., 2007a**). This ΔG rabies is a retrograde tracer comparable to the conventional non-transsynaptic ones to reveal the 1st order neurons that project directly to the region of interest without further spread to 2nd order neurons, but due to its self-amplification nature, the EGFP levels are high enough to visualize the detailed morphology of the infected neurons including the fine cellular process of terminals and dendrites.

V.3.2 Monosynaptic tracing using ΔG rabies virus

In order to understand the detailed construction of complex neuronal circuits, a new method based on the ΔG rabies was developed in Callaway laboratory (**Wickersham et al., 2007b**) to reveal only the 2nd order neurons directly connect to the 1st order neurons, which is a breakthrough in the circuit mapping. ΔG rabies cannot spread beyond the infection of 1st order neurons as described above, however, when the infected cells are able to express G

(G-complementation) by gene-transfer methods, the ΔG rabies can then incorporate the G on its envelop and spread from the primary infected (1st order) neurons to the 2nd order ones without further spread because of the lack of G in the 2nd order neurons (**Figure 26**C), which makes it a monosynaptically restricted transsynaptic tracer to reveal the presynaptic partner of the neurons of interest.

There are different gene-transfer methods to provide G complementation in the 1st order neurons, such as electroporation of G-gene vector (**Wickersham et al., 2007b**), use of helper herpes or adeno-associated viruses (**Esposito et al., 2014**; **Stepien et al., 2010**; **Yonehara et al., 2013**) and Cre/loxP transgenesis mouse system (**Stanek et al., 2014**; **Takatoh et al., 2013**). And by combination with the EnvA/TVA system, in which ΔG rabies is pseudotyped with an avian retrovirus glycoprotein (EnvA) infecting only the neurons that express EnvA-receptor, TVA, which is only expressed in birds and never in mammals in nature, the infection can be restricted to specific class of neurons to reveal their presynaptic partner (**Wickersham et al., 2007b**). Also, many new ΔG rabies variants have been generated by replacing the G gene with other genes to better study the infected neurons, such as the mCherry for red color fluorescent, GCaMP3 for Calcium imaging and Channelrhodopsin-2 for photoactivation (**Osakada et al., 2011**).

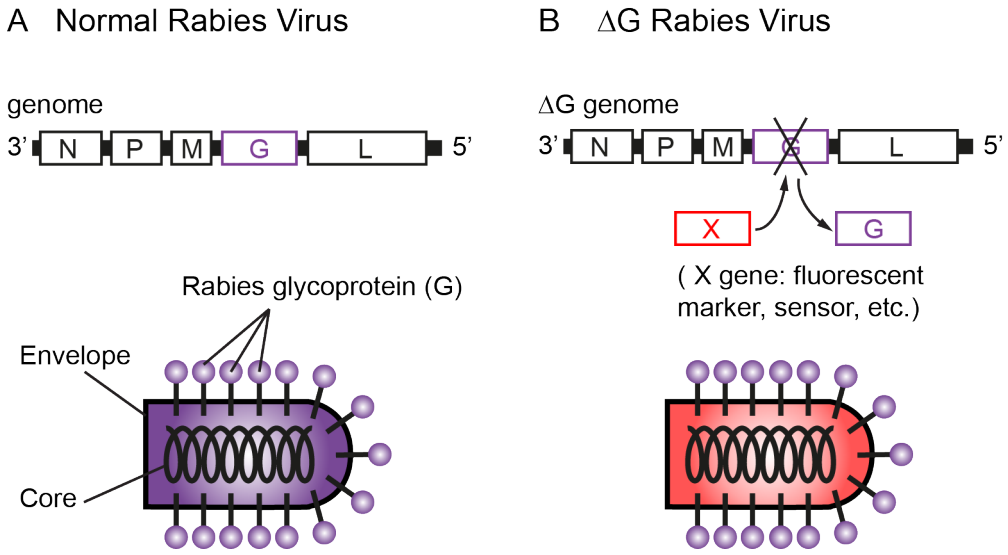

Figure 25. ΔG rabies virion. The G gene in the genome of wild type rabies virus (A) is replaced by a gene of interest encoding fluorescent protein such as GFP and mCherry to better visualize infected neurons, or biosensors to visualize/manipulate neuronal activity and etc. (B).

V.4. Mapping premotor neuronal circuits

In 1925, Sherrington described the motor unit as consisting of a motor neuron, its axon and the muscle fiber it innervates. The motor unit is thus the smallest functional unit in a motor system (**Liddell and Sherrington, 1925**). In 2010, a new method, building on the motor unit of Sherrington, was developed in Silvia Arber's lab to adapt the monosynaptic tracing to reveal the premotor neurons projecting to specific motoneuron pools (**Figure 26**D) (**Stepien et al., 2010**). By injecting a muscle with ΔG rabies coated with original G, specific motoneurons (1^{st} order) can be infected. To deliver G in the same motoneurons, adeno-associated virus (AAV) serotypes 6 modified to carry the G gene was coinjected in the same muscle. AAV is a replication-defective virus, which is able to infect the neurons and incorporate its genes to the genome of host cells but is not able to replicate or spread without the presence of its helper virus-adeno virus. AAV serotypes 6 vectors injected in muscles can deliver genes to motoneurons through retrograde infection of axon at the neuromuscular junctions (**Salegio et al., 2012**; **Towne et al., 2010**). Therefore, G protein can be expressed only in the motoneurons to allow ΔG rabies complementation and spreading to premotor neurons (2^{nd} order). By using this method, in recent years, different premotor circuits controlling specific muscle contraction or coordinate different behaviors have been revealed with high specificity (**Esposito et al., 2014**; **Stanek et al., 2014**; **Takatoh et al., 2013**).

In the respiratory system, the premotor neurons controlling inspiratory motor command are still largely unknown. In this thesis, I injected this virus cocktail in the diaphragm and tongue to infect the phrenic and upper airway motoneurons to visualize their premotor neurons respectively. I combined this monosynaptic tracing method with the Cre-reporter lines to locate the positions of phrenic premotor neurons and identify their developmental origin and through conditional invalidation of Robo3 estimate their contribution to bilateral synchronicity of the inspiratory motor drive.

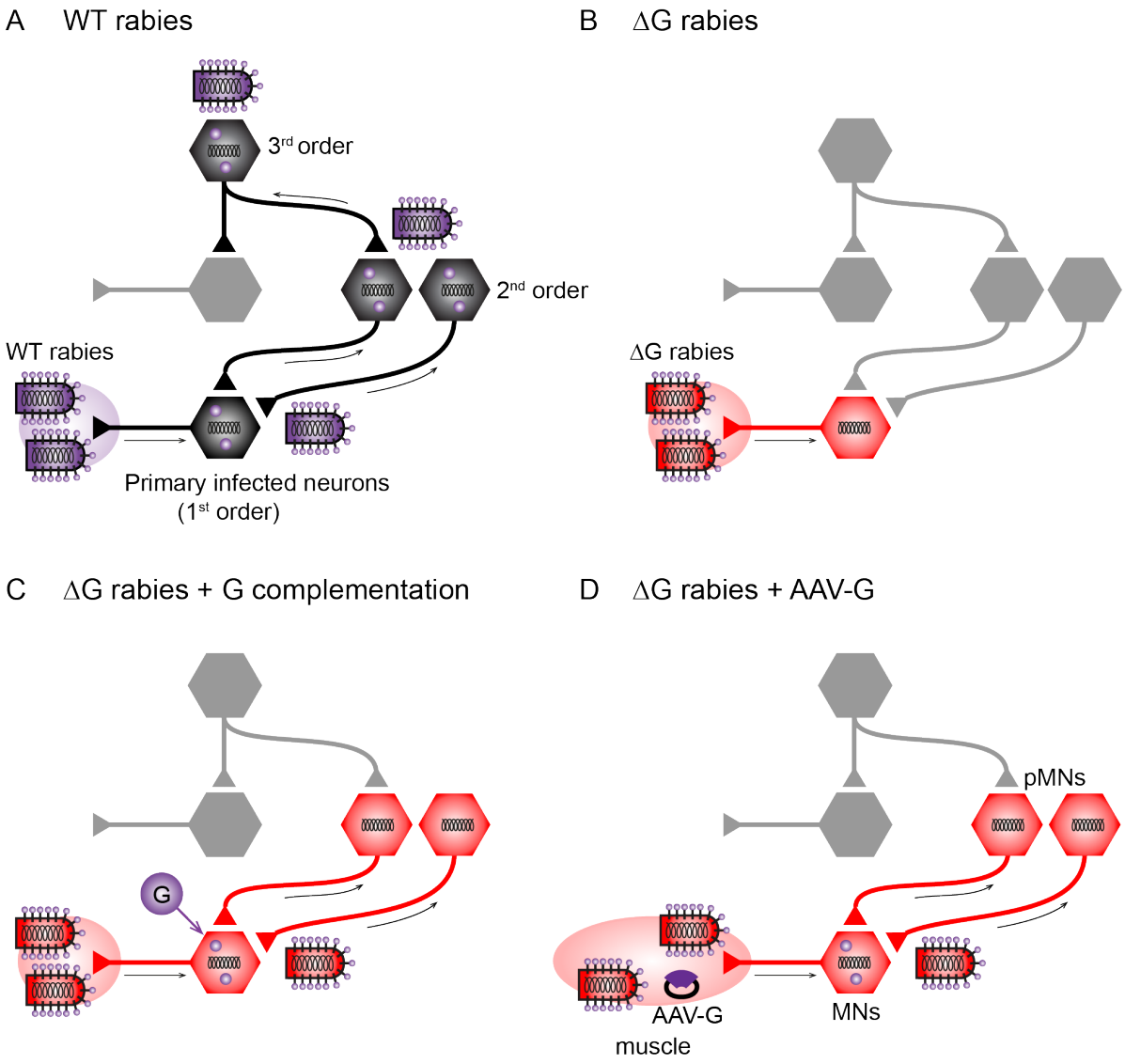

Figure 26. Virus tracing strategy. (A) Rabies virus is able to cross multiple synapses in exclusively retrograde direction in the CNS. (B) G deletion (ΔG) in the genome of rabies virus is sufficient to prevent its transsynaptic spread and results in monosynaptic-restricted vector, which stays in the primary infected neurons (1st order). (C) When 1st order neurons are able to express G (G-complementation) by gene-transfer methods, the ΔG rabies can then incorporate the G on its envelop and spread from 1st order neurons to the 2nd order ones without further spread because of the lack of G in the 2nd order neurons. (D) To perform G-complementation in the motoneurons (MNs), AAV carrying the G gene is coinjected with ΔG rabies in the muscle, thus G protein can be expressed only in the motorneurons to allow ΔG rabies spreading to premotor neurons (pMNs).

THESIS OBJECTIVE

My work is a contribution to the general goal of determining the relationship of defined neuronal subtypes to the organizational logic of interneuron circuitry. More precisely, I'm interested in testing whether individual neuronal subsets can reveal new aspects of the functional logic of interneuron networks controlling breathing.

I focus my attention on phrenic premotor neurons, with yet undefined subtype identities, that interface the inspiratory rhythm generator with the motor neurons innervating its main effector muscle, the diaphragm. Using a monosynaptic viral tracing strategy combined to mouse genetics tools my work investigates the following questions:

1. What is the anatomical distribution of phrenic premotor neurons in early postnatal mice?
2. What is the axonal projection profile of these neurons?
3. Which types of progenitor cells give rise to phrenic premotor neurons?
4. Do premotor neurons contribute to bilateral contraction of the diaphragm?

My data demonstrate the prominent role of V0 type interneurons in the architecture of the executive control circuit for inspiration. These data may bear relevance to evolution of breathing strategies in tetrapods for which motorizing the diaphragm is a "central" problem.

MATERIALS AND METHODS

This section provides basic principles and procedures of the methods used in this thesis. Only methods performed by the author of this thesis are presented.

I. Mouse strains

All the experiments presented in this thesis were conducted on mice. Transgenic mouse is a valuable tool to study gene function. In this thesis, I mainly took advantage of the Cre/lox system to drive expression of reporter molecules such as LacZ, insert light-gated channelrhodopsin (ChR) in the cells to control electrical excitability, or generate a conditional knockout of the gene. The mouse strains used in the thesis are described in **Table 1**. And transgenic mice were genotyped by PCR using the primers described in **Table 2**.

I.1. Cre/lox system

Cre/lox is a site-specific recombinase technology, which allows DNA modification on specific cell type or to be triggered by specific external stimulus. Cre protein is a site-specific DNA recombinase that recognizes a pair of 34 bp sequence named loxP. When cells that have loxP sites in their genome express Cre, DNA recombination can occur between two loxP sites. Placing the loxP sequence properly allows gene of interest to be activated, suppressed or replaced by other genes. The Flp/FRT system is very similar to the Cre/lox recombination system.

I.2. CreER/lox system

To add inducibility to the Cre/lox system, a ligand-dependent Cre recombinase name CreER has been developed (**Feil et al., 1996**, **1997**, **2009**). CreER is a Cre fusion protein with a tamoxifen- responsive Estrogen Receptor ligand-binding domain. The administration of tamoxifen confers a conformational change on CreER, which allows it to be translocated to the nucleus where it induces recombination between loxP sites (**Figure 27**). By combining tissue-specific expression of a CreER with its tamoxifen-dependent activity, the splicing of floxed DNA sequence can be controlled both in space and time. In addition, this CreER/lox system can be used to limit temporally Cre- recombination in relation to its expression dynamics for instance to alleviate early spurious ubiquitous expressions during development.

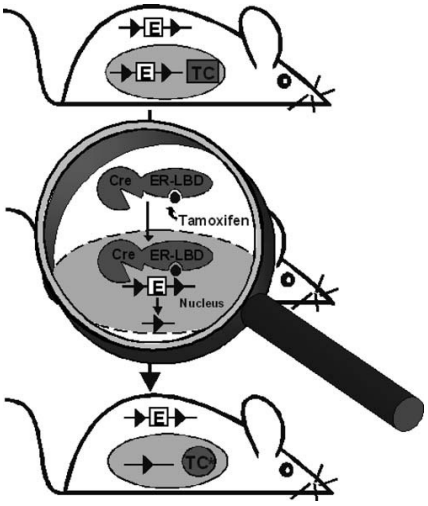

Figure 27. CreER/lox system. Inducible gene inactivation is based on tamoxifen-inducible excision of a loxP (triangle)-flanked exon (E) in cells expressing a tamoxifen-dependent CreER recombinase (TC). TC consists of Cre fused to a mutated ligand-binding domain (LBD) of the estrogen receptor (ER). In the absence of tamoxifen, CreER is retained in the cytoplasm. Binding of tamoxifen to the LBD results in the translocation of TC into the nucleus, where it can recombine its loxP-flanked DNA substrate. Reproduced from Feil et al., 2009.

	Locus	**Transgenic description**	**Ref.**
$Dbx1^{cre}$	Dbx1	Insertion of an IRES-CRE-pGK-Hygro cassette into the BamHI site in the 3'UTR of the Dbx1 gene	(**Bielle et al., 2005**)
$Dbx1^{creER}$	Dbx1	Insertion of an IRES-CreERT2 cassette into the 4th exon of Dbx1.	(**Hirata et al., 2009**)
$Dbx1^{LacZ}$	Dbx1	An nlsLacZ/pGKneo cassette replaces the Dbx1 coding sequence	(**Pierani et al., 2001**)
$Wnt1^{cre}$	Wnt1	cDNA for Cre was placed under the control of the Wnt1 enhancer	(**Danielian et al., 1998**)
$Lbx1^{cre}$	Lbx1	Cre sequences replace exon 1 of Lbx1	(**Sieber et al., 2007**)
$En1^{cre}$	En1	Insertion of a Cre PGK-neopA cassette to exon 1 of En1	(**Sapir et al., 2004**)
$Sim1^{cre}$	Sim1	Cre cassettes were inserted into the 1st exon of the Sim1 gene	(**Zhang et al., 2008**)
$vGlut2^{cre}$	vGlut2	Ires-Cre cassette were inserted just after the vGlut2 stop codons	(**Vong et al., 2011**)
$vGAT^{cre}$	vGAT	Ires-Cre cassette were inserted just after the vGAT stop codons	(**Vong et al., 2011**)
$Robo3^{lox/lox}$	Robo3	Exons 12-14 were flanked with loxP sites	(**Renier et al., 2010**)
ChR2-Tdt	Rosa26	ChR2 (H134R)-tdTomato was cloned into a Rosa26-pCAG-LSL-WPRE-bGHpA targeting vector, between LSL and WPRE sequences. LSL sequence contains loxP-stop-loxP	(**Madisen et al., 2012**)
$Tau^{SynGFP\text{-}nlsLacZ}$	Tau	A loxP-stop-loxP-synaptophysin-GFP-Nls-lacZ-pA targeting cassette was integrated into exon 2 of the Tau locus	(**Tripodi et al., 2011**)

Table 1. Transgenic mouse lines used in this thesis.

Mouse strain	Sequence detected	Primers (5'>3')	Band size (bp)	Tm (ºC)
cre line	Cassette	Sense:GTCCAATTTACTGACCGTACACC	WT:ø Mut:706	62
		Antisense:GTTATTCGGATCATCAGCTACACC		
$Dbx1^{creER}/Dbx1^{cre}$	Cassette	TGGAAACTGGAGAGGGAACGC	WT:ø Mut:743	60-62
		TGTCCATCAGGTTCTTGCGA		
$Wnt1^{cre}$	Cassette	TAAGAGGCCTATAAGAGGCGG	WT:ø Mut:500	62
		AGCCCGGACCGACGATGAA		
$Robo3^{lox}$	Cassette	CCAAGGAAAAACTTGAGGTTGCAGCTAG	WT: 150 Mut: 200	62
		GATTAGGGGAGGTGAGACATAGGG		
$Dbx1^{LacZ}$	neo	GATCGGCCATTGAACAAGATG	WT:ø Mut: 100	66
		AGAGCAGCCGATTGTCTGTTG		

Table 2. Primers used for genotyping. Mut: mutated sequence. Tm: optimal hybridization temperature for a primer pair.

II. Tamoxifen administration

Tamoxifen is an antagonist of the estrogen receptor and it is used to activate the CreER recombinase in the CreER/lox system.

II.1. Oral gavage

The oral gavage of tamoxifen was used in this thesis because it gives more robust recombination with less embryonic toxicity. For our $Dbx1^{CreERT2}$, we administer 2-4mg Tamoxifen (20mg/ml in corn oil) per 30g pregnant mouse at embryonic day 10.5 to cause massive Cre-Lox recombination.

II.2. Litter fostering after tamoxifen gavage

Because tamoxifen blocks the action of estrogen, the pregnant mice with tamoxifen administration are not able to give birth to the pups naturally or eat them after delivery. Therefore proper litter fostering is required to obtain pups in postnatal stage.

Swiss CD-1 is a good foster mother line. The foster mother must have a healthy and well-fed litter of her own that is one or two days older than the fostered litter pups. At embryonic day 18.5, the pups to be fostered are taken out from the donor mother by caesarean section, this step must be done as fast as possible. Once all the pups are removed, the amniotic fluid on each pup should be clean off by soft rotation on a clean paper. A light

pressure should be put on the chest of the pups and the fluid that bubbles out from the mouth should be cleaned out. It is important that the pups are put on a warm surface and kept under massaging until a regular breathing is established (the skin will turn pink). Then the fosterlings should be placed with the nest material or bedding from the cage of foster mother to acquire adequate odor prior to placement with the foster mother. Note that displacement of the foster mother's nest is detrimental. The next day, if the foster mother is feeding the pups, the litter fostering is successful.

III. Retrograde labeling by dextran

Dextrans are hydrophilic polysaccharides characterized by their good water solubility and low toxicity. They are widely used as anterograde and retrograde neuronal tracers according to their molecular weight and different conjugations. The 3000MW dextran is preferentially transported retrogradely with fast speed in alive tissue (**Fritzsch, 1993**).

To reveal the phrenic premotor neurons at embryonic stage, hindbrain-spinal cord of E15 mouse was dissected out and kept in artificial cerebrospinal fluid (aCSF) (see Materials and Methods VIII.1) and a cut was made at the ventral lateral part of cervical level 4 (C4) of the spinal cord to facilitate tracer uptake. Then 3000MW TRITC dextran crystals (D3308, Molecular Probes) were applied to the cut and were incubated in the oxygenated (95% O_2, 5% CO_2) aCSF at RT. After 12h, samples were fixed, embedded and sectioned.

IV. Monosynaptic labeling of premotor neurons by virus

For diaphragm muscle injections, P1 mice were anesthetized by hypothermia. To inject virus in the diaphragm, an incision (~5 mm) was made in intercostal muscles between the 9th and 10th ribs of anesthetized P1 mice to visualize the diaphragm. Then 2µl of virus cocktail (1µl ΔG rabies-mCherry/GFP titered ~1e+8 and 1µl AAV6-G titered ~3e+12) was slowly injected into the costal part of the hemi-diaphragm by using a microinjector (Picospritzer III, Parker, USA) equipped with a pulled fine glass capillary (tip diameter 10µm). After the injections, the ribs and the skin were carefully sutured (B7718, Ethilon), placed on a warm surface until regular breathing was fully restored and put back with their mothers. At 8 days post injection, animals were sacrificed and samples were collected at P9. To trace the hypoglossal premotor neurons, similar injections were made in the genioglossus muscle of the

tongue of P1 mice.

V. Tissue processing

For E15 embryos, brains were dissected out and fixed in 4% paraformaldehyde (PFA) for 4 hours at 4ºC and cryoprotected 24 hours in 30% sucrose/PBS at 4°C. The brains were incubated with 1:1 30% sucrose/PBS: OCT (Optimum Cutting Temperature compound, Tissue-Tek) for 2 hours at 4ºC and followed by 1 hour in pure OCT. Then the brains were embedded in the OCT and sectioned on a cryostat with the thickness of 20µm.

For P9 pups, animals were deeply anesthetized with ketamine (100 mg/kg)/xylazine (10 mg/kg) by IP injection and transcardially perfused with PBS followed by 20ml ice-cold 4% PFA. Then the brains were dissected out and postfixed in 4% PFA for 24 hours at 4°C and cryoprotected 48 hours in 20-30% sucrose/PBS at 4°C. Then the brains were embedded in the OCT and 20~60µm sections were made on a cryostat.

VI. Immunostaining

Immunostaining takes advantage of antigen-antibody binding reaction to detect the localization of proteins in tissues, cells and subcellular compartments.

The immunostaining procedures are described as follows: cryostat sections were washed with PBST (0.2%Triton-X100 in PBS) for 3 times (10min each) at room temperature (RT) and incubated with blocking buffer (0.2%Triton-X100 and 1%FCS in PBS) 1h at RT. Sections were then incubated with primary antibodies diluted with blocking buffer at 4°C. After 1~3 days, sections were washed with PBST 3 times (10min each) and then incubated with appropriate secondary antibodies with blocking buffer overnight at 4°C. The next day, sections were washed with PBST 3 times and mounted with Vectashield. Primary antibodies used in this study are described in **Table 3** and the secondary antibodies in **Table 4**.

For the embryonic and neonatal 20µm sections, the immunostaining was processed on the slides, whereas the 60µm neonatal sections (floating tissue sections) were incubated with antibodies in individual wells and mounted for imaging in serial order.

Species	Antigen	Company	Final concentration
Chicken	GFP	Aves Labs	1/2000
Rabbit	GFP	Invitrogen	1/2000
Chicken	ßgalactosidase	Millipore	1/2000
Goat	ChAT	Millipore	1/100
Rabbit	RFP	Rockland	1/1000
Rat	RFP	ChromoTek	1/1000
Rabbit	Pax2	Covance	1/300
Rabbit	Tlx3	Gift from C.Birchmeier	1/5000
Rabbit	Phox2b	Gift from JF Brunet	1/500
Rabbit	NK1R	Sigma	1/5000

Table 3. Primary antibodies used in this thesis.

Host	Target species	Fluorescent probe	Company	Final concentration
Donkey	Chicken	Alexa 488	Jackson IR	1/1000
Donkey	Chicken	Cy5	Jackson IR	1/400
Donkey	Goat	DyLight 405	Jackson IR	1/200
Donkey	Goat	Alexa 488	Molecular Probes	1/250
Donkey	Goat	Cy5	Jackson IR	1/400
Donkey	Rabbit	Alexa 488	Molecular Probes	1/400
Donkey	Rabbit	Cy3	Jackson IR	1/1000
Donkey	Rabbit	DyLight 649	Jackson IR	1/500
Donkey	Rat	Cy3	Jackson IR	1/500

Table 4. Secondary antibodies used in this thesis.

VII. Image acquisition and cell counting

Fluorescent images were examined and captured on a Leica TCS SP8 confocal microscope. Full-field views of sections were acquired using a 10x objective with the tile scan function. For the co-localization analysis, Z-stack images were obtained using 25x, 40x and 63x objective.

Rabies labeled phrenic premotor neurons in each of the brainstem areas were counted manually through 60 µm serial sections and 6 mice were used for this quantification. Each nuclei was defined by "The Mouse Brain in stereotaxic coordinates" (Paxinos et Franklin, Academic press). At P9, the three subdivisions of ventral respiratory column (VRC), BötC, preBötC and rVRG, were defined by using previously determined anatomical criteria (**Ellenberger, 1999**; **Ellenberger and Feldman, 1990**), the shape of related nucleus ambiguus (nA) and distance from the caudal end of facial nucleus(VII) (**Figure 28**). The BötC located caudal to the caudal end of VII and ventral to compact formation of nA (nAc). The preBötC were caudal to the BötC and ventral to the semicompact formation of nA (nAsc), started from 300-350µm caudal to caudal end of VII. The rVRG, which was caudal to preBötC, extended from the level of area postrema (AP)(550-600µm caudal to caudal end of VII) to rostral pyramidal decussation (PyX) and it was ventral to the loose formation of nA (nAls) and intermingled with external formation of nA (nAex). Final results were presented as the percent of total labeled premotor neurons within sample, thus normalizing each value to the tracing efficiency.

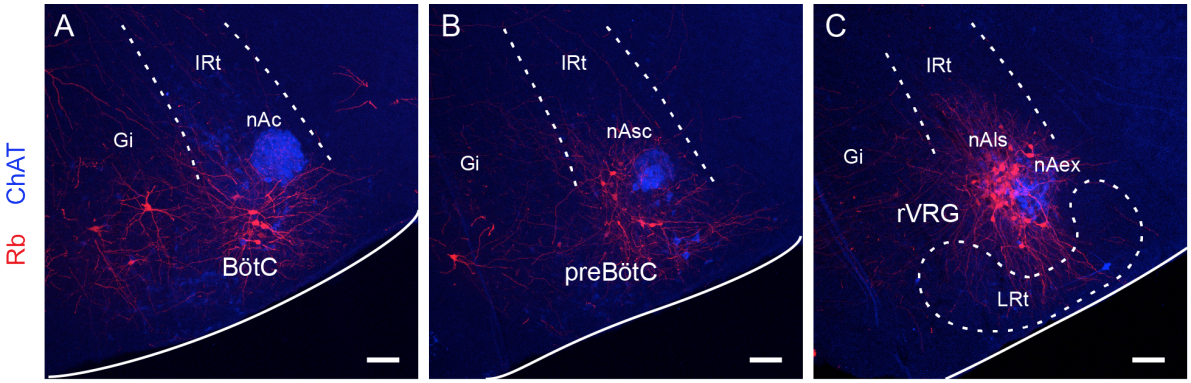

Figure 28. Anatomical definition of BötC, preBötC and rVRG in neonatal mice. (A) The BötC located ventral to compact formation of nA (nAc). (B) The preBötC is ventral to the semicompact formation of nA (nAsc). (C) The rVRG, is caudal to preBötC and ventral to the loose formation of nA (nAls) and intermingled with external formation of nA (nAex). Scale bars, 100µm.

The quantification of co-localization was preformed in Imagej with the "cell-counter" plugin. In order to obtain confident estimation, we only counted neurons with complete cell body volumes in analyzed section.

VIII. In vitro study of respiratory activity

VIII.1. In vitro preparation

A respiratory-like rhythmic activity is maintained in vitro in isolated brainstem-spinal cord en-bloc and transverse slice preparations bathed in artificial cerebrospinal fluid (aCSF) (**Smith et al., 1991**; **Suzue, 1984**). Therefore, in this thesis, we used en bloc / slice preparations from E15 embryos and P0 pup mice to perform calcium imaging, photostimulation and electrophysiological recording to investigate the respiratory activity in vitro. Briefly, the brain of E15 or P0 mice was dissected out in an ice cold, oxygenated (95% O_2, 5% CO_2) aCSF containing (in mM): 128 NaCl, 8 KCl, 1.5 $CaCl_2$, 1 $MgSO_4$, 24 $NaHCO_3$, 0.5 Na_2HPO_4, 30 glucose, pH 7.4. Three reduced preparations were used in my experiments:

The brainstem-spinal cord preparation contained the pons, medulla and proximal cervical segments of the spinal cord (up to C6). The pia mater was removed from the ventral surface of the brainstem in calcium imaging experiments.

For **caudal brainstem-spinal cord preparation**, the E15 brainstem-spinal cord was mounted in an agar block, and a cut (600-650µm caudal to the end of facial nucleus) was made by vibratome (Leica VT1000S) to remove the part rostral than rVRG. Then the agar surrounding the spinal cord was carefully removed without disrupting the agar around the brainstem to facilitate the horizontal exposure of the transverse plane containing the rVRG for optimal orthogonal photostimulation using digital holography through the microscope objective.

For **the preBötC slice**, the E15 brainstem-spinal cord was mounted in agar and serially sectioned by vibratome in the transverse plane from rostral to caudal until the end of the facial nucleus was reached. Using this as a landmark, we further removed a 300 µm-thick slices prior to cutting the 450-µm-thick physiological slice that exposes the preBötC and XII at its rostral surface.

VIII.2. Calcium imaging

Calcium imaging, allows visualization of neural activities, uses fluorescent indicators to monitor changes of intracellular free calcium concentrations, which the membrane-related electrical activity is tightly coupled to.

To monitor the neuronal activity at E15, embryonic en bloc brainstem-spinal cord / slice preparation was incubated for 40min at room temperature with an oxygenated loading solution containing 10µM cell permeable calcium indicator Calcium Green 1AM (C3012, Molecular probes), 2% (v/v) DMSO and 0.2% (v/v) Cremophore EL. After incubation, the preparation was transferred to a recording chamber with the ventral or rostral surface up and 30 min of recovery period was required to wash out the excess dye before monitor any calcium activity.

A conventional epi-fluorescence configuration with a FITC filter cube was used to excite the dye and capture the emitted light. Fluorescence images were captured during periods of 60–180s with a cooled Neo sCMOS CCD camera (ANDOR technology, UK) with an exposure time of 100 ms and bin size of 4 x 4 using Micro-Manager software (https://www.micro-manager.org/ wiki/). The time-series acquisitions were analyzed using custom-made ImageJ software PhysImage (http://physimage.sourceforge.net/) and presented as relative fluorescence changes (ΔF/F).

VIII.3. Photostimulation

Optogenetic is a biological technique that uses light to control neurons that have been genetically modified to express light-sensitive ion channels. Channelrhodopsin 2 (ChR2) is one of the most commonly used fast light-gated cation channels to depolarize membranes of excitable cells with light. In optogenetic experiments, photostimulation was provided by digital holography, where the wavefront of a 473-nm laser was modified by a programmable spatial light modulator (SLM), to re-orient the direction of light propagation onto spatially pre-defined targets (**Lutz et al., 2008**). The laser power density was set to 1–5 mW/mm^2 and individual light pulses of 50ms duration were triggered at random time intervals.

VIII.4. Electrophysiological recordings

Electrophysiological activities were recorded using suction electrodes (tip diameter: 40-160µm) placed on phrenic cervical C4 roots in isolated brainstem spinal cord preparations or on the surface of the hypoglossal motoneurons exposed in transverse slice preparations. The recording chamber had a volume of 2ml and temperature of 30ºC and was constantly perfused with preheated oxygenated (95% O_2, 5% CO_2) aCSF at 30°C at a rate of 2ml/min.

Glass pipettes were pulled from glass tubes (120F-10, Harvard apparatus, USA) using a P97 micropipette puller (Sutter Instruments, USA) and filled with aCSF and connected to an amplificatiuon chain through silver/chloride wire. Nerve or field recording signals were amplified (High-gain AC, 7P511, Grass Technologies, Warwick, RI), filtered (bandwidth 0.3–10 kHz), integrated (time constant 50ms, Neurolog System, Digitimer Ltd, Hertfordshire, UK) before digital sampling at 6 kHz and analysis using pClamp9 (Molecular Devices).

IX. In vivo study of the breathing pattern by plethysmography

Ventilation at birth was monitored using whole-body flow plethysmography (**Chatonnet et al., 2007**), which is a modified barometric method to non-invasively measure the pulmonary ventilation in unrestrained, unanaesthetized animals. Basically, it records the changes of pressure in the chamber generated during breathing. During inspiration, the air inspired from the container into the lungs is warmed and humidified, therefore the total pressure in the animal chamber increases, whereas the opposite occurs during expiration. These changes in chamber pressure can be monitored by a sensitive pressure transducer, and calibrated for tidal volume measurements with appropriate conversion factors.

For neonates, the plethysmograph chamber (30 ml) equipped with a temperature sensor was connected to a reference chamber of the same volume. The pressure difference between the two chambers was measured with a differential pressure transducer connected to a sine wave carrier demodulator. The spirogram was stored on a computer using a Labmaster interface at a sampling frequency of 1 kHz (**Figure 29**). Calibrations were performed at the end of each recording session by injecting 2.5µl of air in the animal chamber with a Hamilton syringe.

Plethysmographic recording were performed within 12h after the birth. P0 mice were removed individually from the litter and placed in the plethysmograph chamber, in which the temperature was kept at 30ºC during the recording period (300 s). For each pup, the periods of

quiet breathing were identified by the absence of limb or body movements, during which the breathing parameters (duration of inspiration [Ti, in s] and expiration [Te, in s], breath duration [T_{TOT}, in s], tidal volume [V_T, in µl/g], and ventilation [$V_E = V_T / T_{TOT}$ in µl/s/g]) (-**Figure 30**) were measured and analyzed using Elphy (developed by Gérard Sadoc at UNIC, CNRS). Frequency plots were used to compare the breathing parameter distribution of control and mutants pups. Density maps were made to relate T_{TOT} and V_T pattern by using a Python based plugin developed by Alexandre Kempf (UNIC, CNRS).

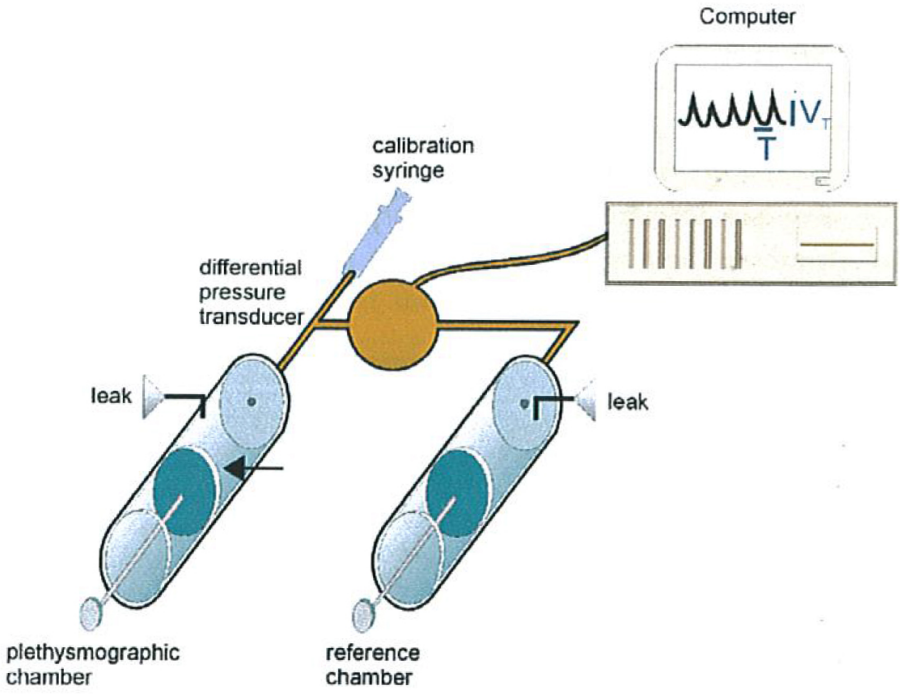

Figure 29. Whole body plethysmograph system. This system is based on a barometric method. The plethysmograph chamber equipped with a temperature sensor is connected to a reference chamber of the same volume. The different pressure between the two chambers is measured with a differential pressure transducer connected to a sine wave carrier demodulator. The spirogram (trace at top) sampled at 1kHz is stored on a computer for later analysis. Reproduced from Guimaraes, 2001.

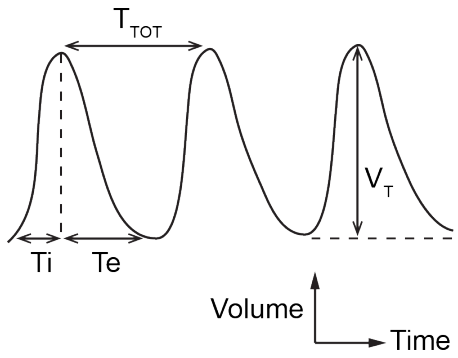

Figure 30. Plethysmographic measurement of respiratory parameters. Upward deflections indicate inspiration. The tidal volume (VT) associated with a tidal breath is calculated by the change of pressure with appropriated factors. Duration of inspiration (Ti) corresponds to the period of time between the beginning and the end of an upward deflection, and duration of expiration (Te) corresponds to the time between the end of an upward deflection and the beginning of the next inspiration. TTOT is the duration of a breath cycle (Ti+Te), equivalent to the duration between two peaks.

X. Statistics

All data are presented as mean ± standard error of the mean (SEM). Statistical significance was tested using unpaired Student's t-test to compare datasets obtained from different mutants and a paired Student's t-test to compare the measurements obtained in two different conditions.

RESULTS

Monosynaptic tracing of phrenic premotor neurons in the mouse

Jinjin Wu[1], Paolo Capelli[2,3], Martyn Goulding[4], Silvia Arber[2,3], Gilles Fortin[1]

[1] Paris-Saclay Institute for Neuroscience, Gif sur Yvette, France,
[2] Biozentrum, Department of Cell Biology, University of Basel, Basel 4056, Switzerland
[3] Friedrich Miescher Institute for Biomedical research, Basel 4058, Switzerland
[4] Salk Institute for Biological Science, La Jolla, CA.

Correspondence should be addressed to G. Fortin NeuroPSI, UMR 9197 CNRS-University Paris-Saclay
Paris-Saclay Institute for Neuroscience, 1 avenue de la terrasse, 91190, Gif sur Yvette France (gilles.fortin@cnrs.fr)

Funding
This work was supported by grants from the Agence Nationale pour la Recherche (ANR-10-BLAN1410-02 and ANR-32-BSV5-0011-02 to G.F.), Fondation pour la Recherche Médicale (DEQ20120323709 to G.F.), the ERC Advanced Grant XXX to S.A., the Swiss National Science Foundation to S.A, J.W. was supported by fellowships from Fondation pour la Recherche Médicale and from Ecole des Neurosciences de Paris, P.C. by XXXX.

SUMMARY

Breathing involves permanent rhythmic contractions of skeletal muscles in a bilaterally synchronized manner. The executive control of respiration relies on sets of brainstem interneurons assembled into an ordered synaptic network: the respiratory central pattern generator (CPG). We investigate the relationship of defined neuronal subtypes to the organization of the respiratory CPG. We have previously demonstrated that the inspiratory rhythm generator —the preBötzinger complex (preBötC)— is composed of V0 glutamatergic neurons that arise from neural progenitors expressing the homeobox gene *Dbx1*. We have now used monosynaptic viral tracing from the inspiratory diaphragm muscle to locate, identify the origin and the excitatory or inhibitory nature of premotor neurons, that are interposed between the preBötC and the main inspiratory motoneurons, the phrenic motoneurons. Phrenic premotor motoneurons (Phr-pMNs) were found to reside exclusively in the brainstem and the cervical spinal cord. We show that the principal Phr-pMNs in the rostral ventral respiratory group (rVRG), are glutamatergic V0 interneurones. Deleting the commissural projections of V0s was found sufficient to left-right desynchronize the inspiratory motor command in reduced brain preparations and breathing at birth. This work reveals the existence of a core inspiratory motor circuit in which V0 cell lineages form both the rhythm generator and its main premotor follower. The V0 core circuit features built-in redundant commissural connectivity to secure bilateral temporal synchronicity and balanced amplitude of rhythmic phrenic motor drives required for efficient aspiration breathing.

INTRODUCTION

In mammals, breathing is a motor behavior generated by a central pattern generator (CPG) located in the brainstem that produces rhythmic contraction of muscles that regulate lung volume and control upper airway patency to maintain bodily homeostasis (Feldman et al., 2013). The respiratory CPG in rodents is precociously active in the fetus at around two thirds through gestation(Greer et al., 2006; Thoby-Brisson et al., 2005), allowing for a "breathing practice" period prior to the challenge of encountering air at birth(Feldman et al., 2009). Starting at birth, the respiratory CPG constantly adapts the frequency and amplitude of the respiratory motor command to metabolic demands linked to exercise and environmental changes (Feldman et al., 2013). Thus, the respiratory CPG must compute the choice, the timing and the intensity of activation of appropriate groups of premotor, motor neurons and their muscle targets. The CPG must do this while respecting two intangible constrains: synchronicity and amplitude balance of the motor drives onto left and right respiratory effector muscles (e.g. left and right costal diaphragm muscles that are the prime movers of tidal air). Together with alternating inspiratory/expiratory phases, left/right balanced motor drives to respiratory muscles is adapted to the design of the upper airways that converge on a unique tract imposing unidirectional air flows, in or out. The identity of neurons in charge of ensuring fail-safe bilaterally synchronized and amplitude balanced inspiratory motor drive is investigated here.

Over the past decade, genetic strategies inspired by the history of gene expression by neural progenitors or precursors have progressed to the point that it has been feasible to manipulate identified neuronal progenies with unprecedented specificity and reveal their role in circuit function and behavior(Goulding, 2009; Grillner and Jessell, 2009; Kiehn, 2016). In that way we established that the preBötzinger Complex (preBötC) that paces inspiration(Smith et al., 1991) is composed of rhythmogenic V0 type interneurons(Bouvier et al., 2010)which are synchronized with their contralateral cognate neurons by commissural projections established through the Robo3 signaling pathway. Therefore, bilateral synchronicity of the respiratory motor command is at least in part built-in at the level of the rhythm generator. In the present work we address the architecture of premotor circuits downstream of the CPG, that control the diaphragm

muscle and report on the contribution of specific synapses to the failsafe transmission of the bilaterally synchronized and balanced inspiratory motor drive.

Using a viral-based circuit-mapping approach (Stepien and Arber, 2008; Stepien et al., 2010) from the diaphragm muscle in early postnatal mice, we find that Phr-pMNs are distributed at several sites of the brainstem and include neurons with bifurcating axons that project onto Phr-MNs on both sides of the midline. An important premotor relay is the rostral ventral respiratory group (rVRG), abutting the preBötC caudally. These rVRG neurons gain prominence over the prenatal period and end up forming at birth, together with the preBötC, the core inspiratory circuit that generates the rhythm and secures its transmission to phrenic motor neurons with the built-in bilateral synchrony and intensity balance required for efficient breathing. Strikingly, this rVRG premotor relay shares with the preBötC, not only a glutamatergic and commissural phenotype but an origin in p0 progenitors, highlighting the centrality of Dbx1-expressing neural progenitors in the advent of aspiration breathing in vertebrates.

RESULTS

Mapping premotor inputs to Phr-MNs in early postnatal mice

To selectively label neurons that synapse onto Phr-MNs, we used transsynaptic rabies technology with monosynaptic restriction. This method makes use of a glycoprotein-G-deleted mutant rabies virus (ΔG-Rb) whose retrograde transsynaptic spread from infected source cells (here Phr-MNs), requires complementation in these cells by the rabies glycoprotein-G (G) (Wickersham et al., 2007; Stepien et al., 2010; Tripodi et al. 2011; Pivetta et al., 2014). Once inside presynaptic neurons, the deficient virus ceases to spread for lack of G, and thus only phrenic premotor neurons are traced. ΔG-Rb-mCherry and an adeno-associated virus (AAV) expressing G (AAV-G), were co-injected in the diaphragm of P1 mice (n=21) to retrogradely infect Phr-MNs and initiate transsynaptic spread to their premotor partners (**Figure 1A**). As expected, at P9, Phr-MNs labeled with Rb-mCherry (thereafter trace^{+}) were found in the ventral spinal cord over the C3-C6 segments exclusively on the injected side (**Figure 1B,C**). Premotor neurons transsynaptically labeled with mCherry were consistently observed

bilaterally in the pons and medulla of the brainstem and in cervical spinal segments, and in no other location. Premotor neurons, counted in six brains, were found in the following locations (in decreasing order of abundance): the rostral ventral respiratory group (rVRG, 399 ± 163 neurons or 70.6 ± 2.7 % of all Phr-pMNs, **Figure 1E**); the Kölliker-Fuse nucleus (KF) and the parabrachial nuclei (PB) in the dorsolateral pons (collectively 51 ± 21 neurons; 9.2 ± 0.6% **Figure 1F**); the area of the preBötzinger complex (preBötC, 28 ± 11 neurons; 5.0 ± 0.5% **Figure 1G**); the Bötzinger complex (BötC, 21 ± 8 neurons; 3.5 ± 0.4% **Figure 1H**); the nucleus of the solitary tract (NTS, 18 ± 7 neurons; 2.7 ± 0.9% **Figure 1I**); the lateral paragigantocellular nucleus (LPGi, 14 ± 7 neurons,; 2.5 ± 0.8% **Figure 1H**), the intermediate reticular nuclei (IRt, 11 ± 5 neurons; 1.7 ± 0.9% **Figure 1K**);the gigantocellular reticular nucleus (Gi, 12 ± 5 neurons; 1.9 ± 0.4 **Figure 1H**); vestibular nuclei (Ve, 12 ± 5 neurons; 1.9 ± 0.5% **Figure 1J**); and the midline raphe nuclei (6 ± 2 neurons, n=6; 0.8 ± 0.4% **Figure 1L**). Virally labeled interneurons were also found in the cervical spinal cord near the central canal in lamina VII and X throughout cervical segments C2-C6. Brainstem areas that comprised Phr-pMNs in fewer numbers, failed to form discernable patterns and were inconsistently detected are not considered here. Thus, the rVRG, that comprises about 70% of all Phr-pMNs, stands out as the main premotor structure (**Figure 1O**). To verify the consistency of the tracing we aligned serial sections from 4 experimental animals and generated a three dimensional (3D) reconstruction of premotor neuronal populations (**Figure 1M,N**). Of note, all premotor stations showed equal proportions of retrogradely traced soma on both sides of the midline except for the PB/KF (ipsi/contra: 78%/22%, $p=2.10^{-4}$), the NTS (ipsi/conta: 78%/22%, p=0.016) and the Gi (ispi/contra: 73%/27%, p=0.021) that showed a significantly higher number of ipsilaterally projecting neurons (**Table 1**).

Since the monosynaptic rabies virus expresses fluorescent protein at high level, the axon terminal of virally infected neurons can be clearly visualized. Strikingly, when the right diaphragm was injected with the virus cocktail, we found that while ipsilateral choline acetyltransferase positive (ChAT+) Phr-MNs were traced as expected, ChAT+ Ph-MNs on the left side were covered by fluorescently labeled axons (**Supplementary Figure 1**) suggesting that some Phr-pMNs bilaterally project to the phrenic motor column. To directly identify Phr-pMNs presynaptic to both left and right Phr-MNs, we injected the left diaphragm with a ΔG-Rab-GFP (green) and the right diaphragm with a ΔG-Rab-mCherry (red) (**Figure 2A**). While, as expected, source Phr-MNs exclusively expressed GFP or m-Cherry, on the left

and right side respectively (**Figure2C**), Phr-pMNs were found that co-expressed GFP and m-Cherry (yellow, **Figure2B**), thus synapsed on both, left and right side Phr-MNs (**Figure2B**). Double-labeled cell soma were present in the rVRG (**Figure 2D,E)** and red or green commissural axons could be seen in the same plane of section (**F**). Double infected neurons were also detected in the PB area (**Figure 2G,H**), the BötC area (**Figure 2I**), the preBötC area (**Figure 2J**) and the NTS area (**Figure 2K**). Double labeled neurons in all these locations represented a small fraction of all virally labeled cells, which probably explains their absence in smaller size premotor stations (not shown). The number of co-infected premotor neurons in a given structure reflects the number of bilaterally projecting Phr-pMNs (**Figure 2L**) but also the competition of the two viral vectors for expression in co-infected cells, precluding quantification of the fractions of ipsi- , contra- and bi-laterally projecting Phr-pMNs. Altogether, these data demonstrate that all of the major phrenic premotor areas comprise neurons bearing a descending branched axon synapsing on Phr-MNs on both side of the midline, a cellular design optimal to secure synchronous and balanced motor drives on left and right diaphragm muscles.

Developmental origin and phenotype of phrenic premotor neurons

We next sought to identify the origin and the excitatory or inhibitory nature of Phr-pMNs and restricted this analysis to the rVRG, the PB, the preBötC, the BötC and the NTS that, collectively, constituted 90% of all Phr-pMNs. To do that we performed viral diaphragm injections in several mouse cre-lines *Wnt1^{cre}, Lbx1^{cre}, Dbx1^{creERT2}, En1^{cre}, Sim1^{cre}, vGlut2^{cre},* and *vGAT^{cre}*, using Tau-nls-lacZ allele as a Cre-dependent reporter. As illustrated in Figure 3, in the rVRG, about two thirds (range 59.3-77.8%, 65.5 ± 4.2%, n=4) of trace^{+} neurons at P9 co-expressed LacZ^{+} in a *Dbx1^{creERT2}* background (**Figure 3A**), 21.9 ± 1.8% (range 18.3-23.6%, n=3) also did in a *Lbx1^{cre}* background (**Figure 3B**) and 18.1 ± 2.7% (range 14.4-26.2%, n=4) in a *Wnt1^{Cre}* background (**Figure 3C**) while none did so, in either *En1^{cre}* (**Figure 3D)** or *Sim1^{cre}* (**Supp Figure 2A**) backgrounds. These data indicate that the majority of rVRG neurons originated in Dbx1-expressing ventral progenitors and have thus a V0 identity while the complement likely originates from more dorsal progenitor domains. Most (74.2 ± 4.0%, n=3) of trace^{+} rVRG neurons were excitatory (vGlut2^{+}, **Figure 3E**) and 17.2 ± 2.5% (n=4) were found inhibitory (vGAT^{+}, **Figure 3F**). In the rVRG, about 90% of vGlut2^{+}/trace^{+} neurons expressed the transcription factor Pax2 while Pax2 expression was missing in all vGAT^{+}/trace^{+} cells (**Figure 3E,F**), suggesting that Pax2 may be associated to the excitatory nature of rVRG neurons. In fact, Pax2 was expressed in about 96% of trace^{+} rVRG neurons with V0 identity (**Figure 3G**)

and in all trace^{+} rVRG neurons with a history of Wnt1 expression, acquired early in dorsal domains giving rise to dA type neurons or possibly later from more ventral domains due to the dynamics of Wnt1 expression (**Figure 3I**). Intriguingly, the fraction (18.3 ± 0.6%) of trace^{+} rVRG neurons that derived from Pax2-negative Lbx1-expressing precursors is similar to the fraction (17.2 ± 2.5%) of trace^{+} rVRG neurons found to express vGAT. This strongly suggested that most of rVRG neurons of the V0 type and all of those derived from Wnt1-expressing progenitors are excitatory while rVRG neurons of dB origin probably contribute the full complement of inhibitory ones. Lbx1 and Pax2 co-expression normally characterize dB1 and dB4 neurons that are the exclusive sources of dB inhibitory neurons. As Pax2 expression is ruled out at P9 by immunostains, we propose that Pax2 expression may have preferentially been down regulated in inhibitory vs excitatory dB premotor neurons. In support of this, we observed that Pax2 was expressed in about 15% of trace^{+} rVRG neurons with dB identity (**Figure 3H**) in keeping with the small contingent (here 3.6 ± 0.7%, n=3) of dB1 neurons known to be excitatory (C. Birchmeier, personal communication). Furthermore, none of trace^{+} rVRG neurons either expressed Phox2b (a dB2 marker, **Supp Figure 2B**) or Tlx3 (a dB3 marker, **Supp Figure 2C**), the inhibitory rVRG neurons likely originate from dB1 and/or dB4 precursors. Therefore, the rVRG, comprises mostly vGlut2^{+} excitatory neurons arising from P0 progenitors (~65%) and possibly from dA/dB1 precursors (~18%), and vGAT^{ON} inhibitory neurons (~17%) from the dB1 and/or dB4 precursors. All Phr-pMNs in the preBötC area were vGlut2^{+}, expressed Pax2 (Cheng et al., 2005; Del Barrio et al., 2013; Goulding, 2009; Huang et al., 2008) but not NK1R (**Supp Figure 3**), derived from P0 progenitors (data not shown) and, apart from their more rostral location, cannot be distinguished from vGlut2^{+} rVRG neurons.

The Phr-pMNs located in the PB nucleus were fully labeled in a *Wnt1^{cre}* (**Supp Figure 2D**) or *En1^{cre}* background (data not shown) as expected from their known rostral and dorsal rhombencephalic origin (Rose et al., 2009b). No other tested cre-line recapitulated trace^{+} PB neurons with the exception of Lbx1^{cre} that picked up about 8% of them, most likely as a consequence of the late phase of Lbx1 expression unrelated to dB identity (Sieber et al., 2007). PB Phr-pMNs were largely excitatory (vGlut2^{+}: 85 ± 7%, vGAT^{+}: 13 ± 5% n=3; data not shown). In the BötC area, Phr-pMNs were all found inhibitory (vGAT^{+}) and derived from Lbx1-expressing precursors (**Supp Figure 2E**)(Pagliardini et al., 2008). All the Phr-pMNs in the NTS were glutamatergic, labeled by Wnt1^{Cre} and expressed Phox2b as expected from their origin in the dA3 domain of progenitors (**Supp Figure 2F)** (Dauger et

al., 2003; Storm et al., 2009). Trace^{+} Phr-pMNs were also present in lamina X of the spinal cord. These neurons derived from Dbx1-expressing progenitors and were cholinergic, thus reminiscent of V0c partition cells (**Supp Figure 2G**) (Miles et al., 2007; Stepien et al., 2010; Zagoraiou et al., 2009).

We conclude that excitatory vGlut^{+} Phr-pMNs reside in the rVRG, the preBötC, the NTS and the PB. The inhibitory vGAT^{+} Phr-pMNs derive almost exclusively from dB origin and reside both in the rVRG and the BötC. By far the largest fraction of Phr-pMNs have a V0 subtype identity and reside in the rVRG. Those Phr-pMNs that are located in the preBötC cannot be distinguished from them due to their shared properties: origin, even bilateral distributions, expression of vGLut2 and absent NK1-R expression **(Supp Figure 3)**.

Because V0 rVRG neurons are numerically the main source of premotor inspiratory drive, we explored their ability to send efferent copy signals to other brainstem neuronal pools. To determine the rVRG axonal targets we used the intense m-Cherry labelling obtained through monosynaptic viral labeling in a *Dbx1^{creERT2};Tau^{synGFP}* mouse where synaptic terminals formed by Dbx1-derived neurons are strongly labeled with GFP. In this context, the synaptic terminals of V0 Phr-pMNs will be double-labeled by mCherry and GFP and will be discriminated from those arising from either non-V0 Phr-pMNs (mCherry^{+} only) or V0 non-Phr-pMNs (GFP^{+} only). Double-labeled synaptic terminals onto brainstem structures are expected to arise almost exclusively from rVRG neurons, since the few spinal V0c partition-like cells are thought to project exclusively on spinal motoneurons(Stepien and Arber, 2008; Zagoraiou et al., 2009). Cranial motor nuclei contained fibers arising from Phr-pMNs (whether V0 or not) (**Supp. Fig. 4, A,D,G,J**) , occasional boutons from non-V0 Phr-pMNs (red), many boutons from non-Phr-pMNs V0 neurons (green, in **Supp. Fig 4**), but virtually no bouton from V0 Phr-pMNs (m-Cherry^{+}/GFP^{+}, thus yellow) (0.12 ± 0.04 / soma, n=67 cells in the trigeminal, 0.10 ± 0.04 / soma, n=67 cells in the facial, 0.06 ± 0.03 / soma, n=50 cells in the hypoglossal and 0.00 ± 0.00 yellow / soma, from 50 cells in the ambiguus)(**Supp. Fig 4**), in contrast with their massive presence on Phr-MN somata in the spinal cord (7.7±0.52/soma, n=62 cells) (**Figure 4A,C**). Of note, the absence of double labeled synapses was also noticed in the rVRG itself (0.07 ± 0.04 boutons / soma, n=54 cells) that featured GFP^{+} only synapses showing that rVRG neurons are not intrinsically connected through ipsilateral or commissural axon collaterals but are connected by V0 interneurones probably including preBötC proper neurons **(Figure 4D-F**)(Tan et al., 2010). Apart from Phr-MNs themselves, rVRG synaptic

terminals were only conspicuously found in the ispi- and contra-lateral lateral reticular nucleus, a pre-cerebellar hub structure that also receives ascending efferent copy signals from multiple spinal premotor sources (**Figure 4G-I**)(Stepien and Arber, 2008). Therefore the rVRG is a source of inspiratory corollary discharge that may help controlling the execution combined respiratory and spinal motor tasks.

V0 type interneurons ensure balanced bilateral drives to phrenic motoneurons and efficient aspiration pumping.

We next explored the ability of rVRG V0 interneurons to control bilaterally the Phr-MNs output during the period of fetal breathing in embryos. We first verified anatomically in brainstem spinal cord preparations from embryonic day (E) 15.5 embryos that a unilateral injection of a rhodamine dextran dye in the phrenic motor column led to bilateral back labeling of rVRG neurons (**Figure 5A,B**). Second, we photostimulated, using digital holography, the V0 rVRG neurons in isolated brainstem spinal cord preparation from *Dbx1^{creERT2};ChR2-tdTomato* E15.5 embryos (**Figure 5C**). The anterior limit of the preparation was set in the transverse plane of the rVRG neurons to optimize its access by light while eliminating the preBötC. In this preparation the phrenic nerves exiting the fourth cervival roots (C4) are spontaneoulsy silent, but when light was targeted to the rVRG on one side of the brainstem, it evoked a bilateral C4 burst of activity (**Figure 5D**). Thus, V0 glutamatergic neurons of the rVRG can transmit their excitation bilaterally to Phr-MNs at E15.5, i.e. at the inception of fetal breathing.

To further investigate the role of the rVRG in ensuring a motor drive that is both synchronized and amplitude balanced to the left and right diaphragms, we prevented the contralateral projection of V0 neurons by deleting *Robo3* with a *Dbx1^{cre}* allele. At E15.5, in en-bloc brainstem spinal cord preparations from wild type embryos, the activities of C4 and of the facial motor nucleus (nVII) were rhythmic and bilaterally synchronized as recorded by electrophysiology and calcium imaging, respectively(**Figure 6A**) (Bouvier et al., 2010). Furthermore, the normalized amplitudes (see material and methods) of the left and right synchronous bouts of C4 activity were similar (1.02 ± 0.01, n=77 bursts from 5 preps, **Figure 6B**). We previously showed that the preBötC of *Dbx1^{cre};Robo3$^{lox/lox}$* mutants maintains a rhythmic activity, albeit left-right desynchronized owing to the loss of intrinsic commissural connectivity. We now show, in en-bloc preparations, that the activities of the nVII are also found left-right de-synchronized suggesting that facial MNs were ispilaterally driven by the left-right uncoupled preBötC (**Supp Figure 5**). Unexpectedly, at the level of the C4 output, bilateral synchronization was

maintained so that each bout of nVII activity present on either side of the midline was systematically associated to bilaterally synchronized bouts of C4 activity (**Figure 6D**). This suggested that this genetic background preserves a sufficient number of Phr-pMNs, other than V0s, able to transmit bilaterally the activity of each preBötC oscillator. These latter neurons derived from the *Wnt1*-expressing progenitors as indicated by a complete left-right decoupling of C4 activities in *Wnt1^{cre};Dbx1^{cre};Robo3$^{lox/lox}$* double mutants, reminiscent of that observed in *Robo3* constitutive null mutants (Bouvier et al., 2010) (**Figure 6G**). If synchronicity of the motor output was maintained in *Dbx1^{cre};Robo3$^{lox/lox}$* mutant preparations, the intensity balance of left and right synchronous C4 bursts was disrupted. In *Dbx1^{cre};Robo3$^{lox/lox}$* preparations, the amplitudes of the left or right synchronized bouts of C4 activity fluctuated according to the side where the nVII —thus probably the preBötC— were active (**Figure 6D**: the amplitudes of normalized C4 discharges recorded from the ipsilateral side to the active nVII and preBötC (ipsi-active) were systematically larger than those recorded from C4 on the contralateral (contra) side (ipsi-active/contra) amplitude ratio: 1.31 ± 0.09, n=127 bursts from 4 preparations, **Figure 6E**). As the invalidation of *Robo3* results in an ipsilateral re-routing of Dbx1-derived axonal projections without changing the identity of postsynaptic targets (Renier et al., 2010), the observed unbalanced left-right C4 amplitudes must reflect an excess of descending ipsilateral projections at the expense of contralateral ones that translates into a systematic motor overdrive on the side hosting the active preBötC. These experiments confirm the early role of V0 rVRG neurons in the mounting of the bilaterally synchronized inspiratory motor command.

When we repeated C4 recordings in *Dbx1^{cre};Robo3$^{lox/lox}$* mutant preparations at birth (P0) when physiological breathing needs to operate reliably, we observed a severe aggravation of the unbalance of the amplitudes of the left and right C4 outputs. Indeed, the ratio of ipsi-active/contra amplitude of C4 activity was increased to 4.68 ± 0.46 (n=76 bursts from 4 preparations, **Figure 6J,K**) and for some events could not be determined as contralateral bursts could not be detected. To estimate directly the impact on breathing, we performed plethysmographic recordings of the ventilation in unrestrained *Dbx1^{cre};Robo3$^{lox/lox}$* P0 pups. The mutant pups revealed atypical ventilation profiles when compared to wildtypes. First, the distribution of breath durations (T_{TOT}) showed an abnormally high incidence of breath separated by short intervals (**Figure 7A-D,G**) as expected from independent generation of inspiratory motor commands on both side of the midline. In fact, the breathing pattern of this mutant was comparable to that of double *Wnt1^{cre};Dbx1^{cre};Robo3$^{lox/lox}$* mutant pups (**Figure 7E,F,G**). Furthermore, the

distribution of tidal volumes (V_T) for both, the single or double conditional *Robo3* null mutants showed a left shift towards small amplitudes breath (**Figure 7H**, the peak of the V_T distribution in both mutants corresponding to about half that of wild type littermates (5.1 ± 0.4 µl/g, n=2192 breath events from 8 pups in $Dbx1^{cre};Robo3^{lox/lox}$ and 7.5 ± 1.0 µl/g, n=1617 breath from 4 pups in $Wnt1^{cre};Dbx1^{cre};Robo3^{lox/lox}$, versus 11.8 ± 0.7µl/g, n=3034 breath events from 13 pups in wild types). Yet, both single and double conditional mutants had ventilation ($V_E = V_T/T_{TOT}$) distributions comparable to that of wildtype pups (**Figure 7 I).** This owed to the large fraction of breaths, in the two mutants, characterized by both low V_T and low T_{TOT} values as revealed by density maps of (V_T,T_{TOT}) plots (**Figure 7J-L**). Altogether, these data indicate that the shallow breathing of mutants is brought about by mobilizing about half the lung capacity about twice as frequently as could produce two free-running unilateral rhythmic motor commands targeting each a hemi-diaphragm (**Supplementary video 1-3**). All $Dbx1^{cre};Robo3^{lox/lox}$ (13/13) and all $Wnt1^{cre};Dbx1^{cre};Robo3^{lox/lox}$ (4/4) newborn pups died within 24 hours. These data suggest that highly unbalanced intensities of the motor drives to the left and right diaphragms observed in $Dbx1^{cre};Robo3^{lox/lox}$ mutants, is functionally as poor as the full left/right desynchronization realized in $Wnt1^{cre};Dbx1^{cre};Robo3^{lox/lox}$ mutants. In both mutants the fully decoupled drive to the MoVII might contribute to the breathing deficiency by diminishing airway patency. At E15.5, Dbx1- and Wnt1-derived Phr-pMNs both convey bilaterally the motor drive to C4 phrenic motoneurons. During prenatal maturation the prominent contribution of V0s, expected from their much greater abundance is progressively established.

V0 type interneurons are not required for bilateral synchronicity of the genioglossus upper airway controlling muscle.

To estimate more widely the importance of V0 interneurons in supporting respiratory premotor drives we have considered that to the tongue protruding genioglossus muscle, an effector contributing to the control of upper airways patency (Sawczuk and Mosier, 2001). We have monosynaptically traced premotor neurons (MoXII-pMNs) impinging onto hypoglossal motoneurons (MoXII) innervating the genioglossus muscle. As reported previously, we found that MoXII-pMNs are distributed in multiple sites non-overlapping with Phr-pMNs areas, including the trigeminal sensory regions and dorsal midbrain reticular formation (Stanek et al., 2014). The large majority of MoXII-pMNS (about 80%) reside in the intermediate reticular nuclei (IRt) of the brainstem. The few Phr-pMNs identified in the IRt (**Figure 1K**) occupy the axial position of the rVRG and thus are much more caudally located than MoXII-pMNs. When viral injections were

performed using the *Dbx1^{creERT2}* recombining Tau$^{nls\text{-}lacZ}$ as a reporter, the only subpopulation of MoXII-pMNs found to derive from Dbx1-expressing progenitors was indeed located in the IRt close to the preBötC oscillator (**Figure 8A**). V0 type interneurons represented about a quarter (23 ± 2 %, n=4) of traced MoXII-pMNs in the IRt (**Figure 8B,C**). Then we looked at the left/right synchronicity of the XII nerve roots in *Dbx1^{cre};Robo3$^{lox/lox}$* mutants by electrophysiology in P0 brainstem-spinal cord preparations. We found that disrupting the commissural navigation of Dbx1-derived neurons failed to alter in any obvious manner the synchronicity and the amplitudes of activities recorded from the left and right hypoglossal nerve roots (**Figure 8D-F**). These data indicate that *Robo3* loss of function restricted to Dbx1-derived neurons is not sufficient to induce left-right decoupling of the nXII output suggesting little if any contribution of V0 interneurons at operating re-synchronization of left and right hypoglossal outputs downstream the decoupled preBötC.

We conclude that Dbx1-derived neurons at birth are the prominent neurons on which rely both the generation of the bilaterally synchronized inspiratory rhythm in the preBötC, and redundantly downstream in the rVRG, the ensuing left-right balanced and synchronized premotor drives, required for efficient motor control of the respiratory pump principal muscle.

DISCUSSION

An early hypothesis concerning the neural bases of movements by Broadbent in 1866 stated: "*That where the muscles of the corresponding parts on opposite sides of the body constantly act in concert, and act independently, either not at all, or with difficulty, the nerve-nuclei of these muscles are so connected by commissural fibres as to be pro tanto a single nucleus.*". This hypothesis applies well to respiratory movements controlled by "*nerve nuclei"* having now partially known developmental histories including the rhythm generator in the preBötC (Bouvier et al., 2010; Gray et al., 2010), some of its attendant neuro-modulatory control (Li et al., 2016; Rose et al., 2009a; Ruffault et al., 2015; Thoby-Brisson et al., 2009) and output phrenic motoneurons that innervate the diaphragm (Philippidou et al., 2012). A yet uncharted link concerns the premotor neurons that convey the inspiratory command to phrenic motoneurons. We here report on a group of such neurons that strikingly vindicate the notion that the diaphragm muscle is motorized by "pro tanto a single nucleus".

The phrenic premotor apparatus

We have investigated the organization of inspiratory circuits motorizing the diaphragm in the early postnatal mouse. The tracing scheme strictly restricts the viral spread to the sole premotor neurons and thus allows a definitive establishment of premotor neurons locations and identities (Stepien et al., 2010). While we cannot exclude the possibility that certain populations of premotor neurons remain unlabeled in our experiments, we have at present no evidence that neuronal populations without synaptic connection to doubly infected phrenic motor neurons are labeled. Phr-pMNs were exclusively found to reside in the pons and medulla of the brainstem and in the proximal cervical spinal cord. Phr-pMNs were present in limited numbers in the dorsolateral pons in the parabrachial nuclei and Kölliker-Füse nucleus (PB/KF), within the lateral tegmental area in the lateral paragigantocellular (LPGi) and gigantocellular nuclei (Gi), the intermediate reticular nucleus, in vestibular nuclei, in the midline raphe, in the ventral medulla in the Bötzinger complex (BötC), and in the dorsal medulla in the nucleus of the solitary tract (NTS). In the cervical spinal cord, Phr-pMNs were inconsistently found in territories axially restricted to cervical segments C2-C6 except in the vicinity of the central canal where we identified the presence of partition-like cells, an exclusive source of cholinergic modulation of motor neuron activity (Conradi and Skoglund, 1969; Miles et al., 2007; Stepien et al., 2010; Zagoraiou et al., 2009). The majority of Phr-pMNs were concentrated in the rVRG, abutting caudally the preBötC. They included a small subset of cells at the axial level of the preBötC, that differed from immediate rostral BötC neurons by origin, but were indistinguishable from rVRG neurons by molecular or anatomical criteria confirming little if any contribution of the preBötC to direct transmission of descending drive to Phr-MNs (Dobbins and Feldman, 1994). Quantitatively, the ventral respiratory column (BötC and rVRG) contained 85% of all Phr-pMNs that were distributed evenly across the midline following a unilateral viral injection in the diaphragm. In other locations (NTS, PB/KF, Gi), the bilateral distribution of Phr-pMNs showed an excess of ipsi-laterally projecting cells, an intriguing yet modest asymmetry in the otherwise exhaustively commissural connectivity of Phr-pMNs. Altogether, the present results are in keeping with the previous anatomical and electrophysiological delineations of Phr-pMNs made in the adult mouse (Gaytan et al., 2002), rat (Dobbins and Feldman, 1994; Onai et al., 1987) and cat (Fedorko et al., 1983; Feldman et al., 1985; Onai and Miura, 1986) suggesting that inspiratory descending circuits may both be definitively set one week after birth and largely conserved in mammals.

The above data imply that the vast majority of the Phr-pMNs anatomically lie in the ventral respiratory column and functionally contribute to motorization of the inspiratory pump. Indeed, the presence of both, excitatory and inhibitory Phr-pMNs neurons in the rVRG is well suited to support concurrent glutamatergic and GABAergic drives to Phr-MNs, enabling a specific gain control of the Phr-MNs output during inspiration for shaping discharge pattern, for establishing the recruitment order of Phr-MNs or for smoothing diaphragm force production (Ellenberger and Feldman, 1990b; Parkis et al., 1999; Robertson and Stein, 1988). In addition, the inhibitory Phr-pMNs of the BötC are known to provide synaptic inhibition of Phr-MNs during expiration (Kalia, 1981; Merrill and Fedorko, 1984). Phr-pMNs in the ventral respiratory column thus contrasted with the paucity of Phr-pMNs found in the other respiratory-related structures probably in keeping with the necessary persistence of breathing during REM sleep atonia in the case of the LPGi, (Sirieix et al., 2012) or whose direct connection to Phr-MNs might serve locally homeostatic integrative roles, whatever the precise functions of these secondary inputs are, either to integrate viscero- and chemo-sensory afferent signals in the NTS (Andresen and Paton, 2011) or to coordinate various rhythmic motor activities in the PB/KF (Forster et al., 2014).

V0 interneurons ensure the bilateral coordination of breathing

We have shown that invalidating the commissural axonal projections of V0 type interneurons causes a left-right desynchronized breathing at birth incompatible with survival. This breathing deficit observed in *Dbx1^{cre};Robo3$^{lox/lox}$* mutant pups cannot be reduced to the sole impairment of the preBötC (Bouvier et al., 2010) as the bulk of glutamatergic commissural rVRG neurons was here shown to share with it V0 identity. Intriguingly, the early (E15.5) modest amplitude mismatch of the left and right C4 drives, accentuated by the further lesioning of Wnt1-derived neurons in double *Dbx1^{cre};Wnt1^{cre};Robo3$^{lox/lox}$* mutants, had transformed at birth into a severe unbalance that disrupted the coordination of bilateral breathing similarly in single and double conditional mutants pups, leading to death. This suggested that Wnt1-derived glutamatergic Phr-pMNs of the PB/KF, the NTS and a subset of rVRG neurons, thought to receive inputs from the preBötC (Tan et al., 2010), thus in position to operate re-synchronisation of the rhythm at an early stage somewhat failed to do so at birth. If postnatal maturation of motor behaviors may proceed through timed incorporation of novel premotor modules (Takatoh et al., 2013), inspiratory motor circuits required for efficient breathing at birth, may proceed accordingly but in the prenatal period. Our data suggest that the V0 rVRG premotor module is in-stated

along with the preBötC at the time of onset of fetal breathing (Thoby-Brisson et al., 2005) and thereafter undergoes a maturation that culminates at birth when it becomes the prominent premotor module controlling the inspiratory pump. The importance of V0 pMNs was not verified at the level the hypoglossal motor neurons innervating tongue protruding muscles involved in the regulation of upper airway resistance (Revill et al., 2015) suggesting a profound divergence in the architecture of the two main motor circuits in charge of controlling inspiratory air flows.

A special axonal design for bilateral motor control

A novel trait of the descending inspiratory motor circuit is the finding that Phr-pMNs display a special axonal morphology: a bilaterally branched axon projecting onto phrenic motor pools on both sides of the midline. For technical reasons these neurons are probably underestimated in our study, precluding a measurement of their relative abundance. Nevertheless, this axonal profile was detected in all of the main phrenic premotor areas: the PB/KF, the NTS, the BötC and in the rVRG. This feature has been previously described for components of the premotor circuits that control bilateral whisking (Takatoh et al., 2013) and jaw closing movements (Stanek et al., 2014). This axonal profile is distinct from that of cardinal classes of commissural interneuron subtypes that are born in diverse progenitor domains of the neural tube (Goulding, 2009; Jessell, 2000). Firstly, it characterized Phr-pMNs with both, dorsal and ventral identities and both, excitatory or inhibitory phenotypes. Secondly, it was observed in the NTS which clearly showed predominant ipsilateral projections indicating that this axonal profile had been acquired by only a subset of all the dA3 NTS neurons. The signal that initiates axon collateral branching, which remains to be identified, appears as a crucial morphogenetic influence in several brainstem premotor circuits and ensures the simplest design for bilateral coordination: a single premotor neuron that synapses on equivalent ipsilateral and contralateral motoneurons.

The present tracing experiments revealed that, collectively, Phr-pMNs distribute projections to several brainstem visceral and somatic motor nuclei that innervate oro-facial and upper airway patency regulating muscles. However, these projections did not arise from rVRG Phr-pMNs, which projected instead to the lateral reticular nucleus (LRN), a precerebellar nucleus that, through mossy fibers, relays information from several spinal systems controlling posture, reaching, grasping and locomotion (Alstermark and Ekerot, 2013). A recent study on the connectivity of spinal circuits underpinning voluntary forelimb motor control has also reported

mono-synaptic contralateral projection of the rVRG neurons onto the LRN (Pivetta et al., 2014). The convergence of central inspiratory and locomotor rhythms onto single LRN neurons has been described in the cat (Ezure and Tanaka, 1997). Altogether these findings suggest that the rVRG is a source of corollary discharge (Crapse and Sommer, 2008; Wolpert and Miall, 1996) needed to coordinate breathing with other motor behaviours (e.g. postural, locomotor, feeding, expulsive) that rely on partially shared muscles (Bramble and Carrier, 1983; Grelot et al., 1993; Hodges and Gandevia, 2000)

In sum, the executive control circuit for inspiration mainly comprises a V0 bilaterally synchronized rhythm generator feeding a redundantly bilaterally projecting V0 premotor system, to alleviate the possibility that putative asymmetric synaptic inputs to neurons of the inspiratory circuit at the level of the rhythm generator or of downstream premotor neurons translate in unbalanced motor drives to the left and right hemi-diaphragms. Interestingly, asymmetric volitional and hypercapnia-induced ventilations are attested in patients with vascular hemiplegia, suggesting the absence of bilateral motor representation of each hemi-diaphragm (Similowski et al., 1996) and the presence of unilateral crossed inhibitory cortical control of the ventilatory response to CO_2 (Lanini et al., 2003). However, hemiplegic patients present with symmetric ventilation in basal conditions, suggesting that cortical descending inputs by-pass both the rhythm generator and premotor commissural apparatus. We never detected direct projections from cortical neurons to Phr-pMNs and in humans the descending circuit from the cortex to phrenic motor neurons is thought to be oligo-synaptic (Gandevia and Rothwell, 1987). One possibility is that descending cortical inputs preferentially target the most lateralized Phr-pMNs populations i.e. those with strong ipsi-laterally biased projections to Phr-MNs, such as the PB/KF, NTS and Gi. Alternatively, they may bypass the brainstem altogether and project onto local spinal Phr-pMNs, inconsistently detected in the present work at early postnatal stage.

V0-V0 synapses and the advent of aspiration breathing

A number of studies have alluded to the possibility that specific genes may induce expressing neurons to establish synaptic connections with one another during development to form functional neural networks. This may concerns *Tlx3* (Logan et al., 1998), *Brn3a* (D'Autreaux et al., 2011), *Drg11* (Saito et al., 1995) in the somatic sensory pathways, *Atoh1* in proprioceptive pathways (Bermingham et al., 2001; Wang et al., 2005), *Lhx6* in an amygdalo-hypothalamic pathway (Choi et al., 2005) and *Phox2b* in visceral circuits (Brunet JF, 2008). V0 neurons in the preBötC and the rVRG

recapitulate all of the necessary properties ensuring production and transmission of the rhythmic inspiratory command in a failsafe bilaterally synchronized manner to Phr-MNs for effective muscle contraction powering breathing inflow. Thus synapses in between neurons sharing a common V0 identity, are sufficient for building an inspiratory motor circuit during development and, in a more speculative way, for the advent of aspiration breathing in tetrapods (Perry et al., 2010).

All extant amniotes draw air in by expanding the thorax rather than pumping air into the lung by building up pressure in the buccopharyngeal cavity as amphibians do. Motorizing the diaphragm required in the first amniotes that respiratory activity was shifted from cranial visceral nerves to spinal somatic nerves (e.g. the phrenic nerve) and that a neural module pacing inspirations emerge. Our data touch upon the latter issue. V0 interneurons in the spinal cord, where first described as inhibitory commissural premotor neurons synapsing onto somatic motoneurons that innervate hindlimb muscles (Lanuza et al., 2004). Assuming premotor status as a default fate for V0s, rVRG neurons only differ from their spinal partners by an excitatory glutamatergic nature. They share this trait with PreBötC neurons (this study and Bouvier et al., 2010) yet differ from them by two other essential traits: the latter are rhythmogenic but not premotor, and the former are premotor but not rhythmogenic. We propose that this phenotypic difference is intimately linked with the ability of PreBötC neurons, but not rVRG neurons, to form V0 homotypic synapses. Interestingly in this respect, redundant interconnections of V0 preBötC neurons are central to the group pacemaker hypothesis for rhythm generation(Del Negro and Hayes, 2008). We thus hypothesize that during evolution a signaling mechanism probably restricted to a rhombencephalic segment (Lumsden and Krumlauf, 1996), induced a pool of P0 progenitors lying immediately rostral to that giving rise to the rVRG to connect with their peers: acquisition of V0-V0 synapses would be sufficient to simultaneously establish the preBötC as a group pacemaker and the rVRG as its follower. Thus, a subtle V0 fate change would enable inspiratory rhythm generation and direct its output so as to secure the bilaterally coordinated contractions of inspiratory effector muscle required for aspiration breathing.

MATERIAL AND METHODS

Mouse genetics

Dbx1^{cre} (Bielle et al., 2005), *Dbx1*^{LacZ} (Pierani et al., 2001), *Dbx1*^{creERT2} (Hirata et al., 2009), *Olig3*^{creER} (Storm et al., 2009), *En1*^{cre} (Kimmel et al., 2000),

Lbx1^{cre} (Sieber et al., 2007), *Wnt1*^{cre} (Danielian et al., 1998), *Sim1*^{cre} (Zhang et al., 2008), *VGlut2*^{cre} (Borgius et al., 2010), *vGAT*^{cre} (Vong et al., 2011), *Robo3*$^{lox/lox}$ (Renier et al., 2010), RCL-ChR2(H134R)/EYFP abbreviated Ai32 and RCL-hChR2(H134R)/tdT-D abbreviated Ai27(Madisen et al., 2012), *Tau-lox-stop-lox-Syn-GFP-IRES-nlsLacZpA* (Pecho-Vrieseling et al., 2009).

Retrograde tracing experiments

Production of Rab-mCherry, Rab-GFP and AAV-G for virus experiments with monosynaptic restriction to label premotor neurons were carried out as previously described (Stepien et al., 2010; Tripodi et al., 2011). P1 mouse pups for a given Cre-line, were anaesthetized by hypothermia, prior to receiving viral injections targeted uni- or bi-laterally to the diaphragm muscle or unilaterally to the genioglossus muscle of the tongue. Two microliters of a viral solution containing equal volumes of G-deficient rabies viruses (titers of ~1e+8) and AAV-G of serotype 6 (titers ~3e+12) were injected in individual muscles. Eight days post injection, P9 pups were deeply anesthetized, transcardially perfused with 4% paraformaldehyde (PFA) in phosphate-buffered saline (PBS), post-fixed overnight in 4% PFA, and cryoprotected in 30% sucrose in PBS and were stored at -80°C for later immunohistochemistry (IHC).

The number of traced pMNs counted in six experiments was variable (range: 401-792 neurons; 577 ± 62 neurons) from one injection to the other and according to the quality of viral stocks. However, the relative abundance of neurons in the diverse premotor areas was consistent between experiments. Because rVRG cells are about one order of magnitude more abundant than cells in other premotor areas, when the number of rVRG neurons was inferior to 150 cells, we never observed trace^{+} cells in any other Phr-pMN location.

Retrograde tracing in E15.5 preparations was performed using pressure injection of Rhodamine dextran MW 3000 (Molecular probes) in the C4 ventral spinal cord of isolated brainstem spinal cord preparations in vitro. After injection, preparations were maintained in the perfusing chamber for 12 hours prior to fixation in 4% PFA at 4°C. Transverse and sagittal 60µm thick sections of the entire brain were performed using a cryostat (Leica CM3050, Germany). We checked that injections in the diaphragm did not result in infection of primary sensory fibers through a close inspection of dorsal root ganglia and afferent fibers projecting into the NTS. The diaphragm has minimal innervation by muscle spindles (Duron et al., 1978) and phrenic afferents contribute little to respiratory modulation (Corda et al.,

1965; Jammes et al., 2000).

Histology, imaging and cell counting

Antibodies used for IHC were as follows: Chicken anti-GFP (1/2000, Aves Labs), rabbit anti-GFP (1/2000, Invitrogen), chicken anti-beta-galactosidase (1/2000, Chemicon), goat anti-ChAT (1/100, Millipore), rabbit anti-RFP (1/1000 Rockland), rat anti-RFP (1/1000, ChromoTek), rabbit anti-Pax2 (1/300, Covance), rabbit anti-Tlx3 (kind gift from C. Birchmeier), rabbit anti-Phox2b (kind gift of JF Brunet). The primary antibodies were revealed by alexa 488- (Invitrogen, Carlsbad, CA), Cy3-, alexa 594-, alexa 647-, or Cy5-labeled (Jackson Immunoresearch, Suffolk, UK) secondary antibodies of the appropriate specificity. Slides were visualized using a Leica SP8 confocal microscope.

Neurons were counted on both sides in all 1:1 serial sections. Results are expressed as mean ± SEM.

We use the following nomenclature for brainstem structures: rVRG (rostral ventral respiratory group), PB/KF (Parabrachial nuclei and Kölliker-Füse nucleus; given the lack of defined boundaries we pooled lateral and medial subdivision of the parabrachial nucleus), preBötC (preBötzinger complex), BötC (Bötzinger Complex), NTS (Nucleus of the solitary tract), LPGi , Gi (Gigantocellular reticular nucleus) Ve (includes vestibular nuclei, medial, lateral and spinal parts), IRt (Intermediate reticular formation), Raphe (includes raphe magnus and obscurus).

Anatomical location of the BötC, preBötC and rVRG in neonatal mice

In neonatal mice, at P9, the three subdivisions of the ventral respiratory column: the BötC, preBötC and rVRG, were defined using previously determined anatomical criteria (Ellenberger, 1999; Ellenberger and Feldman, 1990a). From rostral to caudal, the BötC was located caudal to the end of facial motor nucleus (moVII) and ventral to the compact formation of nucleus ambiguus (nAc) (**Supp Figure 3A**). The preBötC caudal to the BötC and ventral to the semicompact formation of nucleus ambiguus (nAsc), started 300-350µm caudal to posterior end of moVII (**Supp Figure 3B**). The rVRG, caudal to preBötC, extended from 550-600µm caudal to the posterior end of moVII to the rostral pyramidal decussation, ventrally to the loose formation of nucleus ambiguus (nAls), intermingled with the external formation of nucleus ambiguus (nAex) and dorsal to the lateral reticular nucleus (lRt) (**Supp Figure 3C**).

Digital three-dimensional brainstem reconstructions

The 3D brainstem reconstruction of the virus-labeled premotor neurons was processed as previously described (Esposito et al., 2014). Briefly, all sections were acquired with a confocal microscope (Olympus) using a 20x objective. In order to cover the full area of the brainstem with labeled premotor neurons, a mosaic 7x5 tiles was acquired for each brain section, and stitched by Fiji software. All stitched images were aligned manually using Amira software to construct the 3D model, in which rabies labeled ($trace^+$) premotor neurons were manually assigned (Imaris Spot Detection), and color-coded according to their location based on Paxinos' mouse brain atlas (Paxinos and Franklin, 2012).

Calcium imaging, electrophysiology and photostimulation

The methods used for preparing mouse brainstem–spinal cord preparations from embryonic day 15.5 embryos and P0 mouse and maintaining them in oxygenated artificial cerebrospinal fluid (a-CSF) have been described (Bouvier et al., 2010; Ruffault et al., 2015; Thoby-Brisson et al., 2009). Briefly, brainstem-spinal cord preparations were dissected in 4°C a-CSF of the following composition (in mM): 128 NaCl, 8 KCl, 1.5 $CaCl_2$, 1 $MgSO_4$, 24 $NaHCO_3$, 0.5 Na_2HPO_4, 30 glucose, pH 7.4. For calcium imaging of MoVII neurons, brainstem-spinal cord preparations were incubated at room temperature for 40–45 min in oxygenated a-CSF containing the cell-permeable calcium indicator dye Calcium Green-1 AM (10 μM; Life Technologies, Paisley, UK) and were transferred to a recording chamber (30°C). Optical recordings started after rinsing out for 30 min the excess of dye using a conventional epifluorescence configuration with a FITC filter cube. Fluorescence images were captured from the ventral surface of brainstem-spinal cord preparations exposing the MoVII region, with a cooled Neo sCMOS camera (Andor Technology Ltd., Belfast, UK) using 4× objectives, an exposure time of 100 ms and bin size of 4 × 4 for periods of 180 s using Micro-Manager software (https://www.micro-manager.org/wiki/). Spontaneous relative fluorescence changes (ΔF/F) in **Figures 6A,D** show the ΔF/F changes detected in the right and left MoVII whose outlines were defined on the image representing the standard deviation of the ΔF/F changes recorded in a 60s imaging time series.

Phrenic nerve activity was recorded on E15.5 and P0 brainstem-spinal cord preparations using suction electrodes positioned on the fourth cervical root (C4) as described (Bouvier et al., 2010; Thoby-Brisson et al., 2009). The raw signals were amplified (High-gain AC, 7P511, Grass Technologies, Warwick,

RI), filtered (bandwidth 0.1–3 kHz) and integrated (time constant 50 ms, Integator 7DAEF, Grass Technologies, Warwick, RI) before digital sampling at 6 kHz and analysis using pClamp9 (Molecular Devices). Values are given as mean + SEM. Statistical significance was tested using a difference Student's t test to compare data sets obtained from different mutants and a paired difference Student's t-test to compare the measurements obtained in two different conditions.

In optogenetic experiments, photostimulation was performed using digital holography (Lutz et al., 2008). Briefly, a 473nm DPSS laser (CNI, Changchun, China) was used to excite ChR2 expressing neurons. The output beam was expanded to match the input window of a spatial light modulator LCOS-SLM (X10468-01, Hamamatsu), operating in reflection mode. A custom-designed software described in Lutz et al.,2008 calculated, given an intensity distribution at the focal plane of the microscope objective, the phase hologram and addressed it to the LCOS-SLM. The SLM plane was imaged at the back aperture of the microscope objective through a telescope. Individual light pulses of 50 ms duration (laser power density 1–5 mW/mm^2) were delivered manually at 7-10s intervals onto a 100µm circular region covering the rVRG exposed transversally in E15.5 preparations (**Figure 5C**) while recording the electrophysiological activities from the left and right C4 motor roots.

In *Robo3* deletion experiments, we used either the $Dbx1^{cre}$ or the inducible $Dbx1^{creERT2}$ for E15.5 preparation recordings as both genotypes yielded similar results. To induce the recombination in $Dbx1^{creERT2}$ pregnant females, we administered tamoxifen (20mg/g) daily for three days starting on E9.5. As the tamoxifen treatment tested in wildtype pregnant females often resulted in offsprings showing signs of respiratory distress, we resorted to the use of the non-inducible $Dbx1^{cre}$ line for P0 ventilation recordings.

To compare the amplitude of activities recorded from the left and right C4 motor roots in wildtype preparations, we first normalized the amplitude of individual bursts on each side to the mean amplitude of all burst recorded on that side during the recording period and then calculated the ratios of the normalized amplitudes of synchronous left and right bursts. To compare the amplitude of C4 activities on either side of the midline in conditional *Robo3* null mutants at E15.5, we first normalized the C4 burst amplitudes as above, and then calculated the ratios of the normalized amplitudes of bursts considering as numerators the bursts ipsilaterally synchronized to MoVII bursts (ipsi-active) and the amplitudes of the contralateral C4 bursts as

denominators. At P0, due to the large unbalance of the amplitudes of left and right C4 bursts, largest peaks were assumed to arise in the ipsi-active side and their amplitude considered as the numerators for calculating ratios.

Plethysmography

Breathing variables of un-anaesthetized, unrestrained P0 pups were measure by whole-body barometric plethysmography as previously described (Ruffault et al., 2015). After a 7 min adaptation period in the plethysmograph chamber, the breathing parameters (breath duration (T_{TOT}), tidal volume (V_T), and ventilation (V_E) calculated as V_T/T_{TOT}) were continuously monitored in apnea free periods and scored using a custom software package (Elphy by G Saddoc, https://www.unic.cnrs-gif.fr/software.html). Values are given as mean ± SEM. Statistical significance was tested using a difference Student's t-test to compare data sets obtained from different mutants. Density maps of breath amplitude and duration (V_T,T_{TOT}) relationships were obtained using a Python custom made plugin.

REFERENCES

Alstermark, B., and Ekerot, C.F. (2013). The lateral reticular nucleus: a precerebellar centre providing the cerebellum with overview and integration of motor functions at systems level. A new hypothesis. The Journal of physiology *591*, 5453-5458.

Andresen, M.C., and Paton, J.F. (2011). The nucleus of the solitary tract: processing information from viscerosensory afferents. Central regulation of autonomic functions, 23-46.

Bermingham, N.A., Hassan, B.A., Wang, V.Y., Fernandez, M., Banfi, S., Bellen, H.J., Fritzsch, B., and Zoghbi, H.Y. (2001). Proprioceptor pathway development is dependent on Math1. Neuron *30*, 411-422.

Bielle, F., Griveau, A., Narboux-Neme, N., Vigneau, S., Sigrist, M., Arber, S., Wassef, M., and Pierani, A. (2005). Multiple origins of Cajal-Retzius cells at the borders of the developing pallium. Nature neuroscience *8*, 1002-1012.

Borgius, L., Restrepo, C.E., Leao, R.N., Saleh, N., and Kiehn, O. (2010). A transgenic mouse line for molecular genetic analysis of excitatory glutamatergic neurons. Mol Cell Neurosci *45*, 245-257.

Bouvier, J., Thoby-Brisson, M., Renier, N., Dubreuil, V., Ericson, J., Champagnat, J., Pierani, A., Chedotal, A., and Fortin, G. (2010). Hindbrain interneurons and axon guidance signaling critical for breathing. Nature neuroscience *13*, 1066-1074.

Bramble, D.M., and Carrier, D.R. (1983). Running and breathing in mammals. Science *219*,

251-256.

Brunet JF, G.C. (2008). Genetic basis for respiratory control disorders. *C Gauthier (eds), Springer Science + Business Media, LLC*.

Cheng, L., Samad, O.A., Xu, Y., Mizuguchi, R., Luo, P., Shirasawa, S., Goulding, M., and Ma, Q. (2005). Lbx1 and Tlx3 are opposing switches in determining GABAergic versus glutamatergic transmitter phenotypes. Nature neuroscience *8*, 1510-1515.

Choi, G.B., Dong, H.W., Murphy, A.J., Valenzuela, D.M., Yancopoulos, G.D., Swanson, L.W., and Anderson, D.J. (2005). Lhx6 delineates a pathway mediating innate reproductive behaviors from the amygdala to the hypothalamus. Neuron *46*, 647-660.

Conradi, S., and Skoglund, S. (1969). Observations on the ultrastruture and distribution of neuronal and glial elements on the motoneuron surface in the lumbosacral spinal cord of the cat during postnatal development. Acta physiologica Scandinavica Supplementum *333*, 5-52.

Corda, M., Voneuler, C., and Lennerstrand, G. (1965). PROPRIOCEPTIVE INNERVATION OF THE DIAPHRAGM. The Journal of physiology *178*, 161-177.

Crapse, T.B., and Sommer, M.A. (2008). Corollary discharge across the animal kingdom. Nature reviews Neuroscience *9*, 587-600.

D'Autreaux, F., Coppola, E., Hirsch, M.R., Birchmeier, C., and Brunet, J.F. (2011). Homeoprotein Phox2b commands a somatic-to-visceral switch in cranial sensory pathways. Proceedings of the National Academy of Sciences of the United States of America *108*, 20018-20023.

Danielian, P.S., Muccino, D., Rowitch, D.H., Michael, S.K., and McMahon, A.P. (1998). Modification of gene activity in mouse embryos in utero by a tamoxifen-inducible form of Cre recombinase. Current biology : CB *8*, 1323-1326.

Dauger, S., Pattyn, A., Lofaso, F., Gaultier, C., Goridis, C., Gallego, J., and Brunet, J.-F. (2003). Phox2b controls the development of peripheral chemoreceptors and afferent visceral pathways. Development *130*, 6635-6642.

Del Barrio, M.G., Bourane, S., Grossmann, K., Schule, R., Britsch, S., O'Leary, D.D., and Goulding, M. (2013). A transcription factor code defines nine sensory interneuron subtypes in the mechanosensory area of the spinal cord. PLoS One *8*, e77928.

Del Negro, C.A., and Hayes, J.A. (2008). A 'group pacemaker' mechanism for respiratory rhythm generation. The Journal of physiology *586*, 2245-2246.

Dobbins, E.G., and Feldman, J.L. (1994). Brainstem network controlling descending drive to phrenic motoneurons in rat. The Journal of comparative neurology *347*, 64-86.

Duron, B., Jung-Caillol, M.C., and Marlot, D. (1978). Myelinated nerve fiber supply and muscle spindles in the respiratory muscles of cat: quantitative study. Anatomy and embryology *152*, 171-192.

Ellenberger, H.H. (1999). Nucleus ambiguus and bulbospinal ventral respiratory group neurons in the neonatal rat. Brain research bulletin *50*, 1-13.

Ellenberger, H.H., and Feldman, J.L. (1990a). Brainstem connections of the rostral ventral respiratory group of the rat. Brain research *513*, 35-42.

Ellenberger, H.H., and Feldman, J.L. (1990b). Subnuclear organization of the lateral tegmental

field of the rat. I: Nucleus ambiguus and ventral respiratory group. The Journal of comparative neurology *294*, 202-211.

Esposito, M.S., Capelli, P., and Arber, S. (2014). Brainstem nucleus MdV mediates skilled forelimb motor tasks. Nature *508*, 351-356.

Ezure, K., and Tanaka, I. (1997). Convergence of central respiratory and locomotor rhythms onto single neurons of the lateral reticular nucleus. Experimental brain research *113*, 230-242.

Fedorko, L., Merrill, E.G., and Lipski, J. (1983). Two descending medullary inspiratory pathways to phrenic motoneurones. Neuroscience letters *43*, 285-291.

Feldman, J.L., Del Negro, C.A., and Gray, P.A. (2013). Understanding the rhythm of breathing: so near, yet so far. Annual review of physiology *75*, 423-452.

Feldman, J.L., Kam, K., and Janczewski, W.A. (2009). Practice makes perfect, even for breathing. Nature neuroscience *12*, 961-963.

Feldman, J.L., Loewy, A.D., and Speck, D.F. (1985). Projections from the ventral respiratory group to phrenic and intercostal motoneurons in cat: an autoradiographic study. J Neurosci *5*, 1993-2000.

Forster, H., Bonis, J., Krause, K., Wenninger, J., Neumueller, S., Hodges, M., and Pan, L. (2014). Contributions of the pre-Botzinger complex and the Kolliker-fuse nuclei to respiratory rhythm and pattern generation in awake and sleeping goats. Progress in brain research *209*, 73-89.

Gandevia, S.C., and Rothwell, J.C. (1987). Activation of the human diaphragm from the motor cortex. The Journal of physiology *384*, 109-118.

Gaytan, S.P., Pasaro, R., Coulon, P., Bevengut, M., and Hilaire, G. (2002). Identification of central nervous system neurons innervating the respiratory muscles of the mouse: a transneuronal tracing study. Brain research bulletin *57*, 335-339.

Goulding, M. (2009). Circuits controlling vertebrate locomotion: moving in a new direction. Nature reviews Neuroscience *10*, 507-518.

Gray, P.A., Hayes, J.A., Ling, G.Y., Llona, I., Tupal, S., Picardo, M.C., Ross, S.E., Hirata, T., Corbin, J.G., Eugenin, J.*, et al.* (2010). Developmental origin of preBotzinger complex respiratory neurons. J Neurosci *30*, 14883-14895.

Greer, J.J., Funk, G.D., and Ballanyi, K. (2006). Preparing for the first breath: prenatal maturation of respiratory neural control. The Journal of physiology *570*, 437-444.

Grelot, L., Milano, S., Portillo, F., and Miller, A.D. (1993). Respiratory interneurons of the lower cervical (C4-C5) cord: membrane potential changes during fictive coughing, vomiting, and swallowing in the decerebrate cat. Pflugers Archiv : European journal of physiology *425*, 313-320.

Grillner, S., and Jessell, T.M. (2009). Measured motion: searching for simplicity in spinal locomotor networks. Current opinion in neurobiology *19*, 572-586.

Hirata, T., Li, P., Lanuza, G.M., Cocas, L.A., Huntsman, M.M., and Corbin, J.G. (2009). Identification of distinct telencephalic progenitor pools for neuronal diversity in the amygdala. Nature neuroscience *12*, 141-149.

Hodges, P.W., and Gandevia, S.C. (2000). Changes in intra-abdominal pressure during postural and respiratory activation of the human diaphragm. Journal of applied physiology *89*, 967-976.

Huang, M., Huang, T., Xiang, Y., Xie, Z., Chen, Y., Yan, R., Xu, J., and Cheng, L. (2008). Ptf1a, Lbx1 and Pax2 coordinate glycinergic and peptidergic transmitter phenotypes in dorsal spinal inhibitory neurons. Developmental biology *322*, 394-405.

Jammes, Y., Arbogast, S., and De Troyer, A. (2000). Response of the rabbit diaphragm to tendon vibration. Neuroscience letters *290*, 85-88.

Jessell, T.M. (2000). Neuronal specification in the spinal cord: inductive signals and transcriptional codes. Nat Rev Genet *1*, 20-29.

Kalia, M.P. (1981). Anatomical organization of central respiratory neurons. Annual review of physiology *43*, 105-120.

Kiehn, O. (2016). Decoding the organization of spinal circuits that control locomotion. Nature reviews Neuroscience *17*, 224-238.

Kimmel, R.A., Turnbull, D.H., Blanquet, V., Wurst, W., Loomis, C.A., and Joyner, A.L. (2000). Two lineage boundaries coordinate vertebrate apical ectodermal ridge formation. Genes Dev *14*, 1377-1389.

Lanini, B., Bianchi, R., Romagnoli, I., Coli, C., Binazzi, B., Gigliotti, F., Pizzi, A., Grippo, A., and Scano, G. (2003). Chest wall kinematics in patients with hemiplegia. Am J Respir Crit Care Med *168*, 109-113.

Lanuza, G.M., Gosgnach, S., Pierani, A., Jessell, T.M., and Goulding, M. (2004). Genetic identification of spinal interneurons that coordinate left-right locomotor activity necessary for walking movements. Neuron *42*, 375-386.

Li, P., Janczewski, W.A., Yackle, K., Kam, K., Pagliardini, S., Krasnow, M.A., and Feldman, J.L. (2016). The peptidergic control circuit for sighing. Nature *530*, 293-297.

Logan, C., Wingate, R.J., McKay, I.J., and Lumsden, A. (1998). Tlx-1 and Tlx-3 homeobox gene expression in cranial sensory ganglia and hindbrain of the chick embryo: markers of patterned connectivity. J Neurosci *18*, 5389-5402.

Lumsden, A., and Krumlauf, R. (1996). Patterning the vertebrate neuraxis. Science *274*, 1109-1115.

Lutz, C., Otis, T.S., DeSars, V., Charpak, S., DiGregorio, D.A., and Emiliani, V. (2008). Holographic photolysis of caged neurotransmitters. Nature methods *5*, 821-827.

Madisen, L., Mao, T., Koch, H., Zhuo, J.M., Berenyi, A., Fujisawa, S., Hsu, Y.W., Garcia, A.J., 3rd, Gu, X., Zanella, S.*, et al.* (2012). A toolbox of Cre-dependent optogenetic transgenic mice for light-induced activation and silencing. Nature neuroscience *15*, 793-802.

Merrill, E.G., and Fedorko, L. (1984). Monosynaptic inhibition of phrenic motoneurons: a long descending projection from Botzinger neurons. J Neurosci *4*, 2350-2353.

Miles, G.B., Hartley, R., Todd, A.J., and Brownstone, R.M. (2007). Spinal cholinergic interneurons regulate the excitability of motoneurons during locomotion. Proceedings of the National Academy of Sciences of the United States of America *104*, 2448-2453.

Onai, T., and Miura, M. (1986). Projections of supraspinal structures to the phrenic motor

nucleus in cats studied by a horseradish peroxidase microinjection method. Journal of the autonomic nervous system *16*, 61-77.

Onai, T., Saji, M., and Miura, M. (1987). Projections of supraspinal structures to the phrenic motor nucleus in rats studied by a horseradish peroxidase microinjection method. Journal of the autonomic nervous system *21*, 233-239.

Pagliardini, S., Ren, J., Gray, P.A., Vandunk, C., Gross, M., Goulding, M., and Greer, J.J. (2008). Central respiratory rhythmogenesis is abnormal in lbx1- deficient mice. J Neurosci *28*, 11030-11041.

Parkis, M.A., Dong, X., Feldman, J.L., and Funk, G.D. (1999). Concurrent inhibition and excitation of phrenic motoneurons during inspiration: phase-specific control of excitability. J Neurosci *19*, 2368-2380.

Paxinos, G., and Franklin, K.B. (2012). The Mouse Brain in Stereotaxic Coordinates (4th edn) (Elsevier 2012).

Pecho-Vrieseling, E., Sigrist, M., Yoshida, Y., Jessell, T.M., and Arber, S. (2009). Specificity of sensory-motor connections encoded by Sema3e-Plxnd1 recognition. Nature *459*, 842-846.

Perry, S.F., Similowski, T., Klein, W., and Codd, J.R. (2010). The evolutionary origin of the mammalian diaphragm. Respiratory physiology & neurobiology *171*, 1-16.

Philippidou, P., Walsh, C.M., Aubin, J., Jeannotte, L., and Dasen, J.S. (2012). Sustained Hox5 gene activity is required for respiratory motor neuron development. Nature neuroscience *15*, 1636-1644.

Pierani, A., Moran-Rivard, L., Sunshine, M.J., Littman, D.R., Goulding, M., and Jessell, T.M. (2001). Control of interneuron fate in the developing spinal cord by the progenitor homeodomain protein Dbx1. Neuron *29*, 367-384.

Pivetta, C., Esposito, M.S., Sigrist, M., and Arber, S. (2014). Motor-circuit communication matrix from spinal cord to brainstem neurons revealed by developmental origin. Cell *156*, 537-548.

Renier, N., Schonewille, M., Giraudet, F., Badura, A., Tessier-Lavigne, M., Avan, P., De Zeeuw, C.I., and Chedotal, A. (2010). Genetic dissection of the function of hindbrain axonal commissures. PLoS biology *8*, e1000325.

Revill, A.L., Vann, N.C., Akins, V.T., Kottick, A., Gray, P.A., Del Negro, C.A., and Funk, G.D. (2015). Dbx1 precursor cells are a source of inspiratory XII premotoneurons. eLife *4*.

Robertson, G.A., and Stein, P.S. (1988). Synaptic control of hindlimb motoneurones during three forms of the fictive scratch reflex in the turtle. The Journal of physiology *404*, 101-128.

Rose, M.F., Ahmad, K.A., Thaller, C., and Zoghbi, H.Y. (2009a). Excitatory neurons of the proprioceptive, interoceptive, and arousal hindbrain networks share a developmental requirement for Math1. Proceedings of the National Academy of Sciences of the United States of America *106*, 22462-22467.

Rose, M.F., Ren, J., Ahmad, K.A., Chao, H.T., Klisch, T.J., Flora, A., Greer, J.J., and Zoghbi, H.Y. (2009b). Math1 is essential for the development of hindbrain neurons critical for

perinatal breathing. Neuron *64*, 341-354.

Ruffault, P.L., D'Autreaux, F., Hayes, J.A., Nomaksteinsky, M., Autran, S., Fujiyama, T., Hoshino, M., Hagglund, M., Kiehn, O., Brunet, J.F., *et al.* (2015). The retrotrapezoid nucleus neurons expressing Atoh1 and Phox2b are essential for the respiratory response to CO2. eLife *4*.

Saito, T., Greenwood, A., Sun, Q., and Anderson, D.J. (1995). Identification by differential RT-PCR of a novel paired homeodomain protein specifically expressed in sensory neurons and a subset of their CNS targets. Mol Cell Neurosci *6*, 280-292.

Sawczuk, A., and Mosier, K.M. (2001). Neural control of tongue movement with respect to respiration and swallowing. Crit Rev Oral Biol Med *12*, 18-37.

Sieber, M.A., Storm, R., Martinez-de-la-Torre, M., Muller, T., Wende, H., Reuter, K., Vasyutina, E., and Birchmeier, C. (2007). Lbx1 acts as a selector gene in the fate determination of somatosensory and viscerosensory relay neurons in the hindbrain. J Neurosci *27*, 4902-4909.

Similowski, T., Catala, M., Rancurel, G., and Derenne, J.P. (1996). Impairment of central motor conduction to the diaphragm in stroke. Am J Respir Crit Care Med *154*, 436-441.

Sirieix, C., Gervasoni, D., Luppi, P.H., and Leger, L. (2012). Role of the lateral paragigantocellular nucleus in the network of paradoxical (REM) sleep: an electrophysiological and anatomical study in the rat. PLoS One *7*, e28724.

Smith, J.C., Ellenberger, H.H., Ballanyi, K., Richter, D.W., and Feldman, J.L. (1991). Pre-Botzinger complex: a brainstem region that may generate respiratory rhythm in mammals. Science *254*, 726-729.

Stanek, E.t., Cheng, S., Takatoh, J., Han, B.X., and Wang, F. (2014). Monosynaptic premotor circuit tracing reveals neural substrates for oro-motor coordination. eLife *3*, e02511.

Stepien, A.E., and Arber, S. (2008). Probing the locomotor conundrum: descending the 'V' interneuron ladder. Neuron *60*, 1-4.

Stepien, A.E., Tripodi, M., and Arber, S. (2010). Monosynaptic rabies virus reveals premotor network organization and synaptic specificity of cholinergic partition cells. Neuron *68*, 456-472.

Storm, R., Cholewa-Waclaw, J., Reuter, K., Brohl, D., Sieber, M., Treier, M., Muller, T., and Birchmeier, C. (2009). The bHLH transcription factor Olig3 marks the dorsal neuroepithelium of the hindbrain and is essential for the development of brainstem nuclei. Development *136*, 295-305.

Takatoh, J., Nelson, A., Zhou, X., Bolton, M.M., Ehlers, M.D., Arenkiel, B.R., Mooney, R., and Wang, F. (2013). New modules are added to vibrissal premotor circuitry with the emergence of exploratory whisking. Neuron *77*, 346-360.

Tan, W., Pagliardini, S., Yang, P., Janczewski, W.A., and Feldman, J.L. Projections of preBotzinger Complex neurons in adult rats. The Journal of comparative neurology *518*, 1862-1878.

Tan, W., Pagliardini, S., Yang, P., Janczewski, W.A., and Feldman, J.L. (2010). Projections of preBotzinger complex neurons in adult rats. The Journal of comparative neurology *518*, 1862-1878.

Thoby-Brisson, M., Karlen, M., Wu, N., Charnay, P., Champagnat, J., and Fortin, G. (2009). Genetic identification of an embryonic parafacial oscillator coupling to the preBotzinger complex. Nature neuroscience *12*, 1028-1035.

Thoby-Brisson, M., Trinh, J.B., Champagnat, J., and Fortin, G. (2005). Emergence of the pre-Botzinger respiratory rhythm generator in the mouse embryo. J Neurosci *25*, 4307-4318.

Tripodi, M., Stepien, A.E., and Arber, S. (2011). Motor antagonism exposed by spatial segregation and timing of neurogenesis. Nature *479*, 61-66.

Vong, L., Ye, C., Yang, Z., Choi, B., Chua, S., Jr., and Lowell, B.B. (2011). Leptin action on GABAergic neurons prevents obesity and reduces inhibitory tone to POMC neurons. Neuron *71*, 142-154.

Wang, V.Y., Rose, M.F., and Zoghbi, H.Y. (2005). Math1 expression redefines the rhombic lip derivatives and reveals novel lineages within the brainstem and cerebellum. Neuron *48*, 31-43.

Wolpert, D.M., and Miall, R.C. (1996). Forward Models for Physiological Motor Control. Neural networks : the official journal of the International Neural Network Society *9*, 1265-1279.

Zagoraiou, L., Akay, T., Martin, J.F., Brownstone, R.M., Jessell, T.M., and Miles, G.B. (2009). A cluster of cholinergic premotor interneurons modulates mouse locomotor activity. Neuron *64*, 645-662.

Zhang, Y., Narayan, S., Geiman, E., Lanuza, G.M., Velasquez, T., Shanks, B., Akay, T., Dyck, J., Pearson, K., Gosgnach, S., *et al.* (2008). V3 spinal neurons establish a robust and balanced locomotor rhythm during walking. Neuron *60*, 84-96.

Table 1. Quantification of the distribution of phrenic premotor neurons.

Premotor region	(%) ipsilateral	(%) contralateral	p-values	
rVRG	35.66 ± 1.55	34.94 ± 2.10	0,7819	ns
KF/PB	7.54 ± 0.60	1.70 ± 0.26	0,0002	***
preBötC	3.09 ± 0.35	1.98 ± 0.42	0,1050	ns
BötC	2.06 ± 0.28	1.40 ± 0.24	0,0591	ns
NTS	2.16 ± 0.64	0.49 ± 0.27	0,0116	*
LPGi	1.80 ± 0.57	0.73 ± 0.29	0,0532	ns
Ve	0.80 ± 0.24	1.13 ± 0.34	0,3118	ns
Gi	1.51 ± 0.31	0.41 ± 0.16	0,0206	*
IRt	1.08 ± 0.56	0.68 ± 0.30	0,2414	ns
Raphe	0.83 ± 0.46			

Percent number of trace$^+$ cell soma counted in premotor nuclei ipsilateral and contralateral to the side of the diaphragm injection (except for neurons of the raphe). Percentages are averages from 6 experiments. Note the equal left-right distribution of retrogradely traced Phr-pMNs in most locations, a significant (t-test) ipsilateral projection bias is only attested in the PB/KF, the NTS and the Gi that altogether represent less than 15% of all Phr-pMNs.

Figure 1

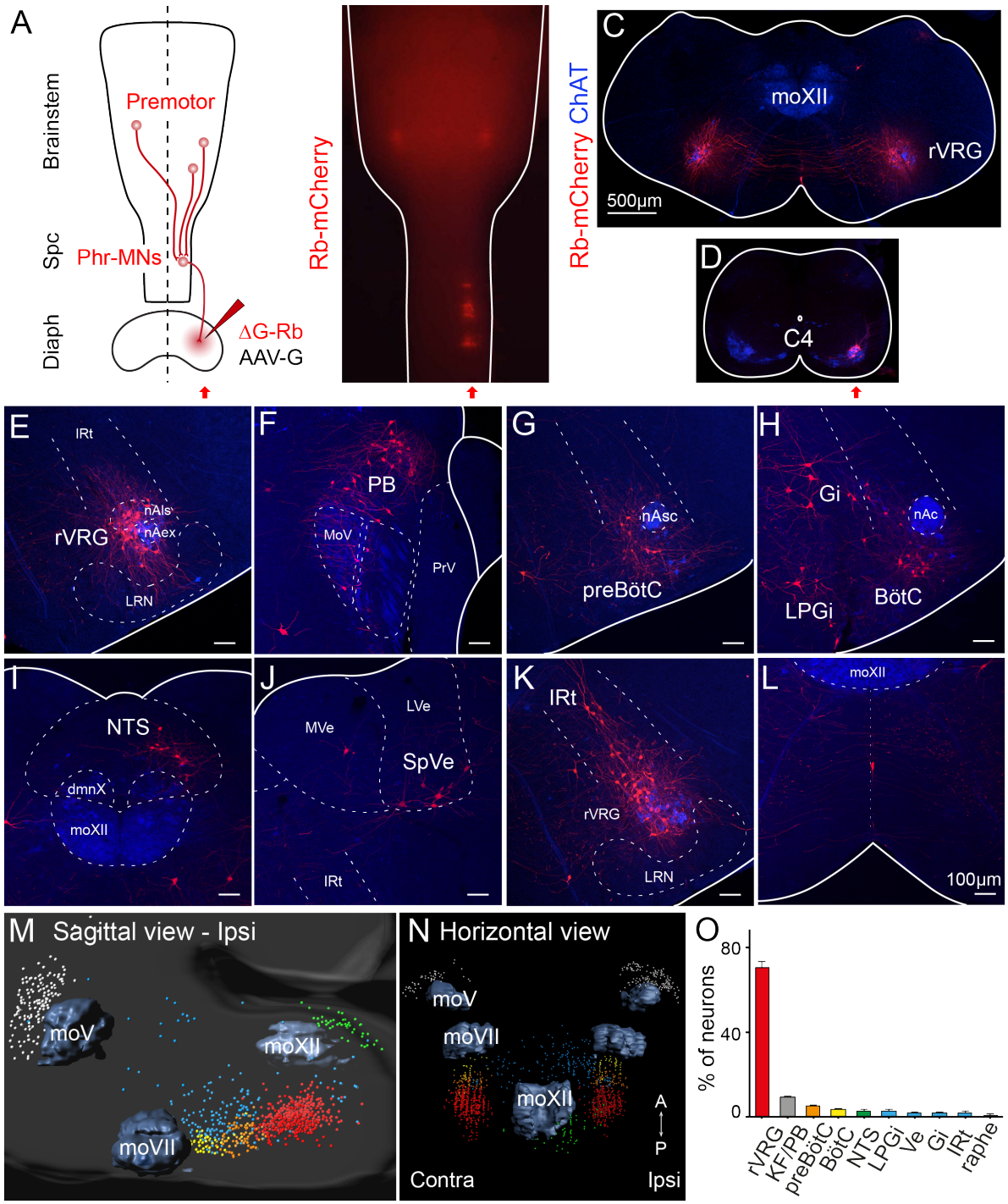
A
Brainstem
Spc
Diaph
Premotor
Phr-MNs
ΔG-Rb
AAV-G
Rb-mCherry
C
Rb-mCherry ChAT
moXII
rVRG
500µm
D
C4
E
IRt
nAIs
rVRG
nAex
LRN
F
PB
MoV
PrV
G
nAsc
preBötC
H
Gi
nAc
LPGi
BötC
I
NTS
dmnX
moXII
J
LVe
MVe
SpVe
IRt
K
IRt
rVRG
LRN
L
moXII
100µm
M Sagittal view - Ipsi
moV
moXII
moVII
N Horizontal view
moV
moVII
moXII
A
P
Contra
Ipsi
O
% of neurons
80
40
0
rVRG
KF/PB
preBötC
BötC
NTS
LPGi
Ve
Gi
IRt
raphe

Figure 1. Distribution of phrenic premotor neurons (Phr-pMNs) in the neonatal mouse at P9. **A**, Scheme illustrating the method used for monosynaptic tracing of Phr-pMNs using unilateral injection of a viral cocktail solution including a G-deficient Rb (ΔG-Rb) virus and a G-coding adeno-associated (AAV-G) virus. **B**, Ventral view (anterior at top) of a wholemount brainstem and proximal spinal cord preparation at P9 following injection at P1, note ipsilateral mCherry$^+$ phrenic motoneurons (C3-C5 segments) and apparent bilateral mCherry expression in the brainstem. **C** and **D** corresponding transverse sections in the brainstem (**C**) and spinal cord (**D,** same calibration bar as C) showing respectively, transynaptically labeled Phr-pMNs of the rVRG and seeding Phr-MNs. **E-L** Representative images of transverse sections of the brainstem showing trace$^+$ Phr-pMNs. Labeled neurons are present in decreasing abundance in the rVRG (**E**), in the PB (**F**), in the preBötC (**G**), in the BötC, Gi and LPGi (**H**), in the NTS (**I**), in Ve nuclei (**J**), in the lRt (**K**) and in the raphe (**L**). **M-N**, 3D reconstructions of the brainstem showing the spatial distribution of Phr-PMNs in sagittal (M) and horizontal (N) views (color coded as indicated by the colors of the bars in the histogram in O). **O**, Distribution histogram of color coded Phr-pMNs. Abbreviations: dmnX: dorsal motor nucleus of the vagus; LRN: lateral reticular nucleus; LVe: lateral vestibular nucleus; MoV: trigeminal motor nucleus; MoXII: hypoglossal motor nucleus; MVe: medial vestibular nucleus, nAc: compact nucleus ambiguus; nAex: external formation of nucleus ambiguus, nAls: loose formation of nucleus ambiguous: nAsc: semi-compact nucleus ambiguus; PrV: principal sensory trigeminal nucleus; Spc: spinal cord; SpVe: spinal vestibular nucleus.

Figure 2

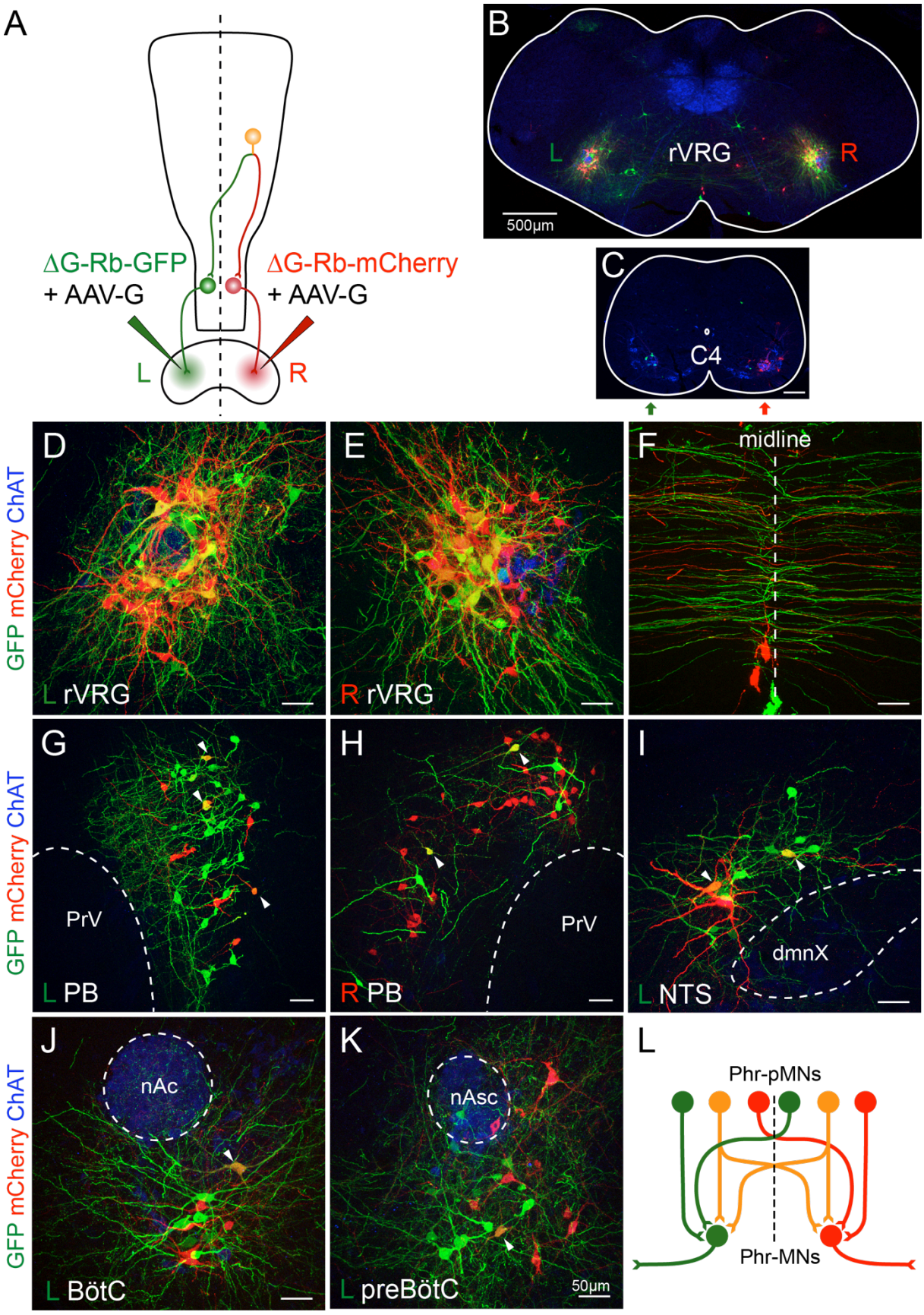
A
ΔG-Rb-GFP
+ AAV-G
ΔG-Rb-mCherry
+ AAV-G
L
R
B
L
rVRG
R
500μm
C
C4
D
L rVRG
E
R rVRG
F
midline
GFP mCherry ChAT
G
PrV
L PB
H
PrV
R PB
I
dmnX
L NTS
J
nAc
L BötC
K
nAsc
L preBötC
50μm
L
Phr-pMNs
Phr-MNs

Figure 2. Individual Phr-pMNs in premotor locations project bilaterally on Phr-MNs. **A,** Schematic showing the tracing strategy based on injections of a green virus (Rb-GFP) on the left diaphragm (L green lettering) and of a red virus (Rb-mCherry) on the right diaphragm (R red lettering). **B** and **C**, transverse sections of the brainstem at the level of the rVRG (**B**) and at the C4 level (**C**). Note the presence of double labeled $GFP^+/mCherry^+$ virally labeled rVRG neurons (yellow) on the left and right side (**B**) while seeding Phr-MNs (**C**) exclusively express either GFP (green) or mCherry (red). **D**-**F**, close up view of the left (**D**) and right (**E**) rVRG showing exclusive green or red cells as well as double labeled (yellow) rVRG cells on either side of the midline. **F,** close-up view of the labeled commissural axons at the level of the midline (dotted line). **G**-**H**, double labeled Phr-pMNs in the PB. Note that the PB bears ipsilaterally biased descending projections as indicated by the excess of green vs red labeled cells in **G** and the converse in **H**. **I**, same for the NTS (only the left side where the green virus has been injected is shown). **J**,**K** double labeled Phr-pMNs in the BötC (**J**) and at the axial level of the preBötC (**K**). **L**, schematic of the labeling of Phr-pMNs somata according to their left or right position and putative projection profiles to Phr-MNs.

Figure 3

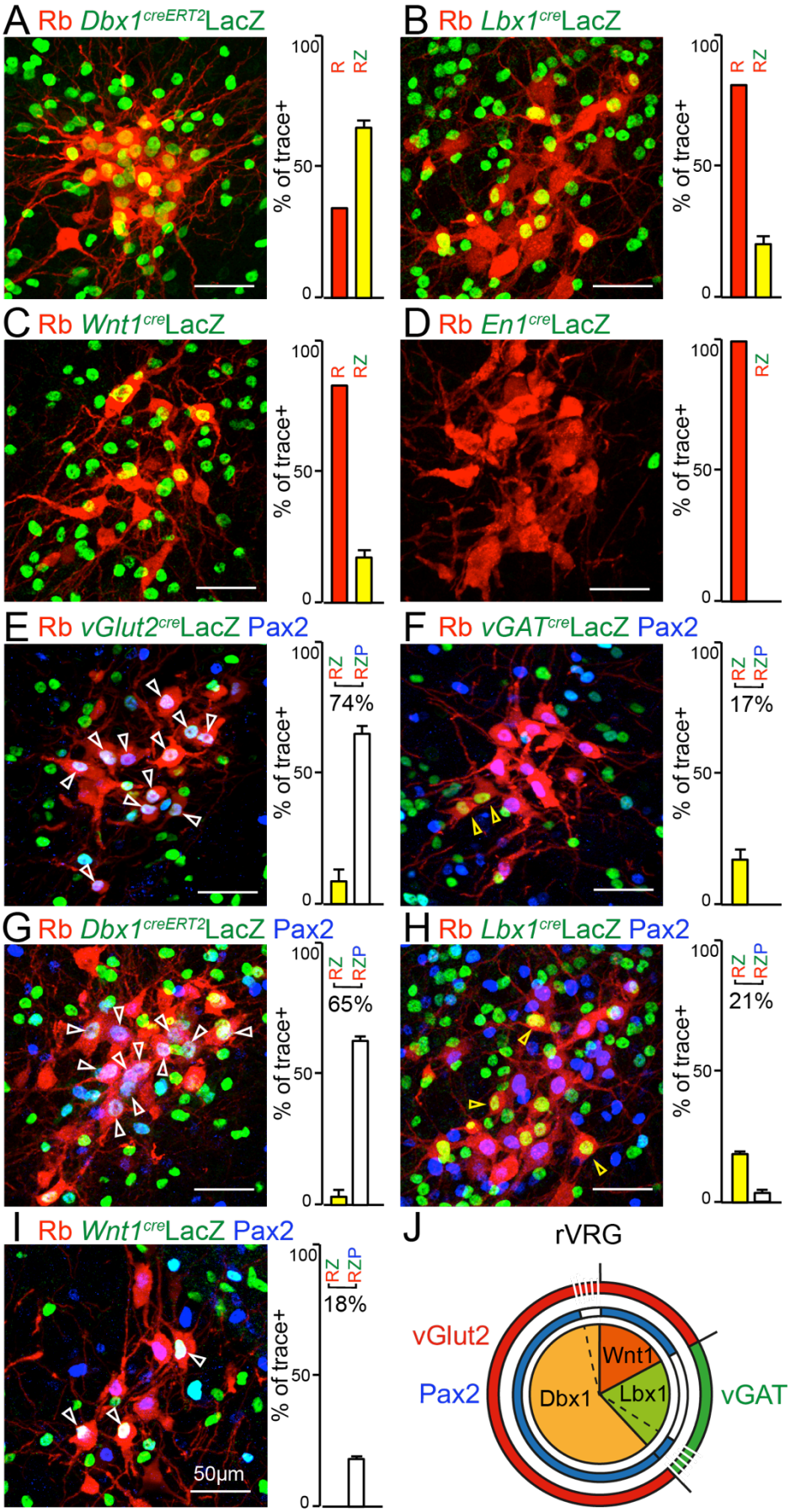
A Rb Dbx1creERT2LacZ
B Rb Lbx1creLacZ
C Rb Wnt1creLacZ
D Rb En1creLacZ
E Rb vGlut2creLacZ Pax2
F Rb vGATcreLacZ Pax2
G Rb Dbx1creERT2LacZ Pax2
H Rb Lbx1creLacZ Pax2
I Rb Wnt1creLacZ Pax2
% of trace+
100
50
0
R
RZ
RZP
74%
17%
65%
21%
18%
50µm
J
rVRG
vGlut2
Pax2
Wnt1
Dbx1
Lbx1
vGAT

Figure 3. Identity of the Phr-pMNs of the rostral ventral respiratory group. Transverse brainstem section showing trace^{+} rVRG neurons labeled by Rb-mCherry (red, R) and counterstained for nuclear expression of LacZ (green, G) and summary histograms featuring the percentage of trace^{+} rVRG neurons expressing LacZ (yellow bars, RZ). **A,** when LacZ is expressed from the Dbx1 locus; **B,** from the Lbx1 locus; **C**, from the Wnt1 locus and **D**, from the En1 locus. Note that the rVRG is comprised of neurons with a history of expression of Dbx1 or Lbx1 or Wnt1 but not of En1. **E**, same as above with additional immunostaining for Pax2 (blue, P) and summary histograms showing the percentage of trace^{+} rVRG neurons expressing LacZ alone (yellow bars, RZ) or co-expressed with Pax2 (white bars, RZP) when LacZ is expressed from the vGlut2 locus; **F**, from the vGAT locus; **G**, from the Dbx1 locus and **H**, from the Lbx1 locus. Note the comparable proportion of triple positive cells in **E** and **G** panels and their virtual absence in **F** and **H** panels. **J**, summary diagram of the proportions of rVRG neurons having a history of expression of Dbx1 (yellow), Wnt1 (orange), Lbx1 (light green), concentric red, green and blue bars indicate respectively the distributions of vGlut2^{+}, vGAT^{+} and Pax2^{+} cells. Dotted lines delineate fractions of rVRG neurons with unknown status that derive from Dbx1-expressing progenitors or Lbx1-expressing precursors found respectively Pax2^{-} and Pax2^{+}. Note that these fractions matching with the those of Pax2^{-},vGlut2^{+} and Pax2^{+},vGAT^{+} cells respectively, have been aligned.

Figure 4

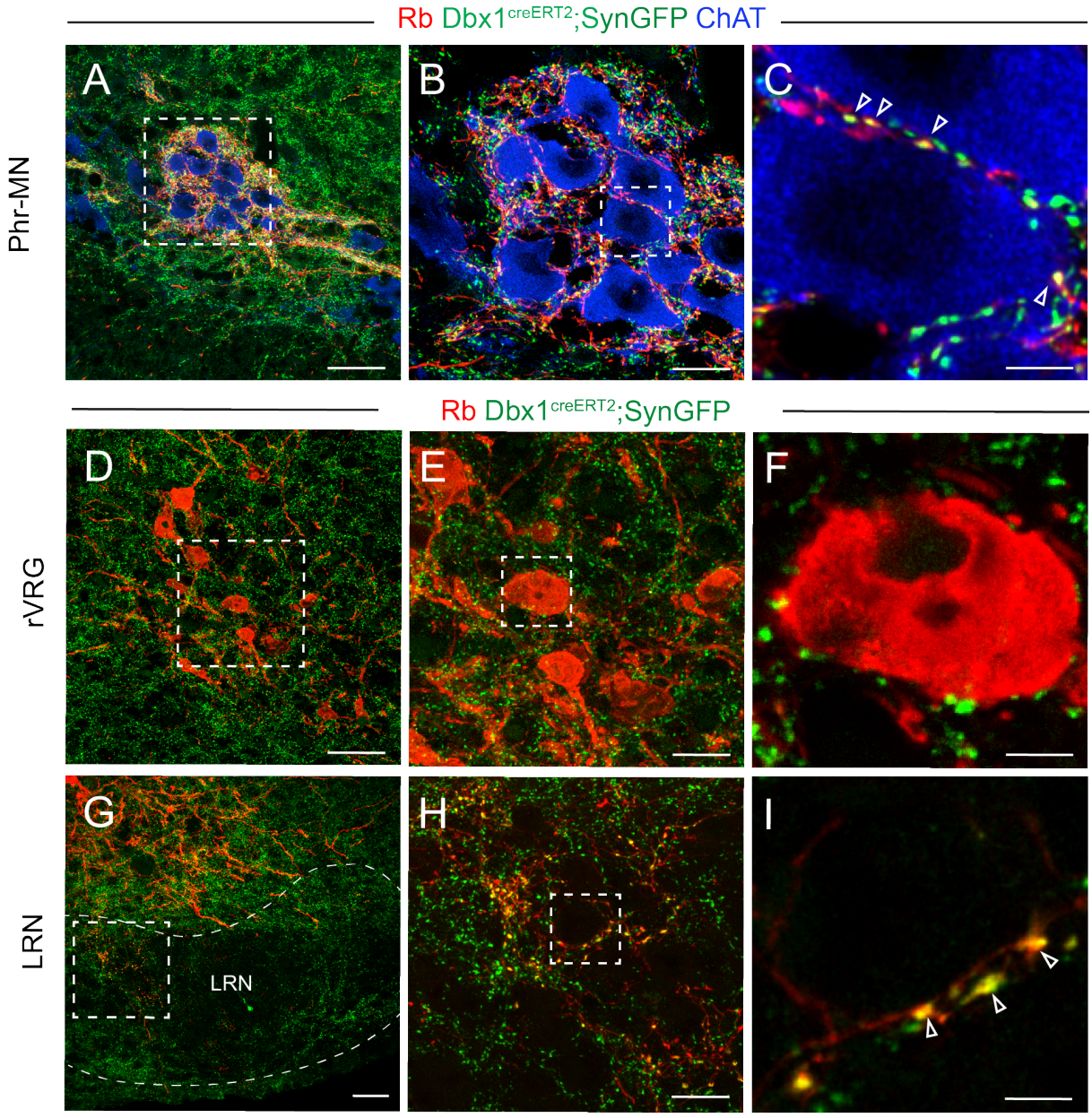

Figure 4. Synaptic targets of V0 rVRG neurons. **A**, V0 rVRG synaptic terminals double labeled (yellow) by rabies-mCherry (Rb, red) and SynGFP (green) are massively present on Phr-MNs (trace$^-$, ChAT$^+$, blue) contralateral to the diaphragm viral injection side. **B,** zoom on the square inset in A. **C**, single optical section of the Phr-MN (inset in B) showing individual synapses (arrowheads). **D-F**, rVRG (trace$^+$, red) neurons devoid of double labeled terminals are not internally connected by either ipsi-or contralateral partners. **E**, zoom of the inset in D. **F**, single optical section of the rVRG neuron (inset in E). **G,** V0 trace$^+$ rVRG neurons project to the lateral reticular nucleus (LRN). **H**, zoom of the inset in G, **I**, single optical section showing individual V0 rVRG synaptic terminals (arrowheads) abutting a LRN soma. Scale bars: A,D,G, 50µm; B,E,H,20µm; C,F,I, 5µm.

Figure 5

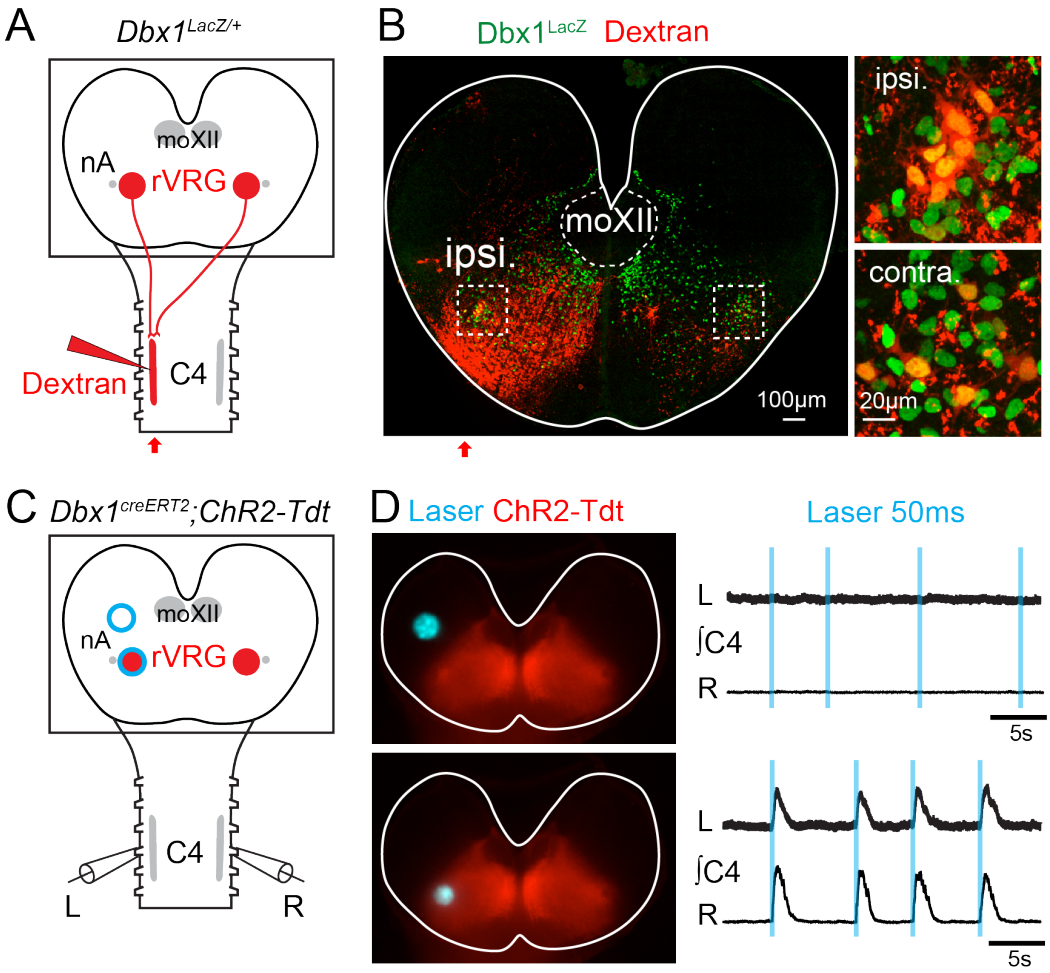

Figure 5. rVRG neurons transmit bilaterally their excitation to Phr-MNs at E15.5. **A**, Schematic of an *Dbx1*$^{LacZ/+}$ E15.5 brainstem spinal cord preparation used to pressure inject a Rhodamine dextran dye unilaterally in the C4 region of Phr-MNs for retrograde staining of rVRG neurons. **B**, low magnification image of a transverse slice in the plane of the rVRG showing the tracer pattern (red) and LacZ counterstain (green). Note at this magnification visible double stained (yellow) cells in the ipsilateral and contralateral rVRG (square dotted insets) shown in close-up views at right. **C**, Schematic showing the *Dbx1*^{creERT2}*;ChR2-Tdt* preparation photo-excited with blue laser light using digital holography in targeted areas (blue empty circles) while recording activities of left and right C4 motor roots. **D**, top, left, image of Tdt expression in the horizontally exposed plane of the rVRG showing the unilateral laser spot, positioned away from the rVRG and applied at times indicated by vertical blue lines systematically failing to evoke C4 activity responses (top right set of traces). Bottom, left, same as top with the light spot positioned on the rVRG now reliably evoking synchronous left and right C4 bursts (bottom right set of traces).

Figure 6

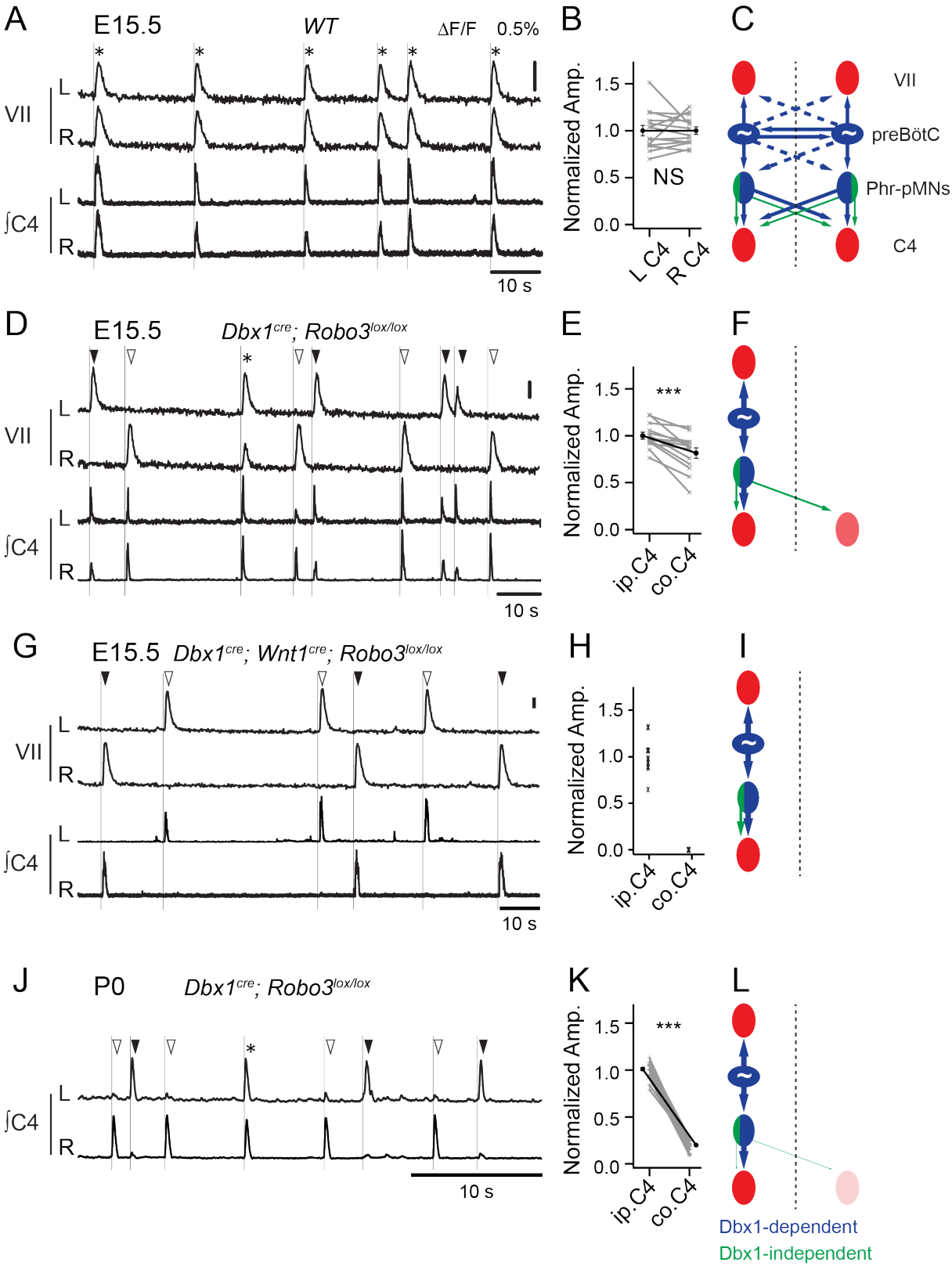
A
E15.5
WT
ΔF/F 0.5%
VII
L
R
∫C4
L
R
10 s
B
Normalized Amp.
1.5
1.0
0.5
0.0
NS
L C4
R C4
C
VII
preBötC
Phr-pMNs
C4
D
E15.5
Dbx1cre; Robo3lox/lox
VII
L
R
∫C4
L
R
10 s
E
Normalized Amp.
1.5
1.0
0.5
0.0
***
ip.C4
co.C4
F
G
E15.5 Dbx1cre; Wnt1cre; Robo3lox/lox
VII
L
R
∫C4
L
R
10 s
H
Normalized Amp.
1.5
1.0
0.5
0.0
ip.C4
co.C4
I
J
P0
Dbx1cre; Robo3lox/lox
∫C4
L
R
10 s
K
Normalized Amp.
1.5
1.0
0.5
0.0
***
ip.C4
co.C4
L
Dbx1-dependent
Dbx1-independent

Figure 6. V0 subtype neurons are critical for bilaterally balanced and synchronized C4 outputs in P0 brainstem spinal cord preparations. **A**, Spontaneous fluorescence (ΔF/F) changes of the left (L) and right (R) facial motor nucleus (VII, top traces) and electrophysiological activities of the left and right C4 motor root (bottom traces) showing phased (*) rhythmic bouts of activity in wildtype preparations. **B**, Histogram of the normalized amplitudes of synchronous left (L C4) and right (R C4) phrenic motor bursts showing their balanced amplitudes. **C**, Schematic of the putative ascending and descending connectivity from the preBötC rhythm generator to respectively facial and phrenic motor outputs (red) assuming (dashed arrows) some of the commissural connectivity from the preBötC and Phr-pMNs. **D**, In *Dbx1^{cre};Robo3$^{lox/lox}$* preparations, the left (black arrowheads) and right (white arrowheads) bouts of VII activity were found de-synchronized but still phased (vertical lines) with bilaterally synchronized bouts of activity of the C4 motor roots. Note the higher amplitude of the burst on the C4 root ipsilateral (ip.C4) to the active VII when compared to that recorded from the contralateral side (Co.C4). **E**, Histogram of the normalized amplitudes of synchronous ip.C4 and Co. C4 showing the reduced amplitude of the latter. **F**, In *Dbx1^{cre};Robo3$^{lox/lox}$* mutants the commissural connectivity (midline crossing blue arrows) of the preBötC, and that of the prominent fraction of rVRG neurons at the Phr-pMNs level is ipsilaterally re-routed while that provided by neurons originating outside the P0 domain of progenitors is spared (midline crossing green arrow). **G**, In double *Dbx1^{cre};Wnt1^{cre};Robo3$^{lox/lox}$* mutant preparations left-right desynchronized bouts of VII activity were phased only with the C4 motor root on the same side. The unilateral restriction of synchronicity results from absent commissural connectivity. **H**, Histogram of the normalized amplitudes of the ip.C4 burst, absent synchronized co.C4 bursts are represented by a zero amplitude symbol. **I**, in the double conditional *Robo3* mutant preparations, the commissural connectivity supporting the rhythmic activity of the motor outputs is lost. **J**, *Dbx1^{cre};Robo3$^{lox/lox}$* mutant preparations, at P0, show an aggravated unbalance of the amplitudes of the synchronous bouts of activity of the left and right C4. **K**, histogram of the normalized amplitudes of yet synchronous ip.C4 and Co. C4 bursts of activity showing the much greater amplitude of ip.C4 relative to Co. C4 bursts suggesting an almost complete loss of commissural connectivity. **L**, at P0 the sole absence of Dbx1-dependent commissural neurons results in a virtually complete left-right unbalance of the C4 motor outputs. Phased activity events (*) were still detected occasionally *in Dbx1^{cre};Robo3$^{lox/lox}$* preparations at both E15.5 (17/144 bursts from 4 preps) and P0 (6/79 bursts from 4 preps) either caused by fortuitous phasing of the independent left and right motor drives or by yet unidentified synchronous bilateral drives of the rhythm generator.

Figure 7

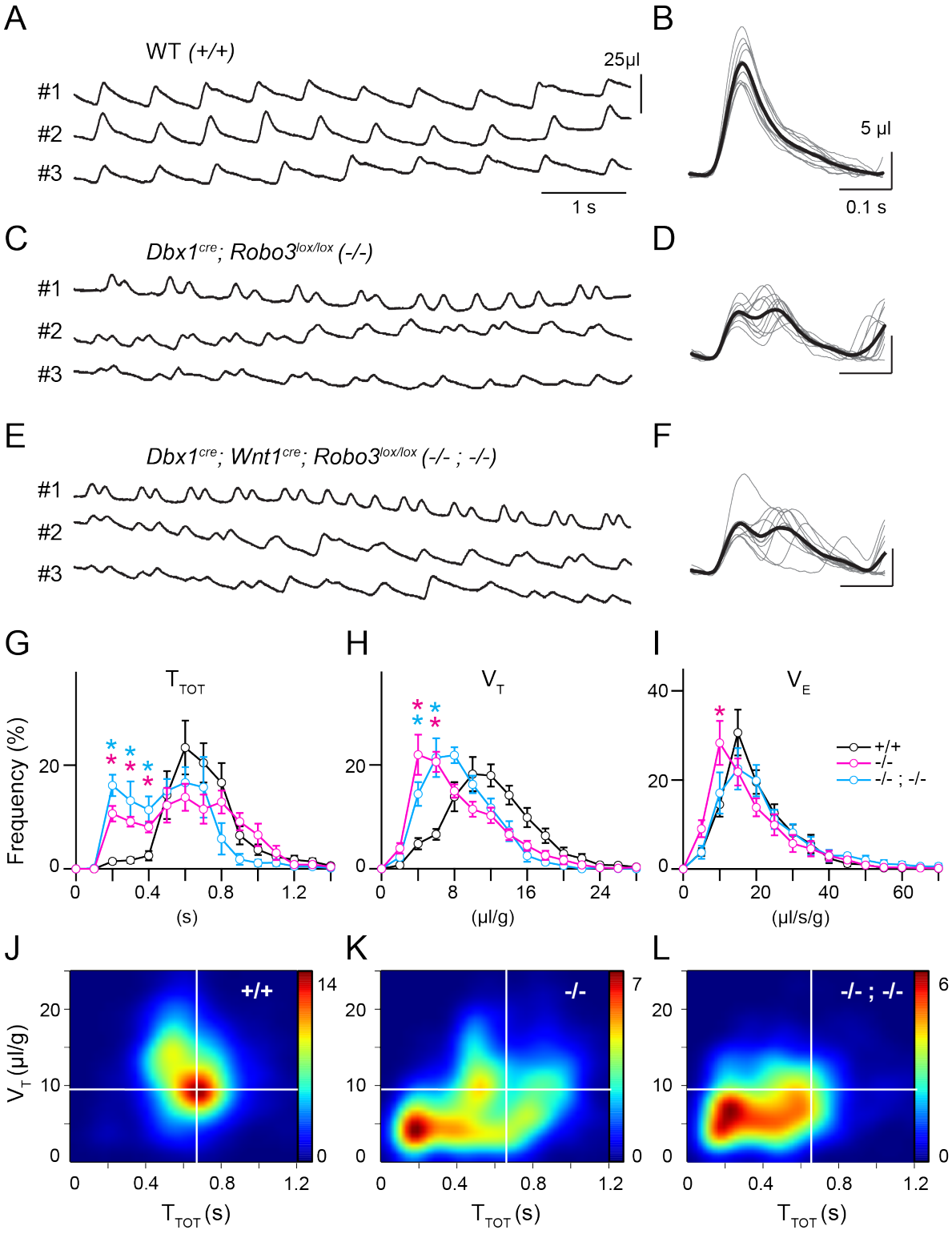
A
WT (+/+)
25µl
#1
#2
#3
1 s
B
5 µl
0.1 s
C
Dbx1cre; Robo3lox/lox (-/-)
#1
#2
#3
D
E
Dbx1cre; Wnt1cre; Robo3lox/lox (-/- ; -/-)
#1
#2
#3
F
G
TTOT
Frequency (%)
20
0
0
0.4
0.8
1.2
(s)
H
VT
20
0
0
8
16
24
(µl/g)
I
VE
40
20
0
0
20
40
60
(µl/s/g)
+/+
-/-
-/- ; -/-
J
+/+
14
0
VT (µl/g)
20
10
0
0
0.4
0.8
1.2
TTOT (s)
K
-/-
7
0
20
10
0
0
0.4
0.8
1.2
TTOT (s)
L
-/- ; -/-
6
0
20
10
0
0
0.4
0.8
1.2
TTOT (s)

Figure 7. Left-right decoupled breathing in *Dbx1^{cre};Robo3$^{lox/lox}$* neonates. **A**, example plethysmographic recordings from three wildtype P0 neonatal pups (#1,#2,#3) during quiet breathing. **B**, ten super imposed representative breath (thin lines) and their average (thick line). **C**, comparable recordings for three *Dbx1^{cre};Robo3$^{lox/lox}$* mutant pups. Note the reduced amplitude of breath and their more frequent occurrence. **D**, super imposed representative mutant breath often appearing as double breath events. **E**, a breathing pattern similar to that of *Dbx1^{cre};Robo3$^{lox/lox}$* is observed in *Dbx1^{cre};Wnt1^{cre};Robo3$^{lox/lox}$* double mutants. **G-I**, summary histograms of the distributions of breath duration (T_{TOT}, **G**), tidal volumes (V_T, **H**) and ventilation (V_E, **I**) in wildtypes (+/+, black trace), *Dbx1^{cre};Robo3$^{lox/lox}$* (-/-, pink trace) and *Dbx1^{cre};Wnt1^{cre};Robo3$^{lox/lox}$* (-/-;-/-, blue trace). Note the left shifted distributions for T_{TOT} and V_T of both mutant types. Stars indicate significant differences with wildtypes, no significant differences were found when comparing values across mutants. **J-K**, Density maps of V_T-T_{TOT} relationships for the breathing of wildtypes (+/+, **J**), *Dbx1^{cre};Robo3$^{lox/lox}$* (-/-, **K**) and *Dbx1^{cre};Wnt1^{cre};Robo3$^{lox/lox}$* (-/-;-/-, **L**). Note in the mutants a concentration of aberrant breath featuring both small V_T and small T_{TOT} values (in the bottom left quadrant) that are absent in wildtype pups.

Figure 8

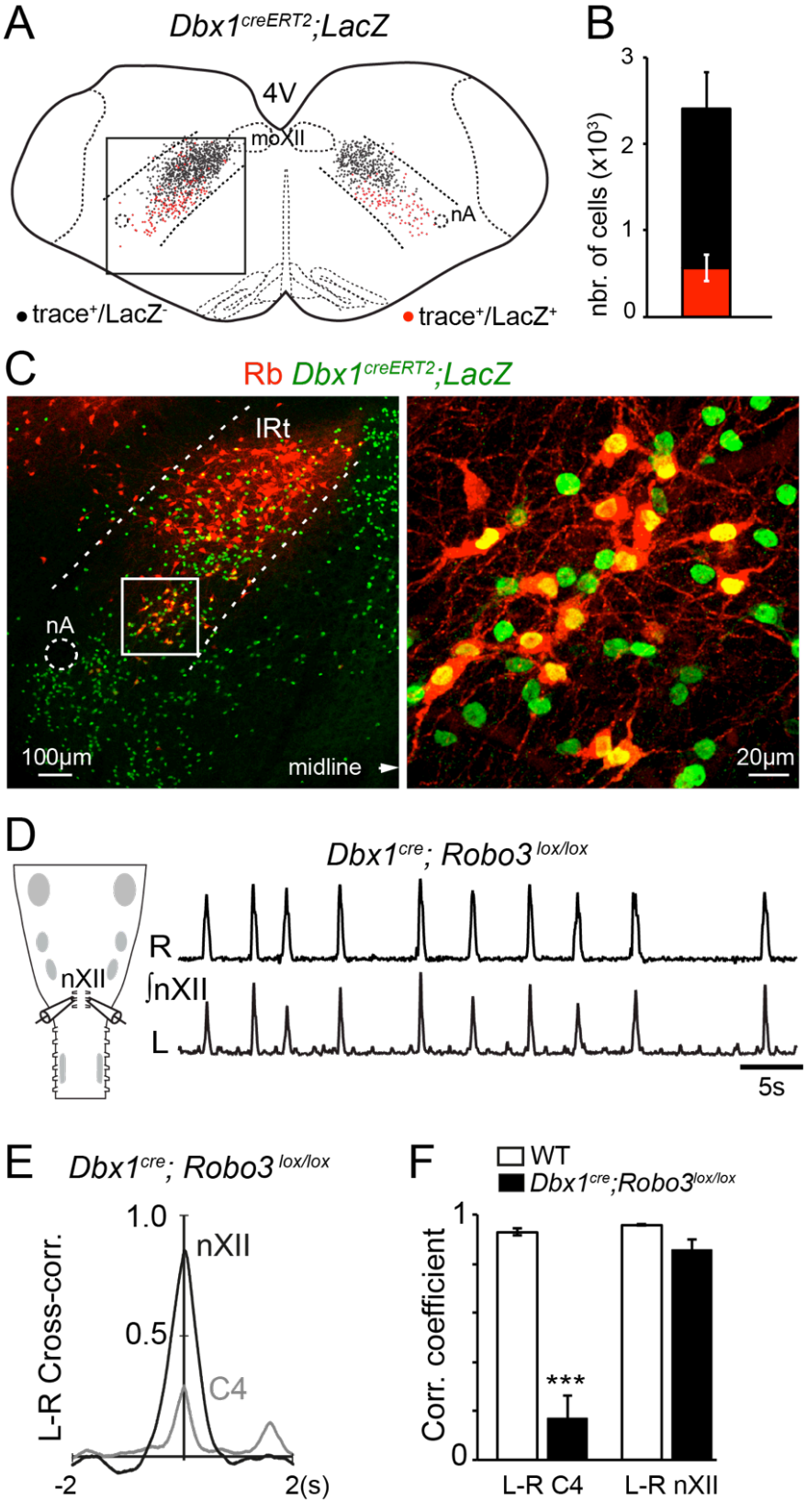
A
Dbx1creERT2;LacZ
4V
moXII
nA
trace+/LacZ-
trace+/LacZ+
B
nbr. of cells (x10³)
3
2
1
0
C
Rb Dbx1creERT2;LacZ
IRt
nA
100µm
midline
20µm
D
Dbx1cre; Robo3 lox/lox
nXII
R
∫nXII
L
5s
E
Dbx1cre; Robo3 lox/lox
1.0
0.5
nXII
C4
L-R Cross-corr.
-2
2(s)
F
WT
Dbx1cre;Robo3lox/lox
Corr. coefficient
1
0
***
L-R C4
L-R nXII

Figure 8. *Dbx1^{cre};Robo3$^{lox/lox}$* neonates maintain left-right synchronized and balanced hypoglossal motor outputs. **A**, Schematic of a transverse brainstem slice between moVII and moXII at P9 showing the bilateral positions of mCherry labeled tongue premotor neurons in the IRt after injection at P1 of DG-Rb/AAV-G viral cocktail into the left genioglossus muscle of a *Dbx1^{creERT2}; LacZ* mouse. The IRt is the only moXII premotor location found to host trace+ V0 subtype identity neurons (trace^{+}/LacZ^{+}, red dots) in ventral and medial location with respect to the bulk of trace+ neurons having no history of Dbx1 expression (trace^{+}/LacZ^{-}, black dots). **B**, summary histogram of the number of trace^{+}/LacZ^{-} (black bar) and trace^{+}/LacZ^{+} (red bar) cells counted in 4 experiments in the IRt extended caudally to the transverse plane of the preBötC and rostrally to that of the moVII. **C**, right, image of the inset in A showing double immunostaining for LacZ (green) and mCherry traced (red) cells. The square inset, at higher magnification on the left, shows the region dorsal and medial to the nucleus ambiguus (nA) where double positive (yellow) cells are most abundant. **D**, Schematic of a *Dbx1^{cre};Robo3$^{lox/lox}$* brainstem spinal cord preparation showing electrodes placed on left (L) and right (R) hypoglossal motor rootlets (nXII). Superposed traces show the corresponding rhythmic and bilaterally synchronized integrated neurograms (the low amplitude events visible on the bottom trace are artefactual). **E**, Cross-correlation plots of the activities of the left-right nXII (black line) and C4 (gray line) activities at P0 recorded in the same *Dbx1^{cre};Robo3$^{lox/lox}$* preparation showing that impaired commissural connectivity of V0 subtype interneurons is sufficient to alter left-right C4 but not nXII motor outputs. **F**, summary histograms showing the average correlation coefficients for L-R C4 and L-R nXII calculated from n=4 wildtype and n=4 *Dbx1^{cre};Robo3$^{lox/lox}$* P0 preparations.

Supplementary Figure 1

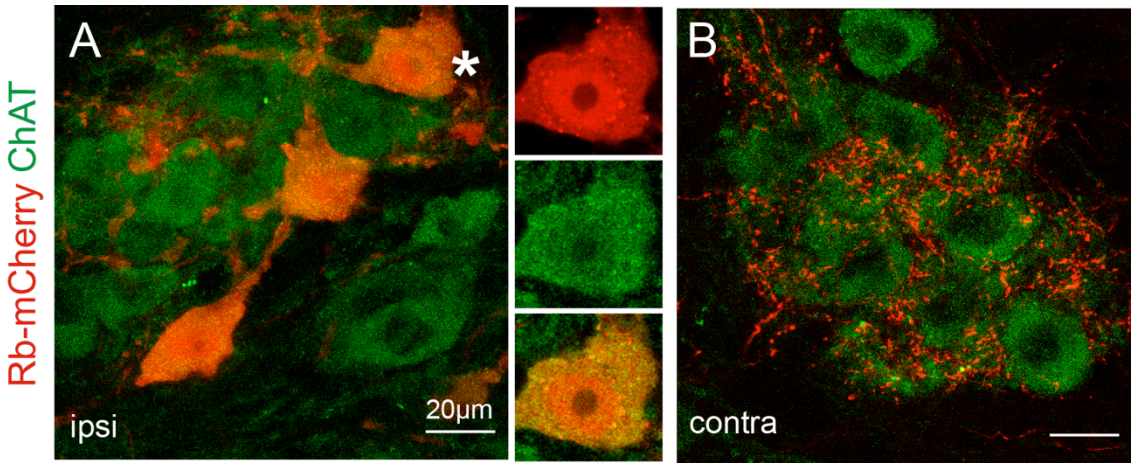

Supplementary Figure 1. A, Example Phr-MNs ipsilateral to the side of diaphragm injection of Rb-mCherry virus co-express (yellow) mCherry (red) and ChAT (green). **B**, contralateral partners receive extensive innervation from labeled Phr-pMNs.

Supplementary Figure 2

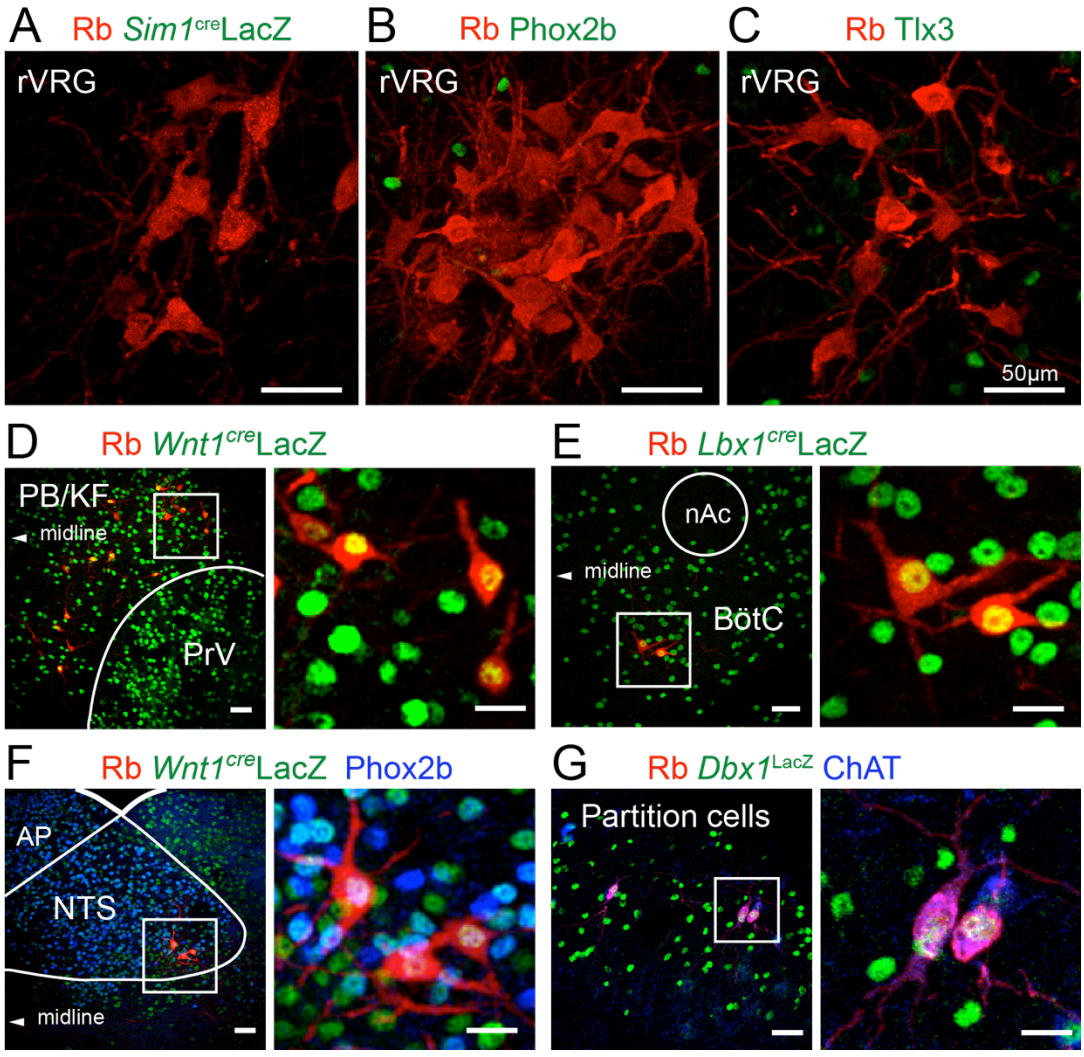

Supplementary Figure 2. Identity of the Phr-pMNs of the rVRG, BötC, PB/KF, NTS, and spinal partition cells. **A-C**, transverse sections showing that traced rVRG neurons have no history of expression of Sim1 (**A**) and express neither Phox2b (**B**) nor Tlx3 (**C**). **D**, traced Phr-pMNs in the PB/KF derive from Wnt1-expressing progenitors. **E**, transverse section showing that traced Phr-pMNs in the BötC derive from Lbx1-expressing precursors. (**F**) traced Phr-pMNs in the NTS derive from Wnt1-expressing progenitors and express Phox2b. **G**, sagittal section showing that traced partition cells in the cervical spinal cord are cholinergic and derive from Dbx1-expressing progenitors. Scale bars: A-C, 50µm; D-G left, 50µm; D-G right, 20µm.

Supplementary Figure 3

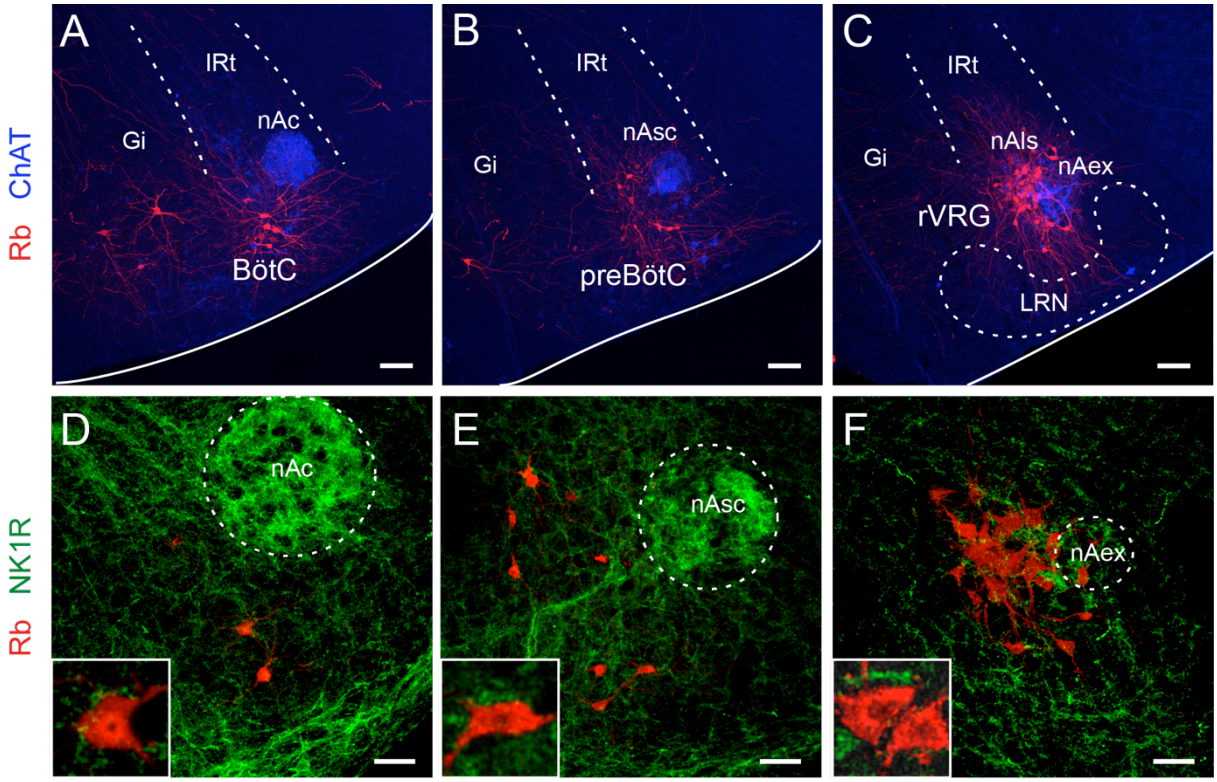

Supplementary Figure 3. The Phr-pMNs in BötC, preBötC and rVRG positions are not NK1R$^+$. **A-C**, transverse sections showing the position of trace$^+$ (red) Phr-pMNs in (**A**) the BötC located ventral to the compact formation of the nucleus ambiguus (nAc), (**B**) the preBötC ventral to the to the semicompact formation of the nA (nAsc) and (**C**) the rVRG ventral to, and intermingled with, respectively the loose formation (nAl) and the external part (nAex) of the nA. **D-F**, Example image of the same regions showing NK1R immunostains (green) and inset higher magnifications of resident trace$^+$ Phr-pMNs immuno-negative for NK1R. Scale bars: 50µm.

Supplementary Figure 4

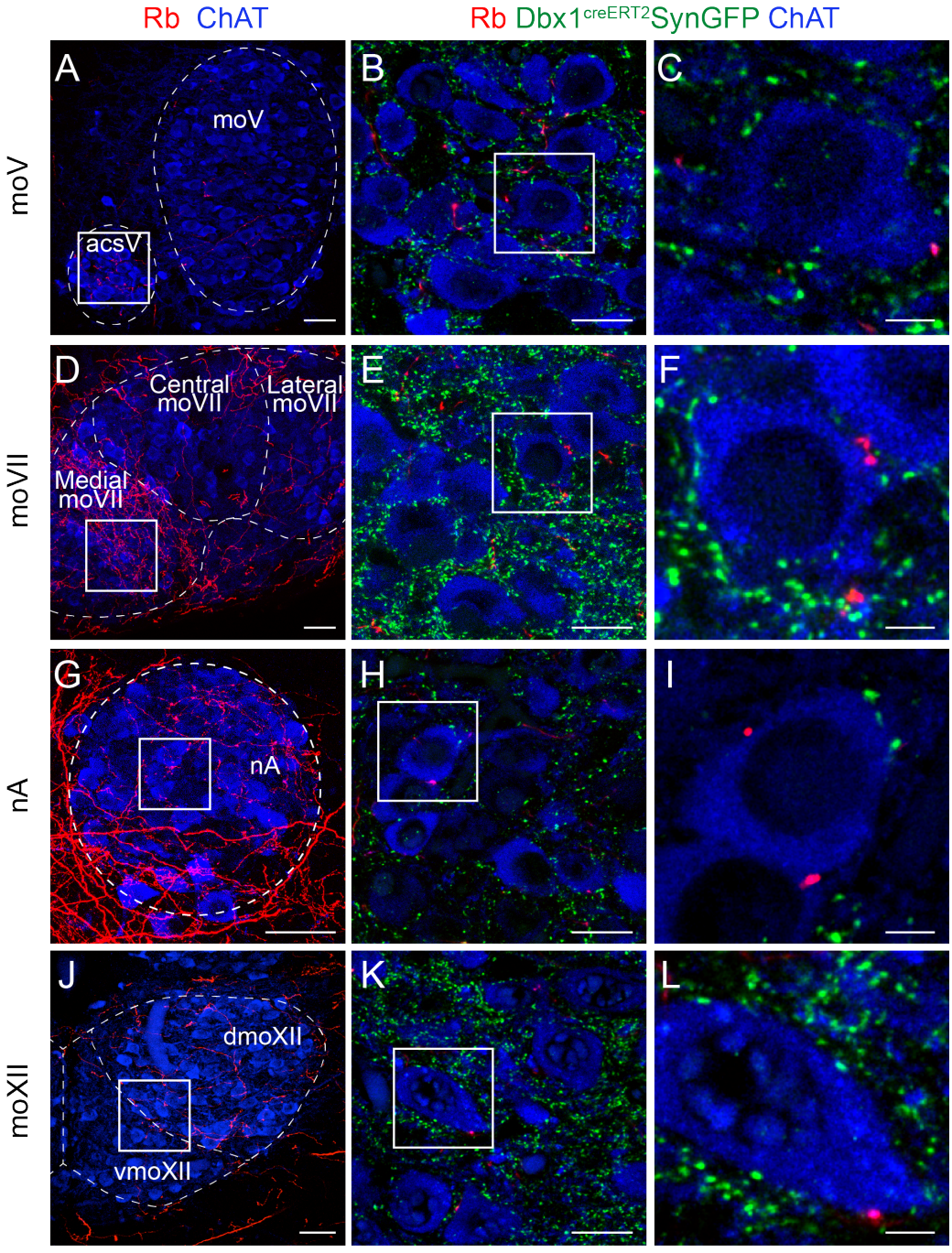

Supplementary Figure 4. V0 Phr-pMNs do not project on cranial motor nuclei. **A,** Trace^{+}(red) projections from Phr-pMNs onto ChAT^{+} (blue) trigeminal (moV) and accessory part of the trigeminal nucleus (acsV). **B**, zoom of the square inset in A showing the presence of non-V0 Phr-pMNs projections (mCherry^{+} only, red) and V0 non-Phr-pMNs synaptic terminals (GFP^{+} only, green) but absent V0 Phr-pMNs double labeled synaptic terminals (mCherry^{+}/ GFP^{+}, yellow). **C**, single optical section of the inset in B. **D-F**, corresponding panels in the facial motor nucleus (moVII), (**G-I**) nucleus ambiguus (nA) and (**J-L**) hypoglossal motor nucleus (moXII). Scale bars: A,D,G,J, 50µm; B,E,H,K, 20µm; C,F,I,L, 5µm.

Supplementary Figure 5

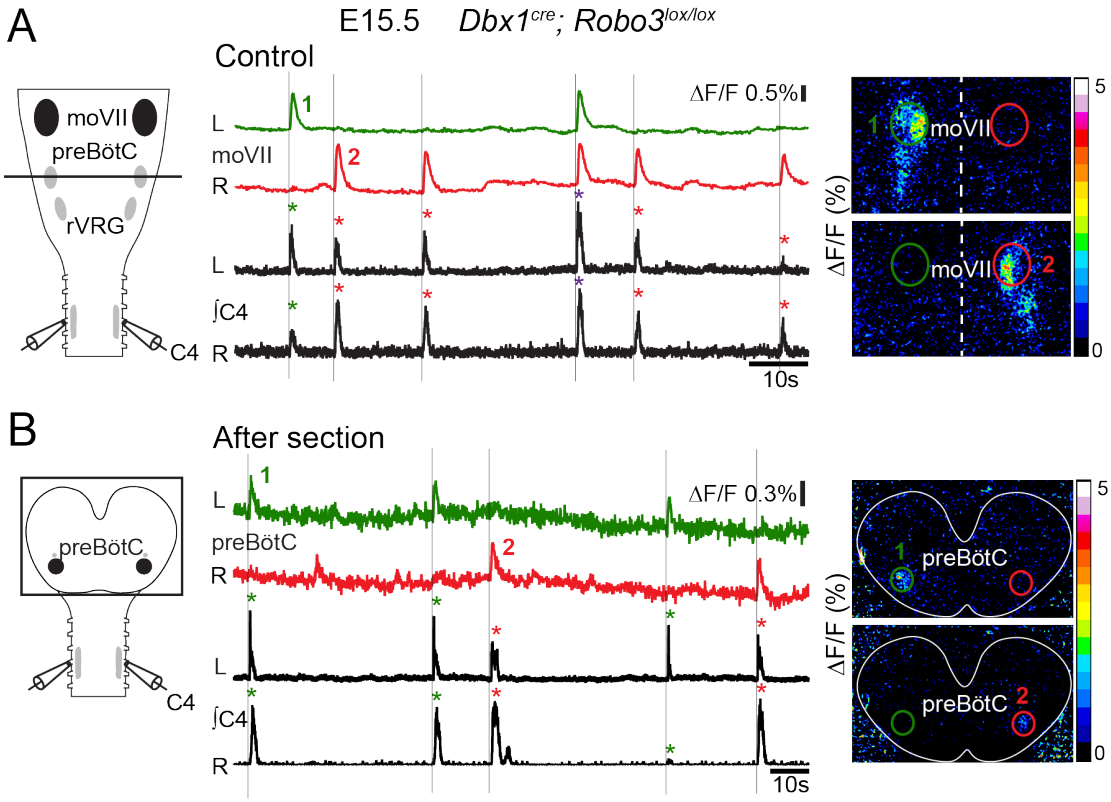

Supplementary Figure 5. At E15.5, facial motor neurons (moVII) are ipsilaterally driven by the left and right decoupled preBötC in *Dbx1*^{cre};*Robo3*$^{lox/lox}$ reduced preparations. **A**, Left, schematic of the in vitro brainstem-spinal cord preparation used to concurrently record control activities, of the left (L, green trace) and right (R, red trace) moVII by calcium imaging, and of the left and right C4 roots by electrophysiology. Generally independent occurrences of activity on the left (example peak 1) and the right (example peak 2) moVII (corresponding ΔF/F fluorescence changes illustrated in panels at right) are associated to synchronous (vertical bars) bilateral discharges of the left and right C4 roots. Note a tendency for C4 bursts ipsilateral to the active moVII to have larger amplitudes than the contralateral ones (green and red asterisks mark respective left active and right active moVII, purple asterisks indicate a rare event of synchronous left and right activation). **B**, Left, schematic of the preparation after a transverse section (black horizontal line on the schematic in A) exposing the preBötC for calcium imaging. Note that independent occurrence of activity on the left (example peak1) and right (example peak2) preBötC (corresponding ΔF/F fluorescence changes are illustrated in panels at right) also lead to bilateral synchronous unbalanced drives of C4 roots.

Supplementary Video 1. Left/right synchronized breathing of a wildtype pup at P0.

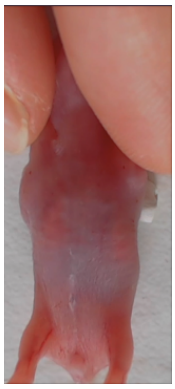

Supplementary Video 2. Decoupled left/right breathing of a *Dbx1^{cre};Robo3$^{lox/lox}$* mutant pup at P0.

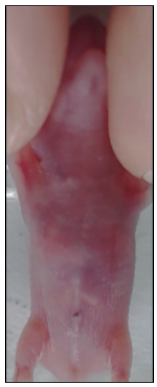

Supplementary Video 3. Decoupled left/right breathing of a *Dbx1^{cre};Wnt1^{cre};Robo3$^{lox/lox}$* double mutant pup at P0.

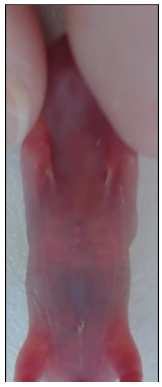

GENERAL DISCUSSION

This PhD work is a contribution to the dissection of the central circuit that controls the breathing behavior. I have focused my attention on premotor neurons impinging on phrenic motoneurons motorizing the diaphragm muscle. These neurons interface the inspiratory rhythm generator to its outputs and must robustly and bilaterally secure the synchronous transmission of amplitude balanced motor drives to left and right diaphragm muscles for efficient breathing. My work touches upon cell specification programs that produce the neurons (the nodes) and viral tracing methods revealing connectivity (the links) of the network.

The results obtained demonstrate the obligatory role of V0-type glutamatergic neurons to ensure the bilaterally synchronized motor control of the left and right hemi-diaphragms. I've shown here that, in addition to composing the preBötC inspiratory rhythm generator, V0 interneurons are also the main premotor neurons transmitting the rhythm to phrenic motoneurons innervating the diaphragm. This work demonstrates the crucial importance of V0 neurons in the functional organization of the inspiratory motor command in mammals and suggests that P0 progenitors may have been candidate targets in the course of evolution for the advent of aspiration breathing in mammals.

I cannot refrain from exposing here an experimental twist that contributed immensely to the development of the present work. When I first started the investigation of the neural bases of left-right synchronicity of the inspiratory drive, we knew that disrupting the commissural navigation of Dbx1-derived neurons forming the preBötC (through conditional invalidation of *Robo3*) resulted in its left-right de-synchronization (**Bouvier et al., 2010**). The prediction was then that should the preBötC be the sole source of left-right synchronization of rhythmic inspiratory activity, in other words if bilateral synchrony was entirely built-in at the level of the rhythm generator, we should observe decoupled activities of the left and right phrenic nerves. The twist is that had I first looked at the outcome of the conditional *Robo3* mutation at birth, I would have witnessed a massive left-right impairment of the left and right motor drives to the phrenic nerves and would have concluded that the preBötC was the unique site ensuring left-right synchronicity of the inspiratory motor drive. Because I first considered activities at E15.5 and observed fully de-synchronized rhythmic activities of facial nerves but the presence of left and right motor drives presenting unbalanced amplitudes at the level of phrenic nerves, the conclusion was that invalidation of *Robo3* in V0s indeed left-right decoupled the preBötC and the premotor drive to facial motoneurons, but was not sufficient to

fully de-synchronize the motor drive to phrenic motoneurons. This rather suggested that descending premotor neurons other than V0s had to participate in “re-synchronizing” the activities of phrenic motor pools on either side of the midline. This experiment prompted the investigation of the identities and of axonal projections of phrenic premotor neurons. The second twist is that had we proceeded the other way, the conclusion as to the importance of V0s at birth for bilateral synchronicity of the inspiratory drive would have been true. However, assuming that the importance of V0s can be reduced to the sole preBötC would have been misleading for a comprehensive understanding of the organization of inspiratory executive control circuit. In particular, the present demonstration that V0 commissural interneurons form both the preBötC and the rVRG, the main premotor station, may prove an essential finding for speculating on the mechanisms that may have instated during evolution the neuronal machinery allowing aspiration breathing. The present discussion section will end with a synthetic presentation of my views on this issue.

I. Methodological concerns

All anatomical studies must address the issue of false positive and negative results. Although it is impossible to rule out that the monosynaptic method might not label all premotor neurons, there is no reason to believe that neurons not connected to phrenic motoneurons may have been labeled. Rabies virus transsynaptic labeling may depend on the number and location of synaptic contacts and on various cellular susceptibilities to the viral infection. When relatively fewer neurons were found in a premotor area compared to others it remains unclear whether this was due to its sparser connectivity or its overall smaller count of neurons or a combination of both. For instance premotor areas such as the LPGi, Gi and Ve comprise reduced numbers of neurons compared to the rVRG. When injections were done using a low volume of virus or lower titer solutions, only the Phr-pMNs in rVRG could be traced. In fact, the abundance of Phr-pMNs in the rVRG was a good predictor of the presence of premotor neurons in other premotor sites. When less than 100 rVRG neurons were labeled in an experiment no other premotor site hosted labeled cells. As the number of labeled rVRG neurons increased, neurons began to appear in other premotor areas starting with the ones that featured the highest effective of neurons. Because the rabies virus is replicative the labeling was equally strong in the cells belonging to either small or large premotor population. Finding that the relative size of virally traced premotor populations compared to the rVRG maintained

a fixed proportionality irrespective the efficiency of the viral injection probably indicates that the virus transsynaptic labeling doesn't introduce sampling biases per se in the effective of traced premotor neurons. As rabies viruses are cytotoxic, it is important to restrict the propagation time of the virus to prevent the apoptosis of infected neurons and spurious glial infections around dying cells. It has been observed that the survival of infected cells is compromised 12 days after infection (**Wickersham et al., 2007b**). Therefore, in this study, we allowed the virus to spread for 8 days to optimize viral expression and minimize detrimental effects.

Although rabies viral spread is known to operate in a retrograde direction in the CNS, it has been found that the rabies viral vectors are also able to infect the terminal endings of sensory neurons and yield anterograde transsynaptic spread (**Zampieri et al., 2014**). This probably has minor impact in the present study. First, appropriate afferent information for respiratory muscle (e.g. indicating accuracy of ventilator efforts) must reflect lung volume and chest wall distention. Accordingly, respiratory muscles such as the diaphragm have minimal innervation by muscle spindles (**Duron et al., 1978**), and phrenic afferents contribute little to respiratory modulation (**Corda et al., 1965**; **Jammes et al., 2000**). Second, sensory inputs from the diaphragm that are conveyed through the vagus nerve (**Young et al., 2010**) arise from the crural diaphragm muscle while our injections target the costal diaphragm muscles. Third, the very limited sensory innervation from the costal diaphragm courses through the dorsal root ganglia. Viral labeling there, was inconsistent in our experiments, and if anterograde transsynaptic spread had occurred the presumptive labeled spinal sensory neurons wouldn't have interfered with our analysis of brainstem premotor neurons. As it turns out, it has been shown that the same pattern of transsynaptically labeled premotor neurons in the spinal cord was obtained when either applying the present viral approach or an alternative method in which the transsynaptic spread is conditional to motoneurons themselves (**Goetz et al., 2015**). Altogether, the monosynaptic tracing method used here provides the most selective strategy to map phrenic premotor neurons.

As mentioned above depending on the efficiency of the viral infection the number of transsynaptically traced premotor neurons changed indicating that the virus likely subsampled the pool of Phr-pMNs, however due to convergence of my findings with those of previous studies the present tracing scheme is unlikely to have failed to detect at all a phrenic premotor population. This technique allows qualitative estimates of the left-right distributions of

premotor neurons but doesn't allow a quantitative determination of the number of Phr-pMNs bearing ispi-only or contra- only or both ipsi- and contra-lateral projection to Phr-MNs. This can be simply explained if we consider double injections made with two viruses encoding distinct reporter proteins in the left and right diaphragm respectively to reveal premotor neurons bearing bilaterally branched axons. In these cases, biases may arise from failures to infect left and right pairs of Phr-MNs sharing a common premotor neuron. Moreover, rabies viral vectors may compete for expression in co-infected neurons putting at risk detections of the both labels introducing a special case of false negative results. Altogether, because Phr-pMNs were always found bilaterally distributed, the above limitations preclude the countings of bilaterally vs unilaterally (ipsi- or contra-) projecting neurons. Even in premotor areas like the NTS or the PB/KF where bilaterally located cells are ipsilaterally over-represented, the reasoning cannot go beyond a mere conclusion that these premotor stations must comprise an excess of ipsilaterally projecting neurons.

II. Distribution of phrenic premotor neurons: mapping the direct control of the inspiratory motor command

Deciphering the neuronal circuits supporting specific behaviors is challenging but essential to understand the principles of information processing in the brain. My thesis work examines the neural bases of the breathing behavior. More specifically, this thesis is focused on the organization of premotor neurons that directly control the phrenic motor neurons responsible for contraction of the diaphragm. Although previous studies in rodents have provided valuable knowledge about the distribution of Phr-pMNs (phrenic premotor neurons), the methods previously used had important limitations. For example, injection of conventional retrograde tracers (e.g. HRP, Fluoro-gold, CTB) in the phrenic nucleus (**Ellenberger, 1999**; **Song et al., 2000**; **Yokota et al., 2004**) may label not only premotor inputs to Phr-MNs (phrenic motoneurons) but also the neurons with passing by axons at the injected site. Injections of transsynaptic neurotropic virus such as PRV and rabies virus in the diaphragm or phrenic nerve (**Dobbins and Feldman, 1994**; **Gaytán et al., 2002**) provide more specificity for entry into the Phr-MNs, but these viruses propagate through multiple orders of synapses and label neurons whose precise position in the multi-synaptic circuit cannot be determined. In the present study, I've used a genetically modified virus based monosynaptic tracing method (**Stepien et al., 2010**) to trace the premotor inputs to Phr-MNs

in newborn mice. This method overcomes the limitations described above by restricting the viral spread to the immediate presynaptic partners of motor neurons infected from their muscle target.

The largest fraction (70%) of traced Phr-pMNs is located in the rVRG, which had previously been suggested to be a prominent premotor station transmitting the inspiratory rhythm to Phr-MNs during inspiration on both anatomical (**Dobbins and Feldman, 1994**; **Ellenberger et al., 1990**; **Saji and Miura, 1990**) and electrophysiological grounds (**Fedorko et al., 1983**; **Feldman et al., 1985**; **Stornetta et al., 2003a**). My work also indicates that rVRG neurons are by and large glutamatergic excitatory neurons. They were shown to receive direct excitatory inputs from the preBötC inspiratory oscillator and inhibitory inputs from BötC as well as other modulatory drives such as from the Kölliker-Fuse (**Ezure et al., 2003b**; **Tan et al., 2010**; **Yokota et al., 2007**). Therefore, the rVRG is a site on which converge multiple inputs that participate in patterning the activity of inspiratory Phr-MNs. Besides this major excitatory drive to Phr-MNs from the rVRG, we have also revealed for the first time the existence within the rVRG of a subpopulation of inhibitory Phr-pMNs intermingled with the excitatory ones. Inhibitory neurons from the rVRG have long been suspected to exist but had never been identified. First, the existence of inhibitory rVRG neurons was anticipated from the electron microscopic observation of symmetrical densities at rVRG-Phr-MNs synapses (**Ellenberger et al., 1990**). Second, GABAergic inhibitory inputs in synchrony with and of similar shape to the inspiratory excitatory drive to Phr-MNs have been described that reduce inspiratory output of the C4 nerves in a BötC independent manner (**Parkis et al., 1999**). The presently identified $vGAT^{ON}$ inhibitory rVRG neurons are indeed GABAergic and are in a position with other rVRG glutamatergic Phr-pMNs to provide concurrent inhibition and excitation during inspiration thus enabling a specific gain control of the Phr-MNs output during inspiration that may shape discharge pattern, establish recruitment order or smooth force production (**Parkis et al., 1999**; **Robertson and Stein, 1988**).

Besides the inhibitory inputs from a subpopulation of rVRG, the Phr-MNs were also found to receive monosynaptic inhibitory inputs from the BötC, consistent with previous results (**Dobbins and Feldman, 1994**; **Ezure et al., 2003b**; **Peever et al., 1998**; **Tian et al., 1999**). The BötC mainly contains glycinergic neurons that likely account for the synaptic inhibition that Phr-MNs receive during expiration (**Fedorko and Merrill, 1984**; **Kalia, 1981**). They may also control the inspiratory-expiratory phase transition during normal

breathing (**Abdala et al., 2015**; **Ezure et al., 2003a**; **Richter and Smith, 2014**; **Schreihofer et al., 1999**; **Tian et al., 1998**). The BötC, together with a subpopulation of rVRG, provide the main monosynaptic inhibitory drive to Phr-MNs.

In this study, I also found some Phr-pMNs in the preBötC region. Because the BötC, preBötC and rVRG form a continuous column of cells, the labeled phrenic projecting neurons counted in the preBötC region may be rostral most rVRG neurons or caudal most BötC neurons as suggested by Dobbins et al 1994. The preBötC is a functionally defined area and the specificity of its described anatomical markers is questionable and at most a relative one. The neurokinin type 1 receptor NK1R, one of these preBötC markers, absent in rVRG cells, was rarely found expressed in Phr-pMNs located in the preBötC area, indicating that there might be only a few preBötC neurons projecting to Phr-MNs directly. The paucity of bulbospinal premotor neurons in the preBötC has been previously observed by anterograde tracing from preBötC (**Tan et al., 2010**) and transsynaptic retrograde tracing from Phr-MNs (**Dobbins and Feldman, 1994**) in adult rats, which is consistent with its essential role in rhythmogenesis rather than in the direct transmission of activity to motor neurons (**Feldman et al., 2012**; **Smith et al., 1991**, **2013**).

The PB/KF is a functionally heterogeneous group of respiratory neurons in the pons. The electrical or chemical stimulation of PB results in different respiratory responses, according to different sites of stimulation (**Alheid et al., 2004**; **Chamberlin and Saper, 1994**). In this study, Phr-pMNs in the PB region are mainly located in the anterior and medial portion of the KF and are mainly excitatory neurons, consistent with previous studies in adult rats (**Dobbins and Feldman, 1994**; **Yokota et al., 2004**, **2007**). It has been reported that injections of glutamate in this region of the KF results in a facilitation of inspiration (**Chamberlin and Saper, 1994**), that our result suggest may be caused by a direct increase of the excitability of Phr-MNs.

In addition, we identify a collection of excitatory Phr-pMNs in the NTS which had been previously shown in adult rats (**Castro et al., 1994**; **Dobbins and Feldman, 1994**). The NTS is the site of projection of the tractus solitarius which contains primary sensory afferents fibers from a number peripheral sensors (e.g. baro-, chemo- and stretch receptors from the lung) that report the metabolic status and the dynamics of ventilation to initiate regulatory reflexes (**Chitravanshi et al., 1994**; **Kubin et al., 2006**). The Phr-pMNs in the NTS are likely in pivotal position in respiratory reflex circuits including the Hering-Breuer lung deflation

reflex that causes a powerful increase of the inspiratory effort.

Brainstem raphe nuclei, especially the RO contains a few neurons that project to Phr-MNs (**Dobbins and Feldman, 1994**; **Hosogai et al., 1998**), and in our study we have confirmed their existence, although these neurons are very few. The RO contains mainly excitatory serotonergic neurons involved in somatic and autonomic control of respiration. It has been shown that the photostimulation of serotonergic neurons in the RO activates breathing and potentiates the chemoreflex *in vivo* (**Depuy et al., 2011**).

I have also identified Phr-pMNs in small numbers in several areas of the reticular formation that by nature lacks both precise localization and functional role. These include the LPGi and Gi that are thought to modulate neural activities in relation to the arousal state. Projection from these areas to phrenic nucleus has previously been suggested by conventional tracers and transsynaptic virus (**Dobbins and Feldman, 1994**; **Gaytán et al., 2002**). There neurons are best known for their role in enforcing REM sleep atonia through decreasing the excitability of medullary and spinal motoneurons (**Sirieix et al., 2012**). In this respect, it is interesting to note that only very few gigantocellular neurons were found to project onto Phr-MNs whereas they massively project onto spinal motoneurons that control locomotion (**Esposito et al., 2014**). This reduced projection may be in keeping with the obligatory persistence of breathing whatever the arousal state. It is likely that these reticular neurons project on multiple circuits and participate in the integration of breathing with other behaviors. Neurons of the IRt have been shown to take part in orofacial behaviors such as licking, sucking and whisking. It has been shown that neuronal output from this region is reset at each inspiration by direct input from the pre-Bötzinger complex, such that high-frequency sniffing has a one-to-one relationship with whisking. Thus, respiratory nuclei, which project to other premotor regions for oral and facial control, function as a master clock for behaviors that coordinate with breathing (**Moore et al., 2013**). Phr-pMNs were also found in vestibular nuclei (Ve) and it has been reported that the phrenic nerve activity in cat is influenced by head rotations (**Rossiter et al., 1996**), and that the stimulation of vestibular nuclei modulates ventilation in rats (**Xu et al., 2002**).

Although the interneurons in the spinal cord are not the focus of this study, I also observed some Phr-pMNs in the lamina VII and X in the cervical spinal cord. These phrenic projecting interneurons have been described previously (**Dobbins and Feldman, 1994**; **Lane, 2011**; **Lane et al., 2008a**), and they are suggested to play a role in the respiratory modulation

during normal breathing and in neuroplasticity following spinal cord injury (**Lane, 2011**; **Lane et al., 2008a**, **2008b**). I have identified a special class of spinal pMNs also present in other spinal motor circuits known as partition cells (**Miles et al., 2007**; **Stepien et al., 2010**; **Zagoraiou et al., 2009**) that constitute the exclusive source of cholinergic modulation onto motoneurons .

A general finding of this tracing scheme is that monosynaptic tracing following unilateral infection of Phr-MNs results in bilateral labeling of Phr-pMNs in all the premotor areas. Furthermore, about 80% of premotor neurons were equally distributed on the ipsilateral and contralateral sides, only the PB/KF, the NTS and the Gi showed an excess of ipsilaterally located cells. These results are in keeping with those obtained in previous tracing studies with two notable exceptions: the equal left and right distribution of bulbospinal neurons in the BötC and the bilateral rather than ipsilateral restricted presence of neurons in the PB/KF described by Dobbins and Feldman (**Dobbins and Feldman, 1994**). These differences probably owe to the unlimited spread of the virus in the latter study that imposes the use of a temporal logic for distinguishing directly connected and indirectly connected neurons to Phr-MNs assuming a somehow fix delay for viral crossing of one synapse. It is likely that at the post injection time (56-72 hours) when results were collected in the previous study, a fraction only of premotor neurons were labeled, resulting in systematic underestimations of neuronal counts. In our case, the selective trapping of the virus in Phr-pMNs allowed to triple the expression time of the virus resulting in optimized detection of the premotor neurons.

Finally, my study did not reveal Phr-pMNs in the retrotrapezoid nucleus, a respiratory site crucial for the CO_2 chemoreflex that up-regulates the respiratory rhythm frequency at birth probably through impinging onto the preBötC rhythm generator (**Dobbins and Feldman, 1994**; **Guyenet et al., 2005**; **Rosin et al., 2006**). The absence of transsynaptically traced neurons in cortical areas suggest that the volitional control of breathing or of diaphragm contractions operates through an oligosynaptic descending circuit or that the descending connectivity is not yet established in the early postnatal mouse.

III. Identity of Phr-pMNs

In this work I also have begun to assign the origin of the diverse phrenic premotor population in dorsal and ventral pools of progenitors that form the developing neural tube. This

description is yet lacunar as it lacks any anchoring in the anterior-posterior regionalization scheme of rhombencephalic segmentation (**Lumsden and Keynes, 1989**; **Lumsden and Krumlauf, 1996**) but still can orient future studies aiming at refining the role of individual subsets of premotor neurons. I will first briefly summarize the results obtained some of which are confirmatory to findings obtained in other labs and proceed on with a main novelty, the special case of V0 interneurons.

This analysis was limited to the main premotor areas i.e. those representing about 90% of all Phr-pMNs. Premotor neurons of the Gi, LPGi, IRt and in vestibular nuclei are not documented. Premotor neurons in the NTS were found to be excitatory glutamatergic neurons derived from dorsal dA3 progenitors (**Dauger et al., 2003**; **Storm et al., 2009**). In the PB/KF premotor neurons were glutamatergic (85%) complemented by $vGAT^{ON}$ inhibitory interneurons and were recapitulated by recombination using $Wnt1^{cre}$ and $En1^{cre}$ suggesting their origin in dorsal and anterior most progenitor domains of the hindbrain (**Rose et al., 2009**). In the BötC, Phr-pMNs were all inhibitory and arose from precursors that expressed Lbx1 (**Pagliardini et al., 2008**).

Finally, the origin of the rVRG that compose by and large the largest Phr-premotor pool had never been reported. I have found that the rVRG was composed for the most part of $vGlut2^{ON}$ excitatory neurons (75%) complemented by about 20% of $vGAT^{ON}$ inhibitory interneurons. These two fractions of rVRG neurons differ in origin. Excitatory rVRG neurons were found to derive from P0 progenitors expressing the homeobox transcription factor Dbx1 and have a V0 subtype identity. In the rVRG all of the inhibitory cells derived from Lbx1-expressing precursors and have a dB1/4 identity also shared by the Phr-pMNs of the BötC. Schematically, all of inhibitory Phr-pMNs share a common dB1/4 identity. Although this was not investigated in detail here, Lbx1-expressing neurons are also present at the axial level of the preBötC in limited numbers and have a likely inhibitory nature. Therefore, the part of the ventral respiratory column that contains about 90% of Phr-pMNs hosts from rostral to caudal the BötC, the preBötC and the rVRG in which Lbx1-derived inhibitory interneurons seems to form a continuous column of cells. In the ventral respiratory column, excitatory interneurons are massively of the V0 subtype and are absent from the BötC but present both in the preBötC and rVRG the two neural modules most crucial to generate and transmit the inspiratory rhythm to downstream phrenic motoneurons.

IV. The rVRG is a source of corollary respiratory discharges

The central nervous system to perform accurate motor tasks relies on comparison of planned and executed actions. To do so, it relies (i) on sensory feedback to report on the performed action and (ii) on axon collaterals at many levels sending efference copy signals or corollary discharges of the planned action to recipient neurons. Together these two information streams are used to adjust and modify the motor commands (**Crapse and Sommer, 2008**; **Wolpert and Miall, 1996**). I have considered the possibility that the main Phr-pMNs could represent a neuronal source broadcasting efference copy signals to other brainstem motoneuronal pools. Analysis of the V0 terminals of virally labeled rVRG neurons using a Dbx1^{creERT2};synGFP line revealed that they were lacking in trigeminal, facial, vagal, hypoglossal motor nuclei that innervate oro-facial muscles and upper airway patency regulating muscles. Interestingly, collateral terminal endings of rVRG neurons were notably detected in the lateral reticular nucleus (LRN). The lateral reticular nucleus is a precerebellar nucleus that relays through mossy fibers information from several spinal systems controlling posture, reaching, grasping and locomotion (**Alstermark and Ekerot, 2013**). Evidences have been reported on the convergence of central respiratory and locomotor rhythms onto single LRN neurons in the cat (**Ezure and Tanaka, 1997**) although the source of the respiratory drive to LRN neurons was not identified. In the latter study, about two thirds of respiratory-modulated LRN neurons showed an inspiratory discharge pattern. We therefore, propose that rVRG neurons may be a source of inspiratory inputs to the LRN. A recent study has identified the connectivity matrix of the C3-C4 propriospinal system implicated in voluntary forelimb motor control to the LRN and has also reported monosynaptic contralateral projection of the rVRG neurons onto the LRN (**Pivetta et al., 2014**). Altogether, my work suggests that the LRN known as a major hub for selective combinations of functionally diverse ascending spinal information also receives from the rVRG propriobulbar respiratory information needed for the execution of postural and locomotor motor tasks that engage shared respiratory and locomotor muscles (**Bechbache and Duffin, 1977**; **Hodges and Gandevia, 2000**).

V. A premotor apparatus functional at birth

The phrenic premotor organization described here in the early postnatal mouse is grossly comparable to that found in the adult rat suggesting that inspiratory descending circuits may both be definitive one week after birth and conserved between the mouse and the rat.

A recent study has demonstrated that the maturation of motor behaviors may proceed through timed incorporation of novel premotor modules (**Takatoh et al., 2013**). In this view, addition of premotor module in respiratory circuits, if any, might take place during the prenatal development. Incidentally, our experiments suggest indeed that the organization of Phr-pMNs circuits may change between E15.5, the date of inception of fetal breathing, and birth. Indeed, Dbx1-derived Phr-pMNs invalidated for *Robo3* that were found to cause only modest unbalances of the left and right phrenic motor drives at E15.5, caused much more severe ones at birth. The mechanisms underlying this progressive establishment of V0 rVRG as the prominent inspiratory premotor module in developing respiratory circuits will need to be investigated further. One possibility is that, at E15.5, V0 interneurons are still migrating to the rVRG area and developing their connections with Phr-MNs. Another possibility is that among early set (e.g. present at E15.5) premotor populations some undergo a regressive maturation. This may be the case for dorsal Wnt1-derived premotor neurons whose functional importance appears inversely to decline over the period.

Altogether, our data indicate that the architecture of breathing circuits at birth may already be the definitive one. This is not intended to deny the importance of postnatal maturation of the breathing behavior rather it suggests that respiratory circuits and their permanent rhythmic activity constitute a primitive organization, a blue print, upon which additional functional modules may be built.

A striking example is that of the circuits controlling orofacial movements and in particular exploratory whisking behavior that appears to build upon respiratory circuits. Axons from the preBötzinger complex project to neuronal centers that are involved in the patterning of breathing phases including Phr-pMNs, as well as to neuronal oscillators that are presynaptic to the orofacial motoneurons that drive whisking and licking; the case for chewing is equivocal. It has been shown that a dramatic maturation of whisking behavior occurs about one week after birth when a novel premotor module is incorporated in whisking circuits to impose bilateral synchrony the whisker movements (**Takatoh et al., 2013**). This premotor module is paced by the respiratory clock and allows coincident olfactory and mechanical sensory detection to perceive the environment. The use of a common clock, the early set inspiratory rhythm generator, to actively sample the sensory environment probably simplifies the problem of binding inputs arising from different modalities (e.g. smell, touch, and taste) into a common percept (**Kleinfeld et al., 2014a**, **2014b**).

VI. A special axonal design ensures bilaterally synchronized and balanced inspiratory motor drives.

A previously unsuspected aspect of the connectivity of Phr-pMNs revealed in my study is the presence of neurons featuring a special axonal design: a bilaterally branched axon projecting onto corresponding motoneurons on either side of the midline. These neurons identified by double viral labeling experiments were present in all premotor areas although for the reasons exposed above it is yet impossible to estimate quantitatively the contribution of this particular cell type to the global pool of premotor neurons. The link between this axonal morphology and the molecular identity of Phr-pMNs deserves some discussion. Because this axonal profile was present in all the main phrenic premotor areas (rVRG, BötC, NTS and PB/KF) this clearly indicates that a common axonal design can be acquired by neurons with different subtype identities and excitatory or inhibitory nature. In addition, in the NTS where we observed a pronounced ipsilateral premotor projection bias the presence of this morphotype suggests that conversely the bilaterally branched axonal design can be differentially acquired by neurons that share a common (dA3) identity.

Neurons with such an axonal morphology have been reported in yet a few other brainstem premotor circuits. Such neurons were demonstrated in the premotor circuitry controlling movements of the whiskers. More precisely using a comparable double viral tracing scheme Takatoh and colleagues (**Takatoh et al., 2013**) found that neurons in the LPGi were double labeled and thus projected bilaterally onto facial motoneurons innervating muscle controlling vibrissa movements thus enabling bilaterally synchronized whisking. A second example is trigeminal premotor neurons controlling the jaw closing masseter muscle. In this case these premotor neurons were observed in many brainstem regions including the IRt and Gi and the peri-trigeminal region (**Stanek et al., 2014**). It thus appears that many orofacial movements are controlled by premotor circuits that include the simplest configuration for bilateral coordination: a single premotor neuron that synapses on equivalent ipsilateral and contralateral motoneurons.

The bilateral branching design of axons together with establishment of synapses on corresponding pools of motoneurons across the midline is a most parsimonious way to secure left-right symmetric drives for muscle contraction. How this special axonal profile articulates with the cardinal classes of commissural interneurons defined originally in the spinal cord

(**Goulding, 2009**; **Jessell, 2000**) is unclear and further double tracing experiments are required to estimate whether this axonal property may be over-represented by neurons of rhombencephalic vs spinal origins.

An early hypothesis concerning the neural bases of movements by Broadbent in 1866 stated: "*That where the muscles of the corresponding parts on opposite sides of the body constantly act in concert, and act independently, either not at all, or with difficulty, the nerve-nuclei of these muscles are so connected by commissural fibres as to be pro tanto a single nucleus.*" These interneurons directly substantiate the notion that the control of inspiratory pump muscle is operated by "pro tanto a single nucleus".

I have described anatomically the populations of Phr-pMNs but for a comprehensive understanding of the circuit one would need to know about their inputs. The literature is replete with evidences that all of these premotor populations receive projection from the preBötC and that considered individually they may also be connected to one another. For instance individual KF neurons were described to project both to Phr-MNs and to the rVRG (**Yokota et al., 2004**). This, is also the case of inhibitory neurons of the BötC in the cat that were shown to directly project to phrenic motoneurons and also indirectly through impinging inspiratory bulbospinal neurons possibly from the rVRG (**Jiang and Lipski, 1990**; **Tian et al., 1999**). In addition, many of these premotor populations may also be targeted by specific motor circuits outside of respiration. Classic examples include those underlying expulsive behaviors like emesis and defecation during which respiratory neurons were described to re-configure their activity (**Grélot et al., 1990**). It seems impossible to relate simply my novel connectivity results to the complexity of described interactions between circuits supporting often interdependent functions.

The main feature of respiratory circuits provided by my results is an architecture whereby rhythm generation and bilateral synchronicity of inspiratory activity first established at the level of the rhythm generator is redundantly ensured by a commissural apparatus of premotor neurons that innervates phrenic motor neurons. This belt and suspender system probably alleviates the possibility that putative asymmetric synaptic inputs to neurons of the inspiratory circuit at the level of the rhythm generator or at the downstream premotor level may translate in de-balanced left and right motor drives to the left and right hemi-diaphragms.

Asymmetric volitional and hypercapnia-induced ventilations have been attested in

patients with vascular hemiplegia that suggested the absence of bilateral motor representation of each hemidiaphragm (**Similowski et al., 1996**) and the presence of unilateral crossed inhibitory cortical control of the ventilatory response to CO_2 (**Lanini et al., 2003**). However, hemiplegic patients present with symmetric ventilation in basal condition. Intriguingly, these data point to the existence of cortical descending inputs that may by-pass the rhythm generator and the premotor commissural apparatus. The possibility that corticospinal inputs directly contact Phr-MNs is unlikely, indeed, the descending circuit from the cortex to phrenic motor neurons is thought to be oligo-synaptic in humans and monosynaptically labeled neurons in cortical areas were never detected in the present work. A possibility would be that descending cortical inputs access phrenic motor neurons through preferential targeting of the most lateralized premotor population i.e. with most pronounced ipsi-laterally biased projections to phrenic motor neurons as described here for the PB/KF, NTS or Gi.

VII. Dbx1: a gene specifying core inspiratory circuits

Understanding the developmental programs that build up specific neuronal circuits is a challenging issue in neuroscience. In the respiratory field, the transcription factor Dbx1, which is expressed specifically in p0 progenitors giving rise to V0 type interneurons (**Pierani et al., 2001**) has gained attention due to its essential role for the development and function of the preBötC inspiratory rhythm generator. In the absence of Dbx1, the preBötC doesn't form and mutants are unable to breathe and die at birth with lungs that never experience inflation (**Bouvier et al., 2010**). Before discussing the importance of V0 of the rVRG premotor neurons I would like to mention two other sites where V0 premotor neurons have been identified in my tracing scheme. One in the spinal cord and concerns Phr-pMNs the other one is in the brainstem reticular formation and concerns premotor neurons of the hypoglossal motoneurons controlling the protrusion of the tongue.

A few phrenic premotor elements were detected in the cervical spinal cord located in the vicinity of the central canal that was also found to derive from P0 progenitors. These commissural and cholinergic spinal V0 premotor neurons also featured bilaterally branched axons and are reminiscent of partition cells described in spinal locomotor circuits (**Stepien et al., 2010**), which constitute an exclusive source of cholinergic inputs to motoneurons through C-bouton synapses to regulate their excitability by reducing the action potential afterhyperpolarization during locomotion (**Miles et al., 2007**) and are involved in locomotor

task-dependent motoneuron firing and muscle activation (**Zagoraiou et al., 2009**).

Beyond spinal motor neurons that innervate respiratory pump muscles, breathing also relies on cranial motor neurons innervating muscles modulating airway resistance (**Euler, 1986**). The latter involve laryngeal and pharyngeal (skeletal muscles), bronchial (smooth muscles) and extrinsic muscles that control protrusion of the tongue innervated by the hypoglossal nerve (**Peever et al., 2002**; **Woch et al., 2000**). One of these muscles the genioglossus muscle attaches the base of the tongue to the jawbone in front and when relaxed causes a narrowing of the airway that can be a cause of obstructive sleep apnea. Hypoglossal motor neurons and nerve roots show respiratory-like bilaterally synchronized rhythmic activity in reduced en bloc and slice in vitro preparations (**Hilaire et al., 1989**; **Paton et al., 1994**; **Smith et al., 1991**). I have traced transsynaptically hypoglossal premotor neurons following viral infections of the genioglossus muscle and found that Dbx1-derived V0 interneurons contribute to part (23%) of the bulk of premotor neurons that is located in the IRt (**Stanek et al., 2014**). However, in *Dbx1*^{cre}*;Robo3*$^{lox/lox}$ mutants, contrary to the phrenic outputs, I have found that the left and right synchronous hypoglossal motor drives was maintained unaffected. Therefore, the V0 hypoglossal premotor neurons per se appear not to contribute to bilateral synchronicity of the motor output. This is in keeping with a recent demonstration that unilateral laser ablation of these V0 neurons in slices results in an exclusive ipsilateral reduction of the amplitude of the hypoglossal nerve motor discharges (**Revill et al., 2015**). The means by which left-right synchronicity of the hypoglossal output may be maintained are at present unclear. It may rely on hypoglossal motoneurons themselves possessing dendrites that extend to the contralateral nucleus (**Altschuler et al., 1994**) and also likely on premotor commissural interneurons with yet unknown identities. Therefore, if premotor neurons controlling the hypoglossal nerve include a fraction of V0 interneurons, these have little if any role in bilateral control of the respiratory-like motor output. This probably denotes a divergence from the premotor organization that prevails for respiratory pump muscles.

Although the diaphragm is innervated by cervical spinal motor neurons the very large majority of its premotor elements reside in the brainstem. None of Phr-pMNs were of the spinal proper V3 type although these interneurons are both commissural and for part premotor in the spinal cord (**Borowska et al., 2013**). These findings confirm the notion that motorizing the diaphragm is a spinal issue but “pre-motorizing” the diaphragm is a brainstem one in

which V0 interneurons play a major role. Indeed, my work has shown that Dbx1 is also required for the specification of main group of Phr-pMNs that form the rostral ventral respiratory group. I have shown that disrupting the commissural navigation of V0s in *Dbx1^{cre};Robo3lox/lox* mutants was sufficient to left-right de-synchronize the inspiratory motor drive recorded from the C4 phrenic root in P0 reduced brainstem spinal cord preparation and altogether breathing at birth. This indicates that left-right synchrony of the rhythm and its transmission to phrenic motoneurons exhaustively relies on V0 interneurons and that other non-Dbx1 derived commissural Phr-pMNs cannot supplement the deficit.

The commissural and glutamatergic nature of preBötC and rVRG are two properties directly linked to their function in rhythm generation and fail-safe bilateral synchrony but these two groups of interneurons notably differ by a few traits. The preBötC neurons express NK1R and Sst, but not rVRG neurons and most conspicuously the preBötC is rhythmogenic while the rVRG is not, but can transmit the rhythmic activity to motor neuronal targets and an efferent copy to the LRN. These neurons arise from a continuous anterior-posterior (AP) column of P0 progenitor but are probably originating from distinct rhombomeres. Rhombomeres are morphogenetic compartments that allow cell lineages variation on a segmental basis. A classic case concerns the sequential generation of visceral motor neurons and serotonergic neurons from a common pool of ventral most neural progenitors. The temporal specification of these neurons varies along the anterior-posterior axis and depends on the integrated activities of Nkx- and segmentally expressed Hox-class homeodomain proteins (**Pattyn et al., 2003**). This sort of mechanisms may be at play to differently engage along the AP axis P0 progenitors to give rise to distinct V0 interneurons destined to form anteriorly the preBötC and immediately caudal to it the rVRG.

VIII. Dbx1 homotypic synaptic connectivity

The respiratory CPG must compute the choice, the timing and the intensity of activation, of appropriate groups of premotor and motor neurons and their muscle targets. If the ability of the respiratory CPG to profoundly modify both temporal and amplitude aspects of the respiratory command is remarkable, this is done respecting one intangible constrain: the production of synchronous and amplitude balanced motor drives onto corresponding left and right respiratory effector muscles. Together with alternating inspiratory/expiratory phases, left/right balanced motor drives to respiratory muscles is adapted to the design of the upper

airways that end in a unique tract imposing unidirectional air flows, in or out. V0 neurons recapitulate all of the necessary properties ensuring production and transmission of the inspiratory rhythm in a failsafe bilaterally synchronized manner to Phr-MNs that in turn can translate the inspiratory motor command in an effective muscle contraction powering breathing inflow.

This sets the stage for making a case of the importance for the mounting of inspiratory circuits of the establishment of synapses in between neurons sharing a common identity, here the V0 identity. A number of studies have alluded to the possibility that specific genes may constrain expressing neurons to establish synaptic connections with one another during development. This may concerns *Tlx3* (**Logan et al., 1998**), *Brn3a* (**D'Autreaux et al., 2011**), *Drg11* (**Saito et al., 1995**) in the somatic sensory pathways, *Atoh1* in proprioceptive pathways (**Bermingham et al., 2001**; **Wang et al., 2005**), *Lhx6* in an amygdalo-hypothalamic pathway (**Choi et al., 2005**) and *Phox2b* in visceral circuits (**Brunet and Goridis, 2008**).

We propose that the respiratory CPG may be a very good model to begin examining V0 to V0 homotypic connectivity, which would appear crucial both for inspiratory rhythmogenesis in the preBötC and for the broadcasting of the inspiratory motor drive to motor neuronal targets, and through efference copies, to other brain areas. This study has firmly revealed the location of Phr-pMNs, partly unraveled their identity, identified an axonal design dedicated to bilateral control and ends up proposing the importance of a special type of synapses in the brainstem whose establishment during development and evolution (as speculated below) may be of fundamental importance to the emergence of a vital functional module.

IX. Evolution of breathing circuits

I should like to conclude this study by speculating on the importance of my results in the context of the evolution of breathing strategies in tetrapods.

All extant amniotes are aspiration breathers. They draw air in by expanding the thorax rather than pumping air into the lung by building up pressure in the buccopharyngeal cavity. Although the circumstances leading to this major evolutionary change in respiratory mechanisms are largely unknown, the acquisition of the diaphragm for inspiration in mammals must have engaged changes in central networks in charge of activating muscles in

precise temporal and spatial patterns to drive coordinated respiratory motor activity. I here discuss the relevance of the present results to the mechanisms that may have contributed to the reconfiguration of central respiratory circuits for the advent of aspiration breathing using the diaphragm.

Fish ventilate through gills and locomote through body wall muscles. Air breathing in lungfish is still derived from gill ventilation (**McMahon, 1969**) and in the first amniotes, aspiration breathing involves almost exclusively body wall (costal) muscles and their derivatives that once formed the locomotor apparatus in fish. When the same costal muscles must be activated in distinct sequences to allow simultaneous locomotion and breathing, the animal cannot breathe and walk at the same time. This phenomenon called "axial constraint" (**Carrier, 1991**) is present in extant lizards like the green iguana. Mammals can overcome limitations of costal breathing by using a muscular septum—the diaphragm—for inspiration. Motorizing the diaphragm required re-programming in the first amniotes of respiratory activity from cranial visceral nerves to spinal somatic nerves and the emergence of a neural module pacing inspirations. Our data may touch upon these issues.

The diaphragm is a dome-shaped structure consisting of a central tendon (aponeurosis) surrounded by a ring of predominantly radially oriented striated muscles with left and right costal diaphragm muscles being innervated respectively and exclusively by the left and right phrenic nerves. As such this sets a double constraint on the phrenic motor command as optimal inflation of the thoracic cavity will only be obtained if the motor drives to the left and right hemi-diaphragms are balanced in amplitude and synchronously delivered. This conceivably could have been achieved through acquisition of dedicated neuronal modules dealing separately with amplitude and timing. The most parsimonious way, however, would be that a single transformation allows amplitude and timing demands to be met at once. The results of my present work may bear some significance as to the nature of this minimal yet crucial change.

The present consensus regarding the central control of breathing in mammals is that it relies on two essential sites (**Feldman and Del Negro, 2006**): the preBötC for the generation of inspiratory rhythm and the retrotrapezoid nucleus (RTN) (**Guyenet and Bayliss, 2015**) as the principal central respiratory CO_2/low-pH chemoreceptive site that may also be responsible for the generation of active expiration (**Huckstepp et al., 2015**). The RTN is composed of neurons expressing the paired-like homeodomain transcription factor Phox2b, a pan-neuronal

marker expressed in all neurons that go on to form the visceral nervous system (**Pattyn et al., 1999**). This identity, expected for neurons engaged in the control of breathing (one of the three cardinal visceral functions along with cardiovascular and digestive functions), is also that of branchiomotor neurons supporting motor activity to branchial arch derived muscles (that once powered gill ventilation) which are ontogenetically quite distinct from the somite-derived muscles (e.g the diaphragm) innervated by somatic motoneurons (**Pattyn et al., 2000**). Altogether, this indicates that the central respiratory circuits in mammals are still composed of two evolutionary distinct modules, an ancient Phox2b-derived visceral breathing apparatus with a later acquired preBötC rhythmogenic module destined to the control of the diaphragm through somatic spinal motoneurons (phrenic motoneurons).

Regarding the nature of the cells preferentially targeted by the transformation process, the group had previously shown that the preBötC was comprised of excitatory glutamatergic V0 type interneurons derived from P0 progenitors expressing the homeobox transcription factor Dbx1(**Bouvier et al., 2010**). In the present work, I now show that the main phrenic premotor neurons of the rVRG that lie anatomically caudal to, and functionally downstream of, the preBötC are by and large composed of the same type of excitatory glutamatergic V0 interneurons. Moreover, both the preBötC and the rVRG V0 neurons are commissural so that they redundantly alleviate the possibility that asymmetric activity of the left and right phrenic motoneuronal pools may arise from the preBötC or rVRG neurons and from any of their putatively asymmetrically distributed external inputs. Therefore, the double timing/amplitude constraint cited above is largely dealt with by an early selection of P0 progenitors for assembling both the inspiratory rhythm generator and phrenic premotor neurons.

If the preBötC and the rVRG derive from a common pool of progenitors, they are functionally distinct as one is overtly rhythmogenic but not the other. Rhythm generation imparts both on intrinsic membrane properties of preBötC neurons, i.e. specific sodium (I_{NaP}) and calcium (I_{CAN}) ionic conductances in combination with a redundant synaptic connectivity among preBötC neurons (**Del Negro and Hayes, 2008**; **Del Negro et al., 2010**). In what is now called the group pacemaker hypothesis, excitatory synapses between preBötC neurons initiate positive feedback through recurrent excitation where I_{CAN} and I_{NaP} serve to amplify the depolarization and to ease the percolation of excitation across increasing numbers of neurons to generate the collective full drive potential, the inspiratory burst discharge. The burst is terminated by calcium-dependent potassium conductances reverting the positive

feedback process and initiating a refractory period during which the excitability of preBötC neurons is minimal. With progressive relief of refractoriness, most excitable excitatory preBötC neurons regain synaptic access to local partner neurons and re-start the burst generation process so that a permanent generation of rhythmic bursting activity ensues in the preBötC to pace the inspiratory phase of respiration (see **Feldman and Del Negro, 2006** for a review). Therefore, rhythm generation in the preBötC is critically depending on the establishment of redundant synaptic connectivity among its constitutive neurons.

We therefore propose a speculative scenario for the advent of aspiration breathing in mammals whereby the central apparatus driving inspiration and its main specific properties (rhythm generation, bilateral synchrony, and connectivity to respiratory effector hypaxial muscles) may emerge at once through a discrete fate change affecting P0 progenitor or their V0 neuronal derivatives (**Figure 31**).

V0 interneurons in the spinal cord, where first described (**Lanuza et al., 2004**), are inhibitory commissural premotor neurons synapsing onto somatic motoneurons innervating hindlimb muscles. Assuming premotor status as a default fate for V0s, rVRG neurons only differ from their spinal partners by their excitatory glutamatergic nature. PreBötC V0s are also glutamatergic so that this trait may be specific for rhombencephalic vs spinal cord P0-derived lineages. In any case, the prominent difference between rVRG and preBötC V0s is that the latter do not directly project onto motoneurons. As described above the manifest redundant connection of preBötC V0s among themselves is pivotal to its functioning as a rhythm generator. We thus hypothesize the advent during evolution of a rhombencephalic signaling mechanism, probably segmental in range, instating divergence from the V0 default fate in a discrete anterior-posterior segment of P0 progenitors, immediately rostral to that giving rise to the rVRG, that constrains the ensuing V0 neurons to connect with their peers. Acquisition of homotypical V0 to V0 synapses at a discrete level of the rhombencephalon is sufficient to jointly establish the preBötC as a group pacemaker and the rVRG as its follower. Thus, such a subtle V0 fate change would be sufficient to cause rhythm generation and assign its motor ambition through realization of a connectivity design that also secures the bilateral (i) amplitude balance and (ii) temporal synchronicity of activities.

Future experiments will be designed to address and possibly verify the above connectivity hypothesis. To do so, multiple novel viral tracing schemes can be used including some in which the absolute restriction of transsynaptic spread to immediate presynaptic

partners can be transgressed exclusively if synapses are established in between homotype neurons (in practice neurons recapitulated by a common cre line). These experiments may also reveal yet other V0 functional modules that may modulate the inspiratory drive amplitude and duration or its transition to expiration.

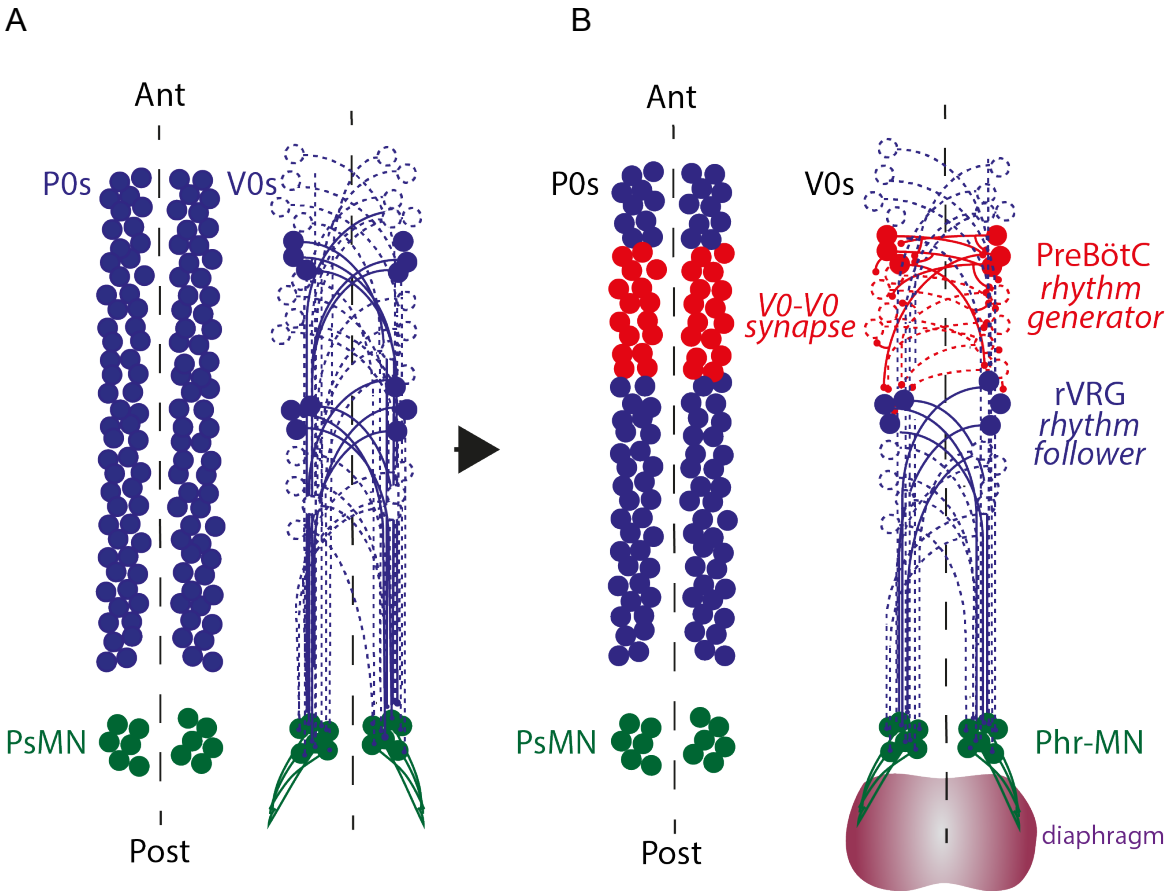

Figure 31. Model hypothesis for the emergence of a central circuit for aspiration breathing. A, Left, schematized bilateral columns of P0 (blue) neural progenitors in the rhombencephalon and PsMN (green) neural progenitors in the spinal cord respectively giving rise, at right, to postmitotic V0 premotor interneurones (blue) projecting onto somatic motor neurons sMN (green) innervating skeletal muscles. B, Left, acquisition by P0 neural progenitors in a discrete rhombencephalic segment (red) or by their ensuing postmitotic V0 interneurons, at right, of the novel capacity to connect other V0 interneurones. As a result novel V0-V0 synapses allow co-emergence of the preBotC as a rhythm generator also able to connect V0 rVRG premotor neurons projecting on somatic Phr-MNs innervating the diaphragm.

REFERENCES

Abdala, A.P., Paton, J.F.R., and Smith, J.C. (2015). Defining inhibitory neurone function in respiratory circuits: Opportunities with optogenetics? J. Physiol. *14*, 3033–3045.

Alaynick, W.A., Jessell, T.M., and Pfaff, S.L. (2011). SnapShot: spinal cord development. Cell *146*, 178–178.e1.

Alheid, G.F., Milsom, W.K., and McCrimmon, D.R. (2004). Pontine influences on breathing: an overview. Respir. Physiol. Neurobiol. *143*, 105–114.

Alheid, G.F., Jiao, W., and McCrimmon, D.R. (2011). Caudal nuclei of the rat nucleus of the solitary tract differentially innervate respiratory compartments within the ventrolateral medulla. Neuroscience *190*, 207–227.

Alsahafi, Z., Dickson, C.T., and Pagliardini, S. (2015). Optogenetic excitation of preBotzinger complex neurons potently drives inspiratory activity in vivo. J. Physiol. *593*, 3673–3692.

Alstermark, B., and Ekerot, C.-F. (2013). The lateral reticular nucleus: a precerebellar centre providing the cerebellum with overview and integration of motor functions at systems level. A new hypothesis. J. Physiol. *591*, 5453–5458.

Altschuler, S.M., Bao, X., and Miselis, R.R. (1994). Dendritic architecture of hypoglossal motoneurons projecting to extrinsic tongue musculature in the rat. J Comp Neurol *342*, 538–550.

Amiel, J., Laudier, B., Attie-Bitach, T., Trang, H., de Pontual, L., Gener, B., Trochet, D., Etchevers, H., Ray, P., Simonneau, M., et al. (2003). Polyalanine expansion and frameshift mutations of the paired-like homeobox gene PHOX2B in congenital central hypoventilation syndrome. Nat. Genet. *33*, 459–461.

Bechbache, R.R., and Duffin, J. (1977). The entrainment of breathing frequency by exercise rhythm. J. Physiol. *272*, 553–561.

Beier, K.T., Saunders, A., Oldenburg, I.A., Miyamichi, K., Akhtar, N., Luo, L., Whelan, S.P., Sabatini, B., and Cepko, C.L. (2011). Anterograde or retrograde transsynaptic labeling of CNS neurons with vesicular stomatitis virus vectors. Proc. Natl. Acad. Sci. U. S. A. *108*,

15414–15419.

Bermingham, N.A., Hassan, B.A., Wang, V.Y., Fernandez, M., Banfi, S., Bellen, H.J., Fritzsch, B., and Zoghbi, H.Y. (2001). Proprioceptor pathway development is dependent on MATH1. Neuron *30*, 411–422.

Bertrand, F., Hugelin, A., and Vibert, J.F. (1973). Quantitative study of anatomical distribution of respiration related neurons in the pons. Exp. Brain Res. *16*, 383–399.

Bianchi, A.L. (1971). [Localization and study of respiratory medullary neurons. Antidromic starting by spinal cord or vagal stimulation]. J. Physiol.Paris *63*, 5–40.

Bianchi, A.L., Denavit-Saubie, M., and Champagnat, J. (1995). Central Control of Breathing in Mammals: Neuronal Circuitry, Membrane Properties, and Neurotransmitters. Physiol. Rev. *75*, 1–45.

Bielle, F., Griveau, A., Narboux-Nême, N., Vigneau, S., Sigrist, M., Arber, S., Wassef, M., and Pierani, A. (2005). Multiple origins of Cajal-Retzius cells at the borders of the developing pallium. Nat. Neurosci. *8*, 1002–1012.

Borday, C., Wrobel, L., Fortin, G., Champagnat, J., Thaëron-Antôno, C., and Thoby-Brisson, M. (2004). Developmental gene control of brainstem function: Views from the embryo. Prog. Biophys. Mol. Biol. *84*, 89–106.

Borowska, J., Jones, C.T., Zhang, H., Blacklaws, J., Goulding, M., and Zhang, Y. (2013). Functional subpopulations of V3 interneurons in the mature mouse spinal cord. J. Neurosci. *33*, 18553–18565.

Bouvier, J., Thoby-brisson, M., Renier, N., Dubreuil, V., Ericson, J., Champagnat, J., Pierani, A., Chedotal, A., and Fortin, G. (2010). Hindbrain interneurons and axon guidance signaling critical for breathing. Nat. Neurosci. *13*, 1066–1074.

Briscoe, J., and Ericson, J. (2001). Specification of neuronal fates in the ventral neural tube. Curr. Opin. Neurobiol. *11*, 43–49.

Brouillette, R.T., and Thach, B.T. (1980). Control of genioglossus muscle inspiratory activity. J. Appl. Physiol. *49*, 801–808.

Brunet, J.-F., and Goridis, C. (2008). Phox2b and the homeostatic brain. In Genetic Basis for Respiratory Control Disorders, (Springer), pp. 25–44.

Callaway, E.M. (2008). Transneuronal circuit tracing with neurotropic viruses. Curr. Opin. Neurobiol. *18*, 617–623.

Carrier, D.R. (1991). Conflict in the hypaxial musculo-skeletal system: documenting an evolutionary constraint. Am. Zool. *31*, 644–654.

Castellani, V., and Kania, A. (2012). Breathless without Hox. Nat. Neurosci. *15*, 1607–1609.

Castro, D.D., Lipski, J., and Kanjhan, R. (1994). Electrophysiological study of dorsal respiratory neurons in the medulla oblongata of the rat. Brain Res. *639*, 49–56.

Chamberlin, N.L., and Saper, C.B. (1994). Topographic Organization of Respiratory Responses to Glutamate Microstimulation of the Parabrachial Nucleus in the Rat. J. Neurosci. *14*, 6500–6510.

Chan, E., Steenland, H.W., Liu, H., and Horner, R.L. (2006). Endogenous Excitatory Drive Modulating Respiratory Muscle Activity across Sleep–Wake States. Am. J. Respir. Crit. Care Med. *174*, 1264–1273.

Chatonnet, F., Domínguez del Toro, E., Voiculescu, O., Charnay, P., and Champagnat, J. (2002). Different respiratory control systems are affected in homozygous and heterozygous kreisler mutant mice. Eur. J. Neurosci. *15*, 684–692.

Chatonnet, F., Wrobel, L.J., Mézières, V., Pasqualetti, M., Ducret, S., Taillebourg, E., Charnay, P., Rijli, F.M., and Champagnat, J. (2007). Distinct roles of Hoxa2 and Krox20 in the development of rhythmic neural networks controlling inspiratory depth, respiratory frequency, and jaw opening. Neural Dev. *2*, 19.

Chitravanshi, V.C., Kachroo, A., and Sapru, H.N. (1994). A midline area in the nucleus commissuralis of NTS mediates the phrenic nerve responses to carotid chemoreceptor stimulation. Brain Res. *662*, 127–133.

Choi, G.B., Dong, H.W., Murphy, A.J., Valenzuela, D.M., Yancopoulos, G.D., Swanson, L.W., and Anderson, D.J. (2005). Lhx6 delineates a pathway mediating innate reproductive behaviors from the amygdala to the hypothalamus. Neuron *46*, 647–660.

Cohen, M.I. (1979). Neurogenesis of respiratory rhythm in the mammal. Physiol. Rev. *59*, 1105–1173.

Corda, M., Von Euler, C., and Lennerstrand, G. (1965). Proprioceptive innervation of the diaphragm. J Physiol *178*, 161–177.

Del Corral, R.D., and Storey, K.G. (2004). Opposing FGF and retinoid pathways: A signalling switch that controls differentiation and patterning onset in the extending vertebrate body axis. BioEssays *26*, 857–869.

Crapse, T.B., and Sommer, M.A. (2008). Corollary discharge across the animal kingdom. Nat. Rev. Neurosci. *9*, 587–600.

D'Autreaux, F., Coppola, E., Hirsch, M.-R., Birchmeier, C., and Brunet, J.-F. (2011). Homeoprotein Phox2b commands a somatic-to-visceral switch in cranial sensory pathways. Proc. Natl. Acad. Sci. *108*, 20018–20023.

Danielian, P.S., Muccino, D., Rowitch, D.H., Michael, S.K., and McMahon, A.P. (1998). Modification of gene activity in mouse embryos in utero by a tamoxifen-inducible form of Cre recombinase. Curr. Biol. *8*, 1323–1326.

Dauger, S., Pattyn, A., Lofaso, F., Gaultier, C., Goridis, C., Gallego, J., and Brunet, J.-F. (2003). Phox2b controls the development of peripheral chemoreceptors and afferent visceral pathways. Development *130*, 6635–6642.

Dawes, G.S., Fox, H.E., Leduc, B.M., Liggins, G.C., and Richards, R.T. (1972). Respiratory movements and rapid eye movement sleep in the foetal lamb. J. Physiol. *220*, 119–143.

Dawid-Milner, M.S., Lara, J.P., Gonzaléz-Barón, S., and Spyer, K.M. (2001). Respiratory effects of stimulation of cell bodies of the A5 region in the anaesthetised rat. Pflügers Arch. *441*, 434–443.

Deegan, P.C., and McNicholas, W.T. (1995). Pathophysiology of obstructive sleep apnoea. Eur. Respir. J. *8*, 1161–1178.

Delcomyn, F. (1980). Neural basis of rhythmic behavior in animals. Science *210*, 492–498.

Depuy, S.D., Kanbar, R., Coates, M.B., Stornetta, R.L., and Guyenet, P.G. (2011). Control of breathing by raphe obscurus serotonergic neurons in mice. J. Neurosci. *31*, 1981–1990.

Derenne, J.-P., Debru, A., Grassino, A.E., and Whitelaw, W.A. (1995). History of diapragm physiology: the achievements of Galen. Eur. Respir. J. *8*, 154–160.

Dobbins, E.G., and Feldman, J.L. (1994). Brainstem network controlling descending drive to phrenic motoneurons in rat. J. Comp. Neurol. *347*, 64–86.

Dobbins, E.G., and Feldman, J.L. (1995). Differential innervation of protruder and retractor muscles of the tongue in rat. J. Comp. Neurol. *357*, 376–394.

Dubreuil, V., Barhanin, J., Goridis, C., and Brunet, J.-F. (2009a). Breathing with phox2b. Philos. Trans. R. Soc. Lond. B. Biol. Sci. *364*, 2477–2483.

Dubreuil, V., Thoby-Brisson, M., Rallu, M., Persson, K., Pattyn, A., Birchmeier, C., Brunet, J.-F., Fortin, G., and Goridis, C. (2009b). Defective respiratory rhythmogenesis and loss of central chemosensitivity in Phox2b mutants targeting retrotrapezoid nucleus neurons. J. Neurosci. *29*, 14836–14846.

Dudanova, I., and Klein, R. (2013). Integration of guidance cues: Parallel signaling and crosstalk. Trends Neurosci. *36*, 295–304.

Duron, B., Jung-Caillol, M.C., and Marlot, D. (1978). Myelinated nerve fiber supply and muscle spindles in the respiratory muscles of cat: quantitative study. Anat Embryol *152*, 171–192.

Dutschmann, M., and Herbert, H. (2006). The Kolliker-Fuse nucleus gates the postinspiratory phase of the respiratory cycle to control inspiratory off-switch and upper airway resistance in rat. Eur. J. Neurosci. *24*, 1071–1084.

Ellenberger, H.H. (1999). Nucleus ambiguus and bulbospinal ventral respiratory group neurons in the neonatal rat. Brain Res. Bull. *50*, 1–13.

Ellenberger, H.H., and Feldman, J.L. (1988). Monosynaptic transmission of respiratory drive to phrenic motoneurons from brainstem bulbospinal neurons in rats. J. Comp. Neurol. *269*, 47–57.

Ellenberger, H.H., and Feldman, J.L. (1990). Subnuclear organization of the lateral tegmental field of the rat. I: Nucleus ambiguus and ventral respiratory group. J. Comp. Neurol. *294*, 202–211.

Ellenberger, H.H., Feldman, J.L., and Goshgarian, H.G. (1990). Ventral respiratory group projections to phrenic motoneurons: electron microscopic evidence for monosynaptic

connections. J. Comp. Neurol. *302*, 707–714.

Esposito, M.S., Capelli, P., and Arber, S. (2014). Brainstem nucleus MdV mediates skilled forelimb motor tasks. Nature.

Etessami, R., Conzelmann, K.-K., Fadai-Ghotbi, B., Natelson, B., Tsiang, H., and Ceccaldi, P.E. (2000). Spread and pathogenic characteristics of a G-deficient rabies virus recombinant: an in vitro and in vivo study. J. Gen. Virol. *81*, 2147–2153.

Euler, C. (1986). Brain stem mechanisms for generation and control of breathing pattern. Compr. Physiol.

Von Euler, C. (1983). On the central pattern generator for the basic breathing rhythmicity. J. Appl. Physiol. *55*, 1647–1659.

Ezure, K., and Tanaka, I. (1997). Convergence of central respiratory and locomotor rhythms onto single neurons of the lateral reticular nucleus. Exp. Brain Res. *113*, 230–242.

Ezure, K., and Tanaka, I. (2006). Distribution and medullary projection of respiratory neurons in the dorsolateral pons of the rat. Neuroscience *141*, 1011–1023.

Ezure, K., Manabe, M., and Yamada, H. (1988). Distribution of medullary respiratory neurons in the rat. Brain Res. *455*, 262–270.

Ezure, K., Tanaka, I., and Kondo, M. (2003a). Glycine is used as a transmitter by decrementing expiratory neurons of the ventrolateral medulla in the rat. J. Neurosci. *23*, 8941–8948.

Ezure, K., Tanaka, I., and Saito, Y. (2003b). Brainstem and spinal projections of augmenting expiratory neurons in the rat. Neurosci. Res. *45*, 41–51.

Fedorko, L., and Merrill, E.G. (1984). Axonal projections from the rostral expiratory neurones of the Botzinger complex to medulla and spinal cord in the cat. J. Physiol. *350*, 487–496.

Fedorko, L., Merrill, E.G., and Lipski, J. (1983). Two descending medullary inspiratory pathways to phrenic motoneurones. Neurosci. Lett. *43*, 285–291.

Feil, R., Brocard, J., Mascrez, B., LeMeur, M., Metzger, D., and Chambon, P. (1996). Ligand-activated site-specific recombination in mice. Proc. Natl. Acad. Sci. U. S. A. *93*,

10887–10890.

Feil, R., Wagner, J., Metzger, D., and Chambon, P. (1997). Regulation of Cre recombinase activity by mutated estrogen receptor ligand-binding domains. Biochem. Biophys. Res. Commun. *237*, 752–757.

Feil, S., Valtcheva, N., and Feil, R. (2009). Inducible cre mice. Methods Mol. Biol. *530*, 343–363.

Feldman, J.L., and Del Negro, C.A. (2006). Looking for inspiration: new perspectives on respiratory rhythm. Nat. Rev. Neurosci. *7*, 232–242.

Feldman, J.L., Loewy, A.D., and Speck, D.F. (1985). Projections from the ventral respiratory group to phrenic and intercostal motoneurons in cat: an autoradiographic study. J. Neurosci. *5*, 1993–2000.

Feldman, J.L., Del Negro, C.A., and Gray, P.A. (2012). Understanding the Rhythm of Breathing: So Near, Yet So Far. Annu. Rev. Physiol. *75*, 121102144047002.

Flourens, M.J.P. (1851). Note sur le point vital de la moelle allongée. CR Seances Soc Biol *33*, 437–439.

Fritzsch, B. (1993). Fast axonal diffusion of 3000 molecular weight dextran amines. J. Neurosci. Methods *50*, 95–103.

Funk, G.D., Smith, J.C., and Feldman, J.L. (1994). Development of thyrotropin-releasing hormone and norepinephrine potentiation of inspiratory-related hypoglossal motoneuron discharge in neonatal and juvenile mice in vitro. J. Neurophysiol. *72*, 2538–2541.

Furley, D.J., and Wilkie, J.S. (1984). Galen on respiration and the arteries (Princeton university).

Gavalas, A., Ruhrberg, C., Livet, J., Henderson, C.E., and Krumlauf, R. (2003). Neuronal defects in the hindbrain of Hoxa1, Hoxb1 and Hoxb2 mutants reflect regulatory interactions among these Hox genes. Development *130*, 5663–5679.

Gaytán, S.P., Pásaro, R., Coulon, P., Bevengut, M., and Hilaire, G. (2002). Identification of central nervous system neurons innervating the respiratory muscles of the mouse: a transneuronal tracing study. Brain Res. Bull. *57*, 335–339.

Ghanem, A., and Conzelmann, K.-K. (2015). G gene-deficient single-round rabies viruses for neuronal circuit analysis. Virus Res.

Ginger, M., Haberl, M., Conzelmann, K.-K., Schwarz, M.K., and Frick, A. (2013). Revealing the secrets of neuronal circuits with recombinant rabies virus technology. Front. Neural Circuits *7*.

Glover, J.C., Renaud, J., and Rijli, F.M. (2006). Retinoic acid and hindbrain patterning. J. Neurobiol. *66*, 705–725.

Goetz, C., Pivetta, C., and Arber, S. (2015). Distinct Limb and Trunk Premotor Circuits Establish Laterality in the Spinal Cord Article Distinct Limb and Trunk Premotor Circuits Establish Laterality in the Spinal Cord. Neuron *85*, 131–144.

Goshgarian, H.G., and Rafols, J.A. (1981). The phrenic nucleus of the albino rat: A correlative HRP and Golgi study. J. Comp. Neurol. *201*, 441–456.

Goshgarian, H.G., and Rafols, J.A. (1984). The ultrastructure and synaptic architecture of phrenic motor neurons in the spinal cord of the adult rat. J. Neurocytol. *13*, 85–109.

Goulding, M. (2009). Circuits controlling vertebrate locomotion: moving in a new direction. Nat. Rev. Neurosci. *10*, 507–518.

Gray, P.A. (2008). Transcription factors and the genetic organization of brain stem respiratory neurons. J. Appl. Physiol. *104*, 1513–1521.

Gray, P.A. (2013). Transcription factors define the neuroanatomical organization of the medullary reticular formation. Front. Neuroanat. *7*, 7.

Gray, P.A., and Janczewski, W.A. (2001). Normal breathing requires preBötzinger complex neurokinin-1 receptor-expressing neurons. Nat. Neurosci. *4*, 927–930.

Gray, P.A., Rekling, J.C., Bocchiaro, C.M., and Feldman, J.L. (1999). Modulation of respiratory frequency by peptidergic input to rhythmogenic neurons in the preBötzinger complex. Science *286*, 1566–1568.

Gray, P.A., Hayes, J.A., Ling, G.Y., Llona, I., Tupal, S., Picardo, M.C.D., Ross, S.E., Hirata, T., Corbin, J.G., Eugenín, J., et al. (2010). Developmental origin of preBötzinger complex respiratory neurons. J. Neurosci. *30*, 14883–14895.

Greer, J.J. (2012). Control of breathing activity in the fetus and newborn. Compr. Physiol. *2*, 1873–1888.

Greer, J.J., Smith, J.C., and Feldman, J.L. (1992). Respiratory and locomotor patterns generated in the fetal rat brain stem-spinal cord in vitro. J. Neurophysiol. *67*, 996–999.

Greer, J.J., Funk, G.D., and Ballanyi, K. (2006). Preparing for the first breath: prenatal maturation of respiratory neural control. J. Physiol. *570*, 437–444.

Grélot, L., Barillot, J.C., and Bianchi, A.L. (1990). Activity of respiratory-related oropharyngeal and laryngeal motoneurones during fictive vomiting in the decerebrate cat. Brain Res. *513*, 101–105.

Guerrier, C., Hayes, J.A., Fortin, G., and Holcman, D. (2015). Robust network oscillations during mammalian respiratory rhythm generation driven by synaptic dynamics. Proc. Natl. Acad. Sci. U. S. A. *112*, 9728–9733.

Guthrie, S. (2007). Patterning and axon guidance of cranial motor neurons. Nat. Rev. Neurosci. *8*, 859–871.

Guyenet, P.G., and Bayliss, D.A. (2015). Neural Control of Breathing and CO2 Homeostasis. Neuron *87*, 946–961.

Guyenet, P.G., and Wang, H. (2001). Pre-Bötzinger Neurons With Preinspiratory Discharges "In Vivo" Express NK1 Receptors in the Rat. J. Neurophysiol. *86*, 438–446.

Guyenet, P.G., Sevigny, C.P., Weston, M.C., and Stornetta, R.L. (2002). Neurokinin-1 receptor-expressing cells of the ventral respiratory group are functionally heterogeneous and predominantly glutamatergic. J. Neurosci. *22*, 3806–3816.

Guyenet, P.G., Mulkey, D.K., Stornetta, R.L., and Bayliss, D.A. (2005). Regulation of ventral surface chemoreceptors by the central respiratory pattern generator. J. Neurosci. *25*, 8938–8947.

Harsløf, M., Müller, F.C., Rohrberg, J., and Rekling, J.C. (2015). Fast neuronal labeling in live tissue using a biocytin conjugated fluorescent probe. J. Neurosci. Methods 1–9.

Hilaire, G., Monteau, R., and Errchidi, S. (1989). Possible modulation of the medullary respiratory rhythm generator by the noradrenergic A 5 area: an in vitro study in the newborn

rat. Brain Res. *485*, 325–332.

Hilaire, G., Viemari, J.-C., Coulon, P., Simonneau, M., and Bévengut, M. (2004). Modulation of the respiratory rhythm generator by the pontine noradrenergic A5 and A6 groups in rodents. Respir. Physiol. Neurobiol. *143*, 187–197.

Hirata, T., Li, P., Lanuza, G.M., Cocas, L. a, Huntsman, M.M., and Corbin, J.G. (2009). Identification of distinct telencephalic progenitor pools for neuronal diversity in the amygdala. Nat. Neurosci. *12*, 141–149.

Hirokawa, N., and Takemura, R. (2005). Molecular motors and mechanisms of directional transport in neurons. Nat. Rev. Neurosci. *6*, 201–214.

Hodges, P.W., and Gandevia, S.C. (2000). Changes in intra-abdominal pressure during postural and respiratory activation of the human diaphragm. J. Appl. Physiol. *89*, 967–976.

Hollinshead, W.H., and Keswani, N.H. (1956). Localization of the phrenic nucleus in the spinal cord of man. Anat. Rec. *125*, 683–699.

Hosogai, M., Matsuo, S., Sibahara, T., and Kawai, Y. (1998). Projection of respiratory neurons in rat medullary raphe nuclei to the phrenic nucleus. Respir. Physiol. *112*, 37–50.

Huckstepp, R.T.R., Cardoza, K.P., Henderson, L.E., and Feldman, J.L. (2015). Role of Parafacial Nuclei in Control of Breathing in Adult Rats. J. Neurosci. *35*, 1052–1067.

Huminiecki, L., Gorn, M., Suchting, S., Poulsom, R., and Bicknell, R. (2002). Magic roundabout is a new member of the roundabout receptor family that is endothelial specific and expressed at sites of active angiogenesis. Genomics *79*, 547–552.

Inanlou, M.R., Baguma-Nibasheka, M., and Kablar, B. (2005). The role of fetal breathing-like movements in lung organogenesis. Histol. Histopathol. *20*, 1261–1266.

Iscoe, S. (1998). Control of abdominal muscles. Prog. Neurobiol. *56*, 433–506.

Jacob, J., Kong, J., Moore, S., Milton, C., Sasai, N., Gonzalez-Quevedo, R., Terriente, J., Imayoshi, I., Kageyama, R., Wilkinson, D.G., et al. (2013). Retinoid acid specifies neuronal identity through graded expression of Ascl1. Curr. Biol. *23*, 412–418.

Jacquin, T.D., Borday, V., Schneider-Maunoury, S., Topilko, P., Ghilini, G., Kato, F., Charnay, P., and Champagnat, J. (1996). Reorganization of pontine rhythmogenic neuronal

networks in Krox-20 knockout mice. Neuron *17*, 747–758.

Jammes, Y., Arbogast, S., and De Troyer, A. (2000). Response of the rabbit diaphragm to tendon vibration. Neurosci. Lett. *290*, 85–88.

Janczewski, W.A., and Feldman, J.L. (2006). Distinct rhythm generators for inspiration and expiration in the juvenile rat. J. Physiol. *570*, 407–420.

Jen, J.C., Chan, W.-M., Bosley, T.M., Wan, J., Carr, J.R., Rüb, U., Shattuck, D., Salamon, G., Kudo, L.C., Ou, J., et al. (2004). Mutations in a human ROBO gene disrupt hindbrain axon pathway crossing and morphogenesis. Science *304*, 1509–1513.

Jessell, T.M. (2000). Neuronal specification in the spinal cord: inductive signals and transcriptional codes. Nat. Rev. Genet. *1*, 20–29.

Jiang, M.C., and Lipski, J. (1990). Extensive monosynaptic inhibition of ventral respiratory group neurons by augmenting neurons in the Bötzinger complex in the cat. Exp. Brain Res. *81*, 639–648.

Jodkowski, J.S., Coles, S.K., and Dick, T.E. (1997). Prolongation in expiration evoked from ventrolateral pons of adult rats. J. Appl. Physiol. *82*, 377–381.

Kalia, M.P. (1981). Anatomical organization of central respiratory neurons. Annu. Rev. Physiol. *43*, 105–120.

Kalia, M., Mesulam, M., and others (1980). Brain stem projections of sensory and motor components of the vagus complex in the cat: II. Laryngeal, tracheobronchial, pulmonary, cardiac, and gastrointestinal branches. J. Comp. Neurol. *193*, 467–508.

Kleinfeld, D., Deschênes, M., Wang, F., and Moore, J.D. (2014a). More than a rhythm of life: breathing as a binder of orofacial sensation. Nat. Neurosci. *17*, 647–651.

Kleinfeld, D., Moore, J.D., Wang, F., and Deschênes, M. (2014b). The brainstem oscillator for whisking and the case for breathing as the master clock for orofacial motor actions. Cold Spring Harb. Symp. Quant. Biol. *79*, 29–39.

Kobayashi, K., Lemke, R.P., and Greer, J.J. (2001). Ultrasound measurements of fetal breathing movements in the rat. J Appl Physiol *91*, 316–320.

Koizumi, H., Koshiya, N., Chia, J.X., Cao, F., Nugent, J., Zhang, R., and Smith, J.C. (2013).

Structural-Functional Properties of Identified Excitatory and Inhibitory Interneurons within Pre-Botzinger Complex Respiratory Microcircuits. J. Neurosci. *33*, 2994–3009.

Koshiya, N., Oku, Y., Yokota, S., Oyamada, Y., Yasui, Y., and Okada, Y. (2014). Anatomical and functional pathways of rhythmogenic inspiratory premotor information flow originating in the pre-Bötzinger complex in the rat medulla. Neuroscience *268*, 194–211.

Krumlauf, R. (2016). Hox Genes and the Hindbrain: A Study in Segments (Elsevier Inc.).

Krumlauf, R., Marshall, H., Studer, M., Nonchev, S., Sham, M.H., and Lumsden, A. (1993). Hox homeobox genes and regionalisation of the nervous system. J. Neurobiol. *24*, 1328–1340.

Kubin, L., Alheid, G.F., Zuperku, E.J., and McCrimmon, D.R. (2006). Central pathways of pulmonary and lower airway vagal afferents. J. Appl. Physiol. *101*, 618–627.

Kuna, S.T., and Remmers, J.E. (1999). Premotor input to hypoglossal motoneurons from Kölliker-Fuse neurons in decerebrate cats. Respir. Physiol. *117*, 85–95.

Kuwana, S., Tsunekawa, N., Yanagawa, Y., Okada, Y., Kuribayashi, J., and Obata, K. (2006). Electrophysiological and morphological characteristics of GABAergic respiratory neurons in the mouse pre-Bötzinger complex. Eur. J. Neurosci. *23*, 667–674.

Lafon, M. (2005). Rabies virus receptors. J. Neurovirol. *11*, 82–87.

Lane, M.A. (2011). Spinal respiratory motoneurons and interneurons. Respir. Physiol. Neurobiol. *179*, 3–13.

Lane, M.A., White, T.E., Coutts, M.A., Jones, A.L., Sandhu, M.S., Bloom, D.C., Bolser, D.C., Yates, B.J., Fuller, D.D., and Reier, P.J. (2008a). Cervical prephrenic interneurons in the normal and lesioned spinal cord of the adult rat. J. Comp. Neurol. *511*, 692–709.

Lane, M.A., Fuller, D.D., White, T.E., and Reier, P.J. (2008b). Respiratory neuroplasticity and cervical spinal cord injury: translational perspectives. Trends Neurosci. *31*, 538–547.

Lanini, B., Bianchi, R., Romagnoli, I., Coli, C., Binazzi, B., Gigliotti, F., Pizzi, A., Grippo, A., and Scano, G. (2003). Chest wall kinematics in patients with hemiplegia. Am. J. Respir. Crit. Care Med. *168*, 109–113.

Lanuza, G., Gosgnach, S., and Pierani, A. (2004). Genetic identification of spinal

interneurons that coordinate left-right locomotor activity necessary for walking movements. Neuron.

Lee, K.J., and Jessell, T.M. (1999). The specification of dorsal cell fates in the vertebrate central nervous system. Annu. Rev. Neurosci. *22*, 261–294.

Li, P., Janczewski, W.A., Yackle, K., Kam, K., Pagliardini, S., Krasnow, M.A., and Feldman, J.L. (2016). The peptidergic control circuit for sighing. Nature *530*, 293–297.

Liddell, E.G.T., and Sherrington, C.S. (1925). Recruitment and some other features of reflex inhibition. Proc. R. Soc. London. Ser. B, Contain. Pap. a Biol. Character *97*, 488–518.

Lindsay, A.D., Greer, J.J., and Feldman, J.L. (1991). Phrenic motoneuron morphology in the neonatal rat. J. Comp. Neurol. *308*, 169–179.

Lipski, J. (1984). Is there electrical coupling between phrenic motoneurons in cats? Neurosci. Lett. *46*, 229–234.

Logan, C., Wingate, R.J., McKay, I.J., and Lumsden, A. (1998). Tlx-1 and Tlx-3 homeobox gene expression in cranial sensory ganglia and hindbrain of the chick embryo: markers of patterned connectivity. J. Neurosci. *18*, 5389–5402.

Long, H., Sabatier, C., Ma, L., Plump, A.S., Yuan, W., Ornitz, D.M., Tamada, A., Murakami, F., Goodman, C.S., and Tessier-Lavigne, M. (2004). Conserved roles for Slit and Robo proteins in midline commissural axon guidance. Neuron *42*, 213–223.

Lumsden, A., and Keynes, R. (1989). Segmental patterns of neuronal development in the chick hindbrain. Nature *337*, 424–428.

Lumsden, A., and Krumlauf, R. (1996). Patterning the Vertebrate Neuraxis. Science *274*, 1109–1115.

Lupo, G., Harris, W.A., and Lewis, K.E. (2006). Mechanisms of ventral patterning in the vertebrate nervous system. Nat. Rev. Neurosci. *7*, 103–114.

Lutz, C., Otis, T.S., DeSars, V., Charpak, S., DiGregorio, D.A., and Emiliani, V. (2008). Holographic photolysis of caged neurotransmitters. Nat. Methods *5*, 821–827.

Madisen, L., Mao, T., Koch, H., Zhuo, J., Berenyi, A., Fujisawa, S., Hsu, Y.-W.A., Garcia, A.J., Gu, X., Zanella, S., et al. (2012). A toolbox of Cre-dependent optogenetic transgenic

mice for light-induced activation and silencing. Nat. Neurosci. *15*, 793–802.

Mantilla, C.B., Zhan, W.Z., and Sieck, G.C. (2009). Retrograde labeling of phrenic motoneurons by intrapleural injection. J. Neurosci. Methods *182*, 244–249.

Marillat, V., Sabatier, C., Failli, V., Matsunaga, E., Sotelo, C., Tessier-Lavigne, M., and Chédotal, A. (2004). The slit receptor Rig-1/Robo3 controls midline crossing by hindbrain precerebellar neurons and axons. Neuron *43*, 69–79.

Martin-Caraballo, M., and Greer, J.J. (1999). Electrophysiological properties of rat phrenic motoneurons during perinatal development. J. Neurophysiol. *81*, 1365–1378.

Mazarakis, N.D., Azzouz, M., Rohll, J.B., Ellard, F.M., Wilkes, F.J., Olsen, A.L., Carter, E.E., Barber, R.D., Baban, D.F., Kingsman, S.M., et al. (2001). Rabies virus glycoprotein pseudotyping of lentiviral vectors enables retrograde axonal transport and access to the nervous system after peripheral delivery. Hum. Mol. Genet. *10*, 2109–2121.

Mazza, E., Núñez-Abades, P. a, Spielmann, J.M., and Cameron, W.E. (1992). Anatomical and electrotonic coupling in developing genioglossal motoneurons of the rat. Brain Res. *598*, 127–137.

McCrimmon, D.R., Milsom, W.K., and Alheid, G.F. (2004). The rhombencephalon and breathing: a view from the pons. Respir. Physiol. Neurobiol. *143*, 103–104.

McMahon, B.R. (1969). A functional analysis of the aquatic and aerial respiratory movements of an African lungfish, Protopterus aethiopicus, with reference to the evolution of the lung-ventilation mechanism in vertebrates. J. Exp. Biol. *51*, 407–430.

Mebatsion, T., Konig, M., and Conzelmann, K.-K. (1996). Budding of rabies virus particles in the absence of the spike glycoprotein. Cell *84*, 941–951.

Mellen, N.M., Janczewski, W.A., Bocchiaro, C.M., and Feldman, J.L. (2003). Opioid-Induced Quantal Slowing Reveals Dual Networks for Respiratory Rhythm Generation. Neuron *37*, 821–826.

Miles, G.B., Hartley, R., Todd, A.J., and Brownstone, R.M. (2007). Spinal cholinergic interneurons regulate the excitability of motoneurons during locomotion. Proc. Natl. Acad. Sci. U. S. A. *104*, 2448–2453.

Milsom, W.K. (2008). Evolutionary trends in respiratory mechanisms. Adv. Exp. Med. Biol.

605, 293–298.

Moore, J.D., Deschênes, M., Furuta, T., Huber, D., Smear, M.C., Demers, M., and Kleinfeld, D. (2013). Hierarchy of orofacial rhythms revealed through whisking and breathing. Nature *497*, 205–210.

Morgado-Valle, C., Baca, S.M., and Feldman, J.L. (2010). Glycinergic pacemaker neurons in preBötzinger complex of neonatal mouse. J. Neurosci. *30*, 3634–3639.

Morin, D., Monteau, R., and Hilaire, G. (1992). Compared effects of serotonin on cervical and hypoglossal inspiratory activities: an in vitro study in the newborn rat. J. Physiol. *451*, 605–629.

Mörschel, M., and Dutschmann, M. (2009). Pontine respiratory activity involved in inspiratory/expiratory phase transition. Philos. Trans. R. Soc. Lond. B. Biol. Sci. *364*, 2517–2526.

Mulkey, D.K., Stornetta, R.L., Weston, M.C., Simmons, J.R., Parker, A., Bayliss, D.A., and Guyenet, P.G. (2004). Respiratory control by ventral surface chemoreceptor neurons in rats. Nat. Neurosci. *7*, 1360–1369.

Muroyama, Y., Fujihara, M., Ikeya, M., Kondoh, H., and Takada, S. (2002). Wnt signaling plays an essential role in neuronal specification of the dorsal spinal cord. Genes Dev. *16*, 548–553.

Del Negro, C.A., and Hayes, J.A. (2008). A “group pacemaker” mechanism for respiratory rhythm generation. J. Physiol. *586*, 2245–2246.

Del Negro, C.A., Morgado-Valle, C., Hayes, J.A., Mackay, D.D., Pace, R.W., Crowder, E.A., and Feldman, J.L. (2005). Sodium and Calcium Current-Mediated Pacemaker Neurons and Respiratory Rhythm Generation. J. Neurosci. *25*, 446–453.

Del Negro, C.A., Hayes, J.A., Pace, R.W., Brush, B.R., Teruyama, R., and Feldman, J.L. (2010). Synaptically activated burst-generating conductances may underlie a group-pacemaker mechanism for respiratory rhythm generation in mammals. Prog. Brain Res. *187*, 111–136.

Onimaru, H., and Homma, I. (2003). A novel functional neuron group for respiratory rhythm

generation in the ventral medulla. J. Neurosci. *23*, 1478–1486.

Onimaru, H., Kumagawa, Y., and Homma, I. (2006). Respiration-related rhythmic activity in the rostral medulla of newborn rats. J. Neurophysiol. *96*, 55–61.

Onimaru, H., Ikeda, K., and Kawakami, K. (2008). CO2-Sensitive Preinspiratory Neurons of the Parafacial Respiratory Group Express Phox2b in the Neonatal Rat. J. Neurosci. *28*, 12845–12850.

Osakada, F., Mori, T., Cetin, A.H., Marshel, J.H., Virgen, B., and Callaway, E.M. (2011). New rabies virus variants for monitoring and manipulating activity and gene expression in defined neural circuits. Neuron *71*, 617–631.

Oztas, E. (2003). Neuronal tracing. Neuroanatomy *2*, 2–5.

Pagliardini, S., Ren, J., and Greer, J.J. (2003). Ontogeny of the pre-Bötzinger complex in perinatal rats. J. Neurosci. *23*, 9575–9584.

Pagliardini, S., Ren, J., Gray, P.A., VanDunk, C., Gross, M., Goulding, M., and Greer, J.J. (2008). Central respiratory rhythmogenesis is abnormal in lbx1-deficient mice. J. Neurosci. *28*, 11030–11041.

Pagliardini, S., Janczewski, W.A., Tan, W., Dickson, C.T., Deisseroth, K., and Feldman, J.L. (2011). Active Expiration Induced by Excitation of Ventral Medulla in Adult Anesthetized Rats. J. Neurosci. *31*, 2895–2905.

Parkis, M.A., Dong, X., Feldman, J.L., and Funk, G.D. (1999). Concurrent inhibition and excitation of phrenic motoneurons during inspiration: phase-specific control of excitability. J. Neurosci. *19*, 2368–2380.

Paton, J.F.R. (1996). A working heart-brainstem preparation of the mouse. J. Neurosci. Methods *65*, 63–68.

Paton, J.F., Ramirez, J.M., and Richter, D.W. (1994). Functionally intact in vitro preparation generating respiratory activity in neonatal and mature mammals. Pflugers Arch. *428*, 250–260.

Pattyn, A., Morin, X., Cremer, H., Goridis, C., and Brunet, J.-F. (1999). The homeobox gene Phox2b is essential for the development of autonomic neural crest derivatives. Nature *399*, 366–370.

Pattyn, A., Hirsch, M.-R., Goridis, C., and Brunet, J.-F. (2000). Control of hindbrain motor neuron differentiation by the homeobox gene Phox2b. Development *127*, 1349–1358.

Pattyn, A., Vallstedt, A., Dias, J.M., Samad, O.A., Krumlauf, R., Rijli, F.M., Brunet, J.-F., and Ericson, J. (2003). Coordinated temporal and spatial control of motor neuron and serotonergic neuron generation from a common pool of CNS progenitors. Genes Dev. *17*, 729–737.

Peever, J.H., Tian, G.-F., and Duffin, J. (1998). Bilaterally independent respiratory rhythms in the decerebrate rat. Neurosci. Lett. *247*, 41–44.

Peever, J.H., Shen, L., and Duffin, J. (2002). Respiratory pre-motor control of hypoglossal motoneurons in the rat. Neuroscience *110*, 711–722.

Pena, F., Parkis, M.A., Tryba, A.K., and Ramirez, J.M. (2004). Differential contribution of pacemaker properties to the generation of respiratory rhythms during normoxia and hypoxia. Neuron *43*, 105–117.

Philippidou, P., Walsh, C.M., Aubin, J., Jeannotte, L., and Dasen, J.S. (2012). Sustained Hox5 gene activity is required for respiratory motor neuron development. Nat. Neurosci. *15*, 1636–1644.

Pierani, A., Moran-Rivard, L., Sunshine, M.J., Littman, D.R., Goulding, M., and Jessell, T.M. (2001). Control of interneuron fate in the developing spinal cord by the progenitor homeodomain protein Dbx1. Neuron *29*, 367–384.

Pivetta, C., Esposito, M.S., Sigrist, M., and Arber, S. (2014). Motor-circuit communication matrix from spinal cord to brainstem neurons revealed by developmental origin. Cell *156*, 537–548.

Prakash, Y.S., Mantilla, C.B., Zhan, W.Z., Smithson, K.G., and Sieck, G.C. (2000). Phrenic motoneuron morphology during rapid diaphragm muscle growth. J. Appl. Physiol. *89*, 563–572.

Qiu, K., Lane, M.A., Lee, K.Z., Reier, P.J., and Fuller, D.D. (2010). The phrenic motor nucleus in the adult mouse. Exp. Neurol. *226*, 254–258.

Rekling, J.C., and Feldman, J.L. (1997). Bidirectional electrical coupling between inspiratory

motoneurons in the newborn mouse nucleus ambiguus. J. Neurophysiol. *78*, 3508–3510.

Renier, N., Schonewille, M., Giraudet, F., Badura, A., Tessier-Lavigne, M., Avan, P., De Zeeuw, C.I., and Chedotal, A. (2010). Genetic dissection of the function of hindbrain axonal commissures. PLoS Biol. *8*, e1000325.

Revill, A.L., Vann, N.C., Akins, V.T., Kottick, A., Gray, P.A., Del Negro, C.A., and Funk, G.D. (2015). Dbx1 precursor cells are a source of inspiratory XII premotoneurons. Elife *4*, 1–15.

Richter, D.W. (1982). Generation and maintenance of the respiratory rhythm. J. Exp. Biol. *100*, 93–107.

Richter, D.W. (1996). Neural regulation of respiration: rhythmogenesis and afferent control. In Comprehensive Human Physiology, (Springer), pp. 2079–2095.

Richter, D.W., and Smith, J.C. (2014). Respiratory rhythm generation in vivo. Physiology (Bethesda). *29*, 58–71.

Richter, D.W., and Spyer, K.M. (2001). Studying rhythmogenesis of breathing: Comparison of in vivo and in vitro models. Trends Neurosci. *24*, 464–472.

Richter, D.W., Ballantyne, D., and Remmers, J.E. (1986). How Is the Respiratory Rhythm Generated? A Model. Physiology *1*, 109–112.

Richter, D.W., Mironov, S.L., Busselberg, D., Lalley, P.M., Bischoff, A.M., and Wilken, B. (2000). Respiratory Rhythm Generation: Plasticity of a Neuronal Network. Neurosci. *6*, 181–198.

Rivera, C., Voipio, J., Payne, J.A., Ruusuvuori, E., Lahtinen, H., Lamsa, K., Pirvola, U., Saarma, M., and Kaila, K. (1999). The K+/Cl- co-transporter KCC2 renders GABA hyperpolarizing during neuronal maturation. *397*, 251–255.

Robertson, G.A., and Stein, P.S. (1988). Synaptic control of hindlimb motoneurones during three forms of the fictive scratch reflex in the turtle. J. Physiol. *404*, 101–128.

Rose, M.F., Ren, J., Ahmad, K.A., Chao, H.-T., Klisch, T.J., Flora, A., Greer, J.J., and Zoghbi, H.Y. (2009). Math1 is essential for the development of hindbrain neurons critical for perinatal breathing. Neuron *64*, 341–354.

Rosin, D.L., Chang, D.A., and Guyenet, P.G. (2006). Afferent and efferent connections of the rat retrotrapezoid nucleus. J. Comp. Neurol. *499*, 64–89.

Rossiter, C.D., Hayden, N.L., Stocker, S.D., and Yates, B.J. (1996). Changes in outflow to respiratory pump muscles produced by natural vestibular stimulation. J. Neurophysiol. *76*, 3274–3284.

Rubin, J.E., Hayes, J.A., Mendenhall, J.L., and Del Negro, C.A. (2009). Calcium-activated nonspecific cation current and synaptic depression promote network-dependent burst oscillations. Proc. Natl. Acad. Sci. U. S. A. *106*, 2939–2944.

Ruffault, P.-L., D'Autréaux, F., Hayes, J. a, Nomaksteinsky, M., Autran, S., Fujiyama, T., Hoshino, M., Hägglund, M., Kiehn, O., Brunet, J.-F., et al. (2015). The retrotrapezoid nucleus neurons expressing *Atoh1* and *Phox2b* are essential for the respiratory response to CO_2. Elife *4*, 1–25.

Rybak, I.A., Paton, J.F.R., and Schwaber, J.S. (1997). Modeling neural mechanisms for genesis of respiratory rhythm and pattern. II. Network models of the central respiratory pattern generator. J. Neurophysiol. *77*, 2007–2026.

Sabatier, C., Plump, A.S., Ma, L., Brose, K., Tamada, A., Murakami, F., Lee, E.Y.H.P., and Tessier-Lavigne, M. (2004). The divergent robo family protein Rig-1/Robo3 is a negative regulator of slit responsiveness required for midline crossing by commissural axons. Cell *117*, 157–169.

Saito, T., Greenwood, A., Sun, Q., and Anderson, D.J. (1995). Identification by differential RT-PCR of a novel paired homeodomain protein specifically expressed in sensory neurons and a subset of their CNS targets. Mol. Cell. Neurosci. *6*, 280–292.

Saji, M., and Miura, M. (1990). Evidence that glutamate is the transmitter mediating respiratory drive from medullary premotor neurons to phrenic motoneurons: a double labeling study in the rat. Neurosci. Lett. *115*, 177–182.

Salegio, E., Samaranch, L., and Kells, A. (2012). Axonal transport of adeno-associated viral vectors is serotype-dependent. Gene Ther. *20*, 348–352.

Sapir, T., Geiman, E.J., Wang, Z., Velasquez, T., Mitsui, S., Yoshihara, Y., Frank, E., Alvarez, F.J., and Goulding, M. (2004). Pax6 and engrailed 1 regulate two distinct aspects of

renshaw cell development. J. Neurosci. *24*, 1255–1264.

Sawczuk, A., and Mosier, K.M. (2001). Neural control of tongue movement with respect to respiration and swallowing. Crit. Rev. Oral Biol. Med. *12*, 18–37.

Schnell, M.J., McGettigan, J.P., Wirblich, C., and Papaneri, A. (2009). The cell biology of rabies virus: using stealth to reach the brain. Nat. Rev. Microbiol. *8*, 51–61.

Schreihofer, A.M., Stornetta, R.L., and Guyenet, P.G. (1999). Evidence for glycinergic respiratory neurons: Bötzinger neurons express mRNA for glycinergic transporter 2. J. Comp. Neurol. *407*, 583–597.

Schwarzacher, S.W., Rub, U., and Deller, T. (2011). Neuroanatomical characteristics of the human pre-Bötzinger complex and its involvement in neurodegenerative brainstem diseases. Brain *134*, 24–35.

Sieber, M.A., Storm, R., Martinez-de-la-Torre, M., Müller, T., Wende, H., Reuter, K., Vasyutina, E., and Birchmeier, C. (2007). Lbx1 acts as a selector gene in the fate determination of somatosensory and viscerosensory relay neurons in the hindbrain. J. Neurosci. *27*, 4902–4909.

Similowski, T., Catala, M., Rancurel, G., and Derenne, J.P. (1996). Impairment of central motor conduction to the diaphragm in stroke. Am. J. Respir. Crit. Care Med. *154*, 436–441.

Sirieix, C., Gervasoni, D., Luppi, P.H., and Leger, L. (2012). Role of the lateral paragigantocellular nucleus in the network of paradoxical (REM) sleep: an electrophysiological and anatomical study in the rat. PLoS One *7*, e28724.

Smith, J.C., Morrison, D.E., Ellenberger, H.H., Otto, M.R., and Feldman, J.L. (1989). Brainstem projections to the major respiratory neuron populations in the medulla of the cat. J. Comp. Neurol. *281*, 69–96.

Smith, J.C., Ellenberger, H.H., Ballanyi, K., Richter, D.W., and Feldman, J.L. (1991). Pre-Bötzinger complex: a brainstem region that may generate respiratory rhythm in mammals. Science *254*, 726–729.

Smith, J.C., Abdala, A.P., Koizumi, H., Rybak, I.A., and Paton, J.F.R. (2007). Spatial and functional architecture of the mammalian brain stem respiratory network: a hierarchy of three oscillatory mechanisms. J. Neurophysiol. *98*, 3370–3387.

Smith, J.C., Abdala, A.P., Borgmann, A., Rybak, I. a, and Paton, J.F.R. (2013). Brainstem respiratory networks: building blocks and microcircuits. Trends Neurosci. *36*, 152–162.

Song, A., Ashwell, K.W., and Tracey, D.J. (2000). Development of the rat phrenic nucleus and its connections with brainstem respiratory nuclei. Anat. Embryol. (Berl). *202*, 159–177.

Stanek, E., Cheng, S., Takatoh, J., Han, B.-X., and Wang, F. (2014). Monosynaptic premotor circuit tracing reveals neural substrates for oro-motor coordination. Elife *3*, e02511.

Stein, E., and Tessier-Lavigne, M. (2001). Hierarchical organization of guidance receptors: silencing of netrin attraction by slit through a Robo/DCC receptor complex. Science *291*, 1928–1938.

Stepien, A.E., Tripodi, M., and Arber, S. (2010). Monosynaptic rabies virus reveals premotor network organization and synaptic specificity of cholinergic partition cells. Neuron *68*, 456–472.

Storm, R., Cholewa-Waclaw, J., Reuter, K., Brohl, D., Sieber, M., Treier, M., Müller, T., and Birchmeier, C. (2009). The bHLH transcription factor Olig3 marks the dorsal neuroepithelium of the hindbrain and is essential for the development of brainstem nuclei. Development *136*, 295–305.

Stornetta, R.L., Sevigny, C.P., and Guyenet, P.G. (2003a). Inspiratory augmenting bulbospinal neurons express both glutamatergic and enkephalinergic phenotypes. J. Comp. Neurol. *455*, 113–124.

Stornetta, R.L., Rosin, D.L., Wang, H., Sevigny, C.P., Weston, M.C., and Guyenet, P.G. (2003b). A group of glutamatergic interneurons expressing high levels of both neurokinin-1 receptors and somatostatin identifies the region of the pre-Bötzinger complex. J. Comp. Neurol. *455*, 499–512.

Stornetta, R.L., Moreira, T.S., Takakura, A.C., Kang, B.J., Chang, D.A., West, G.H., Brunet, J.-F., Mulkey, D.K., Bayliss, D.A., and Guyenet, P.G. (2006). Expression of Phox2b by brainstem neurons involved in chemosensory integration in the adult rat. J. Neurosci. *26*, 10305–10314.

Sun, Q.J., Goodchild, A.K., Chalmers, J.P., and Pilowsky, P.M. (1998). The pre-Bötzinger complex and phase-spanning neurons in the adult rat. Brain Res. *809*, 204–213.

Suzue, T. (1984). Respiratory rhythm generation in the in vitro brain stem-spinal cord preparation of the neonatal rat. J. Physiol. *354*, 173–183.

Suzue, T. (1994). Mouse fetuses in late gestation maintained in vitro by a transplacental perfusion method and their physiological activities. Neurosci. Res. *21*, 173–176.

Takahashi, K., Satomi, H., Ise, H., and Yamamoto, T. (1980). Identification of the phrenic nucleus in the cat as studied by horseradish peroxidase bathing of the transected intrathoracal phrenic nerve. Anat. Anz. *148*, 49—54.

Takatoh, J., Nelson, A., Zhou, X., Bolton, M.M., Ehlers, M.D., Arenkiel, B.R., Mooney, R., and Wang, F. (2013). New modules are added to vibrissal premotor circuitry with the emergence of exploratory whisking. Neuron *77*, 346–360.

Tan, W., Janczewski, W.A., Yang, P., Shao, X.M., Callaway, E.M., and Feldman, J.L. (2008). Silencing preBötzinger complex somatostatin-expressing neurons induces persistent apnea in awake rat. Nat. Neurosci. *11*, 538–540.

Tan, W., Pagliardini, S., Yang, P., Janczewski, W.A., and Feldman, J.L. (2010). Projections of preBötzinger complex neurons in adult rats. J. Comp. Neurol. *518*, 1862–1878.

Thoby-brisson, M., Trinh, J., Champagnat, J., and Fortin, G. (2005). Emergence of the Pre-Bözinger Respiratory Rhythm Generator in the Mouse Embryo. J. Neurosci. *25*, 4307–4318.

Thoby-brisson, M., Karlén, M., Wu, N., Charnay, P., Champagnat, J., and Fortin, G. (2009). Genetic identification of an embryonic parafacial oscillator coupling to the preBötzinger complex. Nat. Neurosci. *12*, 1028–1035.

Tian, G.-F., Peever, J.H., and Duffin, J. (1998). Bötzinger-complex expiratory neurons monosynaptically inhibit phrenic motoneurons in the decerebrate rat. Exp. Brain Res. *122*, 149–156.

Tian, G.-F., Peever, J.H., and Duffin, J. (1999). Bötzinger-complex, bulbospinal expiratory neurones monosynaptically inhibit ventral-group respiratory neurones in the decerebrate rat. Exp. Brain Res. *124*, 173–180.

Towne, C., Schneider, B.L., Kieran, D., Redmond, D.E., and Aebischer, P. (2010). Efficient transduction of non-human primate motor neurons after intramuscular delivery of

recombinant AAV serotype 6. Gene Ther. *17*, 141–146.

Tripodi, M., Stepien, A.E., and Arber, S. (2011). Motor antagonism exposed by spatial segregation and timing of neurogenesis. Nature *479*, 61–66.

Tümpel, S., Cambronero, F., Ferretti, E., Blasi, F., Wiedemann, L.M., and Krumlauf, R. (2007). Expression of Hoxa2 in rhombomere 4 is regulated by a conserved cross-regulatory mechanism dependent upon Hoxb1. Dev. Biol. *302*, 646–660.

Ugolini, G. (2010). Advances in viral transneuronal tracing. J. Neurosci. Methods *194*, 2–20.

Ugolini, G. (2011). Rabies Virus as a Transneuronal Tracer of Neuronal Connections (Elsevier Inc.).

Vardhan, A., Kachroo, A., and Sapru, H.N. (1993). Excitatory amino acid receptors in commissural nucleus of the NTS mediate carotid chemoreceptor responses. Am. J. Physiol. Integr. Comp. Physiol. *264*, R41–R50.

Vasilakos, K., Wilson, R.J.A., Kimura, N., and Remmers, J.E. (2005). Ancient gill and lung oscillators may generate the respiratory rhythm of frogs and rats. J. Neurobiol. *62*, 369–385.

Vercelli, A., Repici, M., Garbossa, D., and Grimaldi, A. (2000). Recent techniques for tracing pathways in the central nervous system of developing and adult mammals. Brain Res. Bull. *51*, 11–28.

Viemari, J.-C., Burnet, H., Bévengut, M., and Hilaire, G. (2003). Perinatal maturation of the mouse respiratory rhythm-generator: In vivo and in vitro studies. Eur. J. Neurosci. *17*, 1233–1244.

Viemari, J.-C., Bévengut, M., Coulon, P., and Hilaire, G. (2004). Nasal trigeminal inputs release the A5 inhibition received by the respiratory rhythm generator of the mouse neonate. J. Neurophysiol. *91*, 746–758.

Vong, L., Ye, C., Yang, Z., Choi, B., Chua, S., and Lowell, B.B. (2011). Leptin action on GABAergic neurons prevents obesity and reduces inhibitory tone to POMC neurons. Neuron *71*, 142–154.

De Vries, J.I.P., Visser, G.H.A., and Prechtl, H.F.R. (1986). Fetal behaviour in early pregnancy. Eur. J. Obstet. Gynecol. Reprod. Biol. *21*, 271–276.

Wallén-Mackenzie, Å., Gezelius, H., Thoby-Brisson, M., Nygård, A., Enjin, A., Fujiyama, F., Fortin, G., and Kullander, K. (2006). Vesicular Glutamate Transporter 2 Is Required for Central Respiratory Rhythm Generation But Not for Locomotor Central Pattern Generation. J. Neurosci. *26*, 12294–12307.

Walton, K.D., and Navarrete, R. (1991). Postnatal changes in motoneurone electrotonic coupling studied in the in vitro rat lumbar spinal cord. J. Physiol. *433*, 283–305.

Wang, H., Stornetta, R.L., Rosin, D.L., and Guyenet, P.G. (2001). Neurokinin-1 receptor-immunoreactive neurons of the ventral respiratory group in the rat. J. Comp. Neurol. *434*, 128–146.

Wang, V.Y., Rose, M.F., and Zoghbi, H.Y. (2005). Math1 expression redefines the rhombic lip derivatives and reveals novel lineages within the brainstem and cerebellum. Neuron *48*, 31–43.

Wickersham, I.R., Finke, S., Conzelmann, K.-K., and Callaway, E.M. (2007a). Retrograde neuronal tracing with a deletion-mutant rabies virus. Nat. Methods *4*, 47–49.

Wickersham, I.R., Lyon, D.C., Barnard, R.J.O., Mori, T., Finke, S., Conzelmann, K.-K., Young, J.A.T., and Callaway, E.M. (2007b). Monosynaptic restriction of transsynaptic tracing from single, genetically targeted neurons. Neuron *53*, 639–647.

Woch, G., Ogawa, H., Davies, R.O., and Kubin, L. (2000). Behavior of hypoglossal inspiratory premotor neurons during the carbachol-induced, REM sleep-like suppression of upper airway motoneurons. Exp. Brain Res. *130*, 508–520.

Wolpert, D.M., and Miall, R.C. (1996). Forward Models for Physiological Motor Control. Neural Netw. *9*, 1265–1279.

Wong, K., Park, H.T., Wu, J.Y., and Rao, Y. (2002). Slit proteins: Molecular guidance cues for cells ranging from neurons to leukocytes. Curr. Opin. Genet. Dev. *12*, 583–591.

Xu, F., Zhuang, J., Zhou, T.-R., Gibson, T., and Frazier, D.T. (2002). Activation of different vestibular subnuclei evokes differential respiratory and pressor responses in the rat. J. Physiol. *544*, 211–223.

Yokota, S., Tsumori, T., Ono, K., and Yasui, Y. (2001). Phrenic motoneurons receive monosynaptic inputs from the Kölliker-Fuse nucleus: a light- and electron-microscopic study

in the rat. Brain Res. *888*, 330–335.

Yokota, S., Tsumori, T., Ono, K., and Yasui, Y. (2004). Glutamatergic pathways from the Kolliker-Fuse nucleus to the phrenic nucleus in the rat. Brain Res. *995*, 118–130.

Yokota, S., Oka, T., Tsumori, T., Nakamura, S., and Yasui, Y. (2007). Glutamatergic neurons in the Kölliker-Fuse nucleus project to the rostral ventral respiratory group and phrenic nucleus: A combined retrograde tracing and in situ hybridization study in the rat. Neurosci. Res. *59*, 341–346.

Yonehara, K., Farrow, K., Ghanem, A., Hillier, D., Balint, K., Teixeira, M., Jüttner, J., Noda, M., Neve, R.L., Conzelmann, K.-K., et al. (2013). The First Stage of Cardinal Direction Selectivity Is Localized to the Dendrites of Retinal Ganglion Cells. Neuron *79*, 1078–1085.

Young, R.L., Page, A.J., Cooper, N.J., Frisby, C.L., and Blackshaw, L.A. (2010). Sensory and Motor Innervation of the Crural Diaphragm by the Vagus Nerves. Gastroenterology *138*, 1091–1101.e5.

Zagoraiou, L., Akay, T., Martin, J.F., Brownstone, R.M., Jessell, T.M., and Miles, G.B. (2009). A cluster of cholinergic premotor interneurons modulates mouse locomotor activity. Neuron *64*, 645–662.

Zampieri, N., Jessell, T.M., and Murray, A.J. (2014). Mapping sensory circuits by anterograde transsynaptic transfer of recombinant rabies virus. Neuron *81*, 766–778.

Zhang, Y., Narayan, S., Geiman, E.J., Lanuza, G.M., Velasquez, T., Shanks, B., Akay, T., Dyck, J., Pearson, K., Gosgnach, S., et al. (2008). V3 spinal neurons establish a robust and balanced locomotor rhythm during walking. Neuron *60*, 84–96.

ÉCOLE DOCTORALE
Signalisation et réseaux intégratifs en biologie (BIOSIGNE)

THESE DE DOCTORAT

DE

L'UNIVERSITE PARIS-SACLAY

PREPAREE A

L'UNIVERSITE PARIS SUD-XI

ECOLE DOCTORALE N° 568 : BIOSIGNE
Signalisations et réseaux intégratifs en biologie

SPÉCIALITÉ :

NEUROSCIENCES

Par

JINJIN WU

Neural bases of breathing in the mouse: monosynaptic tracing and genetic dissection of phrenic premotor neurons

Composition du jury :

Directeur de thèse :	Gilles Fortin
Rapporteurs :	Muriel Thoby-brisson
	Thomas Similowski
Examinateurs :	Alessandra Pierani
Président du jury :	Hervé Daniel

Thèse soutenue le 28.06.2016

Synthèse en français de la thèse de Neurosciences rédigée en anglais par Mlle Jinjin WU, soutenue le 28 juin 2016, à l'institut de Neuroscience de l'université Paris-Saclay, intitulée :

« **Neural bases of breathing in the mouse : monosynaptic tracing and genetic dissection of phrenic premotor neurons** »

Bases neurales de la respiration : traçage monosynaptique et dissection génétique des neurones pré-moteurs phréniques

Résumé

Le comportement respiratoire est unique en ce qu'il requiert l'activation permanente de muscles squelettiques. Le contrôle exécutif de la respiration repose sur des groupes d'interneurones connectés par des synapses et formant un réseau ordonné : le générateur central respiratoire (CPG). Nous cherchons à comprendre l'implication de types neuronaux définis dans la logique de l'organisation du CPG respiratoire. Nous avons précédemment démontré que les neurones constitutifs du – complexe preBötzinger (preBötC) – le générateur du rythme inspiratoire, dérivaient de progéniteurs neuraux exprimant le gène à homéoboite Dbx1. J'étudie ici, par traçage viral monosynaptique chez des souriceaux, les neurones pré-moteurs à l'interface entre le générateur de rythme et les motoneurones phréniques innervant le diaphragme. Je montre que les principaux neurones pré-moteurs formant – le groupe respiratoire ventral rostral (rVRG) – sont aussi des neurones de type V0. Ce travail révèle une organisation des circuits inspiratoires dans laquelle les lignages cellulaires de types V0 sont cruciaux pour établir (i) le preBötC (générateur du rythme) et le rVRG (suiveur du rythme) et (ii) un dessin de connectivité assurant bilatéralement l'amplitude équilibrée et la synchronisation de la commande motrice des nerfs phréniques requise pour respirer efficacement.

Introduction

Chez les mammifères, la respiration est un comportement moteur contrôlé par un générateur central : un réseau neuronal localisé dans le tronc cérébral qui produit et met en forme la contraction rythmique de muscles régulant le volume pulmonaire et la résistance des voies aériennes supérieures(Feldman et al., 2013). Ce générateur central respiratoire dit CPG respiratoire, pour « Central Pattern Generator » respiratoire, est mis en place et devient actif à environ deux tiers de la gestation chez les rongeurs (Greer et al., 2006; Thoby-Brisson et al., 2005) et contrôle l'un des premiers comportements organisés notable chez le fœtus humain. Dès la naissance le comportement respiratoire doit être constamment adapté aux changements de l'environnement et aux actions entreprises dans celui-ci. Ainsi, le réseau central respiratoire doit coordonner le choix, le « timing » et l'intensité d'activation de groupes appropriés de neurones pré-moteurs, moteurs conditionnant la contraction de leurs cibles musculaires. Le CPG respiratoire est donc à la fois robuste, le rythme est permanent tout au long de la vie et les pauses ne peuvent être que courtes, et labile pour satisfaire en toutes circonstances les demandes énergétiques de l'organisme. Ces adaptations doivent néanmoins respecter deux contraintes intangibles : une synchronisation et des amplitudes parfaitement équilibrées des contractions des muscles respiratoires de la partie droite et de la partie gauche du corps. En effet, le principal muscle inspiratoire, le diaphragme est composé de deux hémi-diaphragmes costaux qui sont respectivement innervés par les nerfs phréniques droit et gauche(De Troyer and Estenne, 1988). Avec l'alternance des phases inspiratoires et expiratoires, la synchronisation bilatérale de la commande motrice des muscles respiratoire est adaptée à l'anatomie des voies aériennes supérieures qui convergent en une voie unique imposant des flux d'air unidirectionnels soit entrant (inspiration) soit sortant (expiration). *La caractérisation des neurones responsables de la synchronisation bilatérale et équilibrée en amplitude de la commande inspiratoire est l'objet d'étude de ce travail de thèse.*

Au cours de la dernière décennie, des approches génétiques basées sur l'histoire de développement des neurones du système nerveux central ont progressé de façon spectaculaire au point de permettre désormais de manipuler sélectivement les descendances neuronales établies très tôt au cours du développement du tube neural afin d'en préciser le rôle dans la fonction des circuits neuronaux (Goulding, 2009; Grillner and Jessell, 2009). Cette approche nous avait permis il ya queques années de démontrer que le complexe preBötzinger (preBötC) qui génère le rythme inspiratoire est composé de neurones de type V0 (dérivant de progéniteurs neuraux ayant exprimé le gène codant pour le facteur de transcription Dbx1). De plus, nous avions montré que le générateur du rythme inspiratoire était bilatéralement synchronisé car les neurones V0 le composant sont des neurones commissuraux (dont les axones traversent le plan médian du cerveau). Ces neurones V0 dépendent, pour cette navigation axonale particulière, d'une signalisation reposant sur le récepteur Robo3 (Bouvier et al., 2010) et

l'invalidation de conditionnelle de Robo3 résulte en une désynchronisation des activités des preBötC droit et gauche. Ainsi la synchronisation bilatérale de la commande motrice inspiratoire est en partie réalisée au niveau du générateur de rythme, le preBötC. Dans ce travail de thèse, j'ai cherché à comprendre l'architecture du circuit pré-moteur en aval du générateur qui contrôle la contraction du diaphragme, plus précisément j'ai cherché à identifier les synapses qui assurent que la transmission de la commande motrice inspiratoire maintienne de façon optimale la synchronisation et l'amplitude équilibrée des ordres moteurs droits et gauches dont dépend l'efficience de la contraction du diaphragme.

Pour ce faire, j'ai employé une méthode récente de marquage des circuits neuronaux basée sur l'emploi de vecteurs viraux neurotropes (Stepien and Arber, 2008)(voir la section méthodes). Cette approche permet de marquer de façon exclusive les neurones pré-moteurs établissant des synapses avec les neurones moteurs innervant le diaphragme. Mes travaux démontrent le rôle prépondérant des neurones du groupe respiratoire rostral (rVRG) au sein de l'appareil pré-moteur. Mes travaux démontrent aussi que les neurones du rVRG sont du même type, V0, que ceux composant le générateur de rythme. Par une approche génétique permettant d'invalider le gène Robo3 de façon conditionnelle dans les neurones de type V0, j'ai obtenu à la naissance un découplage des contractions des diaphragmes droit et gauche. Ainsi, mes travaux démontrent le rôle prépondérant des neurones de type V0 au cœur du circuit moteur inspiratoire et suggèrent leur importance pour l'apparition au cours de l'évolution de la stratégie ventilatoire dite de respiration par aspiration.

Objectifs de la thèse

Les principaux objectifs de ce travail sont :

- de localiser de l'ensemble des populations neuronales pré-motrices des neurones moteurs phréniques innervant le diaphragme.
- de décrire les projections des neurones pré-moteurs
- d'identifier l'origine des neurones pré-moteurs
- de comprendre leur contribution à la synchronisation bilatérale de la commande inspiratoire

Méthodes

Notre étude repose sur l'usage de nombreuses lignées de souris transgéniques (système Cre/lox) permettant l'expression conditionnelle d'allèles soit pour marquer ou activer les neurones (par optogénétique) soit pour interférer avec le guidage de leur axone au cours du développement.

Deux grands types de méthodes sont utilisés dans ce travail qui combine investigation anatomique et fonctionnelle. Nous avons d'une part tracé le circuit inspiratoire à partir du muscle diaphragme. Pour ce faire nous avons injecté un cocktail viral composé d'un

vecteur rabique déficient et d'un vecteur AAV (adéno-associated Virus) complémentant la déficience dans le diaphragme de souriceaux à la naissance. Ces deux vecteurs viraux sont neurotropes et infectent les terminaisons axonales des motoneurones phréniques. Le génome du vecteur rabique a été modifié de façon à ce qu'un gène codant pour une glycoprotéine requise à l'assemblage de nouvelles particules virales au sein des cellules primo-infectée soit remplacé par un gène codant pour une protéine fluorescente (GFP ou mCherry). Ainsi ces virus déficients peuvent infecter les neurones et exprimer en leur sein la protéine fluorescente qui permet de les visualiser mais ne peuvent fabriquer de nouvelles particules virales normalement transportée de façon rétrograde (au travers des synapses) dans les neurones pré-synaptiques en l'absence de glycoprotéine. Ce manque est pallié par l'autre vecteur AAV qui code pour la glycoprotéine manquante, on dit qu'il complémente la déficience, et permet donc que seuls les neurones pré-synaptiques (par définition les neurones pré-moteurs) soit trans-synaptiquement infectés et donc visualisables. La beauté de la technique est qu'elle impose que la propagation du virus s'arrête au niveau du neurone pré-moteur dans lequel la complémentation ne peut se faire car l'AAV lui ne franchit pas la synapse(Stepien and Arber, 2008). Pour établir l'origine des neurones pré-moteurs ces expériences de traçage ont été menées dans diverses lignée de souris cre-rapporteur. Les données anatomiques sont capturées par un microscope confocal et des reconstructions 3D de ces populations ont été réalisées permettant de localiser précisément leur position respective dans le volume du tronc cérébral.

Les techniques d'investigation fonctionnelles sont d'une part des enregistrements électrophysiologiques de l'activité des nerfs phréniques et de l'imagerie calcique de l'activité des neurones sur des préparations in vitro de tronc cérébral/moelle épinière isolée. Nous utilisons aussi l'optogénétique pour stimuler les neurones et recueillir des réponses évoquées qui nous permette d'établir le rôle de ces neurones au sein du réseau.

Résultats

Une carte des populations de neurones pré-moteurs du phrénique a été réalisée qui pour la première fois peut être considérée comme définitive en ce qu'elle s'affranchit des biais toujours présents dans les études précédentes soit de spécificité du point d'entrée du traçeur soit de franchissement par le traçeur de plusieurs synapses. Cette carte est établie chez la souris 9 jours après la naissance (**Figure1**).

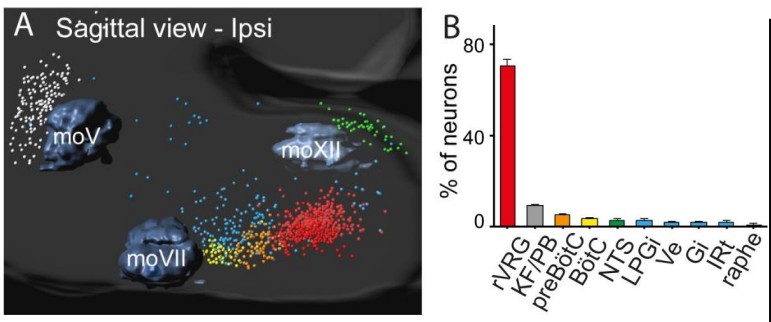

Figure 1. Reconstruction 3D des neurones pré-moteurs phréniques. A, Vue sagittale du tronc cérébral montrant les divers groupes pré-moteurs (code couleur donné en B) et trois groupes de neurones mo-teur crâniens comme repaire ana-tomiques le moV,moVII et moXII. Le principal groupe est le rVRG (rouge). **B**, Distribution des effectifs neuronaux (en pourcentage du nombre total de neurones pré-moteur) dans chacune des régions.

Elle montre que l'ensemble des neurones pré-moteurs phréniques sont localisés dans le tronc cérébral dans plusieurs régions, certaines connues comme respiratoires, d'autres dont l'implication fonctionnelle est moins claire. Une structure ressort particulièrement, le groupe respiratoire ventral rostral (rVRG) qui a lui seul concentre deux tiers de l'effectif total des pré-moteurs et dépasse par un ordre de grandeur l'effectif de toutes les autres populations pré-motrices réunies. Nous avons étudié l'origine de ces diverses populations de neurones pré-moteurs afin d'obtenir des signatures moléculaires susceptibles d'être utilisées pour les manipuler sélectivement. Le résultat le plus remarquable est que les neurones du rVRG sont des neurones issus de progéniteurs neuraux ayant exprimé le gène Dbx1 très tôt pendant le développement du tube neural. Cette observation suffit à leur conférer une identité de neurones dits de type V0 (car issus de progéniteurs dits P0 caractérisés par l'expression du facteur de transcription Dbx1)(Pierani et al., 1999). Nous avons aussi montré que les neurones V0 du rVRG sont excitateurs (glutamatergiques) et comissuraux.

Ainsi, ces neurones pré-moteurs ont exactement la même identité que les neurones du générateur du rythme inspiratoire dont ils reçoivent les projections et dont ils relaient la commande inspiratoire jusqu'au motoneurones phréniques. Ceci constitue un exemple remarquable de l'importance d'un type cellulaire donné à deux niveaux cruciaux d'un réseau neuronal vital.

L'analyse détaillée des profils de projection des neurones pré-moteurs a permis de révéler une propriété anatomique particulière. Dans toutes les régions pré-motrices phréniques nous avons noté l'existence de neurones dont l'axone bifurque en deux branches séparées qui chacune projette sur les motoneurones phréniques situés dans la partie droite et dans la partie gauche de la moelle épinière. Ainsi, l'activation d'un neurone pré-moteur quelle que soit sa position droite ou gauche excitera également les motoneurones phrénique droit et gauche. Il s'agit du « design » le plus simple pour assurer la coordination bilatérale de l'activité inspiratoire. Nous avons pu par optogénétique et en utilisant l'holographie digitale pour restreindre la photoactivation aux seuls neurones du rVRG droit montré que leur activation déclenche des réponses synchrones des motoneurones phréniques droits et gauches (**Figure 2**).

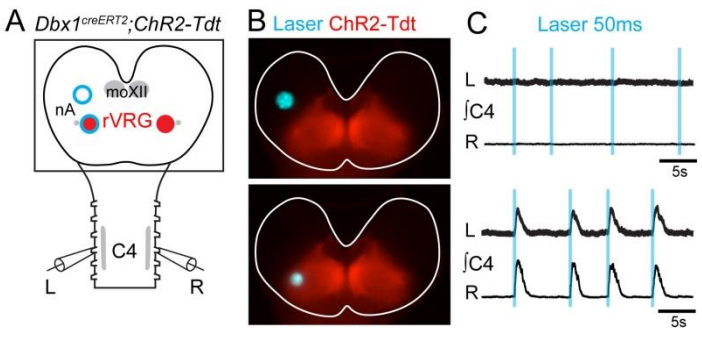

Figure 2. La photostimulation unilatérale du rVRG évoque une réponse bilatérale des motoneurones phréniques. A, préparation in vitro exposant le rVRG et permettant l'enregsitrement de l'activité des nerfs phréniques (C4) droit et gauche. B, Spot lumineux confiné en dehors (haut) et sur le rVRG (bas). C, trace présentant l'absence d'activité évoquée par la lumière (barres verticales bleues) quand le spot est dehors du rVRG, et les activités bilatéralement synchronisées évoquées par le spot sur le rVRG.

Finalement, si le circuit moteur inspiratoire implique au premier chef des neurones V0 à la fois pour la genèse du rythme et pour la transmission pré-motrice de celui-ci, et s'il est possible de d'interdire la navigation commissurale des axones de tous les neurones V0, alors il devait être possible d'observer une dé-synchronisation droite/gauche de l'activité des nerfs phrénique *in vitro* et un découplage droite/gauche des mouvements respiratoires *in vivo*. Nous avons réalisé cette expérience par invalidation conditionnelle du gène Robo3 dans les cellules issues des progéniteurs Dbx1 (lignée *Dbx1^{cre} ;Robo3$^{lox/lox}$*). Conformément à notre prédiction, ces découplages spectaculaires ont été observés (**Figure 3**).

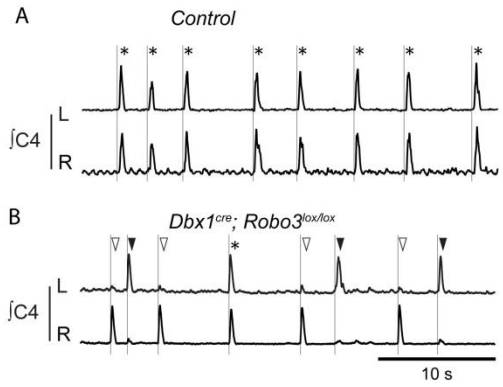

Figure 3. Désynchronisation des nerfs phrénique *in vitro* après invalidation conditionnelle de Robo3 dans les neurones V0s. A, exemple d'enregistrement de l'activité synchronisée des nerfs phréniques (C4) droit et gauche sur une préparation de tronc cérébral moelle épinière isolée d'un souriceau nouveau nés. Les pics correspondants à des décharges d'activité sont synchronisés (trait vertical) chez l'animal contrôle. B, chez le mutant, les bouffées d'activité de C4 gauche (triangles noirs) et de C4 droit (triangles blancs) ne sont pas synchrones. La mutation ayant empêché la connectivité commissurale à la fois au niveau du générateur de rythme et des neurones pré-moteurs du rVRG.

Notre travail permet de conclure que la synchronisation bilatérale de la commande motrice du diaphragme repose sur un appareil neural commissural redondant, composé du générateur du rythme inspiratoire (bilatéralement synchronisé) en amont des pré-moteurs eux-mêmes projetant bilatéralement sur les motoneurones phrénique. Ce système garantit que des inputs asymétriques sur le générateur ou sur les pré-moteurs ne se traduisent pas en des contractions asymétriques du diaphragme qui affecterait l'efficience de la pompe respiratoire. Dans la mesure où les neurones du générateur du rythme inspiratoire et les neurones prémoteurs ciblés par celui-ci sont tous de type V0, cette étude démontre que le cœur du réseau neuronal contrôlant la motorisation du diaphragme repose sur un seul type neuronal dont il est raisonnable de supposer qu'il a été l'objet d'un ciblage particulier au cours de l'évolution lors de la mise en place de la stratégie ventilatoire par aspiration présente chez tous les amniotes.

Références bibliographiques

Bouvier, J., Thoby-Brisson, M., Renier, N., Dubreuil, V., Ericson, J., Champagnat, J., Pierani, A., Chedotal, A., and Fortin, G. (2010). Hindbrain interneurons and axon guidance signaling critical for breathing. Nature neuroscience *13*, 1066-1074.
De Troyer, A., and Estenne, M. (1988). Functional anatomy of the respiratory muscles. Clinics in chest medicine *9*, 175-193.
Feldman, J.L., Del Negro, C.A., and Gray, P.A. (2013). Understanding the rhythm of breathing: so near, yet so far. Annual review of physiology *75*, 423-452.
Goulding, M. (2009). Circuits controlling vertebrate locomotion: moving in a new direction. Nature reviews Neuroscience *10*, 507-518.

Greer, J.J., Funk, G.D., and Ballanyi, K. (2006). Preparing for the first breath: prenatal maturation of respiratory neural control. The Journal of physiology *570*, 437-444.
Grillner, S., and Jessell, T.M. (2009). Measured motion: searching for simplicity in spinal locomotor networks. Current opinion in neurobiology *19*, 572-586.
Pierani, A., Brenner-Morton, S., Chiang, C., and Jessell, T.M. (1999). A sonic hedgehog-independent, retinoid-activated pathway of neurogenesis in the ventral spinal cord. Cell *97*, 903-915.
Stepien, A.E., and Arber, S. (2008). Probing the locomotor conundrum: descending the 'V' interneuron ladder. Neuron *60*, 1-4.
Thoby-Brisson, M., Trinh, J.B., Champagnat, J., and Fortin, G. (2005). Emergence of the pre-Botzinger respiratory rhythm generator in the mouse embryo. J Neurosci *25*, 4307-4318.

université PARIS-SACLAY
ÉCOLE DOCTORALE
Signalisation et réseaux intégratifs en biologie (BIOSIGNE)

Titre : Bases neurales de la respiration : traçage monosynaptique et dissection génétique des neurones pré-moteurs phréniques

Mots clés : pré-moteurs, respiratoire, tronc cérébral

Résumé : Le comportement respiratoire est unique en ce qu'il requiert l'activation permanente de muscles squelettiques. Le contrôle exécutif de la respiration repose sur des groupes d'interneurones connectés par des synapses et formant un réseau ordonné : le générateur central respiratoire (CPG). Nous cherchons à comprendre l'implication de types neuronaux définis dans la logique de l'organisation du CPG respiratoire. Nous avons précédemment démontré que les neurones constitutifs du – complexe preBötzinger (preBötC) – le générateur du rythme inspiratoire, dérivaient de progéniteurs neuraux exprimant le gène à homéoboite *Dbx1*. J'étudie ici, par traçage viral monosynaptique chez des souriceaux, les neurones prémoteurs à l'interface entre le générateur de rythme et les motoneurones phréniques innervant le diaphragme. Je montre que les principaux neurones prémoteurs formant – le groupe respiratoire ventral rostral (rVRG) – sont aussi des neurones de type V0. Ce travail révèle une organisation des circuits inspiratoires dans laquelle les lignages cellulaires de types V0 sont cruciaux pour établir (i) le preBötC (générateur du rythme) et le rVRG (suiveur du rythme) et (ii) un dessin de connectivité assurant bilatéralement l'amplitude équilibrée et la synchronisation de la commande motrice des nerfs phréniques requise pour respirer efficacement.

Title: Neural bases of breathing in the mouse: monosynaptic tracing and genetic dissection of phrenic premotor neurons

Keywords: premotor, respiration, brainstem

Abstract: Breathing uniquely engages permanent rhythmic contractions of skeletal muscles in a bilaterally synchronized manner. The executive control of respiration imparts on sets of brainstem interneurons synaptically assembled into an ordered network: the respiratory central pattern generator (CPG). We investigate the relationship of defined neuronal subtypes to the organizational logic of the respiratory CPG. We have previously demonstrated that neural progenitors expressing the homeobox gene *Dbx1* give rise to V0 neurons that go on forming the – preBötzinger complex (preBötC) – the inspiratory rhythm generator. I now study, via monosynaptic viral tracing in early postnatal mice, the premotor neurons that interface the rhythm generator to output phrenic motor neurons innervating the main inspiratory pump muscle, the diaphragm. I show that the principal premotor neurons in the – rostral ventral respiratory group (rVRG) – are also V0 interneurons. This work reveals an organization of inspiratory circuits in which V0 cell lineages are crucial for establishing (i) the preBötC (rhythm generator) and the rVRG (rhythm follower) and (ii) a connectivity design that secures the bilaterally balanced amplitude and temporal synchronicity of rhythmic phrenic motor drives necessary for efficient breathing.